# Investigation of Small Signal Dynamic Performance of IPFC and UPFC Devices Embedded in AC Networks

By:

**Shan Jiang**

A Thesis

Submitted to the Faculty of Graduate Studies in Partial Fulfillment

of the Requirements for the Degree of

Doctor of Philosophy

Department of Electrical and Computer Engineering

University of Manitoba

Winnipeg, Manitoba

# Acknowledgments

I would never have been able to complete this dissertation without the guidance of my committee members, help of my friend, and support of my family.

I own my deepest gratitude to Professor Ani Gole, the supervisor of this thesis, for his support, encouragement, inspiration, guidance and patience throughout this research. Despite his busy schedule, Professor Gole always provided me with insightful comments and fruitful discussions. It is my greatest honor to work with him, one of the leaders in the area of electromagnetic transient simulation programs.

I would like to express my sincere appreciation to Professor Udaya Annakkage, my co-advisor, for his encouragement and guidance. Whenever we made discussion I gained inspiration and confidence.

I am heartily thankful to Dr. David Jacobson for his highly valuable advices for my research.

I am indebted to Mr. Erwin Dirks for his technical support throughout this research, and the secretarial stuff Ms. Grace McCaskill, Traci Hofer and Amy Dario for their help and consideration.

I would like to thank Dr. Dharshana Muthumuni for relieving me from work to complete my thesis.

I would also like to extend my grateful appreciation to my fellow graduate students Dr. Yi Zhang, Ms. Zheng Zhou, Dr. Hui Ding, Prof. Shaahin Filizadeh, Mr. Yuefeng Liang, Mr. Shaohua Ma, Mr. Ebrahim Rahimi, Mr. Niraj Kshatriya and Dr. Chandana Karawita. Their assistance and friendship have made my life happy and colorful during all my graduate study at the University of Manitoba.

Financial support from the Natural Sciences and Engineering Research Council (NSERC) of Canada and Manitoba Hydro is greatly appreciated.

Finally, I would like to thank my family and my extended family members for their love, caring, understanding, constant support and encouragement. They always stood by me, cheered me up through the times, good and bad.

# Abstract

This thesis proposes the small signal model for the Interline Power Flow Controller (IPFC). Using this model, the damping performance of the IPFC with different power system configuration is investigated and also compared with the AC Transmission System (FACTS) based controllers such as the Unified Power Flow Controller (UPFC).

The IPFC and the UPFC in constant power control mode can be viewed as effectively cutting the connected transmission line. This change on the structure of the network results in a significant change on the small signal stability.

This thesis also addresses issues regarding the different levels of models that are required for the investigation of the behavior of FACTS. An effective validation approach that uses a minimum sized demonstration platform is proposed. This platform is small enough for detailed EMTP validation, yet large enough to exhibit the range of transient electrical and electromechanical behavior which is the focus for FACTS devices. To demonstrate the approach, the small signal models of the system embedded with the IPFC and the UPFC are developed respectively. The results obtained from small signal analysis are validated with EMTP-type simulation and show a close agreement.

# Table of Contents

# List of Figures

# List of Tables

# List of Abbreviations

| | |
|---|---|
| BPA | Bonneville Power Administration |
| EMT | Electromagnetic Transient |
| EMTP | Electromagnetic Transient Program |
| FACTS | Flexible AC Transmission System |
| GTO | Gate Turn_off Thyristor |
| HVDC | High-Voltage Direct Current |
| IGBT | Insulated Gate Bipolar Transistor |
| IPFC | Interline Power Flow Controller |
| PSS | Power System Stabilizer |
| PWM | Pulse Width Modulation |
| SISO | Single Input Single Output |
| SPWM | Sinusoidal Pulse Width Modulation |
| SSSC | Static Synchronous Series Compensator |
| STATCOM | Static Synchronous Compensator |
| SVC | Static Var Compensator |
| TCPAR | Thyristor-Controlled Phase Angle Regulator |
| TCSC | Thyristor-Controlled Series Capacitor |
| TCR | Thyristor-Controlled Reactor |
| TSC | Thyristor-Switched Capacitor |
| UPFC | Unified Power Flow Controller |
| VSC | Voltage Source Converter |

# Chapter 1 Introduction

The electrical power industry has gone through tremendous changes since the 1980s. The power demand has increased rapidly which resulted in the huge expansion of generation and transmission facilities, and interconnections of individual systems have never been tighter than today. At the same time the socioeconomic environment has also experienced dramatic changes with the power industry facing a set of social, economic, and environmental problems. Increasing public concern about the environment and health, and the cost and regulatory difficulties in obtaining the necessary 'right of way' for new projects have often prevented or delayed the construction of new generation facilities and transmission lines.

One of the challenges the power industry faces is deregulation: to build up a competitive market ensuring the buyers and sellers can transact through a non-discriminatory, open access transmission service, which requires the separation of the generation from transmission network. The implementation of deregulation poses challenges to the present power industry: the main economic emphasis of deregulation is to reduce the cost of electricity through competition. This requires a large number of power suppliers in contrast to traditional single-suppler vertically integrated units. The compulsory accommodation of the least expensive power by the transmission network will aggravate the loop-flow problem, possibly resulting in equipment overloading, voltage variation and a decrease of transient stability margin.

The traditional solution for the above problems is the addition of new power flow control devices such as phase shifting transformers. When such options do not solve the problem the next option is to add new lines or to reconstruct the transmission systems to re-establish voltage limit and transient stability while maintain the line load within acceptable limits. Apart from the cost, such a large undertaking would be unacceptable under the present environmental and regulatory constraints. The Flexible AC Transmission System (FACTS), relying on large scale application of power electronics-based, real time computer-controlled compensators and controllers, provides a technical solution to these problems [1].

## 1.1 Flexible AC Transmission System (FACTS)

New power electronic circuit configurations have been developed that are very effective in regulating power flow in AC transmission lines [1]. These configurations are referred as to Flexible AC Transmission System (FACTS). FACTS controllers are used to address three main objectives for power transmission: (1) increasing the power flow in a designated corridor; (2) controlling the precise route of power flow; (3) improving the dynamic performance.

The first objective implies that power flow in a given line may be increased possibly up to its thermal limit by changing the series line impedance. Typically, the power transfer limit of long lines is determined by the stability limit because it is usually lower than the thermal limit. However, with FACTS equipped with proper controllers could increase the stability limit, approaching the thermal limit. The second objective implies that the power flow can be restricted to the selected path. This mitigates the loop-flow of power. The third objective implies that not only the FACTS itself can act as a controller and compensator due to its fast response nature, but also when all the FACTS and other controllers in the system are combined by appropriate control strategies, they can implement an optimal control on the overall system [2].

Based on the type of the power electronic technologies used (thyristor controlled or voltage source converter controlled), FACTS controllers can be classified in two categories (shown in Table 1-1, Figure 1.1, and Figure 1.2) [2].

Table 1-1 The FACTS family

| Type | Thyristor-controlled | | | | Converter-based | | | |
|---|---|---|---|---|---|---|---|---|
| | SVC | | | | | | | |
| | TSC | TCR | TCSC | TCPAR | STATCOM | SSSC | UPFC | IPFC |
| Compensation | shunt | shunt | series | series | shunt | series | both | series |

### 1.1.1 Thyristor Based Controllers

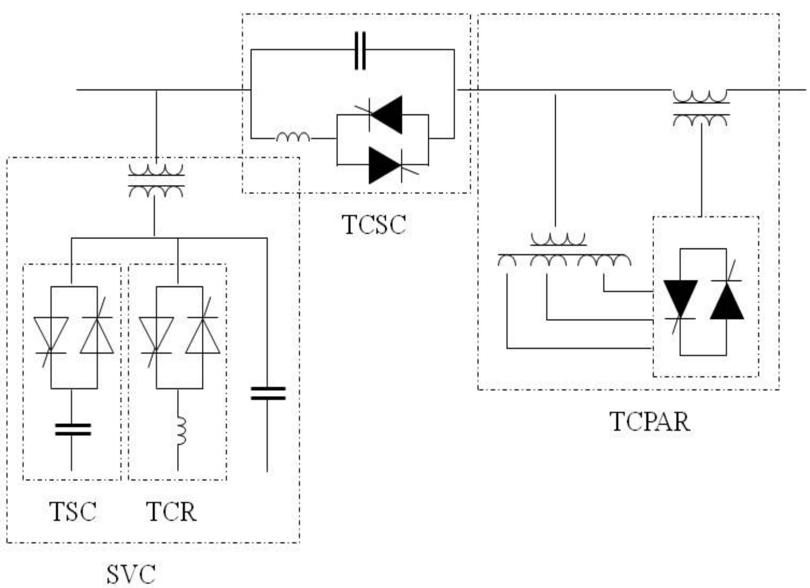


Figure 1.1 Thyristor-controlled FACTS

Thyristor based controllers offer limited controllability because the thyristor device cannot be ordered to turn off. It turns off naturally when system conditions cause the current to reverse direction. However these devices are very robust and have been used extensively in the past. Examples of thyristor based controllers include the Static Var Compensator (SVC), the Thyristor-Controlled Series Capacitor (TCSC) and the Thyristor-Controlled Phase Angle Regulator (TCPAR). Each of them can change one of the three parameters determining power transmission (line impedance, magnitude and phase angle of voltages at both ends of the line). The SVC can change the voltage of the shunt-connected line by controlling the shunt reactors (Thyristor-Controlled Reactor: TCR) or switching capacitors (Thyristor-Switched Capacitor: TSC). The TCSC can change the connected line impedance by controlling series-connected reactor or by switching series-connected capacitors on a transmission line. The TCPAR is similar to a mechanical tap-changer, but has much faster response. It can change the phase angle of the connected line by injecting a voltage in series with the line.

## 1.1.2 Voltage Source Converter (VSC) Based Controllers

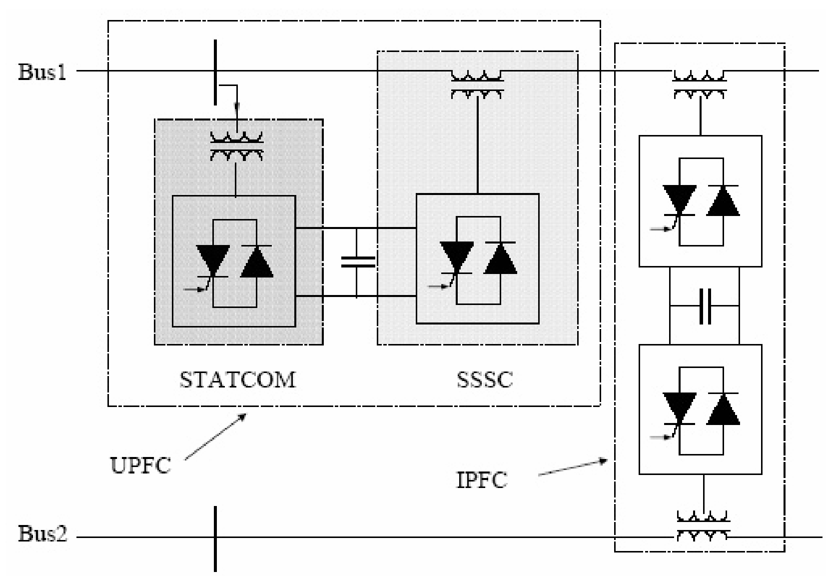


Figure 1.2 Converter-based FACTS

Figure 1.2 shows typical configurations of VSC based FACTS devices. VSC based controllers provide the series or shunt compensation to the system by injecting a series voltage or shunt current into the connected line via a series or shunt voltage-sourced switching converter. Combining shunt and series compensation can provide comprehensive compensation to the system. In contrast to impedance type compensators, they provide compensations via GTO or IGBT switched VSCs, which operate almost instantaneously at fundamental frequency, and do not form a resonance circuit with the transmission network [2]. This group includes the Static Synchronous Compensator (STATCOM), the Static Synchronous Series Compensator (SSSC), the Unified Power Flow Controller (UPFC) and the Interline Power Flow Controller (IPFC). The STATCOM, like the SVC, provides shunt compensation to the system by controlling the reactive current injected into the shunt-connected line thereby affecting the voltage [3]. The SSSC, like the TCSC, provides series compensation, but it relies on controlling the voltage across the series-connected line, thereby controlling the ‘effective’ transmission impedance [4] [5]. The UPFC combines the STATCOM and SSSC by using a common DC capacitor. It can control all three parameters (voltage, effective impedance and angle) to realize shunt and series compensation for a single transmission line [6]. The IPFC combines two SSSCs on the DC side and thus provides series (real and reactive) compensation and real power balancing between two different transmission lines [7].

In this thesis the IPFC and the UPFC are studied. They are relatively new FACTS devices and are versatile as they provide real and reactive compensation functions. Hence they potentially represent the future of FACTS.

## 1.2 Small Signal Stability

Power system stability is the ability of an electric power system, for a given initial operating condition, to regain a state of operating equilibrium after being subjected to a physical disturbance. The classification of power system stability is mainly based on the following considerations: the physical nature of the resulting mode of instability, the size of disturbance, the time span and processes [8]-[11]. A classical classification of power system stability was given by Kundur [11] (also see Figure 1.3).

As shown in Figure 1.3, the small signal rotor angle stability is a factor in system stability. It refers to the ability of the power system to maintain synchronism under small disturbances. These disturbances are considered sufficiently small that the linearization of the system equations is permissible for purposes of analysis.

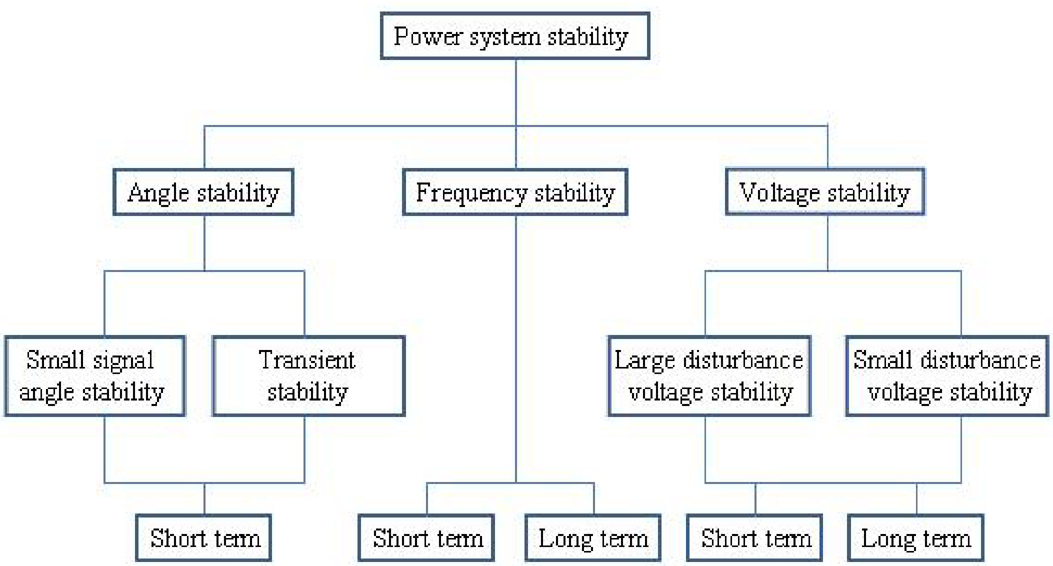


Figure 1.3 Classification of the power system stability [11]

In small signal stability studies, the system is initially modeled using time-domain differential and algebraic equations around the steady-state operating point. After linearization, these equations are transferred to the frequency-domain. Then frequency-domain methods, such as Lyapunov's stability criteria [12] and spectral analysis, are applied in order to obtain the information about the stability and damping by which the system stability and controllers can be designed and analyzed.

In small signal analysis, due to the requirement of linearization, the system is usually a reduced model. The corresponding simulation program permits a large time step. Using such a large time step saves computer time. The frequency-domain methods used are also conceptually clear and efficient for stability analysis and controller design. However, reduced models can lead to misleading results. It is important that the reduced models are validated by comparing results from field measurements or by comparing with results obtained from simulations employing more detailed representation of the power system and related equipment. This is especially the case for systems containing complicated dynamic components, such as FACTS devices.

## 1.3 Electromagnetic Transient Simulation

In all power system simulation programs, the power system is modeled by a set of mathematical equations; the main differences between the programs lie in the detail of modeling and the methods used to solve them [13]. Different levels of detail are required for different research objectives. Hence it is critical to choose the proper approach to analyze and simulate the system according to the desired objective.

Power system simulation programs can be sorted into two main types in terms of the modeling detail and the time span studied: electromechanical transient type programs and electromagnetic transient type programs.

Electromechanical transient type programs are usually used for transient stability studies. These programs represent the network with simple phasor models (compared to EMT programs) and only model the differential equations of equipment such as generators. They allow longer simulation time steps and are suitable for 'large network' studies.

In EMT-type programs (of which PSCAD/EMTDC is an example), the system can be modeled in significant detail, resulting in simulation results which are more accurate. However, due to the high level of detail, the computation is quite time-consuming especially for large systems. Using longer time steps can speed up the process, but at the expense of reduced accuracy.

## 1.4 Main Objectives of the Research

This thesis has three main objectives: **to develop an IPFC small signal model, to investigate the small signal performances of the IPFC in the power system** and **to develop a general approach for validation of the IPFC small signal model that can be applied to other FACTS**.

In the FACTS family of devices, the UPFC and the IPFC are the representatives which have the most complicated configurations and can potentially provide the most comprehensive compensation. A lot of studies on the UPFC have been carried out since Hingorani proposed the concept of FACTS [1], [14]-[23]. The UPFC has been shown by these studies to be a reliable solution that addresses the opposing requirements of increasing power transmission capacity and maintaining the environmental and economic balance. However, very few studies have reported on the IPFC for similar purposes [24]-

[29]. This thesis investigates the performance of the IPFC for increasing power flow and improving controllability while maintaining stability. In order to achieve this, a small signal model for the IPFC had to be developed and validated [30].

As stated in section 1.3, a detailed EMT type simulation provides sufficient credibility for validation, but requires a smaller sized network. Researchers using the method of validating the small signal studies using EMTP have carried out their studies partially and also used very simple systems (such as a single machine infinite bus system) or very simple models of dynamic devices (such as using voltage sources to represent generators) [31]. To address the problems in studying FACTS, an IEEE working group in 2001 (IEEE PES WG 15.05.02, spearheaded by Annakkage and Gole) proposed the creation of a benchmark system for FACTS study. This system is large enough to demonstrate typical problems which can be addressed using FACTS, while being small enough for detailed EMT simulation programs validation [32]. Another important objective of the research in this thesis is to use this test system to validate the IPFC model as well as to demonstrate its typical use.

## 1.5 Thesis Overview

The thesis discusses the approach employed to achieve the above objectives:

Chapter 2 introduces the operating principles of the IPFC and the UPFC. The control algorithm for these devices is also described in detail. The small signal models for these devices are derived.

Chapter 3 introduces the test network, which was specially designed to exhibit behavior that can be improved with FACTS devices. The IPFC and UPFC are embedded into this network at different locations. The IPFC and the UPFC models developed in Chapter 2 are combined with the small signal model of the test system to derive the overall small signal model.

Chapter 4 discusses validation aspects. In this research, the simulations for the small signal models derived in Chapter 2 and 3 are initially run using an analytical formulation in MATLAB. Then the results are compared with a detailed EMT simulation. Using the results of the simulation, the small signal models are further refined and the accuracy is enhanced.

Chapter 5 investigates the damping performance of the IPFC and the UPFC. Small signal analysis shows that the IPFC and the UPFC have a large impact on the electromechanical modes of the network. A simple explanation based on viewing the IPFC as a link that divides the entire network into two independent disconnected parts is proposed. It perfectly explains the observed phenomena.

Finally, in Chapter 6 conclusions are presented and suggestions for future work are given.

The thesis concludes with the list of references cited throughout the thesis and appendices which present the details of the small signal models of the IPFC, the UPFC and the test network.

# Chapter 2 Small Signal Modelling of the Interline Power Flow Controller (IPFC) and the Unified Power Flow Controller (UPFC)

This chapter presents the operating principle for the IPFC and the UPFC, and introduces their small signal models which are validated later in Chapter 4.

## 2.1 FACTS Devices and Modelling

In order to effectively investigate the impact of FACTS devices on the power system, their modeling and implementation in power system software is essential. The modeling methods for FACTS devices vary in terms of different study objectives and detail levels. Generally speaking, there are three levels of modeling: (i) the Electro-Magnetic Transients (EMT) type models for detailed equipment level investigation [33] [34]; (ii) steady-state models for system steady-state operation evaluation [2] [15], such as power flow program; (iii) dynamic models for stability studies [15] [35], such as transient stability program. The small signal model linearizes the system and provides an analytical framework for determining resonance and damping. It can be used to design controllers for power apparatus employing frequency domain method. Of course, unlike the EMT method, it is valid only for small disturbances around a given operating point. The small signal model considers a detailed representation of the mechanical systems, but uses the approximate small signal representation for the electrical network. It is useful for stability studies on very large systems.

A convenient method to validate small signal models is to compare with the most detailed model possible, i.e. the EMT model. One purpose of this work is to validate the small signal model against the accurate EMTP-type model.

The Unified Power Flow Controller (UPFC) and Interline Power Flow Controller (IPFC) are two modern Voltage Source Converter (VSC) based devices for controlling power flow in a network. Their operation will be discussed in the following section.

There is a significant body of work about the UPFC. Since the earliest pioneering concept was proposed [1] [14], the UPFC has been fully demonstrated and proven, from its modeling [14] [17], stability and control [17]-[22], power flow [36]-[40], to its field experience [23] [41]. Literature on the IPFC has been relatively sparse in comparison. The majority of earlier contributions consider only the power flow and operating constraints [24]-[26]. The studies on IPFC's small signal stability performance are even rarer and highly simplified. In these studies, either highly simplified test systems are used [27] [28], or the validation process is entirely omitted [29].

One objective of the research is to investigate the small signal performance of the IPFC in a comprehensive way. The small signal model of the IPFC including the decoupled controller is developed. In this type of controller, the d, q components of the transferred power are decoupled and independent, which reduces the interaction between the real and reactive power controllers [19] [42]. Small signal analysis can be applied to investigate applications of the IPFC for providing damping in realistic power networks and for comparison with other FACTS devices such as the UPFC. This subject will be discussed in Chapter 5.

## 2.2 Operation of the UPFC and the IPFC

The UPFC consists of both series and shunt VSC branches. The IPFC only contains two series branches whose mechanisms are similar with the series branch of the UPFC. Hence the UPFC operating principles will be explained in detail, and the IPFC will be briefly discussed later.

### 2.2.1 Operation of the UPFC

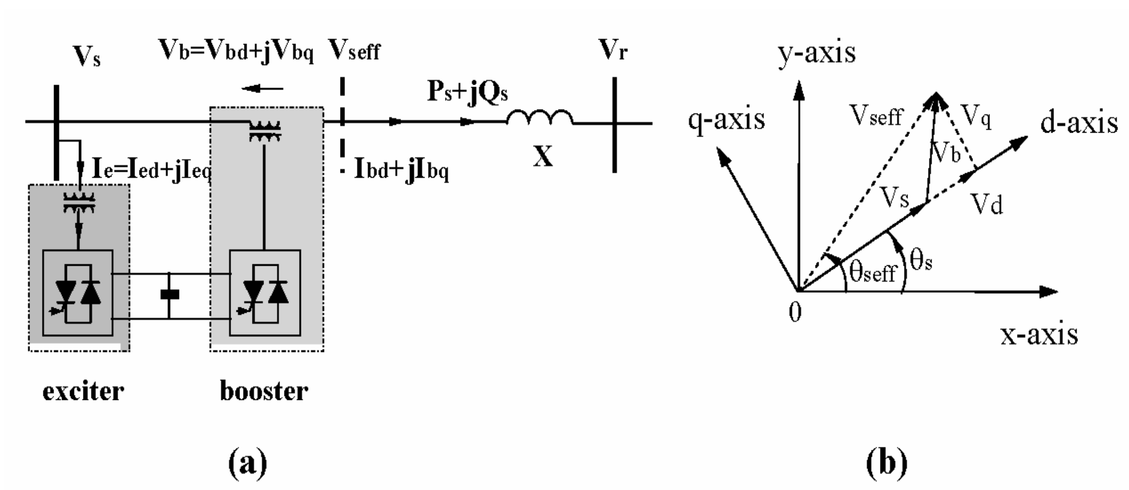


Figure 2.1 Operating principle of the UPFC

Figure 2.1 shows a simple system consisting of two buses connected by a transmission line and a UPFC. Each of the shunt (exciter) and series (booster) branches of the UPFC can be recognized as controllable voltage sources whose magnitude and phase angle can be adjusted. Both of these sources generate the injected AC voltage by converting the DC voltage on the common DC bus capacitor. The voltage sources are not completely independent because the real power balance dictates that the real power entering the shunt converter must be the same as the real power leaving the series converter (ignoring losses). Assume that the injected voltages in the series and shunt branch are $V_b$ and $V_e$ respectively, and that the currents in the series and shunt branch are $I_b$ and $I_e$ respectively.

In the absence of the injected voltage $V_b$, the transmitted real power $P_s$ and reactive power $Q_s$ are described by the well known power flow equations (2.1):

$$P_s = \frac{V_s \cdot V_r}{X} sin(\theta_s - \theta_r)$$
$$Q_s = \frac{V_s^2 - V_s \cdot V_r \cdot cos(\theta_s - \theta_r)}{X} \tag{2.1}$$

With the UPFC placed at the sending end, its series injected voltage $V_b$ boosts the sending end voltage to $V_{seff}$ as shown in Figure 2.1 (b). The sending end power $P_s$ and $Q_s$ are then determined by the "effective" sending voltage magnitude $|V_{seff}|$ and angle $\theta_{seff}$ instead of by $|V_s|$ and $\theta_s$. It can be readily shown that $P_s$ is more sensitive to $\theta_{seff}$ change and $Q_s$ is more sensitive to $V_{seff}$ change. For analysis purposes, the voltage (or current) vectors can be resolved into components in phase with (d) and in quadrature with (q) of the sending end voltage $V_s$. Because the d, q components of the injected voltage ($V_d$, $V_q$) mainly affect $|V_{eff}|$ and $\theta_{eff}$ respectively, the variations of $P_s$ and $Q_s$ are mainly determined by $V_q$ and $V_d$ respectively. In the UPFC, the aims of the shunt exciter are to support the sending end voltage $V_s$ and to keep the DC link voltage constant. The former aim can be implemented by injecting reactive current $I_{eq}$ into the sending bus from the exciter (by controlling $V_e$), while in order to keep the DC link voltage constant, the real power flowing into the exciter must be equal to the real power injected into the line from the booster (neglecting UPFC losses). Therefore there are three independent variables in the UPFC: $P_s$, $Q_s$, and $I_{eq}$, and one dependent variable: $I_{ed}$.

## 2.2.2 Operation of the IPFC

The principle of the IPFC is similar to the UPFC which is illustrated in Figure 2.2. The

IPFC consists of two series VSCs injected into two separate transmission lines. The two VSCs are connected back-to-back by a DC link. Since the IPFC can control the magnitude and phase angle of the injected voltage in both lines, it has 4 degrees of freedom in control. As in the UPFC, one degree is used to keep the DC-link voltage constant and the remaining three degrees are used to control the real **and** reactive power in one line, and the real **or** reactive power in another line.

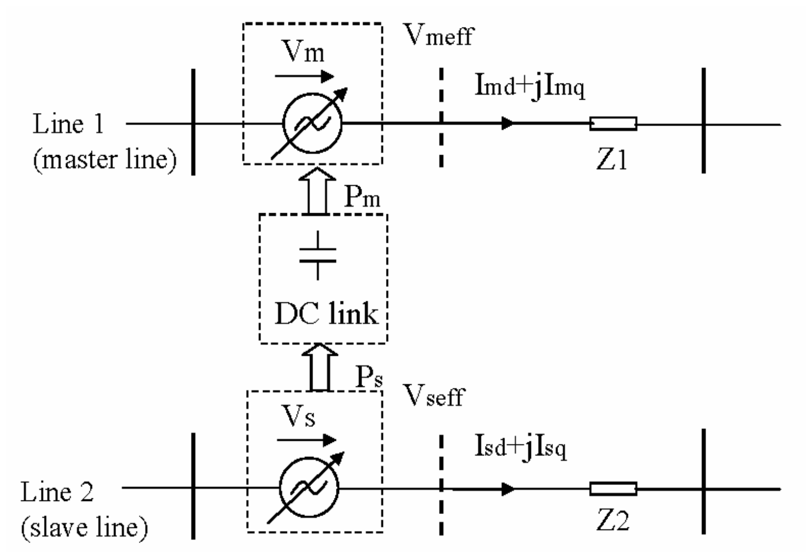


Figure 2.2 Principle of the IPFC

With such an arrangement, the series injection of voltage allows the IPFC to improve the transfer capacity of the transmission line in a similar manner to the UPFC. As the series sources are in two lines, the power flow in each line can be controlled, allowing more equitable use of the transmission capacity. In addition, the individual VSCs of the IPFC can be decoupled and operate as independent Static Synchronous Series Compensators (SSSCs), without any hardware change [43]. The SSSC can not absorb any steady state real power. Although not as versatile as the UPFC and the IPFC, it can introduce a shunt voltage in quadrature with the line current and acts like a variable series capacitor.

### 2.2.3 Control Method for the UPFC and the IPFC

The control strategy plays an important role in the UPFC and IPFC. Decoupled control theory is one popular method for controlling VSC based FACTS devices.

The main principle of decoupled control theory is as follows: any set of three-phase instantaneous variables that sum to zero can be represented by a vector in an orthogonal coordinate system, in which the vector is described by means of its d-axis and q-axis components. This transformation from three-phase variables to d-q vectors is the well known Park's transform [44], which applies to both voltage and current.

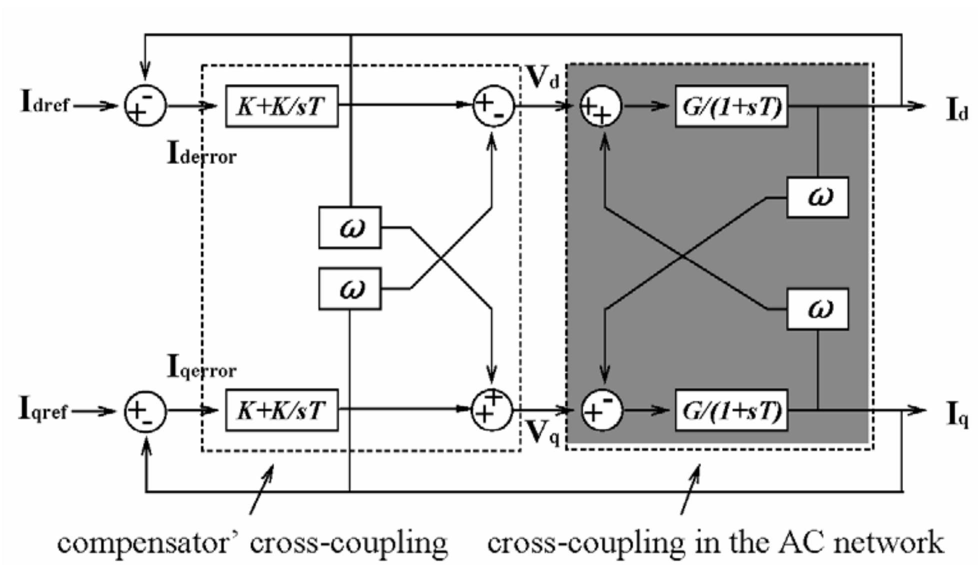


Figure 2.3 Principle of the decoupled controller

As seen in Figure 2.1, changing the d, q components ($V_{bd}$, $V_{bq}$) of the injected voltage ($V_b$) affects both the d, q components ($I_{bd}$, $I_{bq}$) of the line current ($I_b$). This is due to the fact that there is a strong cross-coupling between the d, q components introduced by the connected network. This cross-coupling is represented by the shaded area of Figure 2.3

[19].

Consequently, it is very difficult to independently control the real power without affecting the reactive power or vice versa. Nevertheless, the independent control of active and reactive power is an important desirable feature of the UPFC and the IPFC. In order to achieve this independence, a cross-coupling compensator is introduced by the controller to cancel the cross-coupling of the transmission system [19] [42]. With this compensator, the system resembles two Single Input Single Output (SISO) systems (see Figure 2.3 and equation (2.2)).

$$\begin{matrix} ((I_{dref} - I_d) \cdot K(1+1/sT) - \omega I_q + \omega I_q) \cdot G(1+sT) = I_d \\ ((I_{qref} - I_q) \cdot K(1+1/sT) + \omega I_d - \omega I_d) \cdot G(1+sT) = I_q \end{matrix} \Rightarrow \begin{matrix} I_d / I_{dref} = 1/(1+sT/KG) \\ I_q / I_{qref} = 1/(1+sT/KG) \end{matrix} \quad (2.2)$$

With this modification, control references $I_{dref}$, $I_{qref}$ only affect $I_d$ and $I_q$ respectively which realizes the independent control for the real and reactive power.

Another benefit of the decoupled control is on the modeling and analysis. Without decoupled control, the voltage-current relation has to be described by a set of coupled equations with bus voltages and phase angles as variables. The trigonometric equations with the cross coupled items results in a more complicated linearized model. It usually makes both the derivation and the analysis much harder. Using decoupled control not only simplifies the model, also the straightforward SISO relations between the inputs and outputs can make analysis and controller design much easier.

The EMTP-type models for the UPFC and IPFC are detailed and include power electronic switches to represent the series and shunt converters. They also include the decoupled control method discussed above. They are discussed in more detail in Chapter 4.

## 2.3 Small Signal Model of the IPFC

The nonlinear differential equations are the foundation for developing the small signal model. These same equations can also be directly used in transient stability studies. The difference in the two studies lies in the treatment of these equations. In transient stability studies, the equations are directly integrated numerically to yield the time evolution of the response. In small signal stability studies, they are linearized around the operating point and analyzed using a classical analytical approach to stability: that of examining the system's eigenvalue in the complex plane.

The procedure to form the small signal model is summarized in two main steps:

(1) Describing the dynamics of each dynamic device in the system in the form of differential equations, and describing their interactions with the system in form of algebraic equation;

(2) Linearizing each set of differential/ algebraic equations, and combining them.

The IPFC's two back-to-back inverters can be represented by two voltage sources [7]. The line possessing two degrees of freedom (see Figure 2.2) is called master line, and the other line is called the slave line. All variables related to the master line and slave line are denoted with the subscripts 'm' and 's' respectively. Three coordinate systems are adopted in this model. Master line and slave line sending end voltage vectors ($V_{m1}$, $V_{s1}$) are selected as d-axis of master line's and slave line's coordinate systems separately, thus the real and reactive power ($P_m$, $Q_m$, $P_s$, and $Q_s$) can be represented by their corresponding d, q current components ($I_{md}$, $I_{mq}$, $I_{sd}$ and $I_{sq}$). The other coordinate system is the network's coordinate system (x-y system) which takes the infinite bus voltage as its x-axis. All vectors of the network are finally expressed as x-y components.

The dynamics of the IPFC are represented by two groups of state equations. One represents the dynamics of its DC capacitors; the other group represents the control strategy which plays an important role in FACTS. A well designed controller ensures better performances (such as improved stability and speed of response) of the device. In this research, the decoupled control is used for its simplicity in theoretical analysis.

Figure 2.4 shows the equivalent representation of the IPFC and the phasor relationships between key variables in the small signal model. The derivation of the various quantities is listed below:

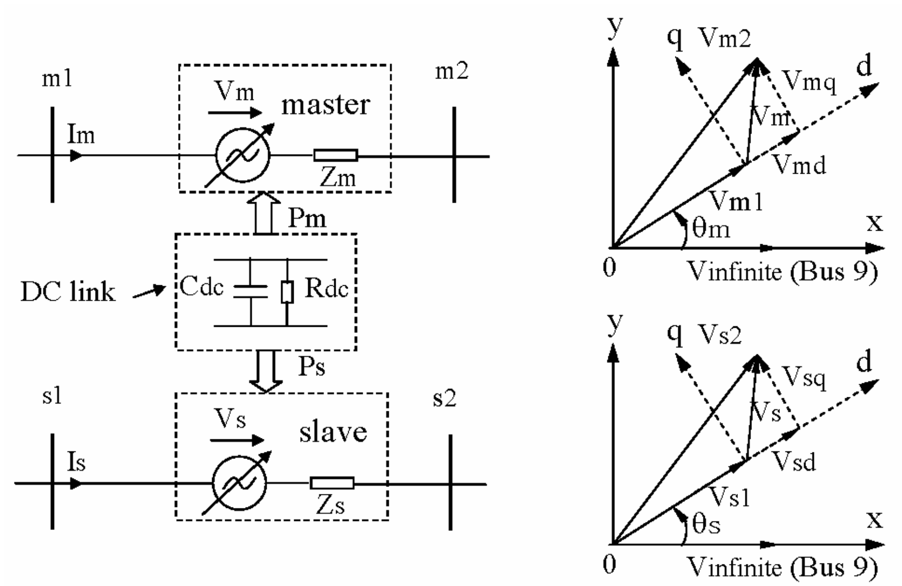


Figure 2.4 Circuit structure and principle variables for the IPFC

The DC link is modeled by:

$$C_{dc} \cdot V_{dc} \cdot \frac{d}{dt} V_{dc} = -S_b \cdot (P_s + P_m) - \frac{V_{dc}^2}{R_{dc}} \tag{2.3}$$

Where:

$C_{dc}$: the capacitance of the dc bus capacitor.

$V_{dc}$: the voltage of the dc bus.

$P_{m}$: the real power flowing out of the dc link into the master line of the IPFC.

$P_{s}$: the real power flowing out of the dc link into the slave line of the IPFC.

The PI Controller that maintains $V_{dc}$ at the reference setting of $V_{dcr}$ is modeled as:

$$U_{sq} = K_{pdc} \cdot (V_{dcr} - V_{dc}) + K_{idc} \cdot \int (V_{dcr} - V_{dc}) \cdot dt \tag{2.4}$$

Here $U_{sq}$ is the reference of the q-axis component of the slave line current. It is the only non-independent reference in the IPFC's four references ($U_{md}$, $U_{mq}$, $U_{sd}$ and $U_{sq}$).

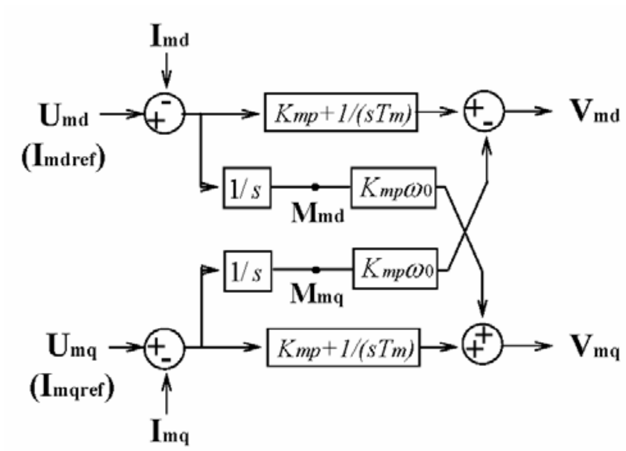


Figure 2.5 The decoupled controller of IPFC master branch

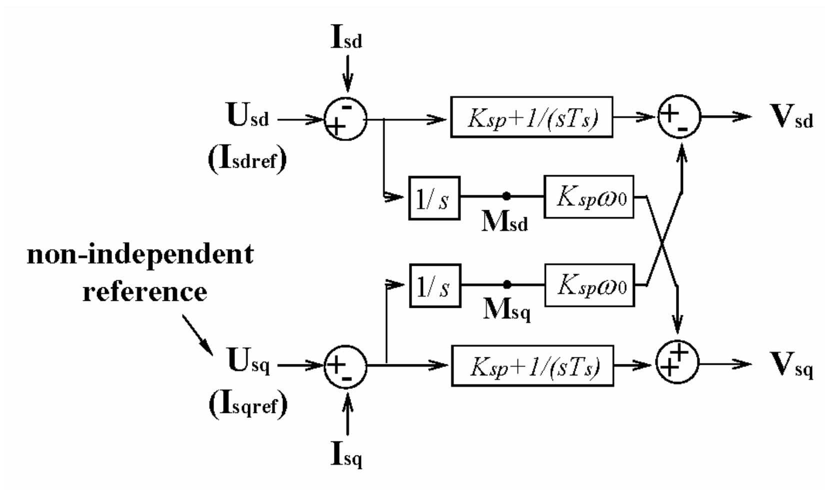


Figure 2.6 The decoupled controller of IPFC slave branch

The decoupled controllers of the IPFC are shown in Figure 2.5 (master branch) and Figure 2.6 (slave branch) respectively.

It should be noted that in the decoupled controller, the controller's setting should be based on the instantaneous value of the system frequency ($\omega/2\pi$) instead of the nominal value ($\omega_0/2\pi$). Here $\omega_0$ is adopted in the study for the following two reasons:

1. In the small signal study, the low frequency oscillation results in the instantaneous system frequency fluctuating around the nominal value ($\omega_0/2\pi$). The average value of the frequency is still the nominal value.
2. In the small signal study, in contrast with the system frequency, the magnitude of the low frequency oscillation is very small, which would not result in a large bias between the instantaneous value and the nominal value of the system frequency.

For an example, in the simulation Case 3 of Chapter 4 the angular frequency $\omega$ changes between 376.985 and 377.015. Hence this trivial difference between $\omega$ and $\omega_0$ can be ignored in the controller.

The decoupled controllers are modeled as:

$$Vm_d = Kmp \cdot (Um_d - Im_d) + \frac{1}{Tm} \cdot Mmd - Kmp \cdot \omega_0 \cdot Mmq \tag{2.5}$$

$$Vm_q = Kmp \cdot (Umq - Im_q) + \frac{1}{Tm} \cdot Mmq + Kmp \cdot \omega_0 \cdot Mmq \tag{2.6}$$

$$Vs_d = Ksp \cdot (Usd - Is_d) + \frac{1}{Ts} \cdot Msd - Ksp \cdot \omega_0 \cdot Msq \tag{2.7}$$

$$Vs_q = Ksp \cdot (Usq - Is_q) + \frac{1}{Ts} \cdot Msq + Ksp \cdot \omega_0 \cdot Msd$$

(2.8)

Here $Mmd$, $Mmq$, $Msd$ and $M_{sq}$ are the integrals of the errors of IPFC's current components ($Imd$, $Imq$, $Isd$ and $Isq$) and their references ($Umd$, $Umq$, $Usd$ and $Usq$).

$$\frac{d}{dt} Mmd = Umd - Im_d \tag{2.9}$$

$$\frac{d}{dt}M_{mq} = U_{md} - I_{m_q} \tag{2.10}$$

$$\frac{d}{dt}M_{sd} = U_{sd} - I_{s_d} \tag{2.11}$$

$$\frac{d}{dt}M_{sq} = U_{sq} - I_{s_q} \tag{2.12}$$

Here, $I_{md}$ and $I_{mq}$ are the d,q components of the master line current; $I_{sd}$ and $I_{sq}$ are the d,q components of the slave line current.

Since the IPFC is incorporated in the power system, the voltage and current variables in the IPFC equations should be expressed with variables in the network x-y plane. Thus the V-I relation of the IPFC can be represented by following equations:

$$V_m = -(V_{m1} - V_{m2}) + Z_m \cdot I_m = -\begin{pmatrix} V_{m1_x} - V_{m2_x} \\ V_{m1_y} - V_{m2_y} \end{pmatrix} + \begin{pmatrix} 0 & -X_m \\ X_m & 0 \end{pmatrix} \cdot \begin{pmatrix} I_{m_x} \\ I_{m_y} \end{pmatrix} \tag{2.13}$$

$$V_s = -(V_{s1} - V_{s2}) + Z_s \cdot I_s = -\begin{pmatrix} V_{s1_x} - V_{s2_x} \\ V_{s1_y} - V_{s2_y} \end{pmatrix} + \begin{pmatrix} 0 & -X_s \\ X_s & 0 \end{pmatrix} \cdot \begin{pmatrix} I_{s_x} \\ I_{s_y} \end{pmatrix} \tag{2.14}$$

$$P_m = (V_{m_x} \quad V_{m_y}) \cdot I_m = -(V_{m1_x} - V_{m2_x}) \cdot I_{m_x} - (V_{m1_y} - V_{m2_y}) \cdot I_{m_y} \tag{2.15}$$

$$P_s = -(V_{s1_x} - V_{s2_x}) \cdot I_{s_x} - (V_{s1_y} - V_{s2_y}) \cdot I_{s_y} \tag{2.16}$$

Where:

$V_{m1} = \begin{pmatrix} V_{m1_x} \\ V_{m1_y} \end{pmatrix}$: the sending end voltage vector of the master branch of the IPFC.

$V_{m2} = \begin{pmatrix} V_{m2_x} \\ V_{m2_y} \end{pmatrix}$: the receiving end voltage vector of the master branch of the IPFC.

$V_{s1} = \begin{pmatrix} V_{s1_x} \\ V_{s1_y} \end{pmatrix}$: the sending end voltage vector of the slave branch of the IPFC.

$V_{s2} = \begin{pmatrix} V_{s2_x} \\ V_{s2_y} \end{pmatrix}$: the receiving end voltage vector of the slave branch of the IPFC.

$V_m = \begin{pmatrix} V_{m_x} \\ V_{m_y} \end{pmatrix} = T_{ip1} \cdot V_{mdq}$ : the injected voltage vector of the master branch of the IPFC.

$V_s = \begin{pmatrix} V_{s_x} \\ V_{s_y} \end{pmatrix} = T_{ip2} \cdot V_{sdq}$ : the injected voltage vector of the slave branch of the IPFC.

$V_{mdq} = \begin{pmatrix} V_{m_d} \\ V_{m_q} \end{pmatrix}$: the d-q vector of the injected voltage of the master branch of the IPFC.

$V_{sdq} = \begin{pmatrix} V_{s_d} \\ V_{s_q} \end{pmatrix}$: the d-q vector of the injected voltage of the slave branch of the IPFC.

$I_m = \begin{pmatrix} I_{m_x} \\ I_{m_y} \end{pmatrix}$: the vector of the current flowing through the master transformer of the IPFC.

$I_s = \begin{pmatrix} I_{s_x} \\ I_{s_y} \end{pmatrix}$: the vector of the current flowing through the slave transformer of the IPFC.

$T_{ip1} = \begin{pmatrix} cos\theta_m & -sin\theta_m \\ sin\theta_m & cos\theta_m \end{pmatrix}$: the dq to xy transformation matrix of the master branch.

$T_{ip2} = \begin{pmatrix} cos\theta_s & -sin\theta_s \\ sin\theta_s & cos\theta_s \end{pmatrix}$: the dq to xy transformation matrix of the slave branch.

$Z_m = \begin{pmatrix} R_m & -X_m \\ X_m & R_m \end{pmatrix}$: the master impedance matrix of the IPFC ($R_m$ is omitted, $R_m$=0 ).

$Z_e = \begin{pmatrix} R_s & -X_s \\ X_s & R_s \end{pmatrix}$: the slave impedance matrix of the IPFC ($R_s$ is omitted, $R_s$=0 ).

Equations (2.3)-(2.16) can be linearized as differential and algebraic equations (2.17)-(2.19) to provide the small signal model. The model has 6 state variables, and three inputs (or references). The detailed derivation of the elements of all coefficient matrices is given in Appendix C.

$$\Delta \dot{X}_{ip} = A_{ip} \cdot \Delta X_{ip} + B_{ip} \cdot \Delta U_{ip} + E_{ip} \cdot \Delta V_{m1} + F_{ip} \cdot \Delta V_{m2} + G_{ip} \cdot \Delta V_{s1} + H_{ip} \cdot \Delta V_{s2} \tag{2.17}$$

$$\Delta I_m = T_{ip39} \cdot \Delta X_{ip} + T_{ip40} \cdot \Delta U_{ip} + T_{ip41} \cdot \Delta V_{m1} + T_{ip42} \cdot \Delta V_{m2} \tag{2.18}$$

$$\Delta I_s = T_{ip43} \cdot \Delta X_{ip} + T_{ip44} \cdot \Delta U_{ip} + T_{ip45} \cdot \Delta V_{s1} + T_{ip46} \cdot \Delta V_{s2} \tag{2.19}$$

Where:

$$\Delta X_{ip} = \begin{pmatrix} \Delta V_{dc} \\ \Delta M_{dc} \\ \Delta M_{md} \\ \Delta M_{mq} \\ \Delta M_{sd} \\ \Delta M_{sq} \end{pmatrix} \qquad \Delta U_{ip} = \begin{pmatrix} \Delta U_{md} \\ \Delta U_{mq} \\ \Delta U_{sd} \end{pmatrix}$$

## 2.4 Small Signal Model of the UPFC

The UPFC’s two back-to-back inverters can be represented either by a shunt current source and a series voltage source [18], or by two voltage sources (one shunt and the other series) [14].

In this thesis, the series part possessing two degrees is called the booster, and the shunt part is called the exciter. All variables and ratios of the booster and exciter sides are denoted with the subscripts ‘b’ and ‘e’ respectively. Two coordinate systems are adopted in this model. The sending end voltage vectors ($V_s$) are selected as the d-axis of the UPFC’s coordinate system, thus the real and reactive power ($P_b$, $Q_b$ and $P_e$, $Q_e$) can be represented by their corresponding d, q current components ($I_{bd}$, $I_{bq}$ and $I_{ed}$, $I_{eq}$). The other coordinate system is the network’s coordinate system (x-y system) which takes the infinite bus voltage as its x-axis. All vectors of the network are finally expressed as x-y components.

The UPFC dynamics is represented by two groups of state equations. One represents the dynamics of its DC capacitors; the other group represents the details of the decoupled controller.

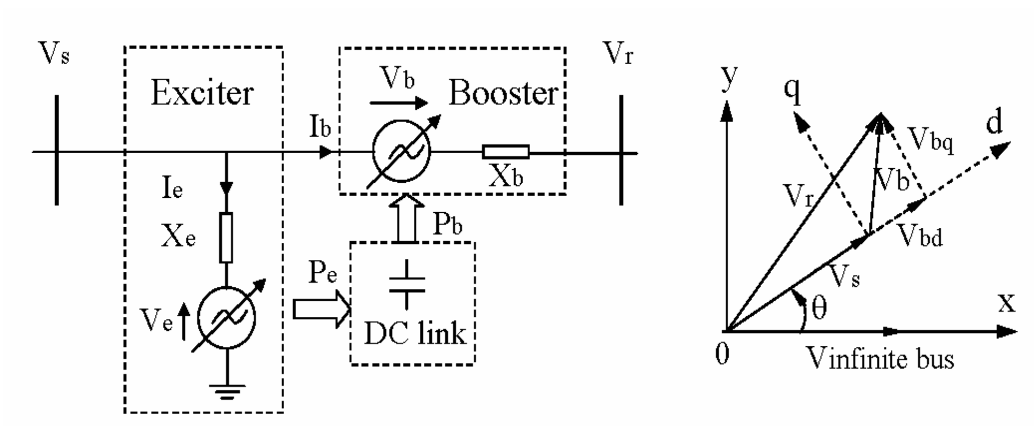


Figure 2.7 Circuit structure and principle variables for the UPFC

Figure 2.7 shows the equivalent representation of the UPFC and the phasor relationships between key variables in the small signal model. The derivation of the various quantities is listed below (the treatment is partly based on the approach suggested by Limyingcharoen [17]):

The dynamics of DC link is modeled as:

$$C_{dc} \cdot V_{dc} \cdot \frac{d}{dt} V_{dc} = S_b \cdot (P_e - P_b) \tag{2.20}$$

Where:

$C_{dc}$: the capacitance of the dc bus capacitor.

$V_{dc}$: the voltage of the dc bus.

$P_e$: the real power drawn into the dc link from the exciter branch of UPFC

$P_b$: the real power flowing out of the dc link into the transmission line through the booster side of UPFC.

The PI Controller that maintains $V_{dc}$ at the reference setting of $V_{dcr}$ is modeled as:

$$U_{ed} = K_{pdc} \cdot (V_{dcr} - V_{dc}) + K_{idc} \cdot \int (V_{dcr} - V_{dc}) \cdot dt \tag{2.21}$$

Where, $U_{ed}$ is the reference of d-axis of the exciter current that is in phase with the voltage $V_s$, and $K_{pdc}$, $K_{idc}$ are PI controller gains.

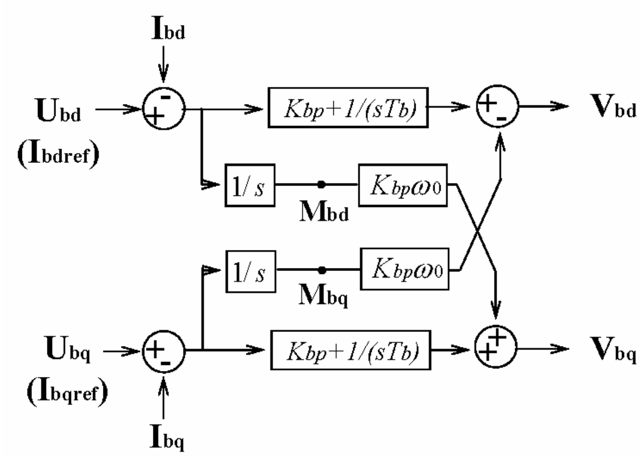


Figure 2.8 The decoupled controller of the UPFC booster branch

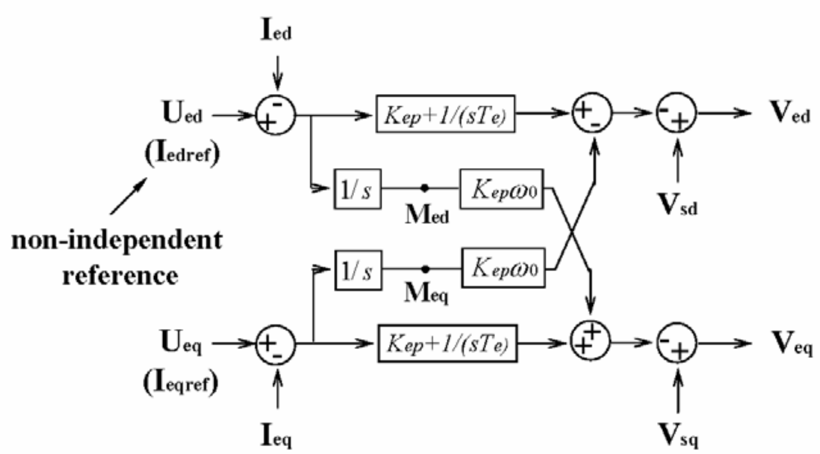


Figure 2.9 The decoupled controller of the UPFC exciter branch

The decoupled controllers of the UPFC are shown in Figure 2.8 (booster branch) and Figure 2.9 (exciter branch) respectively.

They are modeled as:

$$V_{b_d} = K_{bp} \cdot (U_{bd} - I_{b_d}) + \frac{1}{T_b} \cdot M_{bd} - K_{bp} \cdot \omega_0 \cdot M_{bq} \tag{2.22}$$

$$V_{b_q} = K_{bp} \cdot (U_{bq} - I_{b_q}) + \frac{1}{T_b} \cdot M_{bq} + K_{bp} \cdot \omega_0 \cdot M_{bq} \tag{2.23}$$

$$V_{e_d} = V_{s_d} - \left( K_{ep} \cdot (U_{ed} - I_{e_d}) + \frac{1}{T_e} \cdot M_{ed} - K_{ep} \cdot \omega_0 \cdot M_{eq} \right) \tag{2.24}$$

$$V_{e_q} = V_{s_q} - \left( K_{ep} \cdot (U_{eq} - I_{e_q}) + \frac{1}{T_e} \cdot M_{eq} + K_{ep} \cdot \omega_0 \cdot M_{ed} \right) \tag{2.25}$$

Where $M_{bd}$, $M_{bq}$, $M_{ed}$ and $M_{eq}$ are the integrals of the errors of UPFC's current components ($I_{bd}$, $I_{bq}$, $I_{ed}$ and $I_{eq}$) and their references ($U_{bd}$, $U_{bq}$, $U_{ed}$ and $U_{eq}$).

$$\frac{d}{dt} M_{bd} = U_{bd} - I_{b_d} \tag{2.26}$$

$$\frac{d}{dt} M_{bq} = U_{bd} - I_{b_q} \tag{2.27}$$

$$\frac{d}{dt} M_{ed} = U_{ed} - I_{e_d} \tag{2.28}$$

$$\frac{d}{dt} M_{eq} = U_{eq} - I_{e_q} \tag{2.29}$$

Where, $I_{bd}$ and $I_{bq}$ are the in-phase and quadrature component of the booster current; $I_{ed}$ and $I_{eq}$ are the in-phase and quadrature component of the exciter current; $U_{bd}$, $U_{bq}$, $U_{ed}$ and $U_{eq}$ are the reference control settings of $I_{bd}$ , $I_{bq}$, $I_{ed}$ and $I_{eq}$ respectively.

Like the IPFC model, the voltage and current variables in the UPFC equations also need to be expressed with variables in the x-y plane. Thus the V-I relation of the UPFC can be represented by the following equations:

$$V_b = -(V_s - V_r) + Z_b \cdot I_b = -\begin{pmatrix} V_{s_x} - V_{r_x} \\ V_{s_y} - V_{r_y} \end{pmatrix} + \begin{pmatrix} 0 & -X_b \\ X_b & 0 \end{pmatrix} \cdot \begin{pmatrix} I_{b_x} \\ I_{b_y} \end{pmatrix} \tag{2.30}$$

$$V_e = V_s - Z_e \cdot I_e = -\begin{pmatrix} V_{s_x} \\ V_{s_y} \end{pmatrix} - \begin{pmatrix} 0 & -X_e \\ X_e & 0 \end{pmatrix} \cdot \begin{pmatrix} I_{e_x} \\ I_{e_y} \end{pmatrix} \tag{2.31}$$

$$P_b = (V_{b_x} \quad V_{b_y}) \cdot I_b = -(V_{s_x} - V_{r_x}) \cdot I_{b_x} - (V_{s_y} - V_{r_y}) \cdot I_{b_y} \tag{2.32}$$

$$P_e = V_{e_x} \cdot I_{e_x} + V_{e_y} \cdot I_{e_y} = V_{s_x} \cdot I_{e_x} + V_{s_y} \cdot I_{e_y} \tag{2.33}$$

Where:

$V_s = \begin{pmatrix} V_{s_x} \\ V_{s_y} \end{pmatrix}$: the sending end voltage vector.

$V_r = \begin{pmatrix} V_{r_x} \\ V_{r_y} \end{pmatrix}$: the receiving end voltage vector.

$V_b = \begin{pmatrix} V_{b_x} \\ V_{b_y} \end{pmatrix} = T_{up1} \cdot V_{bdq} = T_{up1} \cdot \begin{pmatrix} V_{b_d} \\ V_{b_q} \end{pmatrix}$: the booster voltage vector of the UPFC.

$V_e = \begin{pmatrix} V_{e_x} \\ V_{e_y} \end{pmatrix} = T_{up1} \cdot V_{edq} = T_{up1} \cdot \begin{pmatrix} V_{e_d} \\ V_{e_q} \end{pmatrix}$: the exciter voltage vector of the UPFC.

$V_{b_{dq}} = \begin{pmatrix} V_{b_d} \\ V_{b_q} \end{pmatrix}$: in phase-quadrature (d-q) vector of the booster voltage of the UPFC.

$V_{e_{dq}} = \begin{pmatrix} V_{e_d} \\ V_{e_q} \end{pmatrix}$: in phase-quadrature (d-q) vector of the exciter voltage of the UPFC.

$I_b = \begin{pmatrix} I_{b_x} \\ I_{b_y} \end{pmatrix}$: the line current vector flowing through booster.

$I_e = \begin{pmatrix} I_{e_x} \\ I_{e_y} \end{pmatrix}$: the line current vector flowing through exciter.

$I_{b_{dq}} = \begin{pmatrix} I_{b_d} \\ I_{b_q} \end{pmatrix}$: in phase-quadrature (d-q) vector of the booster current of the UPFC.

$I_{e_{dq}} = \begin{pmatrix} I_{e_d} \\ I_{e_q} \end{pmatrix}$: in phase-quadrature (d-q) vector of the exciter current of the UPFC.

$Z_b = \begin{pmatrix} R_b & -X_b \\ X_b & R_b \end{pmatrix}$: the booster impedance matrix of theUPFC.

$Z_e = \begin{pmatrix} R_e & -X_e \\ X_e & R_e \end{pmatrix}$: the exciter impedance matrix of theUPFC.

$T_{up1} = \begin{pmatrix} cos\theta & -sin\theta \\ sin\theta & cos\theta \end{pmatrix}$: the dq to xy transformation matrix.

Equations (2.20)-(2.33) can be linearized to obtain the set of differential and algebraic equations (2.34)-(2.36). The model has 6 state variables, and three inputs (or references). The detailed derivation of the elements of all coefficient matrices is given in Appendix D.

$$\Delta \dot{X}_{up} = A_{up} \cdot \Delta X_{up} + B_{up} \cdot \Delta U_{up} + E_{up} \cdot \Delta Vs + F_{up} \cdot \Delta Vr \qquad (2.34)$$

$$\Delta I_b = T_{up30} \cdot \Delta X_{up} + T_{up31} \cdot \Delta U_{up} + T_{up32} \cdot \Delta V_s + T_{up33} \cdot \Delta V_r \qquad (2.35)$$

$$\Delta I_e = T_{up34} \cdot \Delta X_{up} + T_{up35} \cdot \Delta U_{up} + T_{up36} \cdot \Delta V_s \qquad (2.36)$$

Where:

$$\Delta X_{up} = \begin{pmatrix} \Delta V_{dc} \\ \Delta M_{dc} \\ \Delta M_{bd} \\ \Delta M_{bq} \\ \Delta M_{ed} \\ \Delta M_{eq} \end{pmatrix} \qquad \Delta U_{up} = \begin{pmatrix} \Delta U_{bd} \\ \Delta U_{bq} \\ \Delta U_{eq} \end{pmatrix}$$

## Summary:

This chapter discussed the operating principle of the IPFC and UPFC devices. The interaction between the d, q control loops was discussed and the method of earlier researchers to eliminate the interaction using decoupled control was presented. Based on a decoupled controller structure, linearized small signal models for the IPFC and UPFC devices were derived. The IPFC small signal model with decoupled control is a contribution of this thesis and is introduced in this chapter. The IPFC and the UPFC models are represented by a sixth order state equation respectively which contains 6 state variables and 3 controller references. These models will be integrated into the linearized network model to form the network small signal model which will be presented in Chapter 3. The full model will be validated by comparison with EMT type simulation in Chapter 4.

# Chapter 3 Development of a Comprehensive Test Platform for Evaluation of FACTS Apparatus

Detailed EMT type programs can be used to validate the results of small signal models. This is best conducted using a suitable test system which should manifest several problems that can be alleviated by FACTS devices. This typically requires a large system. However the detailed EMT type simulation used for validation is practical for a limited size network. As the system size modeled in an EMT type program increases, the computational times can become very long and unfeasible. In this chapter, a test system for FACTS studies is introduced [30]. The details of the system including the transmission problems and eigenvalue information are introduced. Then the small signal models of the system embedded with the UPFC and the IPFC are respectively developed.

## 3.1 Benchmark Platform for Evaluation of FACTS apparatus

The test system (shown in Figure 3.1) has been developed for the IEEE PES WG 15.05.02 as the IEEE FACTS system benchmark. The details of the network are briefly presented below with additional details in the Appendix A.

As a benchmark system for studying the impact of FACTS controllers on improving system performance, it should meet two main requirements. Firstly, it should exhibit poor transmission and stability performance that can be alleviated by FACTS devices, such as transmission congestion, loop flow, inter-area oscillations or over- or under-voltage problems. Secondly, the size of the system should be small enough to be amenable to

EMT-type simulation. Because the EMT-type model is the most detailed, it is also very suitable as the comparison template for validating more approximate models such as small signal models. It is also computationally intensive and time consuming.

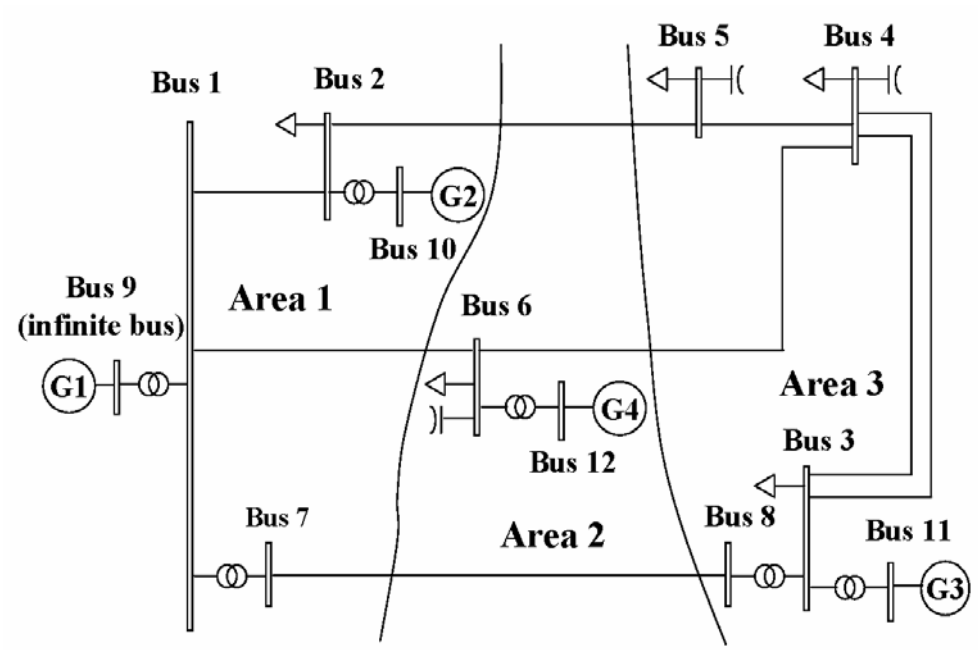


Figure 3.1 Single line diagram of 12 bus system

The proposed test system consists of 12 buses (six 230 kV buses, two 345 kV buses and four 22 kV buses). The test system covers three geographical areas (Area 1, 2, and 3). Area 1 is predominantly a generation area with most of its generation coming from hydro power. Area 2, situated between the main generation area (Area 1) and the main load centre (Area 3), has some hydro generation available, but insufficient to meet local demand. Area 3, situated about 500 km from Area 1, is a load centre with some thermal generation available. Furthermore, as Area 2 generation has limited energy availability, the system demand must often be satisfied through transmission. The transmission system consists of 230 kV transmission lines with the exception of one 345 kV link between areas 1 and 3 (between buses 7 and 8). Areas 2 and 3 have switched shunt capacitors to support the voltage.

Power flow studies (see Table 3.1) reveal that in the event of a loss of generation in area 3, or a loss of the transmission line 4-5, line 1-6 is overloaded while the transmission capacity of the 345 kV transmission line 7-8 is under-utilized. This congestion can be relieved by various FACTS solutions such as TCSCs or SSSCs on line 1-2 or line 7-8; or as in the examples presented here, an IPFC on two of the three lines (line 1-2, 1-6 and 7-8); or a UPFC on line 1-6 or 7-8. Further, the load centre (Area 3) suffers from under-voltage problems, which make this test system suitable for studies on application of SVC or STATCOM.

Table 3-1 Power flow of the system

| | Line 1-6 (limit: 250MVA) | Under-voltage (pu) |
|---|---|---|
| Normal | 210.8 | |
| Line 4-5 tripped | 295.2 | V4=0.943 |
| G3 loss 120 MW | 248.5 | V5=0.922 |
| G4 loss 80 MW | 255.5 | |

Small signal stability studies presented in Chapter 5 show that the platform system has three of the least damped inter-area oscillations (see Table 3.2), and two of them are significantly underdamped (i.e. damping < 5%). It also shows that these poorly damped modes can be improved by FACTS devices at various locations.

Table 3-2 Oscillation modes without FACTS

| Eigenvalues $\lambda = \sigma \pm j\omega$ | Frequency (Hz) | Damping ratio (%) | Dominant generator |
|---|---|---|---|
| -0.058±5.331i | 0.84 | 1.08 | G2 |
| -0.222±7.069i | 1.12 | 3.15 | G3 |
| -0.320±4.728i | 0.75 | 6.76 | G4 |

Another possible application of the platform is to investigate the use of FACTS devices to strengthen the network for the integration of wind generation in Area 2. For example, series FACTS devices on lines 1-6 and/or line 6-4 and/or line 7-8 could make stronger connections from Area 2 (with wind generation) to the other areas.

Thus it can be seen that the proposed platform can be useful for studying FACTS device applications for congestion relief, voltage support, transmission stability and integration of wind generation. It also becomes possible to validate reduced models such as Small Signal Stability models against detailed EMT-type simulation for such FACTS applications. These aspects will be covered in Chapter 4. Data for the benchmark platform are listed in Appendix A.

The procedure for validation is elucidated by connecting a UPFC or an IPFC into the platform and comparing its small signal representation against the detailed EMT-type representation using the technique of Prony Analysis. The Prony analysis is a spectral method which can supply frequency information by extracting all the frequency components from a waveform [45]. The UPFC is installed in line 7-8, of the platform system, its primary purpose being to relieve congestion in line 1-6.

## 3.2 Small Signal Model of the Benchmark System with Embedded IPFC

The small signal model of the system including the IPFC is shown in Figure 3.2. It is divided into two parts: the first part consists of all dynamic components of the network, such as generators, exciters and the IPFC; the second part is the rest of the network which is passive. The IPFC model has been described in Chapter 2. In this section, the generator and exciter model is introduced first, then the passive network is included, and these dynamic components are integrated into the network to form the final system small signal model.

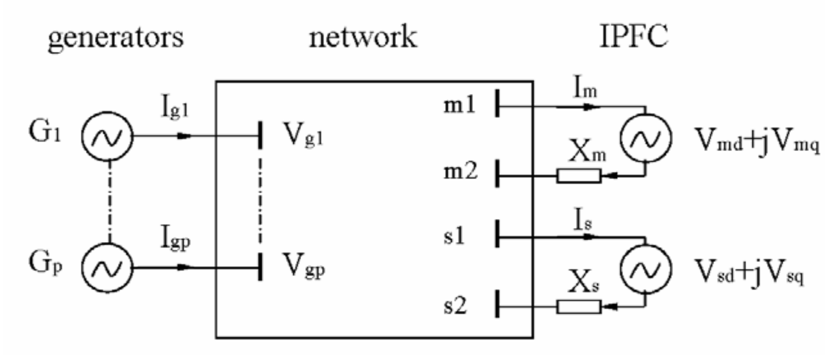


Figure 3.2 The small signal model of the system embedded with the IPFC

## 3.2.1 Generator and Exciter Model

In this system, bus 9 is chosen as the infinite bus, and thus G1 is treated as an ideal voltage source. Three generators (G2, G3 and G4) with their exciters are represented by the typical fourth order dynamic model (third order generator plus first order exciter) [8]. For the k$^{th}$ generator and exciter it has:

$$\dot{\delta}_k = \omega_0(\omega_k - 1) \tag{3.1}$$

$$\dot{\omega}_k = \frac{1}{2H}(Tm_k - E'_{qk}Ig_{kq} - (X_{qk} - X'_{dk})Ig_{kd}Ig_{kq} - KD_k\omega_k) \tag{3.2}$$

$$\dot{E}'_{qk} = \frac{1}{T'_{d0k}}(E_{fdk} - E'_{qk} - (X_{dk} - X'_{dk})Ig_{kd}) \tag{3.3}$$

$$\dot{E}fd_k = -\frac{1}{Ta_k}Efd_k + \frac{Ka_k}{Ta_k}(Vg_{kref} - Vg_k) \tag{3.4}$$

These equations can be linearized and expressed in the compact form for p number of generators as shown in equations (3.5), (3.6). The derivation of this model is found in references [8] [17].

$$\Delta\dot{X}g_k = Ag_k \cdot \Delta Xg_k + Bg_k \cdot \Delta Ug_k + Eg_k \cdot \Delta Vg_k \tag{3.5}$$

$$\Delta Ig_k = Sg_k \cdot \Delta Xg_k - Yg_k \cdot \Delta Vg_k \tag{3.6}$$

Where, k=1….p.

$$\Delta Xg_k = \begin{pmatrix} \Delta\delta_k \\ \Delta\omega_k \\ \Delta E'_{qk} \\ \Delta Efd_k \end{pmatrix} \qquad \Delta Ug_k = \begin{pmatrix} \Delta Tm_k \\ \Delta Vg_{kref} \end{pmatrix} \qquad \Delta Ig_k = \begin{pmatrix} \Delta Ig_{kx} \\ \Delta Ig_{ky} \end{pmatrix} \qquad \Delta Vg_k = \begin{pmatrix} \Delta Vg_{kx} \\ \Delta Vg_{ky} \end{pmatrix}$$

$$Ag_k = \begin{pmatrix} 0 & \omega_0 & 0 & 0 \\ Ag_{k2,1} & \dfrac{-D_k}{2H_k} & \dfrac{-Vg_{kd}}{2H_k \cdot X'_{dk}} & 0 \\ Ag_{k3,1} & 0 & \dfrac{-X_{dk}}{T'_{d0k} \cdot X'_{dk}} & \dfrac{1}{T'_{d0k}} \\ Ag_{k4.1} & 0 & 0 & \dfrac{-1}{Ta_k} \end{pmatrix}$$

$$Bg_k = \begin{pmatrix} 0 & 0 \\ \dfrac{1}{2H_k} & 0 \\ 0 & 0 \\ 0 & \dfrac{Ka_k}{Ta_k} \end{pmatrix} \qquad Eg_k = \begin{pmatrix} 0 & 0 \\ Eg_{k2,1} & Eg_{k2,2} \\ Eg_{k3,1} & Eg_{k3,2} \\ Eg_{k4,1} & Eg_{k4,2} \end{pmatrix} \qquad Sg_k = \begin{pmatrix} Sg_{k1,1} & 0 & \dfrac{sin\delta_k}{X'_{dk}} & 0 \\ Sg_{k2,1} & 0 & \dfrac{-cos\delta_k}{X'_{dk}} & 0 \end{pmatrix}$$

$$Yg_k = \begin{pmatrix} Yga_k & Ygb_k \\ Ygc_k & Ygd_k \end{pmatrix}$$

The detailed derivation of the elements of all coefficient matrices as shown above is given in Appendix B.

### 3.2.2 Network Equation

The transmission lines are represented as Pi-sections, the transformers as leakage impedances, and the loads and shunt capacitors as constant impedances. Hence, the n-bus network can be represented by a 2xn linearized node equation:

$$\begin{pmatrix} YN_{1,1} & YN_{1,2} & \dots & YN_{1,n} \\ YN_{2,1} & YN_{2,2} & \dots & YN_{2,n} \\ \dots & \dots & \dots & \dots \\ YN_{n,1} & YN_{n,2} & \dots & YN_{n,n} \end{pmatrix} \cdot \begin{pmatrix} \Delta V_1 \\ \Delta V_2 \\ \dots \\ \Delta V_n \end{pmatrix} = \begin{pmatrix} \Delta I_1 \\ \Delta I_2 \\ \dots \\ \Delta I_n \end{pmatrix} \tag{3.7}$$

Where the ij$^{th}$ block of admittance matrix is defined as:

$$YN_{i,j} = \begin{pmatrix} GN_{i,j} & -BN_{i,j} \\ BN_{i,j} & GN_{i,j} \end{pmatrix}$$

Note that the small signal model is based on a single line diagram and the number of buses or nodes does consider each phase separately.

### 3.2.3 Small Signal Model of the Network with Generators and Embedded IPFC

The state space representation of the complete power system can be obtained in the format of $\Delta \dot{X} = A \cdot \Delta X + B \cdot \Delta U$ [8] [8], by eliminating *ΔV* and *ΔI* from the differential algebraic equations of the dynamic devices (2.17)~(2.19), (3.5), (3.6), and the network equations (3.7). The derivation procedure is listed below.

The IPFC has two series branches with each introducing one extra bus. Hence the network with the IPFC has 14 buses (the infinite bus is not included). Assuming there are p generators, then the buses of the system are sequenced as follows:

1~p: generator 1 to generator p,

p+1: the sending end bus of the IPFC master branch,

p+2: the receiving end bus of the IPFC master branch,

p+3: the sending end bus of the IPFC slave branch,

p+4: the receiving end bus of the IPFC slave branch, p+5~n: remainder network buses (not including the infinite bus).

The corresponding network node equation (3.7) can be rewritten as:

$$\begin{pmatrix} YN_{g1,1} & \cdots & YN_{g1,p} & YN_{g1,m1} & YN_{g1,m2} & YN_{g1,s1} & YN_{g1,s1} & YN_{g1,s2} & \cdots & YN_{g1,n} \\ \cdots & \cdots & \cdots & \cdots & \cdots & \cdots & \cdots & \cdots & \cdots & \cdots \\ YN_{gp,1} & \cdots & YN_{gp,p} & YN_{gp,m1} & YN_{gp,m2} & YN_{gp,s1} & YN_{gp,s1} & YN_{gp,s2} & \cdots & YN_{gp,n} \\ YN_{m1,1} & \cdots & YN_{m1,p} & YN_{m1,m1} & YN_{m1,m2} & YN_{m1,s1} & YN_{m1,s1} & YN_{m1,s2} & \cdots & YN_{m1,n} \\ YN_{m2,1} & \cdots & YN_{m2,p} & YN_{m2,m1} & YN_{m2,m2} & YN_{m2,s1} & YN_{m2,s1} & YN_{m2,s2} & \cdots & YN_{m2,n} \\ YN_{s1,1} & \cdots & YN_{s1,p} & YN_{s1,m1} & YN_{s1,m2} & YN_{s1,s1} & YN_{s1,s1} & YN_{s1,s2} & \cdots & YN_{s1,n} \\ YN_{s2,1} & \cdots & YN_{s2,p} & YN_{s2,m1} & YN_{s2,m2} & YN_{s2,s1} & YN_{s2,s1} & YN_{s2,s2} & \cdots & YN_{s2,n} \\ YN_{i,1} & \cdots & YN_{i,p} & YN_{i,m1} & YN_{i,m2} & YN_{i,s1} & YN_{i,s1} & YN_{i,s2} & \cdots & YN_{i,n} \\ \cdots & \cdots & \cdots & \cdots & \cdots & \cdots & \cdots & \cdots & \cdots & \cdots \\ YN_{n,1} & \cdots & YN_{n,p} & YN_{n,m1} & YN_{n,m2} & YN_{n,s1} & YN_{n,s1} & YN_{n,s2} & \cdots & YN_{n,n} \end{pmatrix} \cdot \begin{pmatrix} \Delta V_{g_1} \\ \cdots \\ \Delta V_{g_p} \\ \Delta V_{m1} \\ \Delta V_{m2} \\ \Delta V_{s1} \\ \Delta V_{s2} \\ \Delta V_i \\ \cdots \\ \Delta V_n \end{pmatrix}$$

$$= \begin{pmatrix} \Delta IN_{g_1} \\ \cdots \\ \Delta IN_{g_p} \\ \Delta IN_{m1} \\ \Delta IN_{m2} \\ \Delta IN_{s1} \\ \Delta IN_{s2} \\ \Delta IN_i \\ \cdots \\ \Delta IN_n \end{pmatrix} = \begin{pmatrix} \Delta I_{g_1} \\ \cdots \\ \Delta I_{g_p} \\ -\Delta I_m \\ \Delta I_m \\ -\Delta I_s \\ \Delta I_s \\ \Delta IN_i \\ \cdots \\ \Delta IN_n \end{pmatrix}$$

Substituting $\Delta I_{gk}$ of (3.6) into (3.7), the k[th] generator bus node equation is expressed as:

$$S_{g_k} \cdot \Delta X_{g_k} = \sum_{j=1, j\neq k}^{n} YN_{gk,j} \cdot \Delta Vj + (YN_{gk,k} + Y_{g_k}) \cdot \Delta V_{g_k} \tag{3.8}$$

Substituting $\Delta I_m$ , $\Delta I_s$ of (2.18), (2.19) into (3.7), the node equations of the IPFC sending and receiving end bus are expressed as:

$$\begin{aligned} & -T_{ip39} \cdot \Delta X_{ip} - T_{ip40} \cdot \Delta U_{ip} \\ & = \sum_{j=1, j\neq m1,m2}^{n} YN_{m1,j} \cdot \Delta Vj + (YN_{m1,m1} + T_{ip41}) \cdot \Delta V_{m1} + (YN_{m1,m2} + T_{ip42}) \cdot \Delta V_{m2} \end{aligned} \tag{3.9}$$

$$T_{ip39}\cdot\Delta X_{ip}+T_{ip40}\cdot\Delta U_{ip}$$
$$=\sum_{j=1,j\neq m1,m2}^{n} YN_{m2,j}\cdot\Delta Vj+(YN_{m2,m1}-T_{ip41})\cdot\Delta V_{m1}+(YN_{m2,m2}-T_{ip42})\cdot\Delta V_{m2} \tag{3.10}$$

$$-T_{ip43}\cdot\Delta X_{ip}-T_{ip44}\cdot\Delta U_{ip}$$
$$=\sum_{j=1,j\neq s1,s2}^{n} YN_{s1,j}\cdot\Delta V_j+(YN_{s1,s1}+T_{ip45})\cdot\Delta V_{s1}+(YN_{s1,s2}+T_{ip46})\cdot\Delta V_{s2} \tag{3.11}$$

$$T_{ip43}\cdot\Delta X_{ip}+T_{ip44}\cdot\Delta U_{ip}$$
$$=\sum_{j=1,j\neq s1,s2}^{n} YN_{s2,j}\cdot\Delta V_j+(YN_{s2,s1}-T_{ip45})\cdot\Delta V_{s1}+(YN_{s2,s2}-T_{ip46})\cdot\Delta V_{s2} \tag{3.12}$$

For other buses which are not connected to dynamic devices:

$$0=\sum_{j=1}^{n} YN_{i,j}\cdot\Delta V_j \tag{3.13}$$

The above equations (3.8)-(3.13) form a new network equation in which the current components of dynamic devices are eliminated by replacing them with linear combinations of states and reference inputs:

$$\begin{pmatrix} YM_{g,g} & YM_{g,m1} & YM_{g,m2} & YM_{g,s1} & YM_{g,s2} & YM_{g,j} \\ YM_{m1,g} & YM_{m1,m1} & YM_{m1,m2} & YM_{m1,s1} & YM_{m1,s2} & YM_{m1,j} \\ YM_{m2,g} & YM_{m2,m1} & YM_{m2,m2} & YM_{m2,s1} & YM_{m2,s2} & YM_{m2,j} \\ YM_{s1,g} & YM_{s1,m1} & YM_{s1,m2} & YM_{s1,s1} & YM_{s1,s2} & YM_{s1,j} \\ YM_{s2,g} & YM_{s2,m1} & YM_{s2,m2} & YM_{s2,s1} & YM_{s2,s2} & YM_{s2,j} \\ YM_{i,g} & YM_{i,m1} & YM_{i,m2} & YM_{i,s1} & YM_{i,s2} & YM_{i,j} \end{pmatrix}\cdot\begin{pmatrix}\Delta V_g \\ \Delta V_{m1} \\ \Delta V_{m2} \\ \Delta V_{s1} \\ \Delta V_{s2} \\ \Delta V_j\end{pmatrix}$$
$$=\begin{pmatrix} S_g\cdot\Delta X_g \\ -T_{ip39}\cdot\Delta X_{ip}-T_{ip40}\cdot\Delta U_{ip} \\ T_{ip39}\cdot\Delta X_{ip}+T_{ip40}\cdot\Delta U_{ip} \\ -T_{ip43}\cdot\Delta X_{ip}-T_{ip44}\cdot\Delta U_{ip} \\ T_{ip43}\cdot\Delta X_{ip}+T_{ip44}\cdot\Delta U_{ip} \\ 0 \end{pmatrix} \tag{3.14}$$

Where:

$$S_g = \begin{pmatrix} S_{g_1} & \cdots & 0 \\ \vdots & S_{g_k} & \vdots \\ 0 & \cdots & S_{g_p} \end{pmatrix} \qquad \Delta X_g = \begin{pmatrix} \Delta X_{g_1} \\ \ldots \\ \Delta X_{g_p} \end{pmatrix}$$

$$YM_{g,g} = \begin{pmatrix} YN_{gk,1} + Y_{g_1} & \ldots & YN_{g1,p} \\ \ldots & \ldots & \ldots \\ YN_{gp,1} & \ldots & YN_{gp,p} + Y_{g_{p,p}} \end{pmatrix} \qquad YM_{g,m1} = \begin{pmatrix} YN_{g1,m1} \\ \ldots \\ YN_{gp,m1} \end{pmatrix}$$

$$YM_{g,m2} = \begin{pmatrix} YN_{g1,m2} \\ \ldots \\ YN_{gp,m2} \end{pmatrix} \qquad YM_{g,s1} = \begin{pmatrix} YN_{g1,s1} \\ \ldots \\ YN_{gp,s1} \end{pmatrix} \qquad YM_{g,s2} = \begin{pmatrix} YN_{g1,s2} \\ \ldots \\ YN_{gp,s2} \end{pmatrix}$$

$$YM_{g,j} = \begin{pmatrix} YN_{g1,j} & \ldots & YN_{g1,n} \\ \ldots & \ldots & \ldots \\ YN_{gp,j} & \ldots & YN_{gp,n} \end{pmatrix}$$

$$YM_{i,g} = \begin{pmatrix} YN_{i,j} & \ldots & YN_{i,p} \\ \ldots & \ldots & \ldots \\ YN_{n,1} & \ldots & YN_{n,p} \end{pmatrix} \qquad YM_{i,m1} = \begin{pmatrix} YN_{i,m1} \\ \ldots \\ YN_{n,m1} \end{pmatrix} \qquad YM_{i,m2} = \begin{pmatrix} YN_{i,m2} \\ \ldots \\ YN_{n,m2} \end{pmatrix}$$

$$YM_{i,s1} = \begin{pmatrix} YN_{i,s1} \\ \ldots \\ YN_{n,s1} \end{pmatrix} \qquad YM_{i,s2} = \begin{pmatrix} YN_{i,s2} \\ \ldots \\ YN_{n,s2} \end{pmatrix} \qquad YM_{i,j} = \begin{pmatrix} YN_{i,j} & \ldots & YN_{i,i} \\ \ldots & \ldots & \ldots \\ YN_{n,j} & \ldots & YN_{n,n} \end{pmatrix}$$

$$YM_{m1,g} = \begin{pmatrix} YN_{m1,1} & \ldots & YN_{m1,p} \end{pmatrix} \qquad YM_{m1,m1} = YN_{m1,m1} + T_{ip41} \qquad YM_{m1,m2} = YN_{m1,m2} + T_{ip42}$$

$$YM_{m1,s1} = YN_{m1,s1} \qquad YM_{m1,s2} = YN_{m1,s2} \qquad YM_{m1,j} = \begin{pmatrix} YN_{m1,j} & \ldots & YN_{m1,n} \end{pmatrix}$$

$$YM_{m2,g} = \begin{pmatrix} YN_{m2,1} & \ldots & YN_{m2,p} \end{pmatrix} \qquad YM_{m2,m1} = YN_{m2,m1} - T_{ip41} \qquad YM_{m2,m2} = YN_{m2,m2} - T_{ip42}$$

$$YM_{m2,s1} = YN_{m2,s1} \qquad YM_{m2,s2} = YN_{m2,s2} \qquad YM_{m2,j} = \begin{pmatrix} YN_{m2,j} & \ldots & YN_{m2,n} \end{pmatrix}$$

$$YM_{s1,g} = \begin{pmatrix} YN_{s1,1} & \ldots & YN_{s1,p} \end{pmatrix} \qquad YM_{s1,m1} = YN_{s1,m1} \qquad YM_{s1,m2} = YN_{s1,m2}$$

$$YM_{s1,s1} = YN_{s1,s1} + Tip45 \qquad YM_{s1,s2} = YN_{s1,s2} + Tip46 \qquad YM_{s1,j} = \begin{pmatrix} YN_{s1,j} & \dots & YN_{s1,n} \end{pmatrix}$$

$$YM_{s2,g} = \begin{pmatrix} YN_{s2,1} & \dots & YN_{s2,p} \end{pmatrix} \qquad YM_{s2,m1} = YN_{s2,m1} \qquad YM_{s2,m2} = YN_{s2,m2}$$

$$YM_{s2,s1} = YN_{s2,s1} - Tip45 \qquad YM_{s2,s2} = YN_{s2,s2} - Tip46 \qquad YM_{s2,j} = \begin{pmatrix} YN_{s2,j} & \dots & YN_{s2,n} \end{pmatrix}$$

Equation (3.14) can be rewritten as:

$$\begin{pmatrix} \Delta Vg \\ \Delta Vm1 \\ \Delta Vm2 \\ \Delta Vs1 \\ \Delta Vs2 \\ \Delta V_j \end{pmatrix} = ZM \cdot \begin{pmatrix} Sg \cdot \Delta Xg \\ -Tip39 \cdot \Delta Xip - Tip40 \cdot \Delta Uip \\ Tip39 \cdot \Delta Xip + Tip40 \cdot \Delta Uip \\ -Tip43 \cdot \Delta Xip - Tip44 \cdot \Delta Uip \\ Tip43 \cdot \Delta Xip + Tip44 \cdot \Delta Uip \\ 0 \end{pmatrix} \tag{3.15}$$

Where:

$$ZM = YM^{-1} = \begin{pmatrix} ZM_{g,g} & ZM_{g,m1} & ZM_{g,m2} & ZM_{g,s1} & ZM_{g,s2} & ZM_{g,j} \\ ZM_{m1,g} & ZM_{m1,m1} & ZM_{m1,m2} & ZM_{m1,s1} & ZM_{m1,s2} & ZM_{m1,j} \\ ZM_{m2,g} & ZM_{m2,m1} & ZM_{m2,m2} & ZM_{m2,s1} & ZM_{m2,s2} & ZM_{m2,j} \\ ZM_{s1,g} & ZM_{s1,m1} & ZM_{s1,m2} & ZM_{s1,s1} & ZM_{s1,s2} & ZM_{s1,j} \\ ZM_{s2,g} & ZM_{s2,m1} & ZM_{s2,m2} & ZM_{s2,s1} & ZM_{s2,s2} & ZM_{s2,j} \\ ZM_{i,g} & ZM_{i,m1} & ZM_{i,m2} & ZM_{i,s1} & ZM_{i,s2} & ZM_{i,j} \end{pmatrix}$$

Equation (3.14) can be split into following five equations:

$$\begin{aligned} \Delta Vg_k = & \sum_{j=1}^{p} ZM_{gk,gj} \cdot Sg_j \cdot \Delta Xg_j \\ & -((ZM_{gk,m1} - ZM_{gk,m2}) \cdot Tip39 + (ZM_{gk,m1} - ZM_{gk,m2}) \cdot Tip43) \cdot \Delta Xip \\ & -((ZM_{gk,m1} - ZM_{gk,m2}) \cdot Tip40 + (ZM_{gk,s1} - ZM_{gk,s2}) \cdot Tip44) \cdot \Delta Uip \end{aligned} \tag{3.16}$$

$$\begin{aligned} \Delta Vm1 = & \sum_{j=1}^{p} ZM_{m1,gj} \cdot Sg_j \cdot \Delta Xg_j \\ & -((ZM_{m1,m1} - ZM_{m1,m2}) \cdot Tip39 + (ZM_{m1,s1} - ZM_{m1,s2}) \cdot Tip43) \cdot \Delta Xip \\ & -((ZM_{m1,m1} - ZM_{m1,m2}) \cdot Tip40 + (ZM_{m1,s1} - ZM_{m1,s2}) \cdot Tip44) \cdot \Delta Uip \end{aligned} \tag{3.17}$$

$$\Delta V_{m2} = \sum_{j=1}^{p} ZM_{m2,gj} \cdot Sg_j \cdot \Delta Xg_j$$
$$- ((ZM_{m2,m1} - ZM_{m2,m2}) \cdot T_{ip39} + (ZM_{m2,s1} - ZM_{m2,s2}) \cdot T_{ip43}) \cdot \Delta X_{ip} \quad (3.18)$$
$$- ((ZM_{m2,m1} - ZM_{m2,m2}) \cdot T_{ip40} + (ZM_{m2,s1} - ZM_{m2,s2}) \cdot T_{ip44}) \cdot \Delta U_{ip}$$

$$\Delta V_{s1} = \sum_{j=1}^{p} ZM_{s1,gj} \cdot Sg_j \cdot \Delta Xg_j$$
$$- ((ZM_{s1,m1} - ZM_{s1,m2}) \cdot T_{ip39} + (ZM_{s1,s1} - ZM_{s1,s2}) \cdot T_{ip43}) \cdot \Delta X_{ip} \quad (3.19)$$
$$- ((ZM_{s1,m1} - ZM_{s1,m2}) \cdot T_{ip40} + (ZM_{s1,s1} - ZM_{s1,s2}) \cdot T_{ip44}) \cdot \Delta U_{ip}$$

$$\Delta V_{s2} = \sum_{j=1}^{p} ZM_{s2,gj} \cdot Sg_j \cdot \Delta Xg_j$$
$$- ((ZM_{s2,m1} - ZM_{s2,m2}) \cdot T_{ip39} + (ZM_{s2,s1} - ZM_{s2,s2}) \cdot T_{ip43}) \cdot \Delta X_{ip} \quad (3.20)$$
$$- ((ZM_{s2,m1} - ZM_{s2,m2}) \cdot T_{ip40} + (ZM_{s2,s1} - ZM_{s2,s2}) \cdot T_{ip44}) \cdot \Delta U_{ip}$$

Substituting equation (3.16) into (3.5); and (3.17) ~ (3.20) into (2.17) gives the linearized state equations of the system:

$$\Delta \dot{X}g_k = \sum_{j=1}^{p} AGG_{k,j} \cdot \Delta Xg_j + AGI_k \cdot \Delta X_{ip} + \sum_{j=1}^{p} BGG_{k,j} \cdot \Delta Ug_j + BGI_k \cdot \Delta U_{ip} \quad (3.21)$$

$$\Delta \dot{X}_{ip} = \sum_{j=1}^{p} AIG_j \cdot \Delta Xg_j + A_{II} \cdot \Delta X_{ip} + B_{II} \cdot \Delta U_{ip} \quad (3.22)$$

Where:

$$AGG_{k,j} = Eg_k \cdot ZM_{gk,gj} \cdot Sg_j \qquad (\mathrm{j} \neq k)$$

$$AGG_{k,k} = -Eg_k \cdot ZM_{gk,gk} \cdot Sg_k + Ag_k$$

$$AGI_k = -Eg_k \cdot ((ZM_{gk,m1} - ZM_{gk,m2}) \cdot T_{ip39} + (ZM_{gk,s1} - ZM_{gk,s2}) \cdot T_{ip43})$$

$$BGG_k = Bg_k$$

$$BGG_j = 0 \qquad (\mathrm{j} \neq \mathrm{k})$$

$$BGI_k = -Eg_k \cdot ((ZM_{gk,m1} - ZM_{gk,m2}) \cdot T_{ip40} + (ZM_{gk,s1} - ZM_{gk,s2}) \cdot T_{ip44})$$

$$AIG_j = (E_{ip} \cdot ZM_{m1,gj} + F_{ip} \cdot ZM_{m2,gj} + G_{ip} \cdot ZM_{s1,gj} + H_{ip} \cdot ZM_{s2,gj}) \cdot Sg_j \qquad (\mathrm{j=1,...,p})$$

$$\begin{aligned} A_{II} = A_{ip} - E_{ip} \cdot ((ZM_{m1,m1} - ZM_{m1,m2}) \cdot T_{ip39} + (ZM_{m1,s1} - ZM_{m1,s2}) \cdot T_{ip43}) \\ - F_{ip} \cdot ((ZM_{m2,m1} - ZM_{m2,m2}) \cdot T_{ip39} + (ZM_{m2,s1} - ZM_{m2,s2}) \cdot T_{ip43}) \\ - G_{ip} \cdot ((ZM_{s1,m1} - ZM_{s1,m2}) \cdot T_{ip39} + (ZM_{s1,s1} - ZM_{s1,s2}) \cdot T_{ip43}) \\ - H_{ip} \cdot ((ZM_{s2,m1} - ZM_{s2,m2}) \cdot T_{ip39} + (ZM_{s2,s1} - ZM_{s2,s2}) \cdot T_{ip43}) \end{aligned}$$

$$\begin{aligned} B_{II} = B_{ip} - E_{ip} \cdot ((ZM_{m1,m1} - ZM_{m1,m2}) \cdot T_{ip40} + (ZM_{m1,s1} - ZM_{m1,s2}) \cdot T_{ip44}) \\ - F_{ip} \cdot ((ZM_{m2,m1} - ZM_{m2,m2}) \cdot T_{ip40} + (ZM_{m2,s1} - ZM_{m2,s2}) \cdot T_{ip44}) \\ - G_{ip} \cdot ((ZM_{s1,m1} - ZM_{s1,m2}) \cdot T_{ip40} + (ZM_{s1,s1} - ZM_{s1,s2}) \cdot T_{ip44}) \\ - H_{ip} \cdot ((ZM_{s2,m1} - ZM_{s2,m2}) \cdot T_{ip40} + (ZM_{s2,s1} - ZM_{s2,s2}) \cdot T_{ip44}) \end{aligned}$$

Equations (3.21) and (3.22) can be written in matrix form to give the linearized state equation:

$$\begin{pmatrix} \Delta \dot{X}_g \\ \Delta \dot{X}_{ip} \end{pmatrix} = \begin{pmatrix} A_{GG} & A_{GI} \\ A_{IG} & A_{II} \end{pmatrix} \cdot \begin{pmatrix} \Delta X_g \\ \Delta X_{ip} \end{pmatrix} + \begin{pmatrix} B_{GG} & B_{GI} \\ B_{IG} & B_{II} \end{pmatrix} \begin{pmatrix} \Delta U_G \\ \Delta U_{ip} \end{pmatrix} \tag{3.23}$$

Or: $\Delta \dot{X} = A \cdot \Delta X + B \cdot \Delta U$

Where:

$$A_{GG} = \begin{pmatrix} A_{GG_{1,1}} & \dots & A_{GG_{1,p}} \\ \dots & \dots & \dots \\ A_{GG_{p,1}} & \dots & A_{GG_{p,p}} \end{pmatrix} \qquad A_{GI} = \begin{pmatrix} A_{IG_1} \\ \dots \\ A_{IG_p} \end{pmatrix} \qquad A_{IG} = \begin{pmatrix} A_{IG_1} & \dots & A_{IG_p} \end{pmatrix}$$

$$B_{GG} = \begin{pmatrix} B_{GG_{1,1}} & \dots & 0 \\ \dots & \dots & \dots \\ 0 & \dots & B_{GG_{p,p}} \end{pmatrix} \qquad B_{GI} = \begin{pmatrix} B_{GI_1} \\ \dots \\ B_{GI_p} \end{pmatrix} \qquad B_{IG} = \begin{pmatrix} B_{IG_1} & \dots & B_{IG_p} \end{pmatrix}$$

$\Delta \dot{X} = \begin{pmatrix} \Delta \dot{X}_{g1} \\ \dots \\ \Delta \dot{X}_{gp} \\ \Delta \dot{X}_{ip} \end{pmatrix}$: 1x18 matrix (3 generator and exciters, 4 states from each generator and exciter unit; 6 states from the IPFC);

$$\Delta U = \begin{pmatrix} \Delta U_{g1} \\ \dots \\ \Delta U_{gp} \\ \Delta U_{ip} \end{pmatrix}$$: 1x9 matrix (2 inputs from each generator and exciter, 3 inputs from the IPFC).

In this thesis, the impact of the generator on the network is not the main concern, thus the generator governor and exciter input vector $\Delta U_g$ is set to zero. Then equation (3.23) can be written as:

$$\begin{pmatrix} \Delta \dot{X}_g \\ \Delta \dot{X}_{ip} \end{pmatrix} = \begin{pmatrix} A_{GG} & A_{GI} \\ A_{IG} & A_{II} \end{pmatrix} \cdot \begin{pmatrix} \Delta X_g \\ \Delta X_{ip} \end{pmatrix} + \begin{pmatrix} B_{GI} \\ B_{II} \end{pmatrix} \Delta U_{ip}$$

Using equations (3.6) and (3.16) output equations of the k$^{th}$ generator can be derived as (details see Appendix C):

$$\Delta P_{g_k} = CPG_{g_k} \cdot \Delta X_g + CPG_{ip_k} \cdot \Delta X_{ip} + DPG_k \cdot \Delta U_{ip}$$

$$\Delta Q_{g_k} = CQG_{g_k} \cdot \Delta X_g + CQG_{ip_k} \cdot \Delta X_{ip} + DQG_k \cdot \Delta U_{ip}$$

Similarly the output equations of the master branch and slave branch of the IPFC can be derived by equations (2.18), (2.19), (3.17) and (3.19) as:

$$\Delta P_m = V_{m1}^T \cdot \Delta I_m + I_m^T \cdot \Delta V_{m1} = CPM_g \cdot \Delta X_g + CPM_{ip} \cdot \Delta X_{ip} + DPM \cdot \Delta U_{ip}$$

$$\begin{aligned} \Delta Q_m &= (V_{m1_y} \quad -V_{m1_x}) \cdot \Delta I_m + (-I_{m_y} \quad I_{m_x}) \cdot \Delta V_{m1} \\ &= CQM_g \cdot \Delta X_g + CQM_{ip} \cdot \Delta X_{ip} + DQM \cdot \Delta U_{ip} \end{aligned}$$

$$\Delta P_s = CPS_g \cdot \Delta X_g + CPS_{ip} \cdot \Delta X_{ip} + DPS \cdot \Delta U_{ip}$$

$$\Delta Q_s = CQS_g \cdot \Delta X_g + CQS_{ip} \cdot \Delta X_{ip} + DQS \cdot \Delta U_{ip}$$

## 3.3 Small Signal Model of the System with Embedded UPFC

The derivation of the small signal model of system embedded with the UPFC is similar to that of the IPFC.

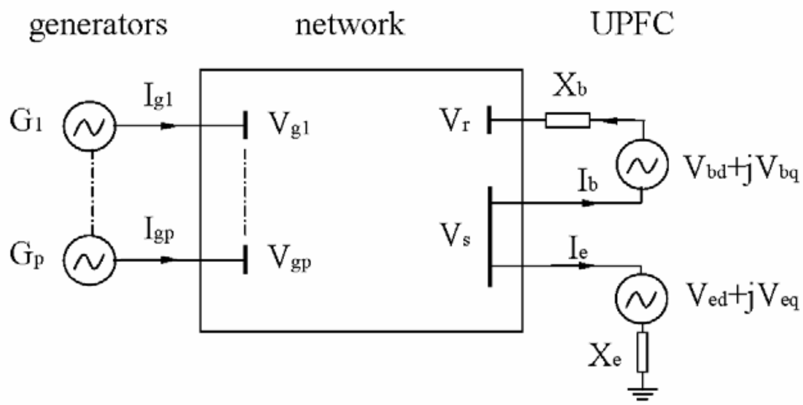


Figure 3.3 The small signal model of the system embedded with the UPFC

The small signal model of the system embedded the UPFC is shown in Figure 3.3. The UPFC model has been described in Chapter 2, and the generator and network equation are described in section 3.2.1 and 3.2.2 respectively. Described here is only how to incorporate these equations into the network to obtain the linearized state equation of the network.

The UPFC has one series branch which introduces one extra bus. Hence the network with the UPFC has 13 buses (the infinite bus is not included). The buses of the system are sequenced as follows:

1~p: generator 1 to generator p,

p+1: the sending end bus of the UPFC,

p+2: the receiving end bus of the UPFC,

p+3~n: remainder network buses (not including the infinite bus).

Thus equation (3.7) can be rewritten as:

$$\begin{pmatrix} YN_{g1,1} & \dots & YN_{g1,p} & YN_{g1,s} & YN_{g1,r} & YN_{g1,i} & \dots & YN_{g1,n} \\ \dots & \dots & \dots & \dots & \dots & \dots & \dots & \dots \\ YN_{gp,1} & \dots & YN_{gp,p} & YN_{gp,s} & YN_{gp,r} & YN_{gp,i} & \dots & YN_{gp,n} \\ YN_{s,1} & \dots & YN_{s,p} & YN_{s,s} & YN_{s,r} & YN_{s,i} & \dots & YN_{s,n} \\ YN_{r,1} & \dots & YN_{r,p} & YN_{r,s} & YN_{r,r} & YN_{r,i} & \dots & YN_{r,n} \\ YN_{i,1} & \dots & YN_{i,p} & YN_{i,s} & YN_{i,r} & YN_{i,i} & \dots & YN_{i,n} \\ \dots & \dots & \dots & \dots & \dots & \dots & \dots & \dots \\ YN_{n,1} & \dots & YN_{n,p} & YN_{n,s} & YN_{n,r} & YN_{n,i} & \dots & YN_{n,n} \end{pmatrix} \cdot \begin{pmatrix} \Delta V_{g_1} \\ \dots \\ \Delta V_{g_p} \\ \Delta V_s \\ \Delta V_r \\ \Delta V_i \\ \dots \\ \Delta V_n \end{pmatrix} = \begin{pmatrix} \Delta I_{g_1} \\ \dots \\ \Delta I_{g_p} \\ -\Delta I_b - \Delta I_e \\ \Delta I_b \\ \Delta IN_i \\ \dots \\ \Delta IN_n \end{pmatrix} \quad (3.7)$$

Substituting $\Delta I_b$ , $\Delta I_e$ of (2.35), (2.36) into (3.7) the node equations of the UPFC sending and receiving end bus are expressed as:

$$\begin{aligned} &-(T_{up30} + T_{up34}) \cdot \Delta X_{up} - (T_{up31} + T_{up35}) \cdot \Delta U_{up} \\ &= \sum_{j=1, j\neq s,r}^{n} YN_{s,j} \cdot \Delta Vj + (YN_{s,s} + T_{up32} + T_{up36}) \cdot \Delta V_{g_s} + (YN_{s,r} + T_{up33}) \cdot \Delta V_r \end{aligned} \quad (3.24)$$

$$\begin{aligned} &T_{up30} \cdot \Delta X_{up} + T_{up31} \cdot \Delta U_{up} \\ &= \sum_{j=1, j\neq s,r}^{n} YN_{r,j} \cdot \Delta V_j + (YN_{r,s} - T_{up32}) \cdot \Delta V_s + (YN_{r,r} - T_{up33}) \cdot \Delta V_r \end{aligned} \quad (3.25)$$

Equations (3.24), (3.25) together with (3.8) and (3.13) form a new network equation in which the current components of dynamic devices are replaced with state variables and reference inputs:

$$\begin{pmatrix} YM_{g,g} & YM_{g,s} & YM_{g,r} & YM_{g,j} \\ YM_{s,g} & YM_{s,s} & YM_{s,r} & YM_{s,j} \\ YM_{r,g} & YM_{r,s} & YM_{r,r} & YM_{r,j} \\ YM_{i,g} & YM_{i,s} & YM_{i,r} & YM_{i,j} \end{pmatrix} \cdot \begin{pmatrix} \Delta V_g \\ \Delta V_s \\ \Delta V_r \\ \Delta V_j \end{pmatrix} = \begin{pmatrix} S_g \cdot \Delta X_g \\ -(T30 + T34) \cdot \Delta X_{up} - (T31 + T35) \cdot \Delta U_{up} \\ T30 \cdot \Delta X_{up} + T31 \cdot \Delta U_{up} \\ 0 \end{pmatrix} \quad (3.26)$$

Where:

$$S_g = \begin{pmatrix} S_{g_1} & \cdots & 0 \\ \vdots & S_{g_k} & \vdots \\ 0 & \cdots & S_{g_p} \end{pmatrix} \qquad \Delta X_g = \begin{pmatrix} \Delta X_{g_1} \\ \dots \\ \Delta X_{g_p} \end{pmatrix}$$

$$YM_{g,g} = \begin{pmatrix} YN_{gk,1} + Yg_1 & \dots & YN_{g1,p} \\ \dots & \dots & \dots \\ YN_{gp,1} & \dots & YN_{gp,p} + Yg_{p,p} \end{pmatrix} \qquad YM_{g,s} = \begin{pmatrix} YN_{g1,s} \\ \dots \\ YN_{gp,s} \end{pmatrix} \qquad YM_{g,r} = \begin{pmatrix} YN_{g1,r} \\ \dots \\ YN_{gp,r} \end{pmatrix}$$

$$YM_{g,j} = \begin{pmatrix} YN_{g1,j} & \dots & YN_{g1,n} \\ \dots & \dots & \dots \\ YN_{gp,j} & \dots & YN_{gp,n} \end{pmatrix}$$

$$YM_{i,g} = \begin{pmatrix} YN_{i,j} & \dots & YN_{i,p} \\ \dots & \dots & \dots \\ YN_{n,1} & \dots & YN_{n,p} \end{pmatrix} \qquad YM_{i,s} = \begin{pmatrix} YN_{i,s} \\ \dots \\ YN_{n,s} \end{pmatrix} \qquad YM_{i,r} = \begin{pmatrix} YN_{i,r} \\ \dots \\ YN_{n,r} \end{pmatrix}$$

$$YM_{i,j} = \begin{pmatrix} YN_{i,j} & \dots & YN_{i,i} \\ \dots & \dots & \dots \\ YN_{n,j} & \dots & YN_{n,n} \end{pmatrix}$$

$$YM_{s,g} = \begin{pmatrix} YN_{s,1} & \dots & YN_{s,p} \end{pmatrix} \qquad YM_{s,s} = YN_{s,s} + Tup32 + Tup36 \qquad YM_{s,r} = YN_{s,r} + Tup33$$

$$YM_{s,j} = \begin{pmatrix} YN_{s,j} & \dots & YN_{s,n} \end{pmatrix}$$

$$YM_{r,g} = \begin{pmatrix} YN_{r,1} & \dots & YN_{r,p} \end{pmatrix} \qquad YM_{r,s} = YN_{r,s} - Tup32 \qquad YM_{r,r} = YN_{r,r} - Tup33$$

$$YM_{r,j} = \begin{pmatrix} YN_{r,j} & \dots & YN_{r,n} \end{pmatrix}$$

Equation (3.26) can be rewritten as:

$$\begin{pmatrix} \Delta V_g \\ \Delta V_s \\ \Delta V_r \\ \Delta V_j \end{pmatrix} = ZM \cdot \begin{pmatrix} S_g \cdot \Delta X_g \\ -(T30 + T34) \cdot \Delta X_{up} - (T31 + T35) \cdot \Delta U_{up} \\ T30 \cdot \Delta X_{up} + T31 \cdot \Delta U_{up} \\ 0 \end{pmatrix} \tag{3.27}$$

Where:

$$ZM = YM^{-1} = \begin{pmatrix} ZM_{g,g} & ZM_{g,s} & ZM_{g,r} & ZM_{g,j} \\ ZM_{s,g} & ZM_{s,s} & ZM_{s,r} & ZM_{s,j} \\ ZM_{r,g} & ZM_{r,s} & ZM_{r,r} & ZM_{r,j} \\ ZM_{i,g} & ZM_{i,s} & ZM_{i,r} & ZM_{i,j} \end{pmatrix}$$

Equation (3.27) can be split into following three equations:

$$\begin{aligned} \Delta Vg_k = &\sum_{j=1}^{p} ZM_{gk,gj} \cdot Sg_j \cdot \Delta Xg_j - ((ZM_{gk,s} - ZM_{gk,r}) \cdot Tup30 + ZM_{gk,s} \cdot Tup34) \cdot \Delta Xup \\ &- ((ZM_{gk,s} - ZM_{gk,r}) \cdot Tup31 + ZM_{gk,s} \cdot Tup35) \cdot \Delta Uup \end{aligned} \tag{3.28}$$

$$\begin{aligned} \Delta Vs = &\sum_{j=1}^{p} ZM_{s,gj} \cdot Sg_j \cdot \Delta Xg_j - ((ZM_{s,s} - ZM_{s,r}) \cdot Tup30 + ZM_{s,s} \cdot Tup34) \cdot \Delta Xup \\ &- ((ZM_{s,s} - ZM_{s,r}) \cdot Tup31 + ZM_{s,s} \cdot Tup35) \cdot \Delta Uup \end{aligned} \tag{3.29}$$

$$\begin{aligned} \Delta Vr = &\sum_{j=1}^{p} ZM_{r,gj} \cdot Sg_j \cdot \Delta Xg_j - ((ZM_{r,s} - ZM_{r,r}) \cdot Tup30 + ZM_{r,s} \cdot Tup34) \cdot \Delta Xup \\ &- ((ZM_{r,s} - ZM_{r,r}) \cdot Tup31 + ZM_{r,s} \cdot Tup35) \cdot \Delta Uup \end{aligned} \tag{3.30}$$

Substituting equation (3.28) into (3.5); and (3.29), (3.30) into (2.34) gives the system state equations:

$$\Delta \dot{X}g_k = \sum_{j=1}^{p} AGG_{k,j} \cdot \Delta Xg_j + AGU_k \cdot \Delta Xup + \sum_{j=1}^{p} BGG_{k,j} \cdot \Delta Ug_j + BGU_k \cdot \Delta Uup \tag{3.31}$$

$$\Delta \dot{X}up = \sum_{j=1}^{p} AUG_j \cdot \Delta Xg_j + AUU \cdot \Delta Xup + BUU \cdot \Delta Uup \tag{3.32}$$

Where:

$$AGG_{k,j} = Eg_k \cdot ZM_{gk,gj} \cdot Sg_j \qquad (\text{j} \neq k)$$

$$AGG_{k,k} = -Eg_k \cdot ZM_{gk,gk} \cdot Sg_k + Ag_k$$

$$AGU_k = -Eg_k \cdot ((ZM_{gk,s} - ZM_{gk,r}) \cdot Tup30 + ZM_{gk,s} \cdot Tup34)$$

$$BGG_k = Bg_k$$

$$B_{GG_j} = 0 \qquad (j \neq k)$$

$$B_{GU_k} = -E_{g_k} \cdot ((ZM_{gk,s} - ZM_{gk,r}) \cdot T_{up31} + ZM_{gk,s} \cdot T_{up35})$$

$$A_{UG_j} = (E_{up} \cdot ZM_{s,gj} + F_{up} \cdot ZM_{r,gj}) \cdot S_{g_j} \qquad (j=1,...,p)$$

$$\begin{aligned} A_{UU} = A_{up} - E_{up} \cdot ((ZM_{s,s} - ZM_{s,r}) \cdot T_{up30} + ZM_{s,s} \cdot T_{up34}) \\ - F_{up} \cdot ((ZM_{r,s} - ZM_{r,r}) \cdot T_{up30} + ZM_{r,s} \cdot T_{up34}) \end{aligned}$$

$$\begin{aligned} B_{UU} = B_{up} - E_{up} \cdot ((ZM_{s,s} - ZM_{s,r}) \cdot T_{up31} + ZM_{s,s} \cdot T_{up35}) \\ - F_{up} \cdot ((ZM_{r,s} - ZM_{r,r}) \cdot T_{up31} + ZM_{r,s} \cdot T_{up35}) \end{aligned}$$

Equations (3.31) and (3.32) can be written as a matrix form to give the standard linearized state equation:

$$\begin{pmatrix} \Delta \dot{X}_g \\ \Delta \dot{X}_{up} \end{pmatrix} = \begin{pmatrix} A_{GG} & A_{GU} \\ A_{UG} & A_{UU} \end{pmatrix} \cdot \begin{pmatrix} \Delta X_g \\ \Delta X_{up} \end{pmatrix} + \begin{pmatrix} B_{GG} & B_{GU} \\ B_{UG} & B_{UU} \end{pmatrix} \begin{pmatrix} \Delta U_G \\ \Delta U_{up} \end{pmatrix} \tag{3.33}$$

or: $\Delta \dot{X} = A \cdot \Delta X + B \cdot \Delta U_{up}$

Where:

$\Delta \dot{X} = \begin{pmatrix} \Delta \dot{X}_{g1} \\ \cdots \\ \Delta \dot{X}_{gp} \\ \Delta \dot{X}_{up} \end{pmatrix}$ : 1x18 matrix (3 generator and exciters, 4 states from each generator and exciter unit; 6 states from UPFC, the total states);

$\Delta U = \begin{pmatrix} \Delta U_{g1} \\ \cdots \\ \Delta U_{gp} \\ \Delta U_{up} \end{pmatrix}$ : 1x9 matrix (2 inputs from each generator and exciter, 3 inputs from the UPFC).

In this thesis, $\Delta U_g$ is set to zero. Then equation (3.33) can be written as:

$$\begin{pmatrix} \Delta \dot{X}_g \\ \Delta \dot{X}_{up} \end{pmatrix} = \begin{pmatrix} A_{GG} & A_{GU} \\ A_{UG} & A_{UU} \end{pmatrix} \cdot \begin{pmatrix} \Delta X_g \\ \Delta X_{up} \end{pmatrix} + \begin{pmatrix} B_{GU} \\ B_{UU} \end{pmatrix} \cdot \Delta U_{up}$$

Using equations (3.6) and (3.28) the output equations of the k$^{th}$ generator can be derived as (details see Appendix D UPFC):

$$\Delta P_{g_k} = V_{g_k}^T \cdot \Delta I_{g_k} + I_{g_k}^T \cdot \Delta V_{g_k} = CPG_{g_k} \cdot \Delta X_g + CPG_{up_k} \cdot \Delta X_{up} + DPG_k \cdot \Delta U_{up}$$

$$\begin{aligned} \Delta Q_{g_k} &= (V_{g_{ky}} \quad -V_{g_{kx}}) \cdot \Delta I_{g_k} + (-I_{g_{ky}} \quad I_{g_{kx}}) \cdot \Delta V_{g_k} \\ &= CQG_{g_k} \cdot \Delta X_g + CQG_{up_k} \cdot \Delta X_{up} + DQG_k \cdot \Delta U_{up} \end{aligned}$$

Similarly the sending end output equations of the UPFC can be derived by equations (2.35), (2.36), (3.29) and (3.30) as:

$$\Delta P_s = V_s^T \cdot (\Delta I_b + \Delta I_e) + (I_b + I_e)^T \cdot \Delta V_s = CPS_g \cdot \Delta X_g + CPS_{up} \cdot \Delta X_{up} + DPS \cdot \Delta U_{up}$$

$$\begin{aligned} \Delta Q_s &= (V_{s_y} \quad -V_{s_x}) \cdot (\Delta I_b + \Delta I_e) + ((-I_{b_y} \quad I_{b_x}) + (-I_{e_y} \quad I_{e_x})) \cdot \Delta V_s \\ &= CQS_g \cdot \Delta X_g + CQS_{up} \cdot \Delta X_{up} + DQS \cdot \Delta U_{up} \end{aligned}$$

## Summary:

In this chapter a benchmark system is proposed for FACTS studies. This system manifests the typical problems that can be solved with FACTS devices, such as congestion and poorly damped modes. Its size is large enough to show typical complex behavior, yet small enough for highly detailed modeling on EMT-type programs. The EMT model is used later for validation. The system's small signal model is developed and linearized for small signal studies in the next chapter.

# Chapter 4 Validation of FACTS Device Using Electromagnetic Transient Simulation

In the last two chapters, the small signal models of the network embedded with the IPFC and the UPFC were derived. The small signal model state equations were implemented in MATLAB. The state variable formulation can be used for small signal stability analysis through eigenvalue calculation. It can also be numerically integrated to produce time-domain results. Results from the numerical simulation can be compared with a detailed EMT model for validation purposes. Such a validation was carried out by comparing the simulation results from the small signal model with an EMT program (PSCAD/EMTDC).

In this chapter, a brief introduction of the validation tool for power system studies-PSCAD/EMTDC is given. Secondly, the implementations of the IPFC, the UPFC and the network in PSCAD/EMTDC are described. Finally, the validation results are presented in contrast with those from small signal models.

## 4.1 PSCAD/EMTDC

The definition and classification of power system stability is complicated because it is based on many considerations such as the physical nature of the resulting instability, the size of the disturbance subjected, and the time span to determine stability [13]. While the classification of power system simulation programs is relatively simple, they can be sorted into two main types in terms of the modelling detail and the time span studied: electromechanical transient type and electromagnetic transient type.

Electromechanical transient type programs usually are used for power flow and transient stability studies. In these programs only some of the dynamic components of the system such as generator, governor, excitation system, Static Var Compensator (SVC), and FACTS devices, are modeled using differential equations. The rest of the network is treated as constant components which are represented with algebraic equations. Because of the assumption that the transmission line is the main part of the network and the integration time step can be very large, these programs can simulate very large networks. Industry standard programs include Siemens PTI's PSS/E, Powertech's DSAT (TSAT/VSAT/SSAT), GE Energy's GEPSLF.

Electromagnetic transient type programs are used to simulate the electromagnetic transients of the power system. In these programs, each component including the transmission line in the network is modeled with differential equations. It allows for a very small time step. Thus it can be used to study the most detailed dynamics of the system, especially because electromagnetic transients pertain to fast switching, significant nonlinearity, and harmonics problems [46]. Conversely, it is considered too detailed for investigating systems on the wider network and over a longer time period. Usually these types of simulation programs are only employed for smaller system studies. Industry standard programs include EMTP, PSCAD/EMTDC and RTDS.

EMTP is the one of earliest EMT type program. It was first developed and applied by Munich Institute of Technology in Germany and Bonneville Power Administration (BPA) in the USA in the 1960s to study electromagnetic transients in power systems and electronic circuits [47]. It has a comprehensive library which contains models for almost every major power system component.

PSCAD/EMTDC appeared later and was developed by the Manitoba HVDC Research Centre to have a greater capability for modeling large power electronic networks containing HVDC and FACTS [46]. Typical applications include design of controllers for power apparatus [48], over-voltage and insulation coordination [49] [50], protection [51], flexible ac transmission systems (FACTS) [32], HVDC [52] [53], and other power electronic applications [54].

It is true that many problems of a power system can be adequately studied on a good load flow and stability program. Transient simulation using EMTDC should not replace the stability study. There are significant reasons why electromagnetic simulation is used rather than a stability program and vice versa. Generally, if a problem can be satisfactorily studied on the load flow and stability program, then there is no need for more complex modelling. Only when it becomes obvious that such a study is inadequate, or **requires confirmation from a different method** of study, then the electromagnetic transients solution should be attempted.

The reason for the need to validate is that some simplifying assumptions are made in modeling the power system for rotor angle stability studies (these include, the transients in the network and the stator winding transients are ignored because they are at higher frequencies than that is interested in a stability study, limits on the control signals are ignored because we are interested in the behavior of the system at a given operating point under small disturbances). Therefore it is important to verify that the effects of these simplifying assumptions do not affect the accuracy at the low frequencies interested in a small signal stability study. Hence it is necessary that these models are validated by more detailed programs, such as PSCAD/EMTDC, EMTP and RTDS. In this research work, PSCAD/EMTDC was selected because of the author's familiarity with this program.

## 4.2 Implementation and Validation of the UPFC and the IPFC in PSCAD/EMTDC

Since the UPFC and the IPFC are the main concern of the project, the implementation of UPFC and the IPFC in PSCAD/EMTDC are detailed in this section. Then the small signal models developed in Chapter 2 and 3 are validated using PSCAD/EMTDC.

### 4.2.1 Implementation of the UPFC and the IPFC in PSCAD/EMTDC

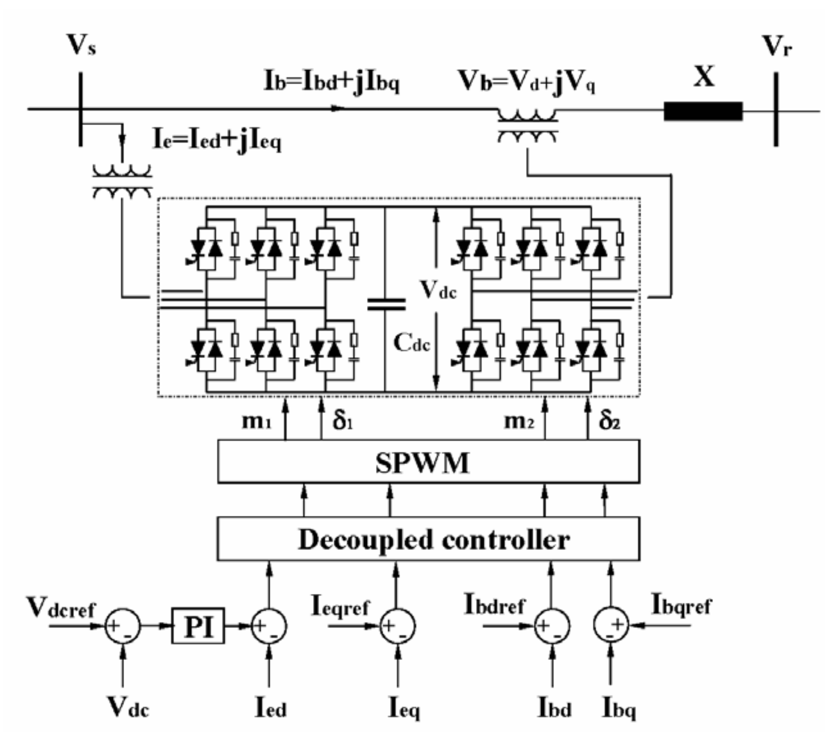


Figure 4.1 The UPFC structure

Since the UPFC contains both shunt and series branches, it has a more comprehensive structure than the IPFC which contains only a series branch. Therefore this section will begin with a detailed description of the UPFC.

Figure 4.1 shows the overall structure of the UPFC. It consists mainly of two voltage source converters designated as exciter and booster respectively. These are shunt- and series-connected to the system through a transformer on the AC side, and linked by a DC capacitor (DC link) on the DC side. Each converter leg contains a gate-controllable valve (GTO, IGBT), an anti-paralleled diode, and an auxiliary snubber circuit. By triggering the valves based on an appropriate control strategy, the UPFC can control the magnitude and phase angle (or d, q components) of shunt and series voltage ($V_e$, $V_b$) of both transformers, thereby giving the system the ability for both shunt and series compensation [55].

There are two popular trigger methods for firing the converter valves [56]: multilevel square wave method and Pulse Width Modulation method (PWM). Using the multilevel method, the VSC circuit generates several square waves, which when superposed, comprise the required sinusoidal waveform. This method gives a low switching frequency, low harmonics, and low operating loss. However, it requires a complicated configuration of the electrical power circuit. In recent years, the PWM method has been used for high power electronic applications. In the PWM converter, the required waveform is generated by repeated operation of switches. The PWM method provides for low harmonics, a simple structure, and near sinusoidal waveform generation but requires a valve capable of a high switching frequency. High switching frequency leads to higher switching losses. In this research, sinusoidal PWM (SPWM) is chosen as the triggering method because this is the most common approach reported in the literature.

The implementation of the IPFC in the PSCAD/EMTDC is similar with that of the UPFC as shown in Figure 4.2. It differs from the UPFC in that the shunt VSC in the

UPFC is replaced by a series VSC (in line 2) which together with the series VSC (in line 1) makes up the IPFC.

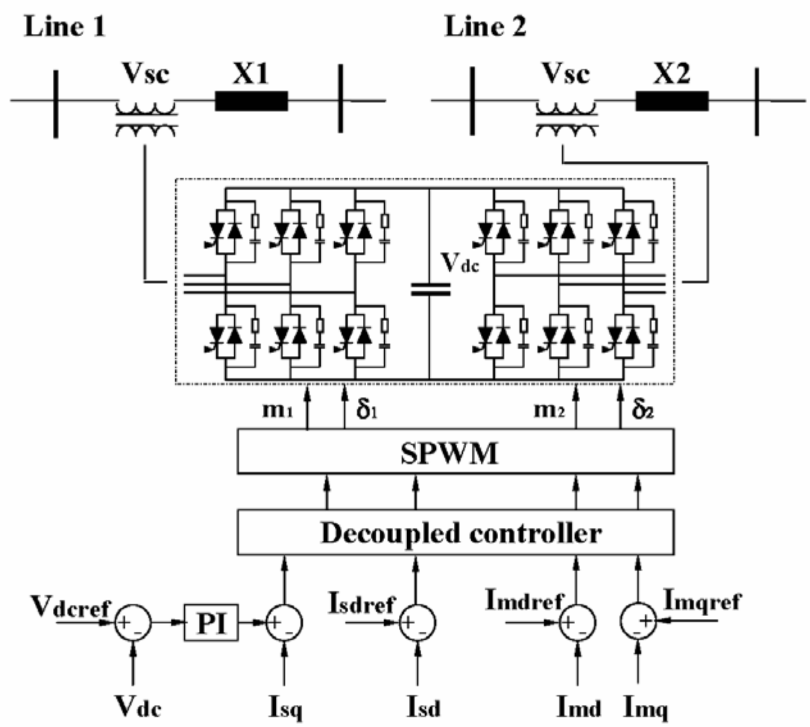


Figure 4.2 The IPFC structure

### 4.2.2 Validation of the UPFC and the IPFC in PSCAD/EMTDC

Two simple test systems were built in PSCAD/EMTDC which are mainly for the purpose of validation debugging of the small signal models of the IPFC and the UPFC. Further comprehensive testing on the larger systems was also carried out and will be described in later sections.

Figure 4.3 shows a three-source simple system for IPFC validation. There are three sources in this system. Source 1 transfers power to source 2 and source 3 through line 1 and line 2 respectively with the IPFC placed in between the two lines. Because the IPFC is the only dynamic device in the system, there are 6 modes in the system (related to the 6 differential equations of the small signal model that describes the IPFC behavior).

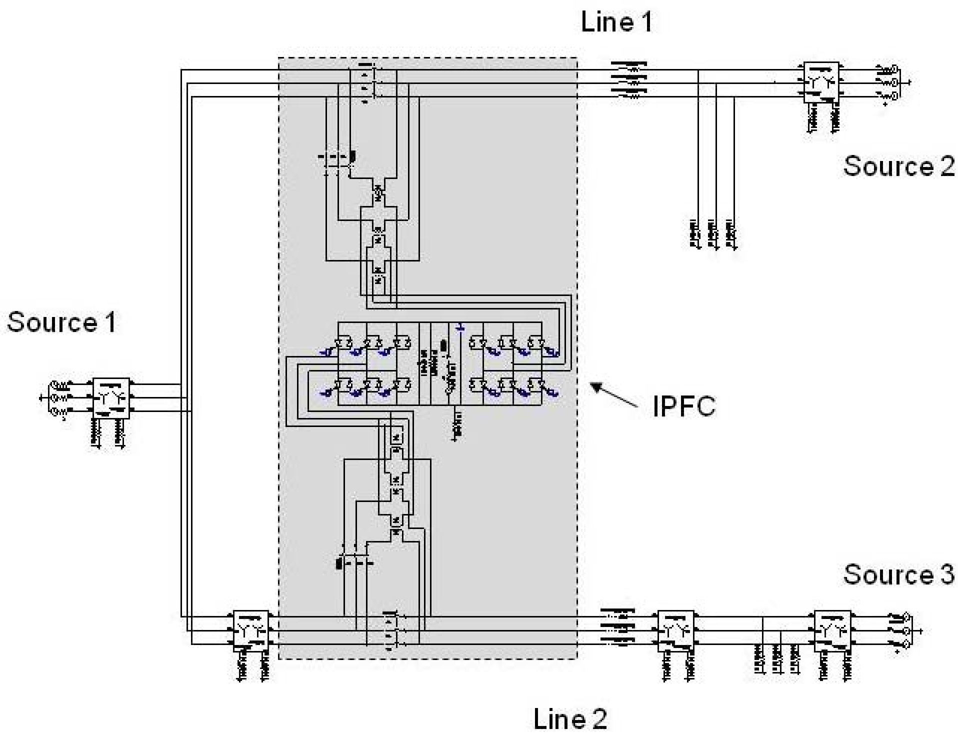


Figure 4.3 The simple test network for the IPFC validation

The small signal model was implemented in MATLAB and results from PSCAD/EMTDC are compared with those from MATLAB. A 2% increase was applied on IPFC's reference $I_{sdref}$. Figure 4.4 shows the step response of the IPFC states from PSCAD and from MATLAB (small signal model response). The responses are close with the steady state values differing slightly due to the non-linear model (large signal) converging to a slightly different steady state. However, the small signal dynamic behaviors are close, verifying the validity of the small signal model that was developed as a part of this research.

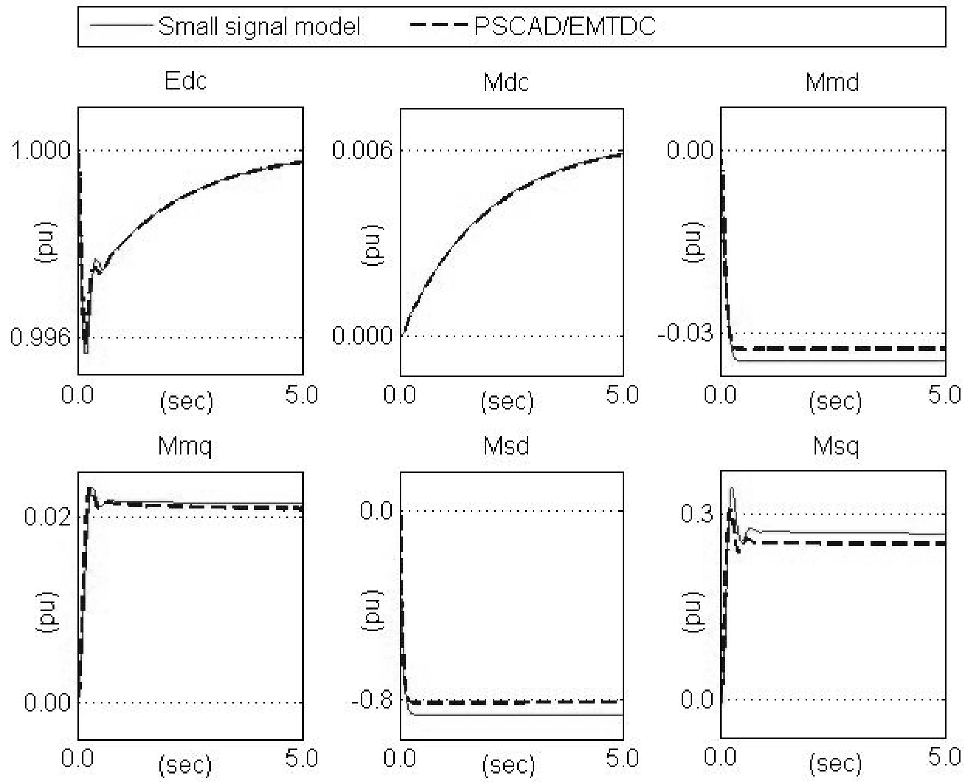


Figure 4.4 States of the simple network embedded with the IPFC

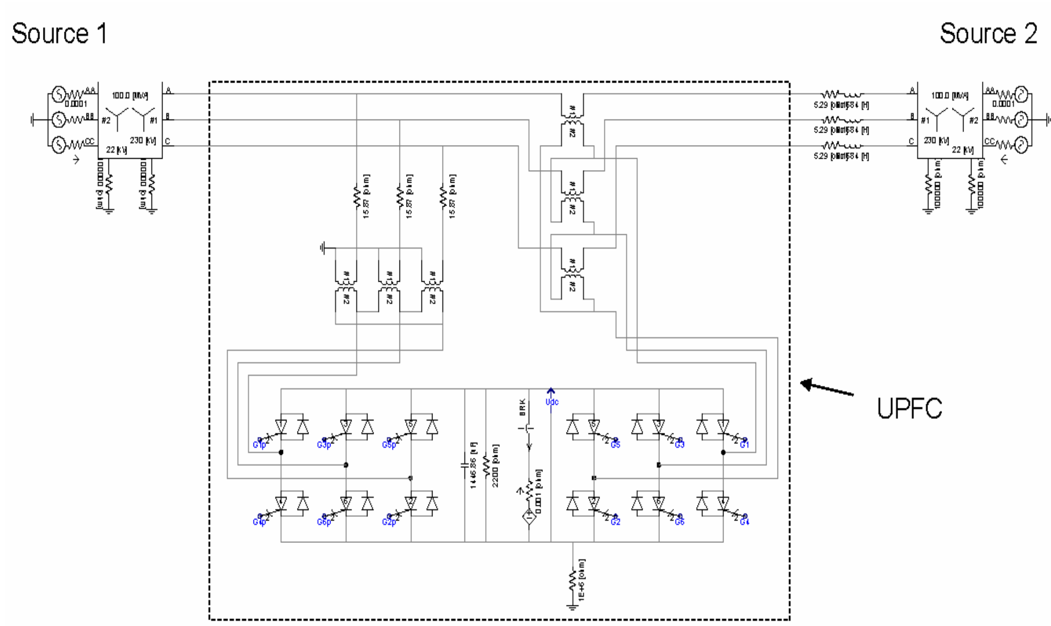


Figure 4.5 The simple test network for the UPFC validation

The UPFC validation is carried out in PSCAD/EMTDC using a two-source system (see

Figure 4.5). A 2% step change was applied on the UPFC's reference $I_{bqref}$. Figure 4.6 shows the step responses of the 6 UPFC states. All the results except state $M_{eq}$ from PSCAD match well with the small signal model. This discrepancy identified the need for more refinement in the model, and a detailed investigation was conducted to find the cause. It turned out that the cause was the fact that dc capacitor voltage change is not reflected in the current equations. Section 4.4 presents the analysis and further model refinement to correct this problem.

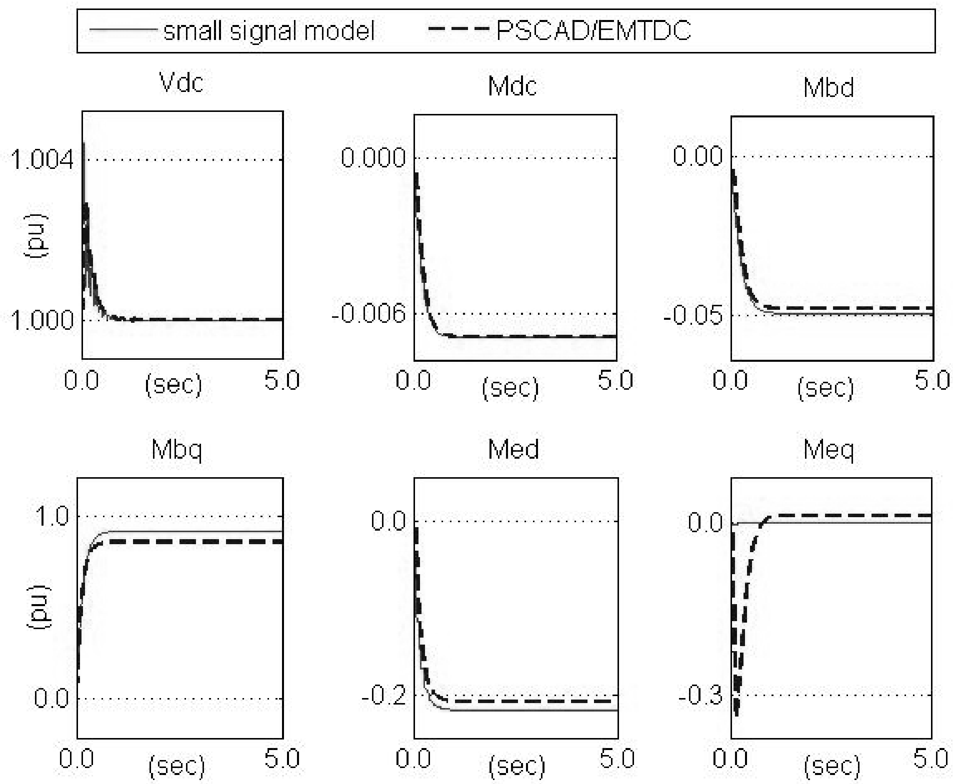


Figure 4.6 States of the simple network embedded with the UPFC

## 4.3 Validation of the IPFC and the UPFC in the 12bus Benchmark System

In PSCAD/EMTDC, the system in Figure 3.1 can be represented with detailed models for the synchronous machines (including full representation of sub-transient effects), exciters and transmission lines. To see if the developed small signal models would provide accurate results in a multi-machine system with several dynamic models, the PSCAD models were implemented in the small signal representation of the 12 bus 3 machine system described in Chapter 3.1. The data for the system is given in Appendix A.

The locations for the IPFC and the UPFC devices are based on power flow control considerations. In this thesis, there are two locations considered for the IPFC (Case 2 and Case 5) and another two for the UPFC (Case 3 and Case 4). The details of the options will be presented in Chapter 5.

### 4.3.1 Validation of the IPFC in the 12bus Benchmark System

In this section, Case 2 is selected for the validation of the IPFC in the 12bus benchmark network. In Case 2, an IPFC is placed in lines 1-6 and 7-8 to relieve congestion of line 1-6 and to improve the utilization of the transfer capacity of line 7-8. There are 18 states in this system: 12 generator states (3x4) and 6 IPFC states.

A 2% step change was applied on the IPFC's reference of the real component of the master line current $I_{mdref}$. Figure 4.7 through 4.9 show the step responses of the system states. Figure 4.10 and Figure 4.11 show the real power of the three generators and the IPFC respectively. The accuracy of the small signal model is evident from the two traces that are virtually overlapping.

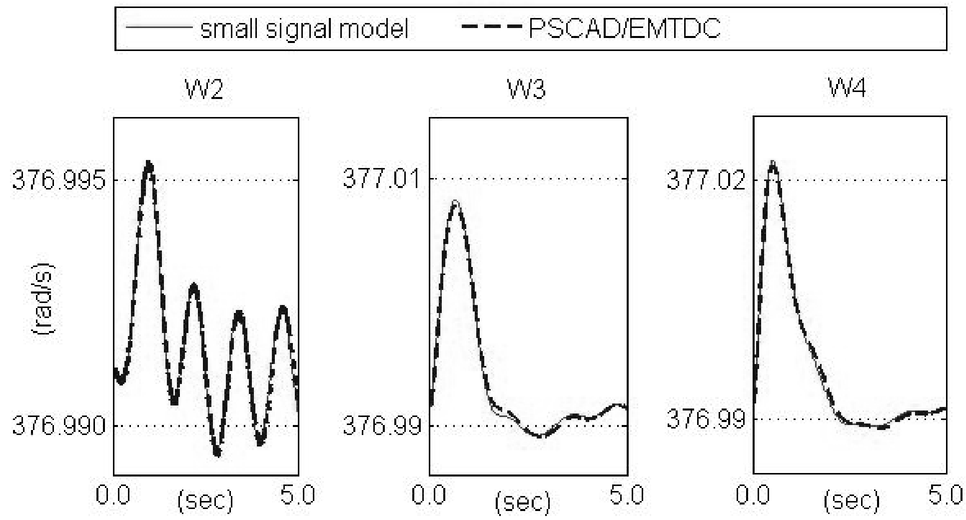


Figure 4.7 Case2: states of the 12 bus network with the IPFC-rotor speed

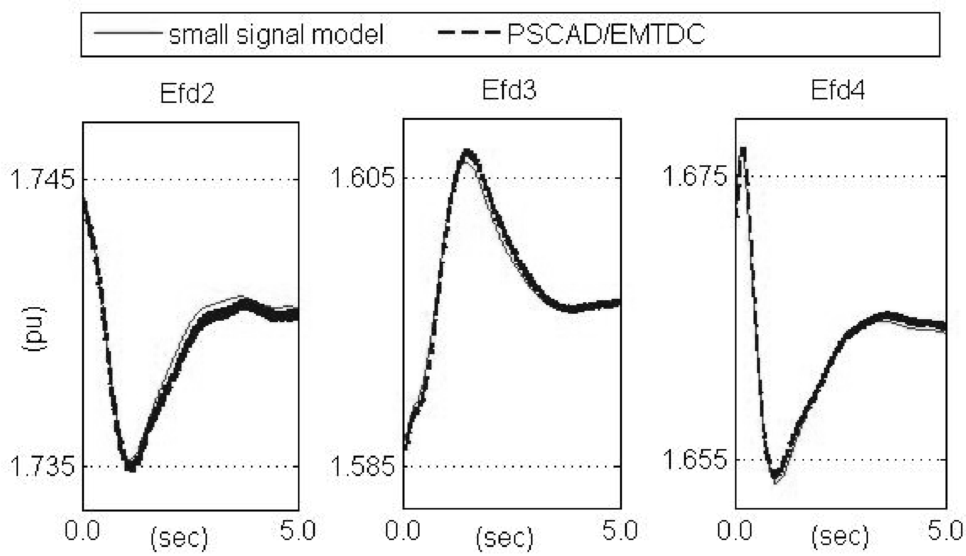


Figure 4.8 Case2: states of the 12 bus network with the IPFC-field voltage

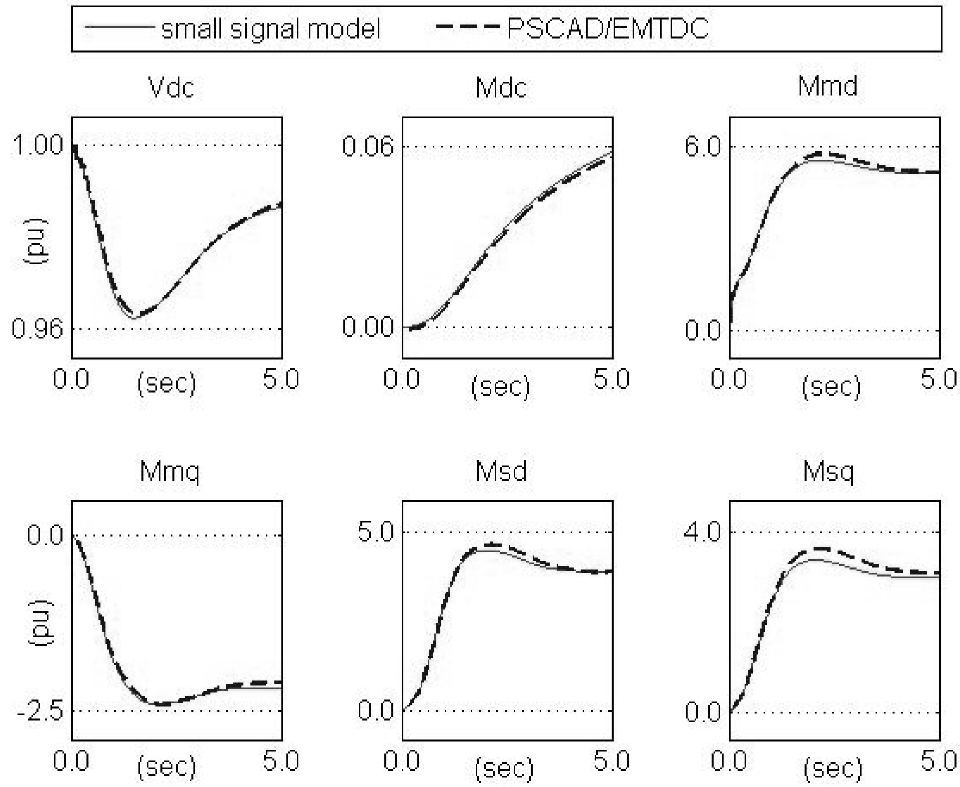


Figure 4.9 Case2: states of the 12 bus network with the IPFC-states of the IPFC

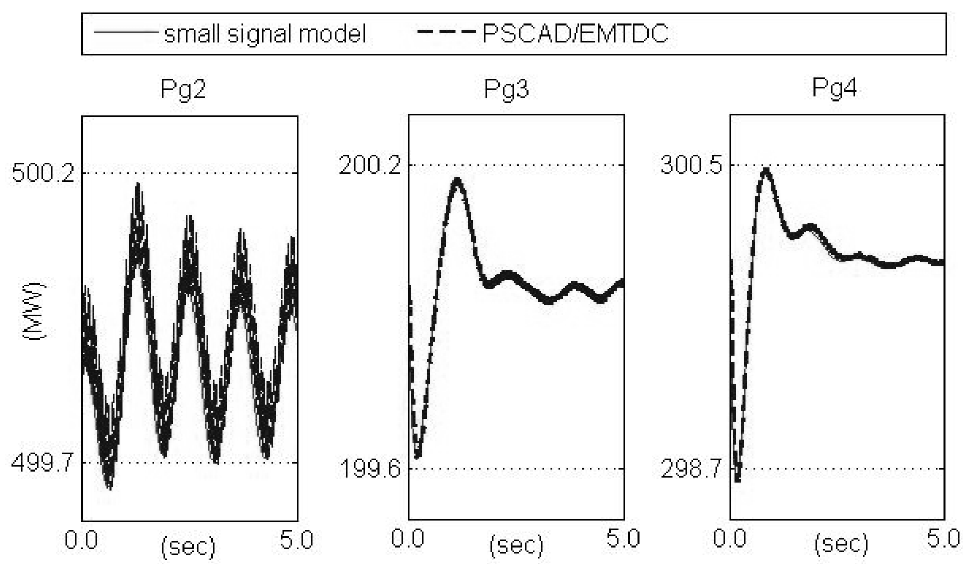


Figure 4.10 Case2: the real power of the generators

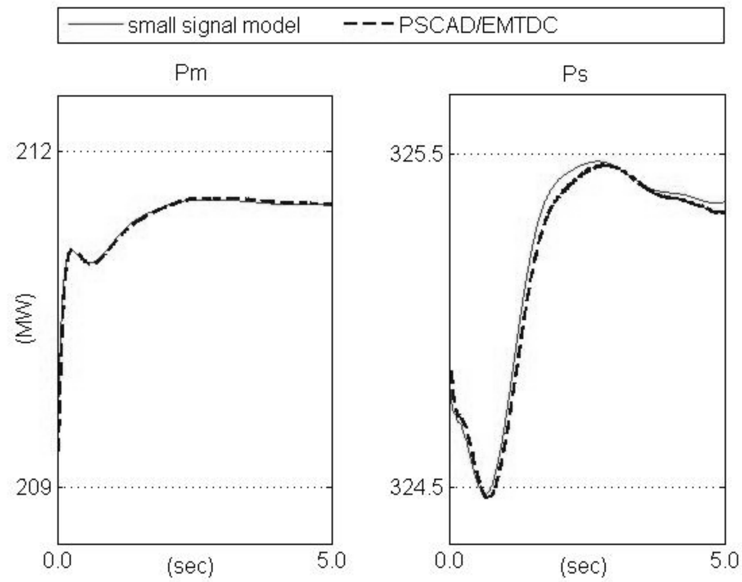


Figure 4.11 Case2: the real power of the master and slave lines of the IPFC

## 4.3.2 Validation of the UPFC in the 12bus Benchmark System

Case 3 is selected for the validation of the UPFC in the system. In Case 3, a UPFC is placed in line 1-6 to relieve the congestion of line 1-6. There are also 18 states in this system.

The disturbance applied was a 2% increase of the UPFC's reference of real component of the series branch current $I_{bdref}$. Figure 4.12 through Figure 4.14 shows the step responses of the system states. Figure 4.15 and Figure 4.16 show the real power of the three generators and the UPFC respectively. All waveforms of the states except the UPFC shunt branch states ($M_{ed}$ and $M_{eq}$) are perfectly superposed.

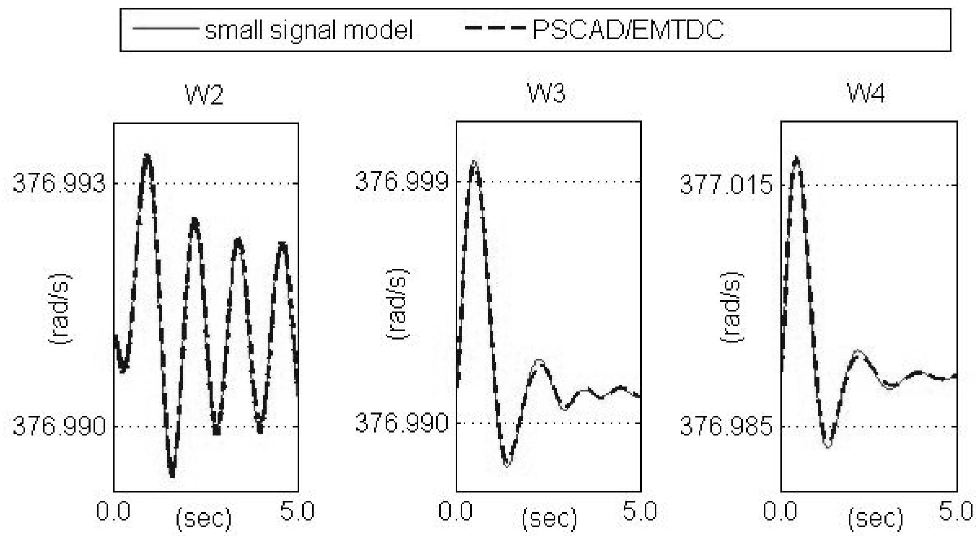


Figure 4.12 Case3: states of the 12 bus network with the UPFC-rotor speed

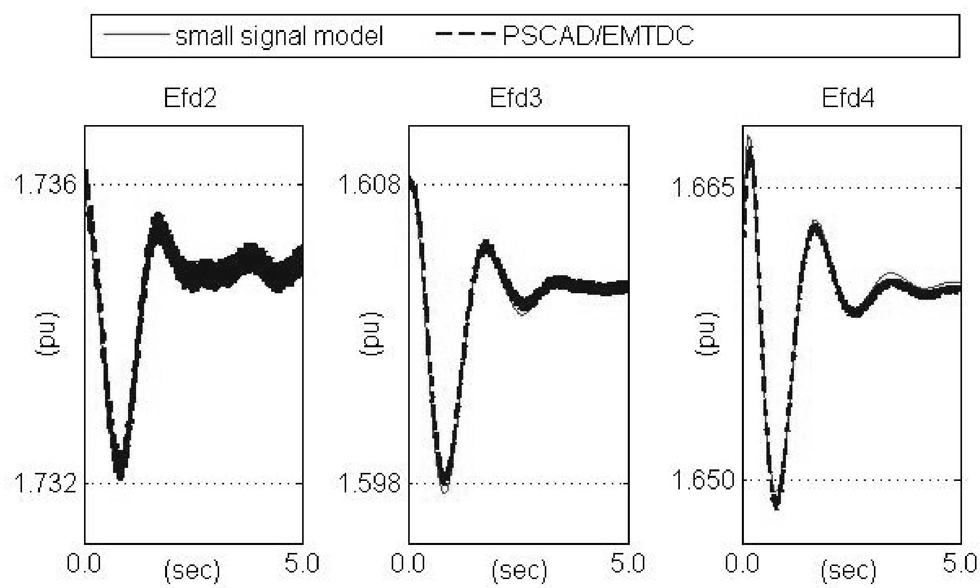


Figure 4.13 Case3: states of the 12 bus network with the UPFC-field voltage

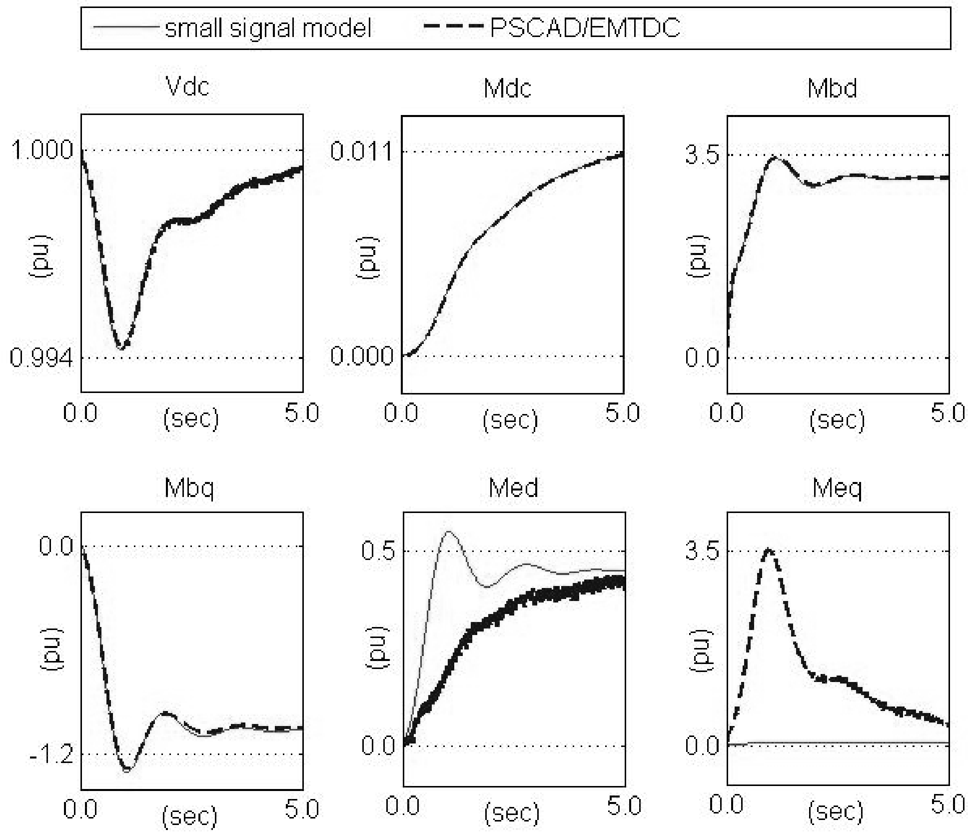


Figure 4.14 Case3: states of the 12 bus network with the UPFC-states of the UPFC

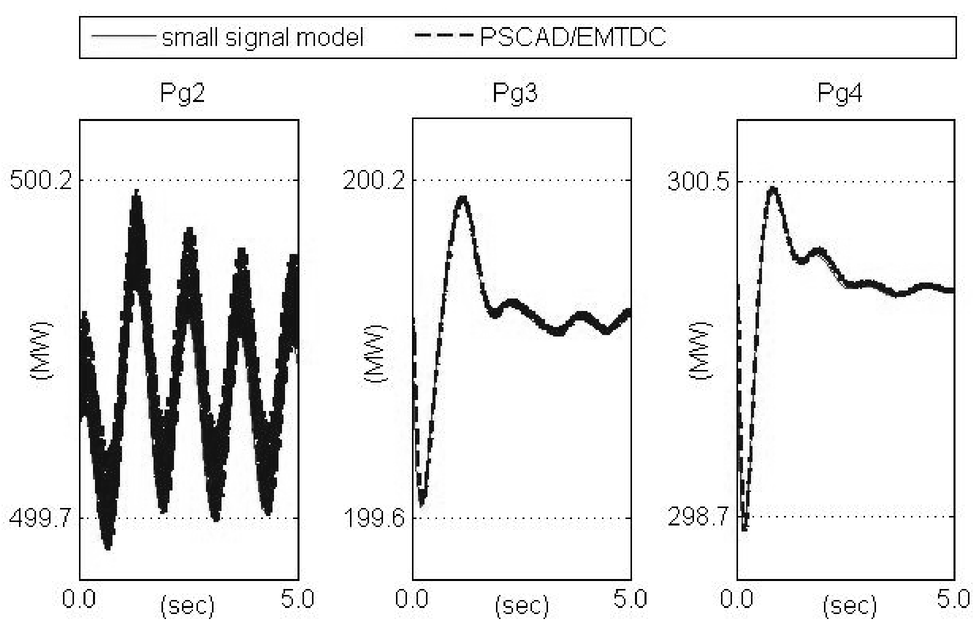


Figure 4.15 Case3: the real power of generators

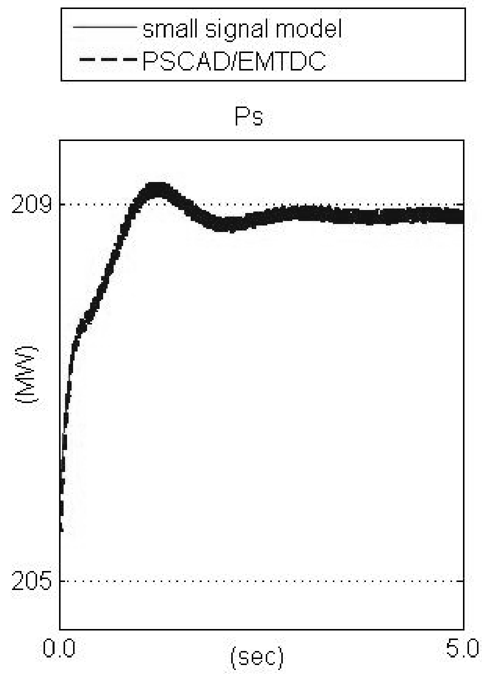


Figure 4.16 Case3: the sending end real power of the UPFC

## 4.4 Explanation of the Validation Errors of the UPFC Model

In order to find the reason of the errors of the states $M_{ed}$ and $M_{eq}$ between the EMT model and the small signal model, the modeling details between the two models are examined.

As seen in Figure 4.17, in PSCAD/EMTDC, the injected voltages are produced by switching devices (shown as the shaded part) instead of by the decoupled controller. The decoupled controller only outputs the ordered injected voltages for the switching devices and does not model detailed switching phenomena. The UPFC final outputs-the injected voltages ($V_{bd}$, $V_{bq}$, $V_{ed}$ and $V_{eq}$) are proportional to the DC capacitor voltage $V_{dc}$. In the small signal models the switching detail (shaded part) are not modeled and the injected voltages are assumed to not be influenced by the change of $V_{dc}$.

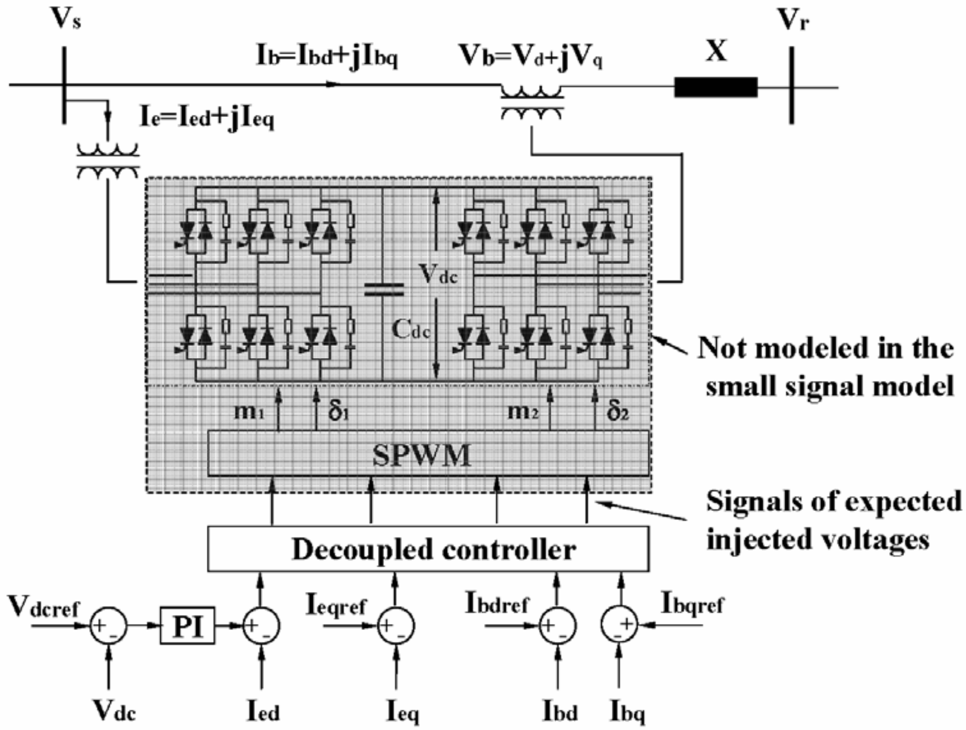


Figure 4.17 The difference between the EMT model and the small signal model of the UPFC

To show the impact of this assumption (the injected voltages are not influenced by the change of $V_{dc}$) on the derivation of the small signal model, the differential equations of the model were re-derived to include the capacitor voltage dependence in an approximate manner.

### 4.4.1 Refinement of System Equation to Include Capacitor Voltage Dependence

Given the assumption that the injected voltages are not influenced by $V_{dc}$, the injected voltages are described by equations (2.22)-(2.25) repeated here for completeness:

$$V_{b_d} = K_{bp} \cdot (U_{bd} - I_{b_d}) + \frac{1}{T_b} \cdot M_{bd} - K_{bp} \cdot \omega_0 \cdot M_{bq} \tag{2.22}$$

$$V_{b_q} = K_{bp} \cdot (U_{bq} - I_{b_q}) + \frac{1}{T_b} \cdot M_{bq} + K_{bp} \cdot \omega_0 \cdot M_{bq} \tag{2.23}$$

$$V_{e_d} = V_{s_d} - (K_{ep} \cdot (U_{ed} - I_{e_d}) + \frac{1}{T_e} \cdot M_{ed} - K_{ep} \cdot \omega_0 \cdot M_{eq}) \tag{2.24}$$

$$V_{e_q} = V_{s_q} - (K_{ep} \cdot (U_{eq} - I_{e_q}) + \frac{1}{T_e} \cdot M_{eq} + K_{ep} \cdot \omega_0 \cdot M_{ed}) \tag{2.25}$$

The corresponding d, q current components ($I_{bd}$, $I_{bq}$ and $I_{ed}$, $I_{eq}$) can be derived by equations (2.22)-(2.25) shown as:

$$\begin{aligned} I_{b_d} = \Big( & (\frac{K_{bp}}{T_b} + K_{bp} \cdot X_b \cdot \omega) \cdot M_{bd} + (\frac{X_b}{T_b} - K_{bp}^2 \cdot \omega) \cdot M_{bq} + K_{bp}^2 \cdot U_{bd} \\ & + K_{bp} \cdot X_b \cdot U_{bq} + K_{bp} \cdot (V_{sd} - V_{rd}) + X_b \cdot (V_{sq} - V_{rq}) \Big) / (X_b^2 + K_{bp}^2) \end{aligned} \tag{4.1}$$

$$\begin{aligned} I_{b_q} = \Big( & (\frac{K_{bp}}{T_b} + K_{bp} \cdot X_b \cdot \omega) \cdot M_{bq} - (\frac{X_b}{T_b} - K_{bp}^2 \cdot \omega) \cdot M_{bd} + K_{bp}^2 \cdot U_{bq} \\ & - K_{bp} \cdot X_b \cdot U_{bd} + K_{bp} \cdot (V_{sq} - V_{rq}) - X_b \cdot (V_{sd} - V_{rd}) \Big) / (X_b^2 + K_{bp}^2) \end{aligned} \tag{4.2}$$

$$I_{e_d} = \Big( (\frac{K_{ep}}{T_e} + K_{ep} \cdot X_e \cdot \omega) \cdot M_{ed} + (\frac{X_e}{T_e} - K_{ep}^2 \cdot \omega) \cdot M_{eq} + K_{ep}^2 \cdot U_{ed} + K_{ep} \cdot X_e \cdot U_{eq} \Big) / (X_e^2 + K_{ep}^2) \tag{4.3}$$

$$I_{e_q} = \Big( (\frac{K_{ep}}{T_e} + K_{ep} \cdot X_e \cdot \omega) \cdot M_{eq} - (\frac{X_e}{T_e} - K_{ep}^2 \cdot \omega) \cdot M_{ed} + K_{ep}^2 \cdot U_{eq} - K_{ep} \cdot X_e \cdot U_{ed} \Big) / (X_e^2 + K_{ep}^2) \tag{4.4}$$

Concerning the impact of $V_{dc}$ on the output voltages, the equations (2.22)-(2.25) should be rewritten as:

$$V_{b_d} = (K_{bp} \cdot (U_{bd} - I_{b_d}) + \frac{1}{T_b} \cdot M_{bd} - K_{bp} \cdot \omega_0 \cdot M_{bq}) \cdot V_{dc} \tag{4.5}$$

$$V_{b_q} = (K_{bp} \cdot (U_{bq} - I_{b_q}) + \frac{1}{T_b} \cdot M_{bq} + K_{bp} \cdot \omega_0 \cdot M_{bq}) \cdot V_{dc} \tag{4.6}$$

$$V_{e_d} = \Big( V_{s_d} - (K_{ep} \cdot (U_{ed} - I_{e_d}) + \frac{1}{T_e} \cdot M_{ed} - K_{ep} \cdot \omega_0 \cdot M_{eq}) \Big) \cdot V_{dc} \tag{4.7}$$

$$V_{e_q} = \Big( V_{s_q} - (K_{ep} \cdot (U_{eq} - I_{e_q}) + \frac{1}{T_e} \cdot M_{eq} + K_{ep} \cdot \omega_0 \cdot M_{ed}) \Big) \cdot V_{dc} \tag{4.8}$$

The currents equations are derived as:

$$I_{b_d} = \Big( (\frac{K_{bp} \cdot V_{dc}^2}{T_b} + K_{bp} \cdot X_b \cdot \omega \cdot V_{dc}) \cdot M_{bd} + (\frac{X_b \cdot V_{dc}}{T_b} - K_{bp}^2 \cdot \omega \cdot V_{dc}^2) \cdot M_{bq} + K_{bp}^2 \cdot V_{dc}^2 \cdot U_{bd} + K_{bp} \cdot X_b \cdot V_{dc} \cdot U_{bq} + K_{bp} \cdot (V_{sd} - V_{rd}) \cdot V_{dc} + X_b \cdot (V_{sq} - V_{rq}) \Big) / (X_b^2 + K_{bp}^2 \cdot V_{dc}^2) \tag{4.9}$$

$$I_{b_q} = \Big( (\frac{K_{bp} \cdot V_{dc}^2}{T_b} + K_{bp} \cdot X_b \cdot \omega \cdot V_{dc}) \cdot M_{bq} - (\frac{X_b \cdot V_{dc}}{T_b} - K_{bp}^2 \cdot \omega \cdot V_{dc}^2) \cdot M_{bd} + K_{bp}^2 \cdot V_{dc}^2 \cdot U_{bq} - K_{bp} \cdot X_b \cdot V_{dc} \cdot U_{bd} + K_{bp} \cdot (V_{sq} - V_{rq}) \cdot V_{dc} - X_b \cdot (V_{sd} - V_{rd}) \Big) / (X_b^2 + K_{bp}^2 \cdot V_{dc}^2) \tag{4.10}$$

$$I_{e_d} = \Big( (\frac{K_{ep} \cdot V_{dc}^2}{T_e} + K_{ep} \cdot X_e \cdot \omega \cdot V_{dc}) \cdot M_{ed} + (\frac{X_e \cdot V_{dc}}{T_e} - K_{ep}^2 \cdot \omega \cdot V_{dc}^2) \cdot M_{eq} + K_{ep}^2 \cdot V_{dc}^2 \cdot U_{ed} + K_{ep} \cdot X_e \cdot V_{dc} \cdot U_{eq} + K_{ep} \cdot (1 - V_{dc}) \cdot V_{dc} \cdot V_{sd} + X_e \cdot (1 - V_{dc}) \cdot V_{sq} \Big) / (X_e^2 + K_{ep}^2 \cdot V_{dc}^2) \tag{4.11}$$

$$I_{e_q} = \Big( (\frac{K_{ep} \cdot V_{dc}^2}{T_e} + K_{ep} \cdot X_e \cdot \omega \cdot V_{dc}) \cdot M_{eq} - (\frac{X_e \cdot V_{dc}}{T_e} - K_{ep}^2 \cdot \omega \cdot V_{dc}^2) \cdot M_{ed} + K_{ep}^2 \cdot V_{dc}^2 \cdot U_{eq} - K_{ep} \cdot X_e \cdot V_{dc} \cdot U_{ed} + K_{ep} \cdot (1 - V_{dc}) \cdot V_{dc} \cdot V_{sq} - X_e \cdot (1 - V_{dc}) \cdot V_{sd} \Big) / (X_e^2 + K_{ep}^2 \cdot V_{dc}^2)$$

(4.12)

Because most state equations contain current components (see Appendix D - the small signal model of the UPFC) with such changes, the subsequent derivation and linearization of the model become significantly more complicated. Therefore the model was simplified to make it more suitable for general use. This procedure is described below.

By comparing equations (4.1)~(4.4) with (4.9)~(4.12), it was found that in addition to the DC voltage $V_{dc}$, there are two extra terms in the accurate shunt current equations (4.11) and (4.12) which do not appear in the original equations (4.3) and (4.4). They are

$(K_{ep} \cdot (1 - V_{dc}) \cdot V_{dc} \cdot V_{sd} + X_e \cdot (1 - V_{dc}) \cdot V_{sq}) / (X_e^2 + K_{ep}^2 \cdot V_{dc}^2)$ and

$(K_{ep} \cdot (1 - V_{dc}) \cdot V_{dc} \cdot V_{sq} - X_e \cdot (1 - V_{dc}) \cdot V_{sd}) / (X_e^2 + K_{ep}^2 \cdot V_{dc}^2)$ respectively. If the change of $V_{dc}$ ($V_{dc} = 1$) is ignored, these two terms would disappear. By observing that the significant errors (Figure 4.6 and Figure 4.14) are only in the shunt branch states $M_{ed}$ and $M_{eq}$, it was decided that only the shunt current equations be changed. The series branch current components ($I_{bd}$, $I_{bq}$) equations were retained as in (4.1)~(4.2), because they appear to be less influenced by $V_{dc}$ (see Figure 4.4 and Figure 4.9). The shunt branch current components ($I_{ed}$, $I_{eq}$) are thus revised as:

$$\begin{aligned} Ie_d = \Big( & (\frac{Kep}{Te} + Kep \cdot Xe \cdot \omega) \cdot Med + (\frac{Xe}{Te} - Kep^2 \cdot \omega) \cdot Meq + Kep^2 \cdot Ued \\ & + Kep \cdot Xe \cdot Ueq + Kep \cdot (1 - Vdc) \cdot Vdc \cdot Vsd + Xe \cdot (1 - Vdc) \cdot Vsq \Big) / (Xe^2 + Kep^2) \end{aligned} \tag{4.13}$$

$$\begin{aligned} Ie_q = \Big( & (\frac{Kep}{Te} + Kep \cdot Xe \cdot \omega) \cdot Meq - (\frac{Xe}{Te} - Kep^2 \cdot \omega) \cdot Med + Kep^2 \cdot Ueq \\ & - Kep \cdot Xe \cdot Ued + Kep \cdot (1 - Vdc) \cdot Vdc \cdot Vsq - Xe \cdot (1 - Vdc) \cdot Vsd \Big) / (Xe^2 + Kep^2) \end{aligned} \tag{4.14}$$

This model is simpler and easier to be linearized as compared with the full modification ((4.9~ (4.12)).

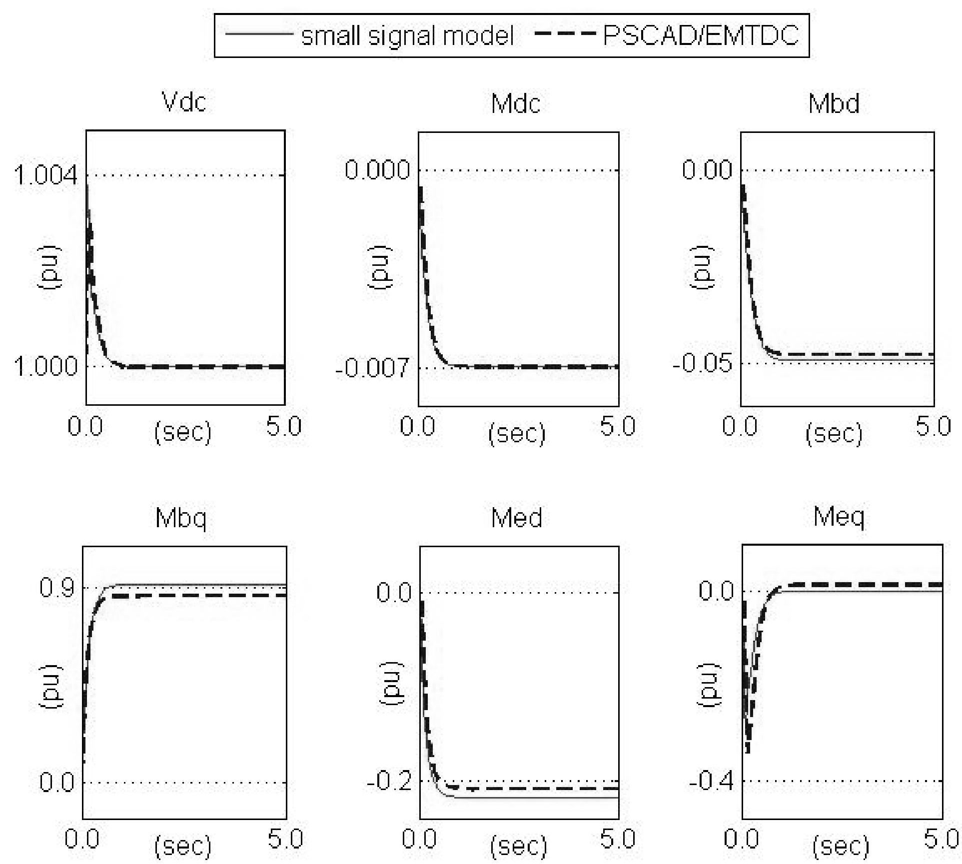


Figure 4.18 States of the revised model

The validation results for the revised model show good agreement between the small signal model and the EMT model (see Figure 4.18). Thereby it was proven that the capacitor voltage variation is the reason why the earlier models were shown some errors.

It should be noted that this modification (added two items in shunt current equations (4.13) and (4.14)) only partly addresses the errors caused by ignoring the change of the DC capacitor voltage. The denominator in equations (4.13), (4.14) is a constant $Xe^2 + Kep^2$ instead of the variable $Xe^2 + Kep^2 \cdot Vdc^2$ as in (4.11), (4.12). This change (replacing $Xe^2 + Kep^2 \cdot Vdc^2$ with $Xe^2 + Kep^2$ ) is based on the numerical consideration that when $Xe >> Kep,\ Xe^2 + Kep^2 \cdot Vdc^2 \approx Xe^2 + Kep^2$. In this case, $Xe = 0.3,\ Kep = 0.019$, and the change in the denominator can be omitted. As a comparison, another setting ( $Xe = 0.3,\ Kep = 0.095$ ) is given to the same case, and the validation results show that the error is enlarged along with a larger $K_{ep}$ (see Figure 4.19).

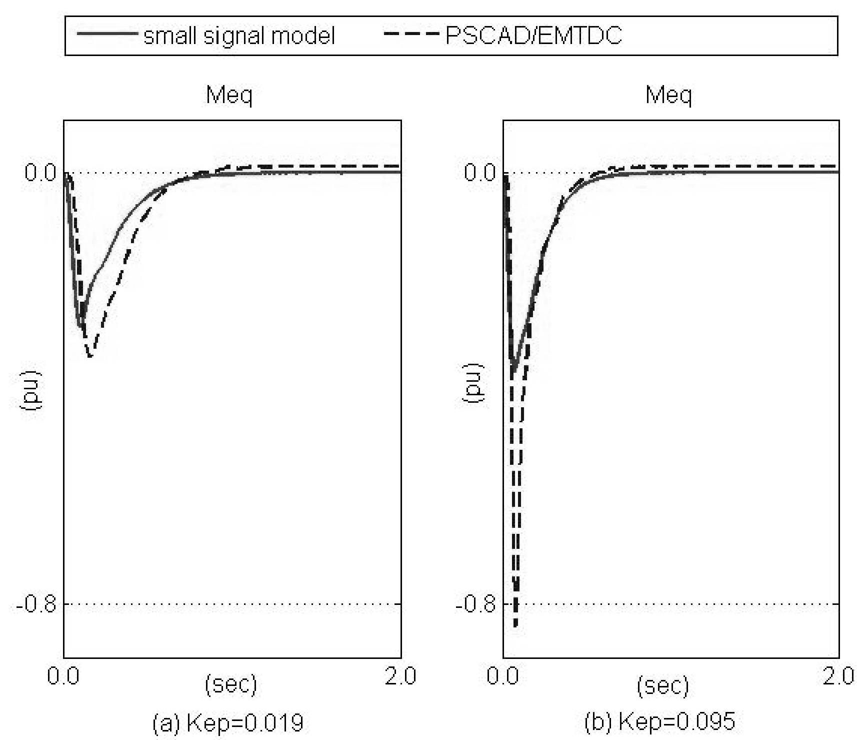


Figure 4.19 The impact of different settings on the revised UPFC model

The same situation happens in Case 3 (12 buses system embedded with a UPFC). Using the revised model, the errors in states $M_{ed}$ and $M_{eq}$ decrease (see Figure 4.20) as compared with the original model (Figure 4.14).

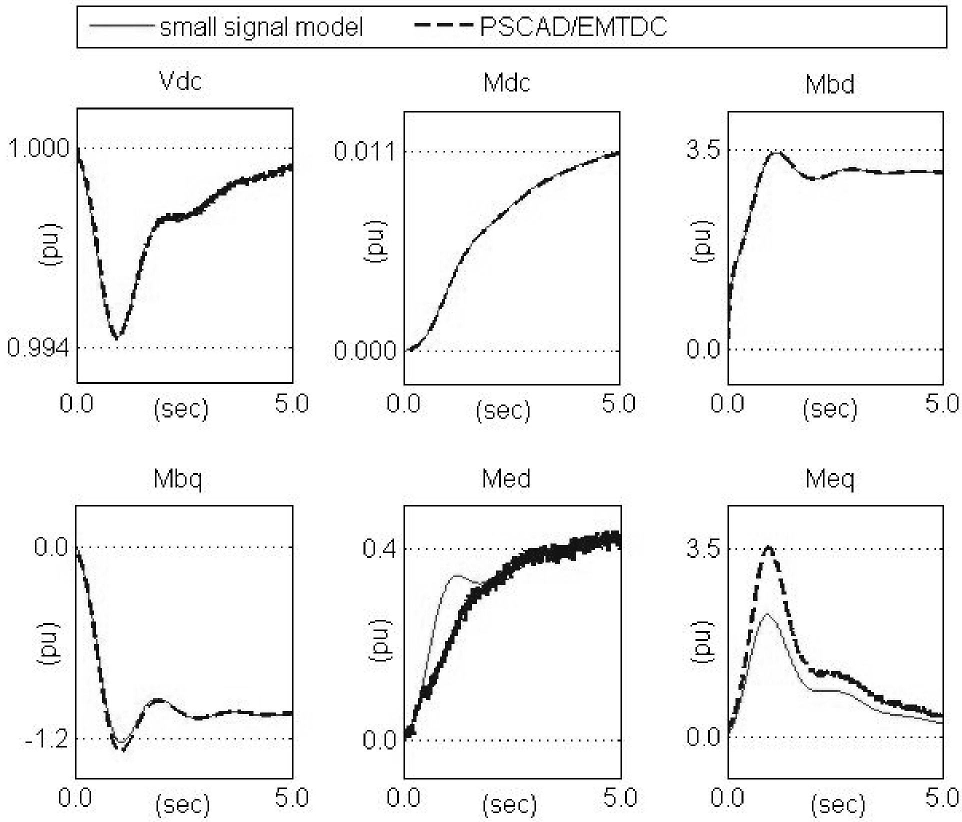


Figure 4.20 Case3: states of the UPFC of the revised model

## 4.4.2 Impact of the DC Capacitor Voltage on the IPFC Model

The above simulations illustrate the reason for the validation errors of the UPFC. Another interesting and puzzling fact is that the IPFC model appears to be accurate without the above refinement regarding dc capacitor voltage that was required for the UPFC. The reason is analyzed and is shown below.

It can be seen that the structures of the decoupled controllers in the series and shunt branches are different (see Figure 4.21). As described in the previous section, the primary impact of dc capacitor voltage is on the shunt current. Indeed, the simplified refined model retains the same equations for the series branch as the original. In the IPFC, there is no shunt branch, and hence the capacitor voltage impact is smaller. Also the injected voltages of the series branch ($V_{bd}$, $V_{bq}$) are much less (<10%) than that of the shunt branch (around 1.0pu, the same level of the line voltage). This largely reduces the impact from the capacitor voltage.

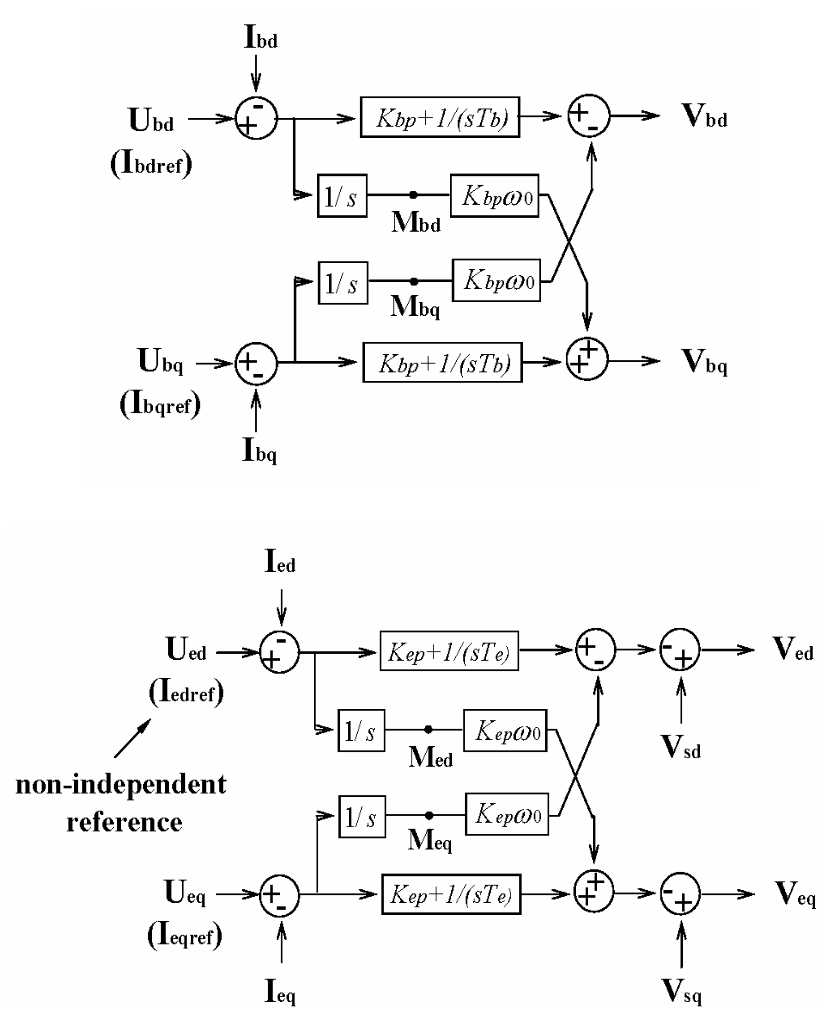


Figure 4.21 The decoupled controllers of the UPFC (repeat of Figure 2.8 and Figure 2.9)

Although there are errors in the shunt branch states in both the simplified and revised UPFC small signal models, it does not have any impact on the small signal analysis of the next chapter. Because the main concern of this research is on the electromechanical oscillation modes, if these modes in the two small signal models match with that of the corresponding EMT model, the errors in the shunt branch states would not affect the analysis.

In Table 4-1, the small signal analysis for both the revised and the simplified small signal models of Case 3 shows that the low frequency oscillation modes of the system are 0.58Hz, 0.84Hz and 1.13 Hz respectively. It also shows that both the frequencies and their damping ratios of the two models are very close. This implies that for a small signal study, the two models would not be significantly different. Another concern is whether or not these modes of the small signal model match with the EMT model. This is addressed by comparing the three modes of the two small signal models with the EMT model (see Table 4-1). The results show a good agreement between the small signal models and the EMT model. Thus the original small signal model of the UPFC is acceptable for the study, and the refined model is not really needed for most generator stability studies.

Table 4-1 Oscillation modes of Case 3 UPFC on line1-6

| Dominant generators | | PSCAD | Small signal model | |
|---|---|---|---|---|
| | | | Revised model | Simplified model |
| G2 | f (hz) | 0.837 | 0.843 | 0.843 |
| | damp | 1.3% | 1.0% | 1.1% |
| G3 | f (hz) | 1.11 | 1.126 | 1.126 |
| | damp | 3.4% | 3.1% | 3.1% |
| G4 | f (hz) | 0.571 | 0.575 | 0.582 |
| | damp | 34.2% | 30.5% | 29.4% |

## 4.5 Concerns for the Small Signal Model Application

This section discusses concerns for the applications of the small signal model, i.e. whether they can easily be used in commercial software, whether they are acceptable when the nonlinearities factors such as the limiter or a larger disturbance are included, and the simulation time required for the system with the FACTS embedded.

## 4.5.1 Effect of non-linearities

Since any non-linearities due to limiters are not typically modeled in a small signal model, it is important to demonstrate that the model is acceptable for a reasonable size of disturbance.

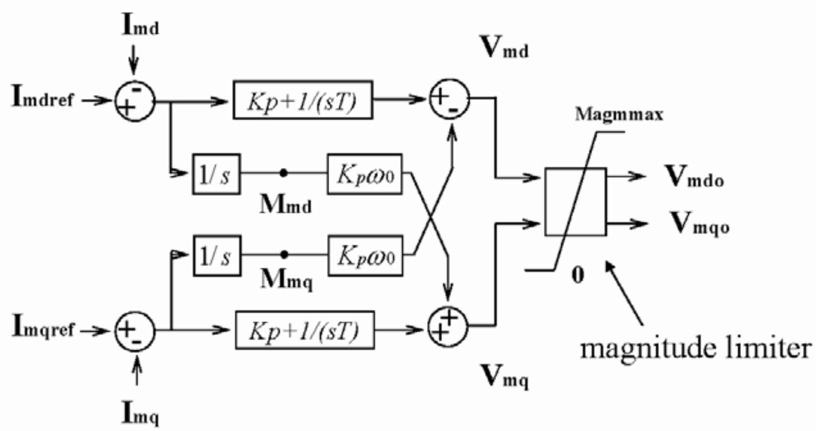


Figure 4.22 Decoupled controller of IPFC's master branch with limiter implemented

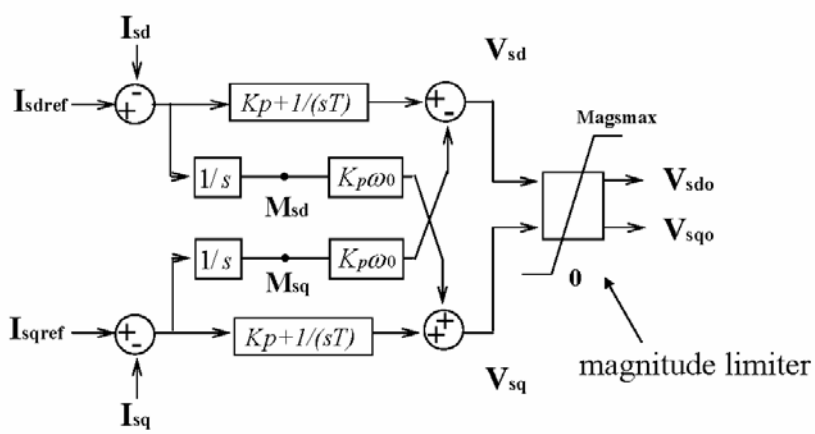


Figure 4.23 Decoupled controller of IPFC's slave branch with limiter implemented

As shown in Figure 4.22 and Figure 4.23, the IPFC controller limits the injected voltage magnitude $\sqrt{Vd0^2 + Vq0^2}$ to the rated maximum (Magmmax and Magsmax, respectively, for the master and slave converters).

Figure 4.24 shows the speed ω3 (also see Figure 4.7), for step changes of 2%, 8% and 14% respectively. The curves are normalized to the step disturbance size, so they can be overlaid for comparison. The IPFC controller ceiling (See Figure 4.24) was found to be reached only for the 14% step. From a visual inspection, the curves for 2% and 8% disturbance have similar shapes, and hence similar frequency and damping to that predicted by the small signal model (note that the curve for 2% damping was earlier shown to be identical to that from the small signal model - Figure 4.7, ω3 graph). However, once a controller limit is reached for the 14% step, the response become oscillatory and completely different from that predicted by the small signal model, indicating that the small signal model is no longer valid for this size of step change.

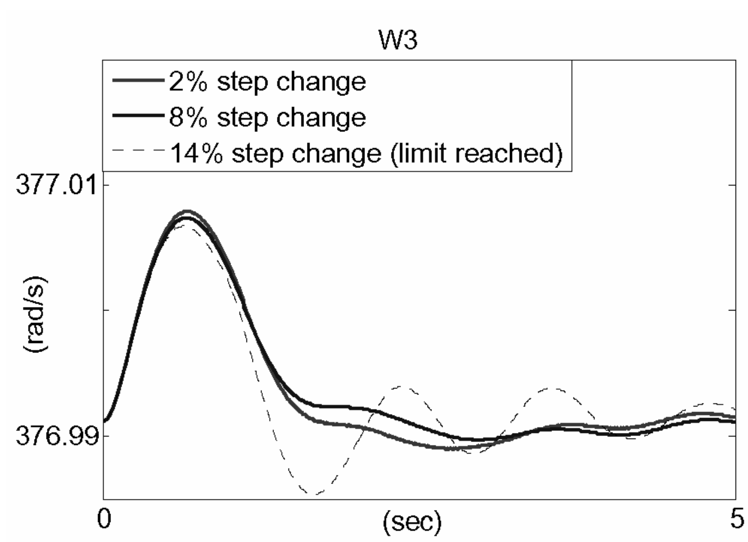


Figure 4.24 The responses of the generator speed for different step changes

### 4.5.2 Computer Simulation Time

The simulation time in the PSCAD/EMTDC for the benchmark system plus the FACTS devices is summarized in Table 4-2. All simulations were done on a 2.6G Hz, 512M Ram Pentium computer running under Window XP. The simulations were for a 5 second real time interval and with a time step of 1μs.

Table 4-2 Simulation time in PSCAD/EMTDC

| Model | Simulation time (hour) |
|---|---|
| Benchmark system | 0.25 |
| Benchmark system + IPFC | 0.50 |
| Benchmark system + UPFC | 0.50 |

These simulation times are large but manageable to conduct many studies. For a bigger system the time would become unmanageably large. As the simulation time is manageable and most typical oscillation modes observed in larger systems are also present, the size of the selected system is acceptable.

### 4.5.3 Incorporating the small signal model into an existing tools

This section briefly discusses how to incorporate the small signal model into an existing small signal analysis tool.

The small signal models of the IPFC and UPFC were thoroughly validated by comparison with detailed EMT simulation. It should be noted that, although a small 12 bus system was used to validate the model, the small signal models of the IPFC and the UPFC devices presented have been developed as sets of equations that are independent of the network. The developed models interact with the network through injection of currents into the network (see equations (2.18), (2.19), (2.35) and (2.36)). These validated models can be included in commercial programs, such as PSSE or SSAT by adding the models into the model library. Both these commercial programs use current injection type models to integrate dynamic devices with the network. Therefore the developed models are compatible with such tools. The computation times mentioned in the previous section is not a concern because PSCAD/EMTDC was used only for the purpose of validating the model. When the developed model is integrated into a small signal analysis tool, the small signal analysis of a given network no longer requires an EMT simulation.

## Summary

In this chapter, the validations for the small signal models of the IPFC and the UPFC were presented. The validations were carried out in the PSCAD/EMTDC simulations, and the results from PSCAD were compared with results from Matlab in which the small signal model state equations were used for numerical simulations.

The validation shows the IPFC small signal model is in agreement with PSCAD, while the UPFC model differs slightly with PSCAD. The errors result from the simplification of the UPFC shunt branch. Validation analysis shows the errors will not have an impact on the small signal studies of major electromechanical oscillation modes. Thus the models can be used for the small signal studies in the next chapter.

# Chapter 5 Small Signal Analysis of Transmission Systems

Once the small signal models of the network are set up and validated, small signal analysis can be carried out to investigate the stability of the system. In this chapter the impacts of FACTS devices on the 12 bus network described in Chapter 3.1 are exhibited by comparing the performance of the network before and after installing FACTS devices. It shows that the IPFC and the UPFC can significantly improve the low frequency oscillation performance and offer other interesting damping solutions.

## 5.1 Small Signal Analysis of the Network Embedded with the IPFC and the UPFC

This section reveals the damping performance of the IPFC and the UPFC. The eigenvalue information of the original network is obtained first. It is then compared with the network with the IPFC and the UPFC respectively.

### 5.1.1 Eigenvalue Information of the Original Network

The preferred location of the IPFC and the UPFC is determined based on power flow control considerations. In the system, (Figure 5.1) the main purpose of the added devices is to relieve the overloading in line 1-6. This can be realized by placing the series branch of the IPFC in line 1-6. Congestion control is also possible with the use of a UPFC type FACTS device, in which the UPFC series element is inserted in line 1-6. However in this case, the power spills over into alternate paths 7-8 and 1-2 based on the relative impedance of each branch.

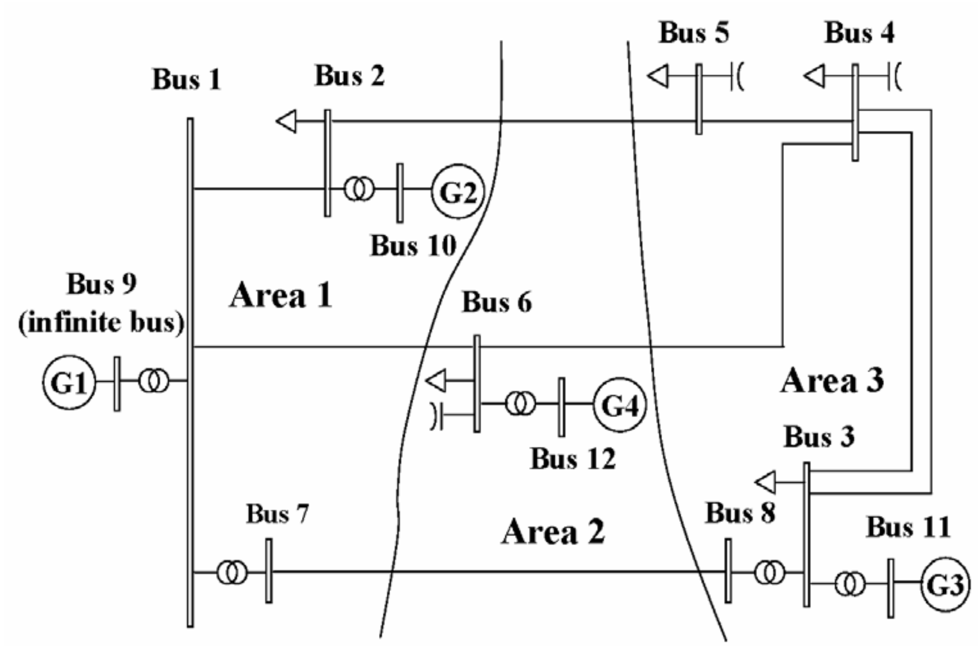


Figure 5.1 Single line diagram of 12 bus system (repeat of Figure 3.1)

With an IPFC, the second branch can be inserted in alternate line 7-8, thereby allowing precise control in two transmission lines. Thus, from the perspective of power flow control, the IPFC is a better option as it allows precise power transfer levels on two lines. Simulations on the UPFC are also conducted to see how the IPFC compares with the UPFC.

The following five cases are considered:

Case 1: the original system without any FACTS device.

Case 2: An IPFC is placed in lines 1-6 and 7-8: it relieves congestion of line 1-6 and improves the utilization of the transfer capacity of line 7-8;

Case 3: A UPFC is placed in line 1-6: it relieves congestion of line 1-6, but the extra power sent to Area 3 is on lines 7-8 and 1-2, which may result in the possibility of loop flow of power.

Case 4: A UPFC is placed in line 7-8: it transfers more power through line 7-8. It will relieve the congestion of line 1-6, but also may result in undesirable loop flow in line 1-2;

Case 5: An IPFC is placed in lines 1-2 and 7-8: it transfers more power through line 7-8, but line 1-6 (congested line) is not directly controlled by the IPFC.

In the above cases, cases 2 & 4 directly control the power flow in line 1-6. In Case 5 the FACTS device does not directly control power flow on the congested line, but indirectly de-congests it by controlling flow on alternate corridors.

The developed small signal models were used to investigate the damping performance of the IPFC and the UPFC. This section summarizes the results of this study.

Table 5-1 Oscillation modes without FACTS

| Eigenvalues $\lambda = \sigma \pm j\omega$ | Frequency (Hz) | Damping ratio (%) | Dominant generator |
|---|---|---|---|
| -0.058±5.331i | 0.84 | 1.08 | G2 |
| -0.222±7.069i | 1.12 | 3.15 | G3 |
| -0.320±4.728i | 0.75 | 6.76 | G4 |

Before the investigation of the performances of the FACTS devices, it is necessary to have a global picture of the small signal stability of the original network. Consider the base case (Case 1) where no FACTS device is installed. Each of the three generators (third order model) and exciter (first order model) introduces four states. Therefore, without any FACTS device the system has 12 states. Eigenvalue analysis shows that there are three pairs of complex conjugate eigenvalues corresponding to lower frequency electromechanical modes (see Table 5.1).

Further information about the oscillation modes can be obtained from mode shapes and the participation factors.

The mode shape given by the right eigenvector reflects the degrees of activity of state variables in a particular mode. The elements of the right eigenvector indicate the response of state variables when the corresponding mode is excited. Therefore, by observing the magnitude and phase of the elements of the eigenvector corresponding to the state variables $\delta_2$, $\delta_3$, and $\delta_4$, one can predict the relative magnitudes and phase angles of the rotor oscillations when the particular mode is excited. This information can be plotted on the complex plane to obtain what is known as the mode shape [8]. The modes shapes of the three oscillatory modes are shown in Figure 5.2, Figure 5.3, and Figure 5.4.

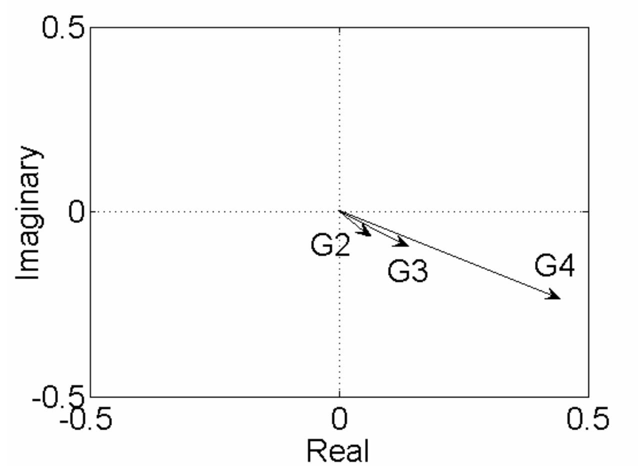


Figure 5.2 Mode shape of 0.75Hz

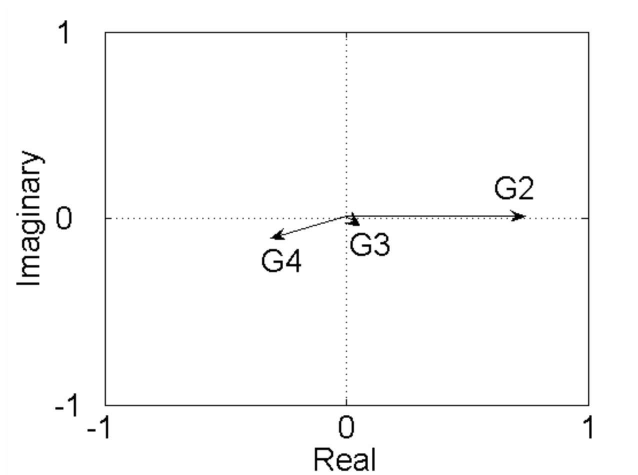


Figure 5.3 Mode shape of 0.85Hz

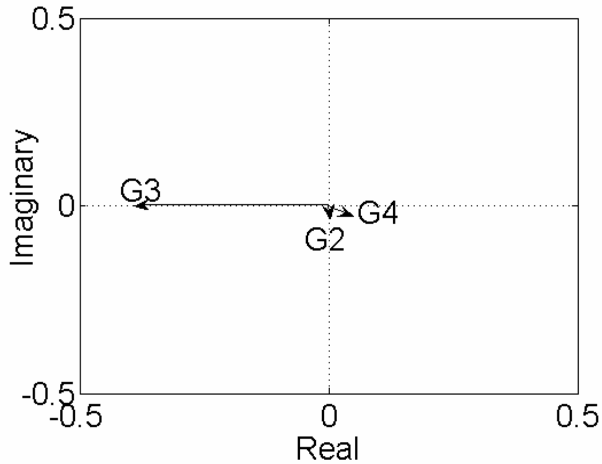


Figure 5.4 Mode shape of 1.12Hz

It is evident from these diagrams that the rotor angle of G4 oscillates when the 0.75 Hz mode is excited (Figure 5.2). Although $\delta_2$ and $\delta_3$ oscillate too, the largest impact of mode 0.75 Hz is on $\delta_4$. Or in other words, the mode 0.75Hz is dominated by generator 4. Similarly Figure 5.3 and Figure 5.4 show that mode 0.85Hz and mode 1.12 Hz are dominated by G2 and G3 respectively. In the following discussion, these modes are referred to as Mode 2, Mode 3 and Mode 4 respectively to associate the mode with the generator (G2, G3 and G4) that dominates the particular mode.

Table 5-2 Participation factors—Case 1 (no FACTS)

| Dynamic device | State | Mode 2 0.85 hz | Mode 3 1.12 hz | Mode 4 0.75 hz |
|---|---|---|---|---|
| G2 | $\delta_2$&$\omega_2$ | **0.46** | 0.00 | 0.04 |
| | $E'_{q2}$ | 0.01 | 0.00 | 0.01 |
| | $E'_{fd2}$ | 0.00 | 0.00 | 0.00 |
| G3 | $\delta_3$&$\omega_3$ | 0.00 | **0.49** | 0.03 |
| | $E'_{q3}$ | 0.00 | 0.04 | 0.01 |
| | $E'_{fd3}$ | 0.00 | 0.01 | 0.00 |
| G4 | $\delta_4$&$\omega_4$ | 0.04 | 0.02 | **0.47** |
| | $E'_{q4}$ | 0.00 | 0.00 | 0.06 |
| | $E'_{fd4}$ | 0.00 | 0.00 | 0.01 |

The participation factor combines the left and right eigenvector to measure the association between the states and the modes. A larger participation factor represents a larger weighting of a state variable in a given mode [57] [58]. The participation factors (Table 5.2) of the three modes also indicate that the three oscillation modes are dominated by generators G2, G3 and G4 respectively. It should be noted that all the three modes have low damping, with Modes 2 and 3 being critical (damping < 5%).

### 5.1.2 Damping Performance Studies

This section discusses the damping performances of the IPFC and the UPFC in the 12 bus network. Through the studies of the five cases, it can be noticed that in all these cases the UPFC and IPFC introduce additional modes but not in the critical low frequency electromechanical range of concern.

The impact of FACTS on electromechanical modes is shown in Table 5.3.

Table 5-3 Oscillation modes of Case1-Case5

| Dominant generators | | **Case 1** No FACTS | **Case 2** IPFC on line 1-6 and 7-8 | **Case 3** UPFC on 1-6 | **Case 4** UPFC on 7-8 | **Case 5** IPFC on line 1-2 and 7-8 |
|---|---|---|---|---|---|---|
| G2 | f (hz) | 0.85 | 0.84 | 0.84 | 0.84 | **0.23** |
| | damp | 1.0% | 1.4% | 1.1% | 0.7% | **35%** |
| G3 | f (hz) | 1.12 | **1.02** | 1.12 | **1.03** | **1.01** |
| | damp | 3.1% | **14%** | 3.1% | **21%** | **14%** |
| G4 | f (hz) | 0.75 | **0.69** | **0.58** | 0.80 | 0.73 |
| | damp | 6.5% | **50%** | **29%** | 11% | 18% |

It is clear from Table 5.3 that once the series branch of the UPFC or the IPFC is inserted at the sending end of a line that has a generator connected close to its receiving end, it changes the dominant oscillation mode associated with that generator, both in frequency and damping. Those modes whose dominant generators are electrically remote to the FACTS installed line are only marginally affected.

To explain the above observation, the participation factors for Cases 2 - 5 are investigated. The participation factors indicate the association of a state with a certain mode.

Table 5-4 Participation factors of Case 3—UPFC in line 1-6

| Dynamic device | State | Mode 2 0.84 hz | Mode 3 1.12 hz | Mode 4 0.57 hz |
|---|---|---|---|---|
| G2 | δ2&ω2 | **0.50** | 0.00 | 0.01 |
| G3 | δ3&ω3 | 0.00 | **0.49** | 0.04 |
| G4 | δ4&ω4 | 0.00 | 0.02 | **0.66** |
| UPFC | $V_{dc}$ | 0.00 | 0.00 | 0.00 |
| | $M_{dc}$ | 0.00 | 0.00 | 0.00 |
| | $M_{bd}$ | 0.00 | 0.00 | **0.13** |
| | $M_{bq}$ | 0.00 | 0.00 | 0.05 |
| | $M_{ed}$ | 0.00 | 0.00 | 0.00 |
| | $M_{eq}$ | 0.00 | 0.00 | 0.00 |

According to Table 5.4, Modes 2 and 3 are still dominated by G2 and G3 because their states δ and ω have the largest participation factors in these modes. This means, the UPFC on line 1-6 did not change the association of G2 and G3 to the Modes 2 and 3 respectively. However, for Mode 4, in addition to G4, the UPFC state $M_{bd}$ also shows a large participation factor. This is expected because the UPFC is located in line 1-6 which is connected to G4.

Note that state $M_{bd}$ is the integral of UPFC's series branch d-axis current component $I_{bd}$. Therefore, the large participation factor means that the series branch of the UPFC has a significant participation in Mode 4.

Similar participation of the Series Branch can be noticed in other cases too. In the case of IPFC (Cases 2 and 5), the difference is that due to the coupling introduced by the IPFC, both generators at the ends of the two lines participate in the corresponding modes. This is evident in Table 5.5 where Mode 4 has both G3 and G4 participating in it in addition to the two series branches of the IPFC. The UPFC on the other hand does not introduce such coupling.

Table 5-5 Participation factors of Case 2— IPFC in line 1-6 and 7-8

| Dynamic device | State | Mode 2 0.84 Hz | Mode 3 1.02 Hz | Mode 4 0.69 Hz |
|---|---|---|---|---|
| G2 | δ2&ω2 | **0.51** | 0.01 | 0.01 |
| G3 | δ3&ω3 | 0.01 | **0.59** | **0.23** |
| G4 | δ4&ω4 | 0.01 | 0.09 | **0.41** |
| IPFC | $V_{dc}$ | 0.00 | 0.00 | 0.00 |
| | $M_{dc}$ | 0.00 | 0.00 | 0.00 |
| | $M_{md}$ | 0.00 | 0.00 | **0.11** |
| | $M_{mq}$ | 0.00 | 0.00 | 0.01 |
| | $M_{sd}$ | 0.00 | **0.15** | **0.48** |
| | $M_{sq}$ | 0.00 | 0.00 | 0.00 |

Another point of interest is determining the effectiveness of different FACTS device types for controlling low frequency oscillations. Inspection of the controllability indices or participation factors of the low frequency modes permits this analysis.

Table 5-6 Controllability indexes of Case 2-5

| | mode | $I_{md}$ (IFPC) $I_{bd}$ (UPFC) | $I_{mq}$ (IFPC) $I_{bq}$ (UPFC) | $I_{sd}$ (IPFC) $I_{eq}$ (UPFC) |
|---|---|---|---|---|
| Case 2 | 2 | -0.2+0.0i | -0.1-0.1i | -0.0-0.3i |
| | 3 | 1.4- 0.4i | -3.4-1.6i | **-12.6-14.7i** |
| | 4 | **21.3+15.2i** | 0.1-5.2i | **2.8+43.1i** |
| Case 3 | 2 | 0.0+0.0i | -0.0-0.0i | -0.02+0.0i |
| | 3 | -0.0+0.0i | 0.0+0.1i | 0.0+0.0i |
| | 4 | **5.3-8.87i** | 4.0-1.6i | -1.3-0.4i |
| Case 4 | 2 | 0.0-0.1i | -0.1+0.1i | 0.0+0.0i |
| | 3 | **-22.2+10.6i** | 1.6-4.7i | -0.1-0.3i |
| | 4 | -4.3-5.5i | 3.4-0.5i | 0.0-0.2i |
| Case 5 | 2 | **-7.7-52.1i** | -11.3-6.0i | **3.4 -37.1i** |
| | 3 | -0.5-0.4i | -0.0-1.0i | **14.2+17.4i** |
| | 4 | -4.8+1.5i | -2.9-1.3i | **24.6-3.9i** |

In small signal analysis, controllability index indicates the influence of a given input to a mode [59]. Table 5.6 shows the controllability indexes of cases 2 - 5. In cases 2 and 5, which consider the IPFC, the column entries are those described by the 'IPFC' headings (i.e., $I_{md}$, $I_{mq}$, $I_{sd}$). For cases 3 and 4 which have the UPFC, the entries are those described by the 'UPFC' headings (i.e., $I_{bd}$, $I_{bq}$ and $I_{eq}$).

It is found that for IPFC cases 2 and 5, the largest controllability index, shown in bold, for any of the modes, is in columns corresponding to real power related variable- i.e. columns $I_{md}$ or $I_{sd}$. Similarly for the UPFC cases (Cases 3 and 4) the largest values appear in the '$I_{bd}$' column, again associated with the real power flow. This is as expected because real power plays a dominant role in sustaining or damping rotor oscillations, and hence, these variables are significantly more effective in damping than those associated with reactive power.

In Cases 2 and 5, the IPFC can control at least two modes, while in Cases 3 and 4, the UPFC can only control one mode. Again, this is as expected, because the IPFC is able to directly control the real power flow in two lines, as opposed to the UPFC which can only control the flow precisely in one line. This shows the IPFC's advantage over the UPFC for low frequency damping control.

As seen from Table 5.3, Mode 2 has very low damping (1%) and remains poorly damped in cases 2 & 4. This mode is associated with G2 oscillating against the infinite bus (See Figure 5.1), and controlling flows in 1-6 or 7-8 (as with cases 2 to 4) has negligible effect on it. On the other hand, controlling the flow in line 1-2, as in Case 5, directly affects the power exchange between G2 and the infinite bus and as seen from Table 5.3, immediately changing the mode frequency to 0.23 Hz as well as introducing significant damping (35%).

## 5.2 Interpretation of the Damping Characteristics

In a conventional damping controller such as a PSS on an electrical machine, changing the PSS gains usually retains the resonance frequencies near their original values but increases the damping. In contrast, when a UPFC or IPFC is included, the above results (Table 5.3) not only indicate improved damping, but also show significant change in the resonant frequencies (eigenvalues) of the network. This section attempts to interpret this seemingly anomalous behaviour. The UPFC is used for the purpose of explanation, but the argument applies to the IPFC as well.

### 5.2.1 Impact of Series Branch on Dynamic Performance

The series branch is the main contributing part of the UPFC and IPFC in controlling power flow. In the UPFC, the series converter is operated to provide the ordered real and reactive power into the line. For power flow control and congestion management, the series branch is given a constant real and reactive power set point, as in example cases 2-5 above. In such operations, the incremental real power $\Delta P$ (and also the reactive power $\Delta Q$) in the line is zero. From a machine acceleration point of view, this is tantamount to having no incremental power transfer through the line. With such control, the system behaves (incrementally) as if the line were not present. The validity of this statement can be checked by modeling the series branch as shown in Figure 5.5 (b), which shows the disconnection. The current sources merely represent steady state real and reactive power levels and hence do not contribute to incremental small signal dynamics.

To validate the above idea, a test case (Case 6) was created by modifying the UPFC controller case (Case 3). Line 1-6 (UPFC series branch) was cut and replaced with an equivalent circuit with one constant current source at each side of the line (Figure 5.5 (b)). The current sources do not contribute to the dynamics but only ensure that the steady state power flow at either end is maintained. If the proposed theory discussed above is valid, then the oscillation frequency and damping ought to be nearly identical to that with the UPFC in line 1-6. The eigenvalue information for the critical modes of Case 6 is shown in Table 5.7.

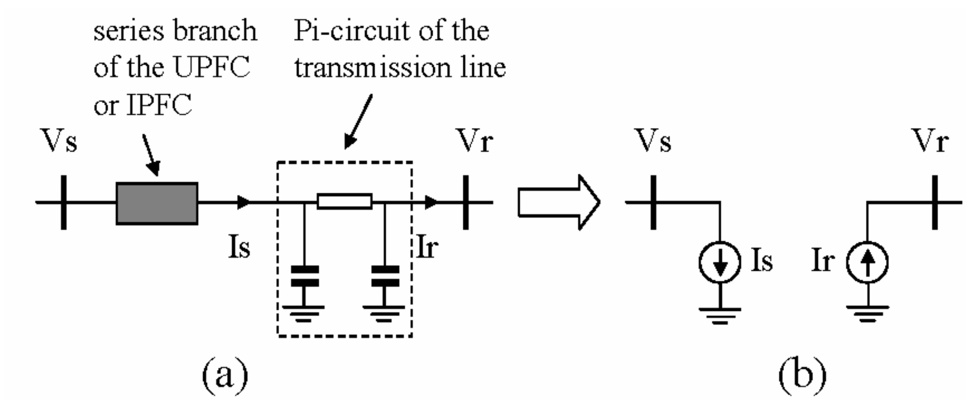


Figure 5.5 Equivalent disconnected circuit of the series branch of the UPFC or the IPFC

Table 5-7 Eigenvalue information—with model as in Figure 5.5 (b) (Case 6)

| Mode | Frequency (Hz) | Damping | Dominant state | Participation factor |
|---|---|---|---|---|
| Mode2 | 0.84 | 1.0% | $\delta 2 \& \omega 2$ | 0.50 |
| Mode3 | 1.12 | 3.1% | $\delta 3 \& \omega 3$ | 0.49 |
| **Mode4** | **0.59** | **14.0%** | $\delta 4 \& \omega 4$ | 0.55 |

In comparison with Case 3 (see Table 5.3), Case 6 (Table 5.7) shows that the frequencies and damping of the modes are in general, close, though not exactly identical. This validates the premise that using a series UPFC branch with P, Q control is tantamount to disconnecting the systems previously connected by the transmission line 1-6.

Although Case 3 and Case 6 modes are close, there is some mismatch, particularly for Mode 4, where Case 3 shows a mode frequency and damping of 0.58 Hz and 29% whereas Case 6 shows 0.59 Hz and 14%. This is due to the fact that in Case 3 the UPFC keeps the real and reactive power constant by regulating the injected voltage and the corresponding line is not really cut. As this regulation process is not perfect, the parameter setting of the UPFC has an impact on the network dynamics. Nevertheless, the mode frequencies are nearly identical and damping values are significantly higher than that for the base Case 1. The 'disconnected line' visualization is thus still generally valid.

The above analysis explains the observed mode frequencies and dampings in Table 5.3. Now the altered mode frequencies and damping can be identified as being those of a new network structure – one in which existing transmission lines have been cut. If the cut is introduced at a suitable location, the new structure can exhibit better damping. For example, segmenting the network by virtual removal of connections to distant networks could alter low frequency inter-area modes, which are often difficult to control [8].

Note that the improved dynamic behavior is a result of the segmentation of the network rather than of the selection of suitable controller parameters. This approach does not require classical feedback controller tuning methods for designing the controller, but merely requires selecting a suitable line to cut. Sometimes, flexibility may not exist in selecting the cut location, as in when a primary objective such as congestion management restricts the location. Then it is possible that the new structure may not be suitably damped. However, there is still the possibility of improving damping by using a regulator to modulate the power order of the UPFC branch in the conventional way.

A similar conclusion can be arrived at regarding the series branches of the IPFC. However, since the IPFC has two series branches, it has even more potential for cutting (i.e. segmenting) the network, in comparison to the UPFC. As seen from Table 5.3 Case 5, a suitably located IPFC is able to damp all critical modes in the test network.

## 5.2.2 Demonstration of "Cutting" Effect of UPFC Series Branch

The above visualization of the UPFC or IPFC (with a series branch operated in power control mode) as an element which disconnects the system can be demonstrated in another way.

The system in Case 3 (UPFC in line 1-6) is remodeled, but now includes an additional gain *KG* in the error paths as shown in Figure 5.6. (Note that if KG is zero, control outputs $V_{bd}$ and $V_{bq}$, and hence the injected voltage is a constant). This effectively means that for incremental small signal purposes the UPFC is not present, as the incremental injected voltage is zero. If *KG* is increased, the controller begins to regulate the real and reactive currents and maintain constant power in the corresponding branch. As discussed before, from a small signal point of view, this is like disconnecting the line that contains the UPFC series branches.

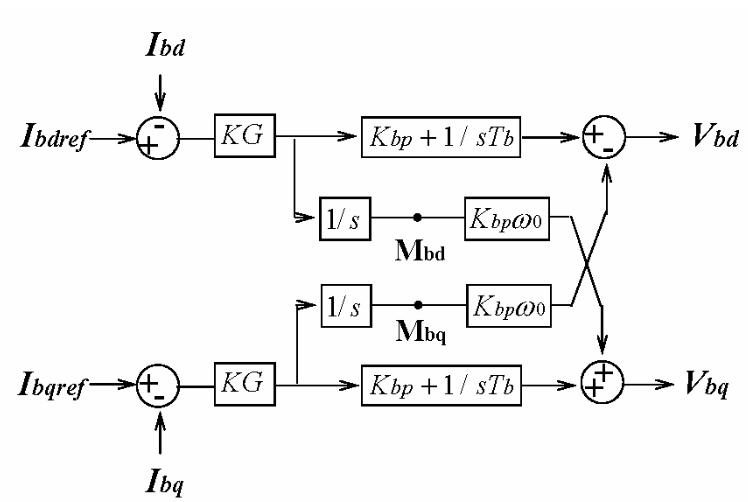


Figure 5.6 The remodelled controller of series branch of UPFC

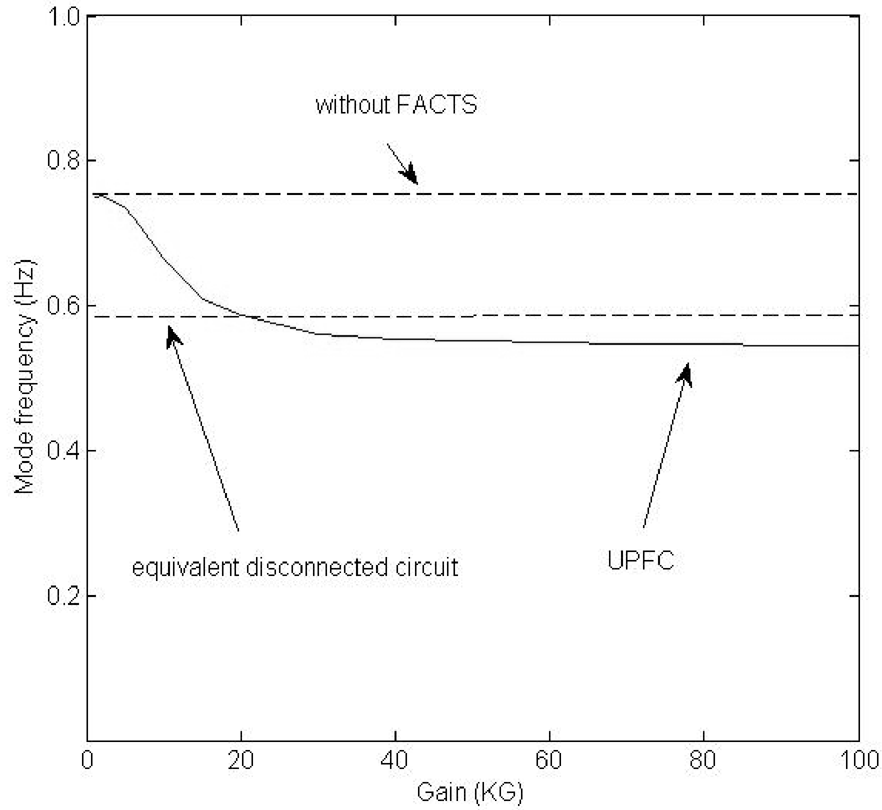


Figure 5.7 The evolution of the mode frequency of Mode 4 during tuning the series branch of UPFC and IPFC

Figure 5.7 shows the frequency of critical Mode 4 of the system for different values of *KG*. For a very small *KG,* the mode frequency is 0.75 Hz which is the same as that of the system without FACTS (Case 1). As *KG* is increased, the mode frequency moves closer to 0.59 Hz for the equivalent disconnected system of Case 6. This shows that the controller has an impact on the mode frequency. However, when the gain is large enough, the line flow is essentially constant and the disconnected visualization becomes valid.

As mentioned earlier, the "disconnection" concept is a useful approximate visualization, but with some differences with the full FACTS device representation.

## 5.3 The Impacts of the Segmentation Effect on the Network

The effect of segmentation has the advantage of mitigating any propagation of disturbances in one area into the wider network. One possible disadvantage that comes with segmentation is that it may reduce the synchronization torque on the generator shafts resulting in reduced transient rotor angle stability margins. This could be addressed by having an auxiliary controller to improve the transient stability during disturbances [60]. HVDC links operated in constant power control mode also provide the same de-coupling between the sending and receiving end systems. The above discussion indicates that the UPFC or the IPFC devices operated in constant power flow also have a similar effect. The MVA rating of the UPFC or IPFC converter branches is only a small fraction of the power transmitted between the subsystem [61]. On the other hand the converters in an HVDC link must carry the full load power. Hence it is likely that the FACTS option is more economical. This needs to be investigated further and is recommended as future work.

## Summary

The damping performance of the IPFC is evaluated using the validated IPFC small-signal model. The damping performance is also compared with that of a UPFC. The following results are obtained:

The effect of installing an IPFC or UPFC in constant power control mode for the series branch is similar to that of disconnecting the transmission line that contains the series branch. This resulting change in network structure introduces significant changes in the corresponding mode frequencies as well as mode damping.

By proper selection of the location of the series branch, the resulting network can be made to exhibit improved damping behaviour.

The improved dynamic performance is essentially caused by a virtual change in the network structure rather than by the tuning of controller parameters as is the case with most traditional approaches such as the PSS. Hence, feedback damping controller design may be avoided.

It is recommended that the open loop dynamics of the changed network be investigated with the FACTS device embedded in the network model to determine the damping of oscillatory modes of the resulting system. If poorly damped modes still exist, a suitable damping controller should be introduced that modulates the power references of the FACTS device.

As the IPFC has more series branches than the UPFC, it provides more opportunities for network segmentation and hence has the potential for greater damping improvement.

# Chapter 6 Conclusions and Future Work

## 6.1 General Conclusions

This thesis was devoted to investigate the small signal performance of FACTS devices in the power system. The small signal models of the IPFC and the UPFC were developed in which the decoupled control method was employed as the control strategy. The thesis employed a specially designed test system which is large enough to manifest typical power system dynamic behavior problems, but is also small enough for detailed EMT type simulation. An approach to validate FACTS models was proposed and tested on the benchmark system. Detailed EMTP-type simulations show close agreements with small signal analysis. From small signal point of view, the series branch of FACTS devices can change the structure of the network by means of 'segmenting' the located line. This function provides a potential approach to improve the small signal stability of the network.

Chapter 2 described the operating principle of the IPFC and UPFC. The power flow control ability of FACTS devices is mainly due to their series branches. By injecting a voltage into the series branch located transmission line, the virtual bus voltage is changed, thus the corresponding power flow can be controlled. The small signal models of the IPFC and the UPFC were derived respectively. The IPFC small signal model is an original contribution of this research. The decoupled control method was introduced in the IPFC and UPFC controllers. The decoupled control addressed the control problem caused by the cross coupling of the d, q components of transmission line voltage and current. It ensures the independent control for the real and reactive power. The details of the decoupled control were also modeled into the small signal models. It made the EMTP validation and the small signal analysis more accurate and easier.

Chapter 3 introduced the benchmark test system for FACTS devices applications. It was developed for IEEE PES WG 15.05.02 as the IEEE HVDC&FACTS system benchmark [32]. It was designed to meet both requirements of FACTS study and EMTP validation. It has typical problems which can be alleviated by FACTS devices, such as transmission congestion, loop flow, inter-area oscillations or over- or under-voltage problems; on the other hand, its adequate size insures the successful implementation of EMTP simulation without concerning the loss of computation speed. In order to make it close to the actual system, all the transmission lines are selected from the real system.

The IPFC and the UPFC were incorporated into the system. The corresponding network small signal model with embedded IPFC and UPFC were derived and linearized respectively.

Chapter 4 proposed using EMT program to validate the small signal models of the UPFC and the IPFC. Electromagnetic Transient (EMT) programs are suitable to investigate the most details of power system phenomenon, such as electromagnetic transients study and controller design. The small signal analysis investigates FACTS devices in the frequency domain. Using PSCAD/EMTDC to validate small signal studies from time domain obviously increases the model credibility.

The corresponding models of the system embedded with a UPFC and an IPFC were also built up in PSCAD/EMTDC respectively. The validation results showed that the IPFC model has a good agreement with the small signal model, while that with the UPFC is slightly different. This error of the UPFC case was determined to be caused by the omission of the impact of DC link voltage on the injected voltages in the UPFC small signal model. A refined UPFC small signal model was introduced and better comparison results were obtained.

Chapter 5 revealed the impacts of FACTS devices on the system by applying eigenvalue based small signal analysis. In contrast with the original network, the UPFC and IPFC have strong impacts on the low frequency oscillation modes, and these changes are brought out by the series branches of FACTS devices. A deduction is thereby obtained that from small signal stability point view the UPFC and the IPFC change the network structure by "cutting" the connected transmission line. The series branches of the UPFC and the IPFC are able to control the real and reactive power which is tantamount to having no incremental power transfer through the line. To examine the deduction, those transmission lines connected to FACTS were cut in the corresponding network, and the comparison results proved the "cutting" effect of the UPFC and the IPFC.

This impact on small signal stability is similar to a back-to-back HVDC link, but with a much lower MVA rating [55] because the device is connected in series and thus the voltage rating is only a fraction of the voltage rating of the power system. This at least provides an option to improve the small signal stability.

## 6.2 Main Contributions

The main contributions of the work presented in this thesis are:

- A platform for FACTS studies was successfully employed to test and validate the thesis models which had a number of problems for FACTS applications [32]. These include congestion relief, voltage support and stability improvement. The system was selected so that it is large enough to show inter-area oscillations and yet manageable so that detailed electromagnetic transient solutions are possible.

- The small signal model of the IPFC is developed. The decoupled control is employed as the control method of these models. The IPFC model with decoupled control is originally proposed. An improved small signal model of the UPFC with decoupled control under constant power control mode is developed, which is also a new contribution. These models are incorporated in the benchmark test system respectively.
- The small signal studies are carried out to investigate the performances of the IPFC and the UPFC. One finding is obtained that the series branch has strong capability to change the low oscillation mode and further to change the small signal stability of the system. As the HVDC system behaves in the system, the FACTS devices possess the function of segmenting the connected line. This structure change might result in the improvement of the small signal stability of the network.
- The comparison of the UPFC and the IPFC performance. Since the IPFC has one more series branches than the UPFC, it provides more opportunities for network segmentation and has the potential for greater damping improvement.

These contributions have led to the following publications:

- Shan Jiang, U. D. Annakkage, A. M. Gole, "A platform for validation of FACTS models", IEEE Trans, Power Delivery, vol. 21, pp. 484–491, 2006.
- Shan Jiang, A. M. Gole, U. D. Annakkage, "Damping Performance Analysis of IPFC and UPFC Controllers Using Validated Small Signal Models", accepted by IEEE Trans, Power Delivery.

## 6.3 Suggestions for Future Studies

The IPFC and UPFC have many applications in the power industry. This thesis reveals their attributes from a small signal point of view. Based on this study, the following aspects need further attention:

- **The extension of the segmentation effect to the transient stability**. In the test system of this study, the UPFC and the IPFC indeed solved congestion issues and improve the small signal stability by "cutting" the network. But it may also create a transient stability problem that did not exist before. The loss of a line implies the equivalent impedance between Area 1 and Area 3 is higher. In other words, the system is weaker, less stable or Area 1 and Area 3 are electrically farther apart. The mode frequency is a good clue: one mode frequency (0.85 Hz originally, it implies a local area damping problem) drops to 0.23 Hz after the cutting. The lower frequency implies systems that are much farther apart. Transient stability studies can be conducted by performing clearing of a three phase fault to examine the impacts on the rotor angles and transient voltages.
- **The comparison with the HVDC system**. From a small signal point of view, FACTS devices containing the series branch can change the structure of the network. This change is limited in the steady state which differs with the HVDC system isolating the network physically. If the dynamic impacts of the IPFC and the UPFC devices prove to be comparable to the HVDC system, this may result in significant cost saving because of reduced power ratings of the FACTS devices.
- **The impacts of different control modes on the small signal stability**. The cutting effect results from the zero change of the power flow under the automatic power

control (or the d, q current control) mode of the series branch. Besides the power modes, there are other optional modes that can be used for the series branch operation. Under the voltage injection mode, the series branch controls the magnitude and phase angle of the injected voltage. Without the fixed power flow, is the impact of the device on small signal stability significant? If the required improvement can not obtained directly under the voltage control mode, if a damping controller can be employed to improve the small signal stability?

# References


[1]. Hingorani, N.G., “Flexible AC transmission”, spectrum, IEEE, vol. 30, pp. 40-45, April 1993.

[2]. Song, Y.H., Allan, T.J., “Flexible ac transmission systems (FACTS)”, IEE press. UK 1999.

[3]. C. Schauder, M. Gernhardt, E. Stacey, T. Lemak, L. Gyugyi, T. W. Cease, and A. Edris, “Development of a 100MVAR static condenser for voltage control of transmission systems”, IEEE Trans, Power Delivery, vol. 10, no.3, pp. 1486–1496, Jul, 1995.

[4]. Gyugyi, L.; Schauder, C.D.; Sen, K.K.; “Static synchronous series compensator: a solid-state approach to the series compensation of transmission lines”, IEEE Trans, Power Delivery, vol. 12, Issue 1, pp.406 – 417, Jan 1997.

[5]. Sen, K.K., “SSSC-static synchronous series compensator: theory, modeling, and application”, IEEE Trans, Power Delivery, vol. 13, Issue 1, pp. 241 – 246, Jan 1998

[6]. Gyugyi, L.; Schauder, C.D.; Williams, S.L.; Rietman, T.R.; Torgerson, D.R.; Edris. A.; “The unified power flow controller: a new approach to power transmission control”, IEEE Trans, Power Delivery, vol. 10, pp. 1085 –1097, April 1995.

[7]. Gyugyi, L.; Sen, K.K.; Schauder, C.D.; “The Interline Power Flow Controller concept: a new approach to power flow management in transmission systems” IEEE Trans, Power Delivery, vol. 14, Issue 3, pp. 1115 – 1123, July 1999.

[8]. Kundur. P., “Power System Stability and Control”, McGraw-Hill, 1994.

[9]. IEEE Task Force, “Proposed terms and definitions for power system stability,” IEEE Trans, Power Apparatus and Systems, vol. PAS-101, pp. 1894–1897, July 1982.

[10]. C .Barbier, L. Carpentier, and F. Saccomanno, CIGRE SC32 Report: “Tentative classification and terminologies relating to stability problems of power systems,” ELECTRA, no. 56, 1978.

[11]. Kundur, P.; Paserba, J.; Vitet, S.; “Overview on definition and classification of

power system stability", Quality and Security of Electric Power Delivery Systems, 2003. CIGRE/PES, 2003. CIGRE/IEEE PES International Symposium, 8-10, Oct 2003.

[12]. A. M. Lyapunov, "Stability of Motion", English Translation. Academic Press, 1967.

[13]. Mohan, N.; Robbins, W.P.; Undeland, T.M.; Nilssen, R.; Mo, O.; "simulation of power electronic and motion control systems-overview", proceedings of the IEEE, vol. 82, pp. 1287-1302, Aug 1994.

[14]. Gyugyi, L., "A unified flow control concept for flexible AC transmission systems", AC and DC Power Transmission, 1991, International Conference on, pp. 19 – 26, 17-20 Sep, 1991

[15]. Nabavi-Niaki, A., Iravani, M.R., "Steady state and Dynamic Models of Unified Power Flow Controller (UPFC) for Power System Studies", IEEE Trans, Power Systems, vol. 11, Issue 4, pp. 1937 – 1943, Nov 1996.

[16]. Keri, A.J.F.; Mehraban, A.S.; Lombard, X.; Eiriachy, A.; Edris, A.A.; "Unified power flow controller (UPFC): modeling and analysis", IEEE Trans, vol. 14, pp. 648 – 654, 1999.

[17]. Limyingcharoen.S, "Application of unified power flow controllers in power system stability enhancement", Ph.D Thesis, Department of Electrical and Electronics Engineering, University of Auckland, New Zealand, March 1999.

[18]. R. Mihalic, P. Zunko, D. Povh, "Improvement of transient stability using unified power flow controller," IEEE Trans, Power Delivery, vol. 11, pp. 485–492, Jan 1996.

[19]. Papic. I., Zunko. P., Povh. D., Weinhold. M., "Basic control of unified power flow controller", IEEE Trans, Power Systems, vol. 4, pp. 1734–1739, 1997.

[20]. Wang, H.F., Swift, F.J., "A unified model for the analysis of FACTS devices in damping power system oscillations. I. Single-machine infinite-bus power systems", IEEE Trans, Power Delivery, vol. 12, Issue 2, pp. 941 – 946, April 1997.

[21]. Zhengyu Huang, Yinxin Ni, Shen, C.M., Wu, F.F., Shousun Chen, Baolin Zhang., "Application of unified power flow controller in interconnected power systems-

modeling, interface, control strategy, and case study", IEEE Trans, Power Systems, vol. 15, Issue 2, pp. 817 – 824 May 2000.

[22]. Larsen, E.V., Sanchez-Gasca, J.J., and Chow, J.H.: "Concepts for Design of FACTS Controllers to Damp Power Swings", IEEE Trans, Power systems, pp. 948 – 956, 1995.

[23]. Schauder, C.D., Gyugyi, L., Lund, M.R., Hamai, D.M., Rietman, T.R., Torgerson, D.R., Edris, A., "Operation of the unified power flow controller (UPFC) under practical constraints", IEEE Trans, Power Delivery, vol. 13, Issue 2, pp. 630 – 639, April 1998.

[24]. Zhang, X. P., "Modelling of the interline power flow controller and the generalised unified power flow controller in Newton power flow Generation, Transmission and Distribution", IEE Proceedings, vol. 150, Issue 3, pp. 268 – 274, May 2003.

[25]. Yankui Zhang, Yan Zhang, Chen Chen, "A Novel Power Injection Model of IPFC for Power Flow Analysis Inclusive of Practical Constraints", IEEE Trans, Power Systems, vol. 21, Issue 4, pp. 1550 – 1556. Nov 2006.

[26]. Arabi, S., Hamadanizadeh, H., Fardanesh, B.B., "Convertible static compensator performance studies on the NY state transmission system", IEEE Trans, Power Systems, vol. 17, pp. 701–706, 2002.

[27]. Parimi, A.M., Elamvazuthi, I., Saad, N., "Damping of inter area oscillations using Interline Power Flow Controller based damping controllers", Power and Energy Conference, 2008. IEEE 2nd International 1-3. pp. 67-72, Dec 2008

[28]. Kazemi, A., Karimi, E., "The Effect of Interline Power Flow Controller (IPFC) on Damping Inter-area Oscillations in the Interconnected Power Systems", Industrial Electronics, 2006 IEEE International Symposium on vol. 3, pp. 1911–1915, 9-13 July 2006

[29]. Xia Jiang, Xinghao Fang, Chow, J.H., Edris, A.-A., Uzunovic, E., "Regulation and Damping Control Design for Interline Power Flow Controllers", Power Engineering Society General Meeting, 2007. pp. 1-8, IEEE 24-28, June 2007

[30]. Shan Jiang, A. M. Gole, U. D. Annakkage, "Damping Performance Analysis of IPFC and UPFC Controllers Using Validated Small Signal Models", accepted by

IEEE Trans, Power Delivery

[31]. Dong, L.Y., Zhang, L., Crow, M.L., “A new control strategy for the unified power flow controller”, PES Winter Meeting, 2002. IEEE, vol. 1, pp. 562-566, Jan, 2002.

[32]. Shan Jiang, U. D. Annakkage, A. M. Gole, “A platform for validation of FACTS models”, IEEE Trans, Power Delivery, vol. 21, pp. 484–491, 2006.

[33]. Lombard, X., Therond, P.G., “Control of unified power flow controller: comparison of methods on the basis of a detailed numerical model”, IEEE Trans, Power systems, vol. 12, pp. 824-830, May 1997.

[34]. Woodford, D.; “How FACTS controllers function in an AC transmission system”, Power Engineering Society General Meeting, 2004. IEEE, vol.2, pp.1263 – 1264, June 2004.

[35]. HaiFeng. Wang, “A unified model for the analysis of FACTS devices in damping power system oscillations. III. Unified power flow controller”, IEEE Trans, Power delivery, vol. 15, pp. 978-9833, July 2000.

[36]. Arabi, S.; Kundur, P.; Adapa, R.; “Innovative techniques in modeling UPFC for power system analysis”, IEEE Trans, Power Systems, vol. 15, Issue 1, pp. 336 – 341, Feb 2000.

[37]. Jun-Yong Liu; Yong-Hua Song; Mehta, P.A.; “Strategies for handling UPFC constraints in steady-state power flow and voltage control”, IEEE Trans, Power Systems, vol. 15, Issue 2, pp. 566 – 571, May 2000.

[38]. Noroozian, M., Angquist, L., Ghandhari,M., and Anderson, G.: “Use of UPFC for Optimal Power Flow Control”, IEEE Trans, Power Delivery, vol. 12, pp. 1629 – 3634, 1997

[39]. Gotham, D.J., and Heydt, G.T.: “Power flow control and power flow studies for system with FACTS devices”, IEEE Trans, Power Systems, pp. 60 – 65, 1998.

[40]. Noroozian, M., and Andersson, G.: “Power flow control by use of controllable series components power flow control”, IEEE Trans, Power Delivery, pp. 1420 – 1429, 1993.

[41]. Kim, S.Y.; Yoon, J.S.; Chang, B.H.; Baek, D.H.; “The operation experience of KEPCO UPFC”, Electrical Machines and Systems, 2005. ICEMS 2005. Proceedings of the Eighth International Conference pp. 2502 - 2505 vol. 3, 2005.

[42]. Schauder.C, Mehta.H, "Vector analysis and control of advanced static Var compensators", Generation, Transmission and Distribution, IEE Proceedings C, vol.140, Issue.4, pp.299-306, July 1993.

[43]. Gyugyi, L., "Converter-based FACTS controllers", Flexible AC Transmission Systems-The FACTS (Ref. No. 1998/500). IET Colloquium, pp. 1/1-111, Nov 1998.

[44]. Park.R.H, "Two-Reaction Theory of Synchronous Machines Generalized Method of Analysis-Part I", AIEE Trans, vol.48, pp.716-730, July 1929.

[45]. Hauer J., C. J. Demeure and L. L. Scharf, "Initial results in Prony analysis of power system response signal", IEEE Trans, Power Systems, vo1. 5, pp. 80-89, 1990.

[46]. S. Filizadeh, M. Heidari, A. Mehrizi-Sani, J. Jatskevich, J. A. Martinez, "Techniques for Interfacing Electromagnetic Transient Simulation Programs With General Mathematical Tools", IEEE Trans, Power Delivery, vol. 23, no. 4, pp. 2610 – 2622, Oct 2008.

[47]. H. W. Dommel, "Digital computer solution of electromagnetic transients in single and multiphase networks", IEEE Trans, Power Apparatus and Systems, vol. PAS-88, no. 4, pp. 388-399, April 1969.

[48]. D. A. Woodford, A. M. Gole and R. W. Menzies, "Digital simulation of dc links and ac machines", IEEE Trans, Power Apparatus and Systems, vol. PAS-102, no. 6, pp. 1616-1623, June 1983.

[49]. N. Kolcio, J. A. Halladay, G. D. Allen, and E. N. Fromholtz, "Transient overvoltages and overcurrents on 12.47 kV distribution lines: Computer modeling results", IEEE Trans, Power Delivery, vol. 8, no. 1, pp. 359–366, Jan 1993.

[50]. Q. Bui-Van, G. Beaulieu, H. Huynh, and R. Rosenqvist, "Overvoltage studies for the St. Lawrence River 500-kV DC cable crossing", IEEE Trans, Power Delivery., vol. 6, no.3, pp. 1205–1215, Jul 1991.

[51]. A. K. S. Chaudhary, K.-S. Tam, and A. G. Phadke, "Protection system representation in the electromagnetic transients program", IEEE Trans, Power Delivery, vol. 9, no. 2, pp. 700–711, Apr 1994.

[52]. M. Saeedifard, H. Nikkhajoei, and R. Iravani, "A space vector modulation

approach for a multimodule HVDC converter system", IEEE Trans, Power Delivery, vol. 22, no. 3, pp. 1643–1654, Jul 2007.

[53]. A. M. Gole and M. Meisingset, "An AC active filter for use at capacitor commutated HVDC converters", IEEE Trans, Power Delivery, vol. 16, no. 2, pp. 335–341, Apr 2001.

[54]. C. K. Sao, P. W. Lehn, and M. R. Iravani, "A benchmark system for digital time-domain simulation of a pulse-width-modulated D-STATCOM", IEEE Trans, Power Delivery, vol. 17, no. 4, pp. 1113–1120, Oct 2002.

[55]. Hingorani, N.G., Gyugyi, L., "Understanding FACTS: Concepts and Technology of Flexible AC Transmission Systems", IEEE press. 1999.

[56]. Joseph, V., "Power Electronics Principles and Applications", McGraw-hill press, Jan 2000.

[57]. Perez-Arriaga, I.J.; Verghese, G.C.; Schweppe, F.C.; "Selective modal analysis with application to electrical power systems, Part I: Heuristic introduction", IEEE Trans, Power Apparatus and Systems, vol. PAS-101, pp. 3117-3125, 1982.

[58]. Verghese, G.C.; Perez-Arriaga, I.J.; Schweppe, F.C.; "Selective modal analysis with application to electrical power systems, Part II: the dynamic stability problem", IEEE Trans, Power Apparatus and Systems, vol. PAS-101, pp. 3126-3134, 1982.

[59]. R. E. Kalman, "Contributions to the Theory of Optimal Control", Bol. Soc. Mat. Mex. vol.5, pp. 102-199, 1960.

[60]. S. Limyingcharoen, U.D. Annakkage, N.C. Pahalawaththa, "Effects of unified power flow controllers on transient stability", IEE Proc. - Generation Trans. and Distr., vol 145, No. 2, pp 182-188, Mar 1998.

[61]. Mehraban, A.S.; Edris, A.; Schauder, C.D.; Provanzana, J.H.; "Installation, commissioning, and operation of the world's first UPFC on the AEP system", Power System Technology, 1998. Proceedings. 1998 International Conference on Volume 1, pp. 323–327, 1998.

[62]. Transmission Line Reference Book (345 kV and Above), 2nd Ed. Revised, EPRI, 1987, Palo Alto, CA, USA, page 39.

# List of Symbols

| | |
|---|---|
| $V_s$: | sending end voltage vector of the UPFC |
| $V_{sx}$: | real component of $V_s$ |
| $V_{sy}$: | imaginary component of $V_s$ |
| $V_{m1}$: | sending end voltage vector of the master branch of the IPFC |
| $V_{m1x}$: | real component of $V_{m1}$ |
| $V_{m1y}$: | imaginary component of $V_{m1}$ |
| $V_{m2}$: | receiving end voltage vector of the master branch of the IPFC |
| $V_{m2x}$: | real component of $V_{m2}$ |
| $V_{m2y}$: | imaginary component of $V_{m2}$ |
| $V_m$: | injected voltage vector of the master branch of the IPFC |
| $V_{mx}$: | real component of $V_m$ |
| $V_{my}$: | imaginary component of $V_m$ |
| $V_{s1}$: | sending end voltage vector of the slave branch of the IPFC |
| $V_{s1x}$: | real component of $V_{s1}$ |
| $V_{s1y}$: | imaginary component of $V_{s1}$ |
| $V_{s2}$: | receiving end voltage vector of the slave branch of the IPFC |
| $V_{s2x}$: | real component of $V_{s2}$ |
| $V_{s2y}$: | imaginary component of $V_{s2}$ |
| $V_s$: | injected voltage vector of the slave branch of the IPFC |
| $V_{sx}$: | real component of $V_s$ |
| $V_{sy}$: | imaginary component of $V_s$ |
| | |
| $V_r$: | receiving end voltage vector of the UPFC |
| $V_{rx}$: | real component of $V_r$ |
| $V_{ry}$: | imaginary component of $V_r$ |
| $V_b$: | booster voltage vector of the UPFC |
| $V_e$: | exciter voltage vector of the UPFC |
| $V_{bdq}$: | in phase-quadrature (d-q) vector of the booster voltage of the UPFC |

| | |
|---|---|
| $V_{bd}$: | d component of $V_{bdq}$ |
| $V_{bq}$: | q component of $V_{bdq}$ |
| $V_{edq}$:I | in phase-quadrature (d-q) vector of the exciter voltage of the UPFC |
| $V_{ed}$: | d component of $V_{edq}$ |
| $V_{eq}$: | q component of $V_{edq}$ |
| $V_{mdq}$: | in phase-quadrature (d-q) vector of the injected voltage of the master branch of the IPFC |
| $V_{md}$: | d component of $V_{mdq}$ |
| $V_{mq}$: | q component of $V_{mdq}$ |
| $V_{sdq}$: | in phase-quadrature (d-q) vector of the injected voltage of the slave branch of the IPFC |
| $V_{sd}$: | d component of $V_{sdq}$ |
| $V_{sq}$: | q component of $V_{sdq}$ |
| | |
| $V_{dc}$: | voltage of the DC bus of the UPFC and the IPFC |
| $V_{dcr}$: | reference of the DC bus voltage of the UPFC and the IPFC |
| $I_b$: | vector of the current flowing through the booster transformer of the UPFC |
| $I_{bx}$: | real component of $I_b$ |
| $I_{by}$: | imaginary component of $I_b$ |
| $I_{bdq}$: | in phase-quadrature (d-q) vector of the booster current of the UPFC |
| $I_{bd}$: | d component of $I_{bdq}$ |
| $I_{bq}$: | q component of $I_{bdq}$ |
| $I_e$: | vector of the current flowing through the exciter transformer of the UPFC |
| $I_{ex}$: | real component of $I_e$ |
| $I_{ey}$: | imaginary component of $I_e$ |
| $I_{edq}$: | in phase-quadrature (d-q) vector of the exciter current of the UPFC |

| | |
|---|---|
| $I_{ed}$: | d component of $I_{edq}$ |
| $I_{eq}$: | q component of $I_{edq}$ |
| $I_m$: | vector of the current flowing through the master transformer of the IPFC |
| $I_{mx}$: | real component of $I_m$ |
| $I_{my}$: | imaginary component of $I_m$ |
| $I_{mdq}$: | in phase-quadrature (d-q) vector of the master line current of the IPFC |
| $I_{md}$: | d component of $I_{mdq}$ |
| $I_{mq}$: | q component of $I_{mdq}$ |
| $I_s$: | vector of the current flowing through the slave transformer of the IPFC |
| $I_{sx}$: | real component of $I_s$ |
| $I_{my}$: | imaginary component of $I_s$ |
| $I_{sdq}$: | in phase-quadrature (d-q) vector of the slave lineh current of the IPFC |
| $I_{sd}$: | d component of $I_{sdq}$ |
| $I_{sq}$: | q component of $I_{sdq}$ |
| $T1$: | transform matrix from d-q coordinate to x-y coordinate |
| $C_{dc}$: | capacitance of the DC link of the UPFC and the IPFC |
| $Z_b=R_b+jX_b$: | impedance of the booster transformer of the UPFC |
| $R_b$: | resistance of the booster transformer of the UPFC |
| $X_b$: | reactance of the booster transformer of the UPFC |
| $Z_e=R_e+jX_e$: | impedance of the exciter transformer of the UPFC |
| $R_e$: | resistance of the exciter transformer of the UPFC |
| $X_e$: | reactance of the exciter transformer of the UPFC |
| $Z_m=R_m+jX_m$: | impedance of the master transformer of the IPFC |
| $R_m$: | resistance of the master transformer of the IPFC |
| $X_m$: | reactance of the master transformer of the IPFC |
| $Z_s=R_s+jX_s$: | impedance of the salve transformer of the IPFC |
| $R_s$: | resistance of the slave transformer of the IPFC |

| | |
|---|---|
| $X_s$: | reactance of the slave transformer of the IPFC |
| $S_b$: | system base MVA |
| $P_b$: | real power flowing from the DC bus to the booster transformer of the UPFC |
| $P_e$: | real power flowing from the exciter transformer to the DC bus of the UPFC |
| $P_m$: | real power flowing from the DC bus to the master transformer of the IPFC |
| $P_s$: | real power flowing from the DC bus to the slave transformer of the IPFC |
| $K_{pdc}$: | proportional gain of DC link PI controller of the UPFC or the IPFC |
| $K_{idc}$: | integral gain of DC link PI controller of the UPFC or the IPFC |
| $U_{bd}$: | control input of d component of booster current of the UPFC |
| $U_{bq}$: | control input of q component of booster current of the UPFC |
| $U_{ed}$: | control input of d component of exciter current of the UPFC |
| $U_{eq}$: | control input of q component of exciter current of the UPFC |
| $U_{md}$: | control input of d component of master line current of the IPFC |
| $U_{mq}$: | control input of q component of master line current of the IPFC |
| $U_{sd}$: | control input of d component of slave current of the IPFC |
| $U_{sq}$: | control input of q component of slave current of the IPFC |
| $M_{dc}$: | state variable introduced by the DC link PI controller of the UPFC or the IPFC |
| $M_{bd}$, $M_{bq}$: | state variables introduced by the decoupled controller of the booster branch of the UPFC |
| $M_{ed}$, $M_{eq}$: | state variables introduced by the decoupled controller of the exciter branch of the UPFC |
| $M_{md}$, $M_{mq}$: | state variables introduced by the decoupled controller of the master branch of the IPFC |
| $M_{sd}$, $M_{sq}$: | state variables introduced by the decoupled controller of the slave branch of the IPFC |

$K_{bp}$: proportional gain of the decoupled controller of the booster branch of the UPFC

$T_b$: time constant of the decoupled controller of the booster branch of the UPFC

$K_{ep}$: proportional gain of the decoupled controller of the exciter branch of the UPFC

$T_e$: time constant of the decoupled controller of the exciter branch of the UPFC

$K_{mp}$: proportional gain of the decoupled controller of the master branch of the IPFC

$T_m$: time constant of the decoupled controller of the master branch of the IPFC

$K_{sp}$: proportional gain of the decoupled controller of the slave branch of the IPFC

$T_s$: time constant of the decoupled controller of the slave branch of the IPFC

$A_{up}$: state matrix of the linearized state-space model of the UPFC

$A_{ip}$: state matrix of the linearized state-space model of the IPFC

$B_{up}$: control matrix of the linearized state-space model of the UPFC

$B_{ip}$: control matrix of the linearized state-space model of the IPFC

$E_{up}$, $F_{up}$: coefficient matrix of the linearized state-space model of the UPFC

$E_{ip}$, $F_{ip}$, $G_{ip}$, $H_{ip}$: coefficient matrix of the linearized state-space model of the IPFC

$const\_M_{bd}$, $const\_M_{bq}$: coefficient of coefficient matrix $E_{up}$

$const\_M_{md}$, $const\_M_{mq}$: coefficient of coefficient matrix $E_{ip}$

$const\_M_{sd}$, $const\_M_{sq}$: coefficient of coefficient matrix $G_{ip}$

$X_{up}$: state vector of the UPFC

$X_{ip}$: state vector of the IPFC

$U_{up}$: control vector of the UPFC

| | |
|---|---|
| $U_{ip}$: | control vector of the IPFC |
| $T2 \sim T46$: | coefficient matrices of the linearized state-space model of the UPFC or the IPFC |
| $\theta$: | phase angle of the sending voltage $V_s$ of the UPFC |
| $\theta_m$: | phase angle of the sending voltage $V_{m1}$ of the IPFC master branch |
| $\theta_s$: | phase angle of the sending voltage $V_{s1}$ of the IPFC slave branch |
| $\omega_0$: | synchronous speed (constant) |
| $\omega$: | rotor angular speed (state variable) |
| $\delta$: | generator rotor angle |
| $E_q'$ : | q-axis voltage behind transient voltage |
| $E_{fd}$: | field voltage referred to the armature circuit of the generator. |
| $X_g$: | state vector of generators |
| $X_{gk}$: | state vector of the k$^{th}$ generator |
| $U_g$: | control vector of generators |
| $I_g$: | current vector of generators |
| $I_{gk}$: | current vector of the k$^{th}$ generator |
| $I_{gd}$: | d component of current vector of generators |
| $I_{gq}$: | q component of current vector of generators |
| $V_g$: | voltage vector of generators |
| $V_{gk}$: | voltage vector of the k$^{th}$ generator |
| $V_{gd}$: | d component of $V_g$ |
| $V_{gq}$: | q component of $V_g$ |
| $V_{gx}$: | real component of $V_g$ |
| $V_{gy}$: | imaginary component of $V_g$ |
| $A_g$: | state matrix of the linearized state-space model of generators |
| $A_{gk}$: | state matrix of the linearized state-space model of the k$^{th}$ generator |
| $B_g$: | control matrix of the linearized state-space model of generators |

| | |
|---|---|
| $B_{gk}$: | control matrix of the linearized state-space model of the k$^{th}$ generator |
| $E_g$: | coefficient matrix of the linearized state-space model of generators |
| $E_{gk}$: | coefficient matrix of the linearized state-space model of the k$^{th}$ generator |
| $Y_g$: | admittance matrix of the linearized state-space model of generators |
| $Y_{gk}$: | admittance matrix of the linearized state-space model of the k$^{th}$ generator |
| $Y_{ga}, Y_{gd}$: | self admittance matrix of $Y_g$ |
| $Y_{gb}, Y_{gc}$: | transfer admittance matrix of $Y_g$ |
| $S_g$: | coefficient matrix of the linearized state-space model of generators |
| $S_{gk}$: | coefficient matrix of the linearized state-space model of the k$^{th}$ generator |
| $K_a$: | gain of the automatic voltage regulator (AVR) |
| $T_a$: | time constant of the AVR |
| $H$: | rotor-turbine inertia constant |
| $D$: | damping coefficient accounting for mechanical damping losses and the effects of damping windings |
| $X_d$: | d-axis synchronous reactance of the generator |
| $X_d'$ : | d-axis transient reactance of the generator |
| $X_q$: | q-axis synchronous reactance of the generator |
| $T_m$: | mechanical torque of the generator |
| $V_{ref}$: | reference voltage of the AVR |
| $T_{d0}'$ : | d-axis open circuit transient time constant of the armature of the generator |
| $YN$: | admittance matrix of the partial network of the system |
| $YM$: | linearized admittance matrix of the system with generators and the UPFC or the IPFC incorporated |

$YM_{g,g}$, $YM_{g,s}$, $YM_{g,r}$, $YM_{g,i}$,
$YM_{s,g}$, $YM_{s,s}$, $YM_{s,r}$, $YM_{s,i}$,
$YM_{r,g}$, $YM_{r,s}$, $YM_{r,r}$, $YM_{r,i}$,
$YM_{i,g}$, $YM_{i,s}$, $YM_{i,r}$, $YM_{i,i}$, sub-matrices of *YM* associated with the UPFC

$YM_{g,g}$, $YM_{g,m1}$, $YM_{g,m2}$,
$YM_{g,s1}$, $YM_{g,s2}$, $YM_{g,i}$,
$YM_{m1,g}$, $YM_{m1,m1}$, $YM_{m1,m2}$,
$YM_{m1,s1}$, $YM_{m1,s2}$, $YM_{m1,i}$,
$YM_{m2,g}$, $YM_{m2,m1}$, $YM_{m2,m2}$,
$YM_{m2,s1}$, $YM_{m2,s2}$, $YM_{m2,i}$,
$YM_{s1,g}$, $YM_{s1,m1}$, $YM_{s1,m2}$,
$YM_{s1,s1}$, $YM_{s1,s2}$, $YM_{s1,i}$,
$YM_{s2,g}$, $YM_{s2,m1}$, $YM_{s2,m2}$,
$YM_{s2,s1}$, $YM_{s2,s2}$, $YM_{s2,i}$,
$YM_{i,g}$, $YM_{i,m1}$, $YM_{i,m2}$,
$YM_{i,s1}$, $YM_{i,s2}$, $YM_{i,i}$: sub-matrices of *YM* associated with the IPFC

*ZM*: linearized impedance matrix of the system with generators and the UPFC or the IPFC incorporated.

$ZM_{g,g}$, $ZM_{g,s}$, $ZM_{g,r}$, $ZM_{g,i}$,
$ZM_{s,g}$, $ZM_{s,s}$, $ZM_{s,r}$, $ZM_{s,i}$,
$ZM_{r,g}$, $ZM_{r,s}$, $ZM_{r,r}$, $ZM_{r,i}$,
$ZM_{i,g}$, $ZM_{i,s}$, $ZM_{i,r}$, $ZM_{i,i}$: sub-matrices of *ZM* associated with the UPFC

$ZM_{g,g}$, $ZM_{g,m1}$, $ZM_{g,m2}$,
$ZM_{g,s1}$, $ZM_{g,s2}$, $ZM_{g,i}$,
$ZM_{m1,g}$, $ZM_{m1,m1}$, $ZM_{m1,m2}$,
$ZM_{m1,s1}$, $ZM_{m1,s2}$, $ZM_{m1,i}$,
$ZM_{m2,g}$, $ZM_{m2,m1}$, $ZM_{m2,m2}$,
$ZM_{m2,s1}$, $ZM_{m2,s2}$, $ZM_{m2,i}$,
$ZM_{s1,g}$, $ZM_{s1,m1}$, $ZM_{s1,m2}$,
$ZM_{s1,s1}$, $ZM_{s1,s2}$, $ZM_{s1,i}$,
$ZM_{s2,g}$, $ZM_{s2,m1}$, $ZM_{s2,m2}$,

| | |
|---|---|
| $ZM_{s2,s1}$, $ZM_{s2,s2}$, $ZM_{s2,i}$, $ZM_{i,g}$, $ZM_{i,m1}$, $ZM_{i,m2}$, $ZM_{i,s1}$, $ZM_{i,s2}$, $ZM_{i,i}$: | sub-matrices of *YM* associated with the IPFC |
| $A$: | state matrix of the linearized state-space model of the system with generators and the UPFC or the IPFC incorporated |
| $B$: | control matrix of the linearized state-space model of the system with generators and the UPFC or the IPFC incorporated |
| $A_{GG}$, $A_{GU}$, $A_{UG}$, $A_{UU}$: | sub-matrices of $A$ associated with the UPFC |
| $B_{GG}$, $B_{GU}$, $B_{UU}$: | sub-matrices of $B$ associated with the UPFC |
| $A_{GG}$, $A_{GI}$, $A_{IG}$, $A_{II}$: | sub-matrices of $A$ associated with the IPFC |
| $B_{GG}$, $B_{GI}$, $B_{II}$: | sub-matrices of $B$ associated with the IPFC |

# Appendix A 12 Buses 3 Generators Test System

The data pertaining to the power system shown in Figure 3.1 are given in the following tables.

Table.A.1 shows: (a) the loads, and shunt compensation at load buses 1-8, and (b) the specified voltage and real power generation at generator buses 9-12. In the transient model, the loads are represented as fixed impedances.

Table A-1 Bus data

| Bus | Nominal Voltage kV | Specified Voltage kV | Load MVA | Shunt MVar | Generation MW |
|---|---|---|---|---|---|
| 1 | 230 | | | | |
| 2 | 230 | | 280+j200 | | |
| 3 | 230 | | 320+j240 | | |
| 4 | 230 | | 320+j240 | 160 | |
| 5 | 230 | | 100+j60 | 80 | |
| 6 | 230 | | 440+j300 | 180 | |
| 7 | 345 | | | | |
| 8 | 345 | | | | |
| 9 | 22 | 1.04 | | | |
| 10 | 22 | 1.02 | | | 500 |
| 11 | 22 | 1.01 | | | 200 |
| 12 | 22 | 1.02 | | | 300 |

The geometrical and physical parameters for the transmission lines are as shown in Table A-2 and Figure A.1. All 230 kV lines are assumed to have the same geometrical and physical parameters (except for different lengths). The 230 kV line is based on Manitoba Hydro's Glenboro-South to Rugby line. The 345 kV line has a typical structure selected from Table 2.7.1 of the EPRI "transmission line reference book" [62]. Table.A.3 shows the line lengths for each of the 230 kV and 345 kV lines as well as the series impedances and shunt reactances resulting from the above line geometries for an equivalent-π representation corrected for long-line effects.

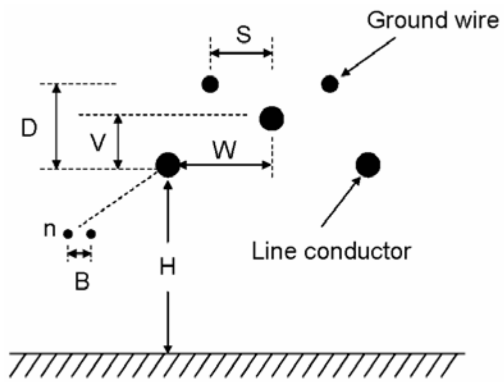


Figure A.1 Transmission line structure

Table A-2 The configuration of transmission line

| Voltage(kV) | 230 | 345 |
|---|---|---|
| Structure type | 3H6 | 3H6 |
| H (m) | 14.4 | 17.526 |
| V (m) | 1.22 | 3.505 |
| W (m) | 5.49 | 7.925 |
| Sag | 5.94 | 7.254 |
| n (Conds/bundle) | 1 | 2 |
| B (m) | 0.4572 | 0.4572 |
| Conductor type | 954ACSR 54/7 | 795ACSR 26/19 |
| DC resistance (ohms/km) | 0.0587 | 0.683 |
| Ground wires | 2 | 2 |
| S(m) | 3.05 | 4.648 |
| D(m) | 3.81 | 5.00 |
| Ground resistivity (ohms·km) | 100 | 100 |
| Sag of GW (m) | 4.45 | 7.254 |

Table A-3 Branch data (system base: 100MVA)

| Line | Voltage(kV) | Length(km) | R(pu) | X(pu) | B(pu) | Rating(MVA) |
|---|---|---|---|---|---|---|
| 1-2 | 230 | 100 | 0.01144 | 0.09111 | 0.18261 | 250 |
| 1-6 | 230 | 300 | 0.03356 | 0.26656 | 0.55477 | 250 |
| 2-5 | 230 | 300 | 0.03356 | 0.26656 | 0.55477 | 250 |
| 3-4(1) | 230 | 100 | 0.01144 | 0.09111 | 0.18261 | 250 |
| 3-4(2) | 230 | 100 | 0.01144 | 0.09111 | 0.18261 | 250 |
| 4-5 | 230 | 300 | 0.03356 | 0.26656 | 0.55477 | 250 |
| 4-6 | 230 | 300 | 0.03356 | 0.26656 | 0.55477 | 250 |
| 7-8 | 345 | 600 | 0.01595 | 0.17214 | 3.28530 | 500 |

Table A-4 Transformer data (system base: 100MVA)

| From-To | Voltage (kV) | Leakage reactance(pu) | Rating(MVA) |
|---|---|---|---|
| 1-7 | 230-345 | 0.0100 | 1000 |
| 1-9 | 230-22 | 0.0100 | 1000 |
| 2-10 | 230-22 | 0.0100 | 1000 |
| 3-8 | 230-345 | 0.0100 | 1000 |
| 3-11 | 230-22 | 0.0100 | 1000 |
| 6-12 | 230-22 | 0.0200 | 500 |

Table A-5 Generator and exciter data

| Bus | H | D | $T_{d0}'$ | Xd | Xq | Xd' | Ka | Ta |
|---|---|---|---|---|---|---|---|---|
| 10(G2) | 5.0 | 1.0 | 5.0 | 1.5 | 1.2 | 0.4 | 20 | 0.05 |
| 11(G3) | 3.0 | 0.0 | 6.0 | 1.4 | 1.35 | 0.3 | 20 | 0.05 |
| 12(G4) | 5.0 | 1.0 | 5.0 | 1.5 | 1.2 | 0.4 | 20 | 0.05 |

Table A-6 UPFC data

| Kbp | Kep | Cdc(μf) | Kpdc | Kidc |
|---|---|---|---|---|
| 20 | 100 | 1446 | 2.0 | 1.0 |

Table A-7 IPFC data

| Kmp | Ksp | Cdc(μf) | Kpdc | Kidc |
|---|---|---|---|---|
| 20 | 20 | 1446 | 2.0 | 1.0 |

# Appendix B Derivation of the Small Signal Model of the Generator and Exciter

The generators (G2, G3 and G4) with their exciters in the test 12 bus system are represented by the typical fourth order dynamic model (third order generator plus first order exciter). The dynamics of the k[th] generator and exciter are given by:

$$\dot{\delta}_k = \omega_0(\omega_k - 1) \tag{A-1}$$

$$\dot{\omega}_k = \frac{1}{2H}(Tm_k - E'_{qk} Ig_{kq} - (X_{qk} - X'_{dk}) Ig_{kd} Ig_{kq} - KD_k \omega_k) \tag{A-2}$$

$$\dot{E}'_{qk} = \frac{1}{T'_{d0k}}(E_{fdk} - E'_{qk} - (X_{dk} - X'_{dk}) Ig_{kd}) \tag{A-3}$$

$$\dot{E}fd_k = -\frac{1}{Ta_k} Efd_k + \frac{Ka_k}{Ta_k}(Vg_{kref} - Vg_k) \tag{A-4}$$

The voltage behind the transient reactance, the terminal voltage, and the terminal current are related by:

$$\begin{pmatrix} E'_{qk} \\ 0 \end{pmatrix} = \begin{pmatrix} Vg_{kq} \\ Vg_{kd} \end{pmatrix} + \begin{pmatrix} 0 & X'_{dk} \\ -Xq_k & 0 \end{pmatrix} \cdot \begin{pmatrix} Ig_{kq} \\ Ig_{kd} \end{pmatrix} \tag{A-5}$$

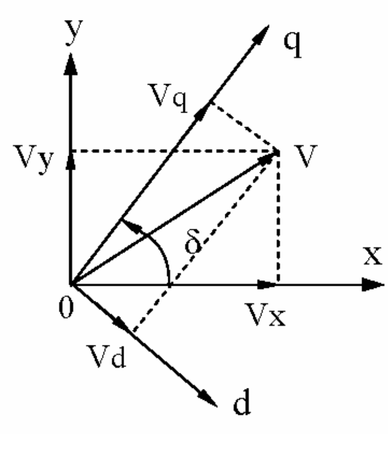


Figure B.1 dq-xy coordinate transformation

The model for synchronous generators is given in the d-q coordinate when connected to the network requiring a coordinate transformation to the x-y coordinate. This dq-xy coordinate transformation is established as shown in Figure B.1.

The relationship between the voltage behind the transient reactance and the generator terminal voltage and current in the x-y coordinate is obtained as:

$$Ig_k = Yg_k \cdot E'_{gk} - Yg_k \cdot Vg_k \tag{A-6}$$

Where:

$$Yg_k = \begin{pmatrix} Yga_k & Ygb_k \\ Ygc_k & Ygd_k \end{pmatrix}$$

$$Yga_k = (\frac{1}{Xd'_k} - \frac{1}{Xq_k}) \cdot cos\delta_k \cdot sin\delta_k \qquad Ygb_k = \frac{1}{Xq_k} \cdot cos\delta_k{}^2 + \frac{1}{Xd'_k} \cdot sin\delta_k{}^2$$

$$Ygc_k = \frac{-1}{Xd'_k} cos\delta_k{}^2 - \frac{1}{Xq_k} sin\delta_k{}^2 \qquad Ygd = -Yga$$

$$E'_{gk} = Tg_k \cdot \begin{pmatrix} E'_{qk} \\ 0 \end{pmatrix} = \begin{pmatrix} E'_{qk} \cdot cos\delta_k \\ E'_{qk} \cdot sin\delta_k \end{pmatrix}$$

$$Sg_k = \begin{pmatrix} cos\delta_k & -sin\delta_k \\ sin\delta_k & cos\delta_k \end{pmatrix}$$

The coordinate transformation between the d-q coordinate and x-y coordinate of the terminal voltage and current is given by:

$$Vg_{kqd} = Sg_k \cdot Vg_k \tag{A-7}$$

$$Ig_{kqd} = Sg_k \cdot Ig_k \tag{A-8}$$

$$Vg_k = Sg_k \cdot Vg_{kqd} \tag{A-9}$$

$$Ig_k = Sg_k \cdot Ig_{kqd} \tag{A-10}$$

Where:

$$Vg_{kqd} = \begin{pmatrix} Vg_{kq} \\ Vg_{kd} \end{pmatrix} \quad Ig_{kqd} = \begin{pmatrix} Ig_{kq} \\ Ig_{kd} \end{pmatrix} \quad Vg_k = \begin{pmatrix} Vg_{kx} \\ Vg_{ky} \end{pmatrix} \quad Ig_k = \begin{pmatrix} Ig_{kx} \\ Ig_{ky} \end{pmatrix}$$

The above equations ((A-1)-( A-10)) can be linearized to give:

$$\Delta \dot{X}g_k = Ag_k \cdot \Delta Xg_k + Bg_k \cdot \Delta Ug_k + Eg_k \cdot \Delta Vg_k \tag{A-11}$$

$$\Delta Ig_k = Sg_k \cdot \Delta Xg_k - Yg_k \cdot \Delta Vg_k \tag{A-12}$$

Where:

$$\Delta Xg_k = \begin{pmatrix} \Delta\delta_k \\ \Delta\omega_k \\ \Delta E'_{qk} \\ \Delta Efd_k \end{pmatrix} \qquad \Delta Ug_k = \begin{pmatrix} \Delta Tm_k \\ \Delta Vg_{kref} \end{pmatrix} \qquad \Delta Ig_k = \begin{pmatrix} \Delta Ig_{kx} \\ \Delta Ig_{ky} \end{pmatrix} \qquad \Delta Vg_k = \begin{pmatrix} \Delta Vg_{kx} \\ \Delta Vg_{ky} \end{pmatrix}$$

$$Ag_k = \begin{pmatrix} 0 & \omega_0 & 0 & 0 \\ Ag_{k2,1} & \frac{-D_k}{2H_k} & \frac{-Vg_{kd}}{2H_k \cdot X'_{dk}} & 0 \\ Ag_{k3,1} & 0 & \frac{-X_{dk}}{T'_{d0k} \cdot X'_{dk}} & \frac{1}{T'_{d0k}} \\ Ag_{k4.1} & 0 & 0 & \frac{-1}{Ta_k} \end{pmatrix} \qquad Bg_k = \begin{pmatrix} 0 & 0 \\ \frac{1}{2H_k} & 0 \\ 0 & 0 \\ 0 & \frac{Ka_k}{Ta_k} \end{pmatrix}$$

$$Eg_k = \begin{pmatrix} 0 & 0 \\ Eg_{k2,1} & Eg_{k2,2} \\ Eg_{k3,1} & Eg_{k3,2} \\ Eg_{k4,1} & Eg_{k4,2} \end{pmatrix} \qquad Sg_k = \begin{pmatrix} Sg_{k1,1} & 0 & \frac{sin\delta_k}{X'_{dk}} & 0 \\ Sg_{k2,1} & 0 & \frac{-cos\delta_k}{X'_{dk}} & 0 \end{pmatrix}$$

$$Yg_k = \begin{pmatrix} Yga_k & Ygb_k \\ Ygc_k & Ygd_k \end{pmatrix}$$

$$Ag_{k2,1} = \frac{1}{2H_k} \cdot ((\frac{Vg_{kd}}{X'_{dk}} - Ig_{kq}) \cdot (Vg_{ky} \cdot cos\delta_k - Vg_{kx} \cdot sin\delta_k) - (\frac{Vg_{kq}}{X_q} + Ig_{kd}) \cdot (Vg_{kx} \cdot cos\delta_k - Vg_{ky} \cdot sin\delta_k))$$

$$Ag_{k3,1} = \frac{1}{T'_{d0k}} \cdot (\frac{X_{dk}}{X'_{dk}} - 1) \cdot (Vg_{ky} \cdot cos\delta_k - Vg_{kx} \cdot sin\delta_k)$$

$$Ag_{k4,1} = \frac{-Ka_k}{Ta_k \cdot |Vg_k|} \cdot (Vg_{kq} \cdot (Vg_{ky} \cdot cos\delta_k - Vg_{kx} \cdot sin\delta_k) + Vg_{kd} \cdot (Vg_{kx} \cdot cos\delta_k + Vg_{ky} \cdot sin\delta_k))$$

$$Eg_{k2,1} = \frac{1}{2H_k} \cdot ((\frac{Vg_{kd}}{X_{dk}^{'}} - Ig_{kq}) \cdot cos\delta_k - (\frac{Vg_{kq}}{X_{qk}} + Ig_{kd}) \cdot sin\delta_k))$$

$$Eg_{k2,2} = \frac{1}{2H_k} \cdot ((\frac{Vg_{kd}}{Xd^{'}} - Ig_{kq}) \cdot sin\delta_k + (\frac{Vg_{kq}}{X_{qk}} + Ig_{kd}) \cdot cos\delta_k))$$

$$Eg_{k3,1} = \frac{1}{T_{d0k}^{'}} \cdot (\frac{Xd_k}{Xd^{'}_k} - 1) \cdot cos\delta_k \qquad Eg_{k3,2} = \frac{1}{T_{d0k}^{'}} \cdot (\frac{Xd_k}{Xd^{'}_k} - 1) \cdot sin\delta_k$$

$$Eg_{k4,1} = \frac{-Ka_k}{Ta_k \cdot |Vg_k|} \cdot (Vg_{kq} \cdot cos\delta_k + Vg_{kd} \cdot sin\delta_k) = \frac{-Ka_k}{Ta_k \cdot |Vg_k|} \cdot Vg_{kx}$$

$$Eg_{k4,2} = \frac{-Ka_k}{Ta_k \cdot |Vg_k|} \cdot (Vg_{kq} \cdot sin\delta_k - Vg_{kd} \cdot cos\delta_k) = \frac{-Ka_k}{Ta_k \cdot |Vg_k|} \cdot Vg_{ky}$$

$$Yga_k = (\frac{1}{Xd^{'}_k} - \frac{1}{Xq_k}) \cdot cos\delta_k \cdot sin\delta_k \qquad Ygb_k = \frac{1}{Xq_k} \cdot cos\delta_k{}^2 + \frac{1}{Xd^{'}_k} \cdot sin\delta_k{}^2$$

$$Ygc_k = \frac{-1}{Xd^{'}_k} cos\delta_k{}^2 - \frac{1}{Xq_k} sin\delta_k{}^2 \qquad Ygd = -Yga$$

$$Sg_{k1,1} = -Ig_{kq} \cdot sin\delta_k + Ig_{kd} \cdot cos\delta_k - Vg_{ky} \cdot Yga_k + Vg_{kx} \cdot Ygb_k$$

$$Sg_{k2,1} = Ig_{kq} \cdot cos\delta_k + Ig_{kd} \cdot sin\delta_k - Vg_{ky} \cdot Ygc_k + Vg_{kx} \cdot Ygd_k$$

# Appendix C Derivation of the Small Signal Model of the 12 Bus Test System with Embedded IPFC

The derivation of the small signal model of the network includes two steps:

(1) To derive the small signal models of all dynamic components of the network, i.e., the small signal models of the IPFC, generators and exciters.

(2) To incorporate the above models into the network in order to obtain the linearized state equation of the network.

## C.1 Small Signal Model of the IPFC

### C.1.1 State Equations and Algebraic Equations of the IPFC

The line possessing two degrees of freedom (see Figure 2.2) is called 'master line', and the other line is called the 'slave line'. All variables related to the master line and the slave line are denoted with the subscripts 'm' and 's' respectively. Three coordinate systems are adopted in this model. The master line and slave line sending end voltage vectors ($V_{m1}$, $V_{s1}$) are selected as the d-axis of the master line's and slave line's coordinate systems separately, thus the real and reactive power ($P_m$, $Q_m$, $P_s$, and $Q_s$) can be represented by their corresponding d, q current components ($I_{md}$, $I_{mq}$, $I_{sd}$ and $I_{sq}$). The other coordinate system is the network's coordinate system (x-y system) which takes the infinite bus voltage as its x-axis. All vectors of the network are finally expressed as x-y components.

The DC capacitor dynamics is modeled by:

$$C_{dc} \cdot V_{dc} \cdot \frac{d}{dt} V_{dc} = -S_b \cdot (P_s + P_m) - \frac{V_{dc}^2}{R_{dc}} \tag{C-1}$$

Where:

$C_{dc}$: the capacitance of the dc bus capacitor.

$V_{dc}$: the voltage of the dc bus.

$P_m$: the real power flowing out of the dc link into the master line of the IPFC.

$P_s$: the real power flowing out of the dc link into the slave line of the IPFC.

The PI Controller that maintains $V_{dc}$ at the reference setting of $V_{dcr}$ is modeled as:

$$U_{sq} = K_{pdc} \cdot (V_{dcr} - V_{dc}) + K_{idc} \cdot \int (V_{dcr} - V_{dc}) \cdot dt \tag{C-2}$$

Here $U_{sq}$ is the reference for the q-axis component of the slave line current. It is the only non-independent reference in the IPFC's four references ($U_{md}$, $U_{mq}$, $U_{sd}$ and $U_{sq}$).

Equation (C-2) can be rewritten as following two equations:

$$\frac{d}{dt} M_{dc} = V_{dcr} - V_{dc} \tag{C-3}$$

$$U_{sq} = K_{pdc} \cdot (V_{dcr} - V_{dc}) + K_{idc} \cdot M_{dc} \tag{C-4}$$

The decoupled controllers of the IPFC are modeled as:

$$V_{m_d} = K_{mp} \cdot (U_{m_d} - I_{m_d}) + \frac{1}{T_m} \cdot M_{md} - K_{mp} \cdot \omega_0 \cdot M_{mq} \tag{C-5}$$

$$V_{m_q} = K_{mp} \cdot (U_{mq} - I_{m_q}) + \frac{1}{T_m} \cdot M_{mq} + K_{mp} \cdot \omega_0 \cdot M_{mq} \tag{C-6}$$

$$V_{s_d} = K_{sp} \cdot (U_{sd} - I_{s_d}) + \frac{1}{T_s} \cdot M_{sd} - K_{sp} \cdot \omega_0 \cdot M_{sq} \tag{C-7}$$

$$V_{s_q} = K_{sp} \cdot (U_{sq} - I_{s_q}) + \frac{1}{T_s} \cdot M_{sq} + K_{sp} \cdot \omega_0 \cdot M_{sd}$$

(C-8)

Here $M_{md}$, $M_{mq}$, $M_{sd}$ and $M_{sq}$ are the integrals of the errors of IPFC's current components ($I_{md}$, $I_{mq}$, $I_{sd}$ and $I_{sq}$) and their references ($U_{md}$, $U_{mq}$, $U_{sd}$ and $U_{sq}$).

$$\frac{d}{dt}M_{md} = U_{md} - I_{m_d} \tag{C-9}$$

$$\frac{d}{dt}M_{mq} = U_{md} - I_{m_q} \tag{C-10}$$

$$\frac{d}{dt}M_{sd} = U_{sd} - I_{s_d} \tag{C-11}$$

$$\frac{d}{dt}M_{sq} = U_{sq} - I_{s_q} \tag{C-12}$$

Here, $I_{md}$ and $I_{mq}$ are the d,q components of the master line current; $I_{sd}$ and $I_{sq}$ are the d,q components of the slave line current.

The V-I relationship of the IPFC can be represented with x-y coordinate vectors by following equations:

$$V_m = -(V_{m1} - V_{m2}) + Z_m \cdot I_m = -\begin{pmatrix} V_{m1_x} - V_{m2_x} \\ V_{m1_y} - V_{m2_y} \end{pmatrix} + \begin{pmatrix} 0 & -X_m \\ X_m & 0 \end{pmatrix} \cdot \begin{pmatrix} I_{m_x} \\ I_{m_y} \end{pmatrix} \quad \text{or}$$

$$V_{mdq} + V_{m1dq} - V_{m2dq} = Z_m \cdot I_{mdq} \tag{C-13}$$

$$V_s = -(V_{s1} - V_{s2}) + Z_s \cdot I_s = -\begin{pmatrix} V_{s1_x} - V_{s2_x} \\ V_{s1_y} - V_{s2_y} \end{pmatrix} + \begin{pmatrix} 0 & -X_s \\ X_s & 0 \end{pmatrix} \cdot \begin{pmatrix} I_{s_x} \\ I_{s_y} \end{pmatrix} \quad \text{or}$$

$$V_{sdq} + V_{s1dq} - V_{s2dq} = Z_s \cdot I_{sdq} \tag{C-14}$$

$$P_m = (V_{m_x} \quad V_{m_y}) \cdot I_m = -(V_{m1_x} - V_{m2_x}) \cdot I_{m_x} - (V_{m1_y} - V_{m2_y}) \cdot I_{m_y} \tag{C-15}$$

$$P_s = -(V_{s1_x} - V_{s2_x}) \cdot I_{s_x} - (V_{s1_y} - V_{s2_y}) \cdot I_{s_y} \tag{C-16}$$

Where:

$V_{m1} = \begin{pmatrix} V_{m1_x} \\ V_{m1_y} \end{pmatrix}$: the sending end voltage vector of the master branch of the IPFC.

$V_{m2} = \begin{pmatrix} V_{m2_x} \\ V_{m2_y} \end{pmatrix}$: the receiving end voltage vector of the master branch of the IPFC.

$V_{s1} = \begin{pmatrix} V_{s1_x} \\ V_{s1_y} \end{pmatrix}$: the sending end voltage vector of the slave branch of the IPFC.

$V_{s2} = \begin{pmatrix} V_{s2_x} \\ V_{s2_y} \end{pmatrix}$: the receiving end voltage vector of the slave branch of the IPFC.

$V_m = \begin{pmatrix} V_{m_x} \\ V_{m_y} \end{pmatrix} = T_{ip1} \cdot V_{mdq}$ : the injected voltage vector of the master branch of the IPFC.

$V_s = \begin{pmatrix} V_{s_x} \\ V_{s_y} \end{pmatrix} = T_{ip2} \cdot V_{sdq}$ : the injected voltage vector of the slave branch of the IPFC.

$V_{mdq} = \begin{pmatrix} V_{m_d} \\ V_{m_q} \end{pmatrix}$: the d-q vector of the injected voltage of the master branch of the IPFC.

$V_{sdq} = \begin{pmatrix} V_{s_d} \\ V_{s_q} \end{pmatrix}$: the d-q vector of the injected voltage of the slave branch of the IPFC.

$I_m = \begin{pmatrix} I_{m_x} \\ I_{m_y} \end{pmatrix}$: the vector of the current flowing through the master transformer of the IPFC.

$I_s = \begin{pmatrix} I_{s_x} \\ I_{s_y} \end{pmatrix}$: the vector of the current flowing through the slave transformer of the IPFC.

$T_{ip1} = \begin{pmatrix} cos\theta_m & -sin\theta_m \\ sin\theta_m & cos\theta_m \end{pmatrix}$: the dq to xy transformation matrix of the master branch.

$T_{ip2} = \begin{pmatrix} cos\theta_s & -sin\theta_s \\ sin\theta_s & cos\theta_s \end{pmatrix}$: the dq to xy transformation matrix of the slave branch.

$Z_m = \begin{pmatrix} R_m & -X_m \\ X_m & R_m \end{pmatrix}$: the master impedance matrix of the IPFC ($R_m$ is omitted, $R_m$=0 ).

$Z_e = \begin{pmatrix} R_s & -X_s \\ X_s & R_s \end{pmatrix}$: the slave impedance matrix of the IPFC ($R_s$ is omitted, $R_s$=0 ).

Substituting equations (C-5), (C-6) into (C-13) gives:

$$-X_m \cdot I_{m_q} = K_{mp} \cdot (U_{md} - I_{m_d}) + \frac{1}{T_m} \cdot M_{md} - K_{mp} \cdot \omega_0 \cdot Mmq + V_{m1_d} - V_{m2_d} \qquad \text{(C-17)}$$

$$X_m \cdot I_{m_d} = K_{mp} \cdot (U_{mq} - I_{m_q}) + \frac{1}{T_m} \cdot M_{mq} + K_{mp} \cdot \omega_0 \cdot M_{md} + V_{m1_q} - V_{m2_q} \tag{C-18}$$

Eliminating the d or q current component in equations (C-17) and (C-18) gives:

$$I_{m_d} = T_{ip3} \cdot \begin{pmatrix} M_{md} \\ M_{mq} \end{pmatrix} + T_{ip4} \cdot \begin{pmatrix} U_{md} \\ U_{mq} \end{pmatrix} + T_{ip5} \cdot \begin{pmatrix} V_{m1_d} - V_{m2_d} \\ V_{m1_q} - V_{m2_q} \end{pmatrix} \tag{C-19}$$

$$I_{m_q} = T_{ip6} \cdot \begin{pmatrix} M_{md} \\ M_{mq} \end{pmatrix} + T_{ip7} \cdot \begin{pmatrix} U_{md} \\ U_{mq} \end{pmatrix} + T_{ip8} \cdot \begin{pmatrix} V_{m1_d} - V_{m2_d} \\ V_{m1_q} - V_{m2_q} \end{pmatrix} \tag{C-20}$$

Where:

$$T_{ip3} = \begin{pmatrix} \dfrac{\dfrac{K_{mp}}{T_m} + K_{mp} \cdot X_m \cdot \omega_0}{X_m^2 + K_{mp}^2} & \dfrac{\dfrac{X_m}{T_m} - K_{mp}^2 \cdot \omega_0}{X_m^2 + K_{mp}^2} \end{pmatrix} \qquad T_{ip4} = \begin{pmatrix} \dfrac{K_{mp}^2}{X_m^2 + K_{mp}^2} & \dfrac{K_{mp} \cdot X_m}{X_m^2 + K_{mp}^2} \end{pmatrix}$$

$$T_{ip5} = \begin{pmatrix} \dfrac{K_{mp}}{X_m^2 + K_{mp}^2} & \dfrac{X_m}{X_m^2 + K_{mp}^2} \end{pmatrix}$$

$$T_{ip6} = \begin{pmatrix} T_{ip_1} & T_{ip6_2} \end{pmatrix} = \begin{pmatrix} -T_{ip3_2} & T_{ip3_1} \end{pmatrix} \qquad T_{ip7} = \begin{pmatrix} T_{ip_1} & T_{ip7_2} \end{pmatrix} = \begin{pmatrix} -T_{ip4_2} & T_{ip4_1} \end{pmatrix}$$

$$T_{ip8} = \begin{pmatrix} T_{ip8_1} & T_{ip8_2} \end{pmatrix} = \begin{pmatrix} -T_{ip5_2} & T_{ip5_1} \end{pmatrix}$$

Similarly equations(C-21) and (C-22) can be obtained from equations (C-7), (C-8) and (C-14):

$$I_{s_d} = T_{ip9} \cdot \begin{pmatrix} M_{sd} \\ M_{sq} \end{pmatrix} + T_{ip10} \cdot \begin{pmatrix} U_{sd} \\ U_{sq} \end{pmatrix} + T_{ip11} \cdot \begin{pmatrix} V_{s1_d} - V_{s2_d} \\ V_{s1_q} - V_{s2_q} \end{pmatrix} \tag{C-21}$$

$$I_{s_q} = T_{ip12} \cdot \begin{pmatrix} M_{sd} \\ M_{sq} \end{pmatrix} + T_{ip13} \cdot \begin{pmatrix} U_{sd} \\ U_{sq} \end{pmatrix} + T_{ip14} \cdot \begin{pmatrix} V_{s1_d} - V_{s2_d} \\ V_{s1_q} - V_{s2_q} \end{pmatrix} \tag{C-22}$$

Where:

$$T_{ip9} = \begin{pmatrix} \dfrac{\dfrac{K_{sp}}{T_s} + K_{sp} \cdot X_s \cdot \omega_0}{X_s^2 + K_{sp}^2} & \dfrac{\dfrac{X_s}{T_s} - K_{sp}^2 \cdot \omega_0}{X_s^2 + K_{sp}^2} \end{pmatrix} \qquad T_{ip10} = \begin{pmatrix} \dfrac{K_{sp}^2}{X_s^2 + K_{sp}^2} & \dfrac{K_{sp} \cdot X_s}{X_s^2 + K_{sp}^2} \end{pmatrix}$$

$$T_{ip11} = \begin{pmatrix} \dfrac{K_{sp}}{X_s^2 + K_{sp}^2} & \dfrac{X_s}{X_s^2 + K_{sp}^2} \end{pmatrix}$$

$$T_{ip12} = \begin{pmatrix} -T_{ip9_2} & T_{ip9_1} \end{pmatrix} \qquad T_{ip13} = \begin{pmatrix} -T_{ip10_2} & T_{ip10_1} \end{pmatrix} \qquad T_{ip14} = \begin{pmatrix} -T_{ip11_2} & T_{ip11_1} \end{pmatrix}$$

The algebraic equations can be obtained by expressing equations (C-19)-(C-22) with x-y coordinate vectors:

$$I_m = \begin{pmatrix} I_{m_x} \\ I_{m_y} \end{pmatrix} = T_{ip1} \cdot \begin{pmatrix} I_{m_d} \\ I_{m_q} \end{pmatrix} = T_{ip15} \cdot \begin{pmatrix} M_{md} \\ M_{mq} \end{pmatrix} + T_{ip16} \cdot \begin{pmatrix} U_{md} \\ U_{mq} \end{pmatrix} + T_{ip17} \cdot \begin{pmatrix} V_{m1_x} - V_{m2_x} \\ V_{m1_y} - V_{m2_y} \end{pmatrix} \tag{C-23}$$

$$I_s = \begin{pmatrix} I_{s_x} \\ I_{s_y} \end{pmatrix} = T_{ip2} \cdot \begin{pmatrix} I_{s_d} \\ I_{s_q} \end{pmatrix} = T_{ip18} \cdot \begin{pmatrix} M_{sd} \\ M_{sq} \end{pmatrix} + T_{ip19} \cdot \begin{pmatrix} U_{sd} \\ U_{sq} \end{pmatrix} + T_{ip20} \cdot \begin{pmatrix} V_{s1_x} - V_{s2_x} \\ V_{s1_y} - V_{s2_y} \end{pmatrix} \tag{C-24}$$

Where:

$$T_{ip15} = \begin{pmatrix} T_{ip15_{1,1}} & T_{ip15_{1,2}} \\ T_{ip15_{2,1}} & T_{ip15_{2,2}} \end{pmatrix} = \begin{pmatrix} cos\theta_m \cdot T_{ip3_1} + sin\theta_m \cdot T_{ip3_2} & -sin\theta_m \cdot T_{ip3_1} + cos\theta_m \cdot T_{ip3_2} \\ sin\theta_m \cdot T_{ip3_1} - cos\theta_m \cdot T_{ip3_2} & cos\theta_m \cdot T_{ip3_1} + sin\theta_m \cdot T_{ip3_2} \end{pmatrix}$$

$$T_{ip16} = \begin{pmatrix} T_{ip16_{1,1}} & T_{ip16_{1,2}} \\ T_{ip16_{2,1}} & T_{ip16_{2,2}} \end{pmatrix} = \begin{pmatrix} cos\theta_m \cdot T_{ip4_1} + sin\theta_m \cdot T_{ip4_2} & -sin\theta_m \cdot T_{ip4_1} + cos\theta_m \cdot T_{ip4_2} \\ sin\theta_m \cdot T_{ip4_1} - cos\theta_m \cdot T_{ip4_2} & cos\theta_m \cdot T_{ip4_1} + sin\theta_m \cdot T_{ip4_2} \end{pmatrix}$$

$$T_{ip17} = \begin{pmatrix} T_{ip5_1} & T_{ip5_2} \\ T_{ip8_1} & T_{ip8_2} \end{pmatrix} \qquad T_{ip18} = T_{ip2} \cdot \begin{pmatrix} T_{ip9_1} & T_{ip9_2} \\ T_{ip12_1} & T_{ip12_2} \end{pmatrix}$$

$$T_{ip19} = T_{ip2} \cdot \begin{pmatrix} T_{ip10_1} & T_{ip10_2} \\ T_{ip13_1} & T_{ip13_2} \end{pmatrix} \qquad T_{ip20} = \begin{pmatrix} T_{ip11_1} & T_{ip11_2} \\ T_{ip14_1} & T_{ip14_2} \end{pmatrix}$$

Substituting equations (C-4), (C-19)-(C-24) into (C-1), (C-3) and (C-9)-(C-12) to eliminate current components and $U_{sq}$. The following state equations are obtained:

$$
\begin{aligned}
\frac{d}{dt}V_{dc} = \frac{S_b}{C_{dc}\cdot V_{dc}}\cdot\Big( & (V_{m1_x}-V_{m2_x})\cdot\big(T_{ip15_{1,1}}\cdot M_{md}+T_{ip15_{1,2}}\cdot M_{mq}+T_{ip16_{1,1}}\cdot U_{md} \\
& \qquad +T_{ip16_{1,2}}\cdot U_{mq}+T_{ip17_{1,1}}\cdot(V_{m1_x}-V_{m2_x})\big) \\
& +(V_{m1_y}-V_{m2_y})\cdot\big(-T_{ip15_{1,2}}\cdot M_{md}+T_{ip15_{1,1}}\cdot M_{mq}-T_{ip16_{1,2}}\cdot U_{md} \\
& \qquad +T_{ip16_{1,1}}\cdot U_{mq}+T_{ip17_{1.1}}\cdot(V_{m1_y}-V_{m2_y})\big) \\
& +(V_{s1_x}-V_{s2_x})\cdot\big(T_{ip18_{1,1}}\cdot M_{sd}+T_{ip18_{1,2}}\cdot M_{sq}+T_{ip19_{1,1}}\cdot U_{sd} \\
& \qquad +T_{ip19_{1,2}}\cdot(K_{pdc}\cdot(V_{dcr}-V_{dc})+K_{idc}\cdot M_{dc}) \\
& \qquad +T_{ip20_{1,1}}\cdot(V_{s1_x}-V_{s2_x})\big) \\
& +(V_{s1_y}-V_{s2_y})\cdot\big(-T_{ip18_{1,2}}\cdot M_{sd}+T_{ip18_{1,1}}\cdot M_{sq}+T_{ip19_{1,2}}\cdot U_{sd} \\
& \qquad +T_{ip19_{1,1}}\cdot(K_{pdc}\cdot(V_{dcr}-V_{dc})+K_{idc}\cdot M_{dc}) \\
& \qquad +T_{ip20_{1,1}}\cdot(V_{s1_y}-V_{s2_y})\big)\Big)
\end{aligned}
\tag{C-25}
$$

$$
\frac{d}{dt}M_{dc} = V_{dcr}-V_{dc} \tag{C-26}
$$

$$
\begin{aligned}
\frac{d}{dt}M_{md} = & -T_{ip3_1}\cdot M_{md}-T_{ip3_2}\cdot M_{mq}+(1-T_{ip4_1})\cdot U_{md}-T_{ip4_2}\cdot U_{mq} \\
& -T_{ip5_1}\cdot(\cos\theta_m\cdot(V_{m1_x}-V_{m2_x})+\sin\theta_m\cdot(V_{m1_y}-V_{m2_y})) \\
& -T_{ip5_2}\cdot(-\sin\theta_m\cdot(V_{m1_x}-V_{m2_x})+\cos\theta_m\cdot(V_{m1_y}-V_{m2_y}))
\end{aligned}
\tag{C-27}
$$

$$
\begin{aligned}
\frac{d}{dt}M_{mq} = & -T_{ip6_1}\cdot M_{md}-T_{ip6_2}\cdot M_{mq}-T_{ip7_1}\cdot U_{md}+(1-T_{ip7_2})\cdot U_{mq} \\
& -T_{ip8_1}\cdot(\cos\theta_m\cdot(V_{m1_x}-V_{m2_x})+\sin\theta_m\cdot(V_{m1_y}-V_{m2_y})) \\
& -T_{ip8_2}\cdot(-\sin\theta_m\cdot(V_{m1_x}-V_{m2_x})+\cos\theta_m\cdot(V_{m1_y}-V_{m2_y}))
\end{aligned}
\tag{C-28}
$$

$$
\begin{aligned}
\frac{d}{dt}M_{sd} = & -T_{ip9_1}\cdot M_{sd}-T_{ip9_2}\cdot M_{sq} \\
& +(1-T_{ip10_1})\cdot U_{sd}-T_{ip10_2}\cdot(K_{pdc}\cdot(V_{dcr}-V_{dc})+K_{idc}\cdot M_{dc}) \\
& -T_{ip11_1}\cdot(\cos\theta_s\cdot(V_{s1_x}-V_{s2_x})+\sin\theta_s\cdot(V_{s1_y}-V_{s2_y})) \\
& -T_{ip11_2}\cdot(-\sin\theta_s\cdot(V_{s1_x}-V_{s2_x})+\cos\theta_s\cdot(V_{s1_y}-V_{s2_y}))
\end{aligned}
\tag{C-29}
$$

$$
\begin{aligned}
\frac{d}{dt}M_{sq} = & -T_{ip12_1}\cdot M_{sd}-T_{ip12_2}\cdot M_{sq} \\
& -T_{ip13_1}\cdot U_{sd}+(1-T_{ip13_2})\cdot(K_{pdc}\cdot(V_{dcr}-V_{dc})+K_{idc}\cdot M_{dc}) \\
& -T_{ip14_1}\cdot(\cos\theta_s\cdot(V_{s1_x}-V_{s2_x})+\sin\theta_s\cdot(V_{s1_y}-V_{s2_y})) \\
& -T_{ip14_2}\cdot(-\sin\theta_s\cdot(V_{s1_x}-V_{s2_x})+\cos\theta_s\cdot(V_{s1_y}-V_{s2_y}))
\end{aligned}
\tag{C-30}
$$

## C.1.2 Linearization of State Equations and Algebraic Equations of the IPFC

The x-y components of the magnitude of voltage vectors can be represented by:

$$\begin{pmatrix} V_{m1_x} \\ V_{m1_y} \end{pmatrix} = |V_{m1}| \cdot \begin{pmatrix} cos\theta_m \\ sin\theta_m \end{pmatrix} \tag{C-31}$$

Linearizing equation (C-31) yields:

$$\begin{pmatrix} \Delta V_{m1_x} \\ \Delta V_{m1_y} \end{pmatrix} = \begin{pmatrix} cos\theta_m & -|V_{m1}| \cdot sin\theta_m \\ sin\theta_m & |V_{m1}| \cdot cos\theta_m \end{pmatrix} \cdot \begin{pmatrix} |\Delta V_{m1}| \\ \Delta\theta_m \end{pmatrix} \tag{C-32}$$

$$\Delta\theta_m = T_{ip21} \cdot \begin{pmatrix} \Delta V_{m1_x} \\ \Delta V_{m1_y} \end{pmatrix} = T_{ip21_1} \cdot \Delta V_{m1_x} + T_{ip21_2} \cdot \Delta V_{m1_y} \tag{C-33}$$

Where:

$$T_{ip21_1} = -\frac{1}{|V_{m1}|} \cdot \sin\theta_m \qquad T_{ip21_2} = \frac{1}{|V_{m1}|} \cdot \cos\theta_m$$

Linearizing equation (C-25) gives:

$$\begin{aligned} \frac{d}{dt}\Delta V_{dc} = {} & A_{ip_{1,1}} \cdot \Delta V_{dc} + A_{ip_{1,2}} \cdot \Delta M_{dc} + A_{ip_{1,3}} \cdot \Delta M_{md} + A_{ip_{1,4}} \cdot \Delta M_{mq} \\ & + A_{ip_{1,5}} \cdot \Delta M_{md} + A_{ip_{1,6}} \cdot \Delta M_{mq} \\ & + B_{ip_{1,1}} \cdot \Delta U_{md} + B_{ip_{1,2}} \cdot \Delta U_{mq} + B_{ip_{1,3}} \cdot \Delta U_{sd} \\ & + E_{ip_{1,1}} \cdot \Delta V_{m1_x} + E_{ip_{1,2}} \cdot \Delta V_{m1_y} + F_{ip_{1,1}} \cdot \Delta V_{m2_x} + F_{ip_{1,2}} \cdot \Delta V_{m2_y} \\ & + G_{ip_{1,1}} \cdot \Delta V_{s1_x} + G_{ip_{1,2}} \cdot \Delta V_{s1_y} + H_{ip_{1,1}} \cdot \Delta V_{s2_x} + H_{ip_{1,2}} \cdot \Delta V_{s2_y} \end{aligned} \tag{C-34}$$

Where:

$$
\begin{aligned}
A_{ip_{1,1}} = \frac{-S_b}{C_{dc}\cdot V_{dc}^2}\cdot\Big(&(V_{m1_x}-V_{m2_x})\cdot\big(T_{ip15_{1,1}}\cdot M_{md}+T_{ip15_{1,2}}\cdot M_{mq}+T_{ip16_{1,1}}\cdot U_{md}\\
&\qquad +T_{ip16_{1,2}}\cdot U_{mq}+T_{ip16_{1,1}}\cdot(V_{m1_x}-V_{m2_x})\big)\\
&+(V_{m1_y}-V_{m2_y})\cdot\big(-T_{ip15_{1,2}}\cdot M_{md}+T_{ip15_{1,1}}\cdot M_{mq}-T_{ip16_{1,2}}\cdot U_{md}\\
&\qquad +T_{ip16_{1,1}}\cdot U_{mq}+T_{ip17_{1,1}}\cdot(V_{m1_y}-V_{m2_y})\big)\\
&+(V_{s1_x}-V_{s2_x})\cdot\big(T_{ip18_{1,1}}\cdot M_{sd}+T_{ip18_{1,2}}\cdot M_{sq}+T_{ip19_{1,1}}\cdot U_{sd}\\
&\qquad +T_{ip19_{1,2}}\cdot(K_{pdc}\cdot V_{dcr}+K_{idc}\cdot M_{dc})+T_{ip20_{1,1}}\cdot(V_{s1_x}-V_{s2_x})\big)\\
&+(V_{s1_y}-V_{s2_y})\cdot\big(-T_{ip18_{1,2}}\cdot M_{sd}+T_{ip18_{1,1}}\cdot M_{sq}-T_{ip19_{1,2}}\cdot U_{sd}\\
&\qquad +T_{ip19_{1,1}}\cdot(K_{pdc}\cdot V_{dcr}+K_{idc}\cdot M_{dc})+T_{ip20_{1,1}}\cdot(V_{s1_y}-V_{s2_y})\big)\Big)
\end{aligned}
$$

$$A_{ip_{1,2}} = \frac{S_b}{C_{dc}\cdot V_{dc}}\cdot((V_{s1_x}-V_{s2_x})\cdot T_{ip19_{1,2}}\cdot K_{idc}+(V_{s1y}-V_{s2}y)\cdot T_{ip19_{1,1}}\cdot K_{idc})$$

$$A_{ip_{1,3}} = \frac{S_b}{C_{dc}\cdot V_{dc}}\cdot((V_{m1_x}-V_{m2_x})\cdot T_{ip15_{1,1}}-(V_{m1_y}-V_{m2_y})\cdot T_{ip15_{1,2}})$$

$$A_{ip_{1,4}} = \frac{S_b}{C_{dc}\cdot V_{dc}}\cdot((V_{m1_x}-V_{m2_x})\cdot T_{ip15_{1,2}}+(V_{m1_y}-V_{m2_y})\cdot T_{ip15_{1,1}})$$

$$A_{ip_{1,5}} = \frac{S_b}{C_{dc}\cdot V_{dc}}\cdot((V_{s1_x}-V_{s2_x})\cdot T_{ip18_{1,1}}-(V_{s1_y}-V_{s2_y})\cdot T_{ip18_{1,2}})$$

$$A_{ip_{1,6}} = \frac{S_b}{C_{dc}\cdot V_{dc}}\cdot((V_{s1_x}-V_{s2_x})\cdot T_{ip18_{1,2}}+(V_{s1_y}-V_{s2_y})\cdot T_{ip18_{1,1}})$$

$$B_{ip_{1,1}} = \frac{S_b}{C_{dc}\cdot V_{dc}}\cdot((V_{m1_x}-V_{m2_x})\cdot T_{ip16_{1,1}}+(V_{m1_y}-V_{m2_y})\cdot T_{ip16_{2,1}})$$

$$B_{ip_{1,2}} = \frac{S_b}{C_{dc}\cdot V_{dc}}\cdot((V_{m1_x}-V_{m2_x})\cdot T_{ip16_{1,2}}+(V_{m1_y}-V_{m2_y})\cdot T_{ip16_{2,2}})$$

$$B_{ip_{1,3}} = \frac{S_b}{C_{dc}\cdot V_{dc}}\cdot((V_{s1_x}-V_{s2_x})\cdot T_{ip19_{1,1}}+(V_{s1_y}-V_{s2_y})\cdot T_{ip19_{2,1}})$$

$$
\begin{aligned}
E_{ip_{1,1}} = \frac{S_b}{C_{dc}\cdot V_{dc}}\cdot\Big(&T_{ip15_{1,1}}\cdot M_{md}+T_{ip15_{1,2}}\cdot M_{mq}+T_{ip16_{1,1}}\cdot U_{md}+T_{ip16_{1,2}}\cdot U_{mq}\\
&+2T_{ip17_{1,1}}\cdot(V_{m1_x}-V_{m2_x})\\
&+(V_{m1_x}-V_{m2_x})\cdot(T_{ip25_{1,1}}\cdot M_{md}+T_{ip25_{1,2}}\cdot M_{mq}+T_{ip27_{1,1}}\cdot U_{md}+T_{ip27_{1,2}}\cdot U_{mq})\\
&+(V_{m1_y}-V_{m2_y})\cdot(T_{ip25_{2,1}}\cdot M_{md}+T_{ip25_{2,2}}\cdot M_{mq}+T_{ip27_{2,1}}\cdot U_{md}+T_{ip27_{2,2}}\cdot U_{mq})\Big)
\end{aligned}
$$

$$E_{ip_{1,2}} = \frac{S_b}{C_{dc} \cdot V_{dc}} \cdot \Big( T_{ip15_{2,1}} \cdot M_{md} + T_{ip15_{2,2}} \cdot M_{mq} + T_{ip16_{2,1}} \cdot U_{md} + T_{ip16_{2,2}} \cdot U_{mq} \\ + 2T_{ip17_{1,1}} \cdot (V_{m1_y} - V_{m2_y}) \\ + (V_{m1_x} - V_{m2_x}) \cdot (T_{ip26_{1,1}} \cdot M_{md} + T_{ip26_{1,2}} \cdot M_{mq} + T_{ip28_{1,1}} \cdot U_{md} + T_{ip28_{1,2}} \cdot U_{mq}) \\ + (V_{m1_y} - V_{m2_y}) \cdot (T_{ip26_{2,1}} \cdot M_{md} + T_{ip26_{2,2}} \cdot M_{mq} + T_{ip28_{2,1}} \cdot U_{md} + T_{ip28_{2,2}} \cdot U_{mq}) \Big)$$

$$F_{ip_{1,1}} = \frac{-S_b}{C_{dc} \cdot V_{dc}} \cdot (T_{ip15_{1,1}} \cdot M_{md} + T_{ip15_{1,2}} \cdot M_{mq} + T_{ip16_{1,1}} \cdot U_{md} \\ + T_{ip16_{1,2}} \cdot U_{mq} + 2T_{ip17_{1,1}} \cdot (V_{m1_x} - V_{m2_x}))$$

$$F_{ip_{1,2}} = \frac{-S_b}{C_{dc} \cdot V_{dc}} \cdot (T_{ip15_{2,1}} \cdot M_{md} + T_{ip15_{2,2}} \cdot M_{mq} + T_{ip16_{2,1}} \cdot U_{bd} \\ + T_{ip16_{2,2}} \cdot U_{mq} + 2T_{ip17_{1,1}} \cdot (V_{m1_y} - V_{m2_y}))$$

$$G_{ip_{1,1}} = \frac{S_b}{C_{dc} \cdot V_{dc}} \cdot \Big( T_{ip18_{1,1}} \cdot M_{sd} + T_{ip18_{1,2}} \cdot M_{sq} + T_{ip19_{1,1}} \cdot U_{sd} \\ + T_{ip19_{1,2}} \cdot (K_{pdc} \cdot (V_{dcr} - V_{dc}) + K_{idc} \cdot M_{dc}) + 2T_{ip20_{1,1}} \cdot (V_{s1_x} - V_{s2_x}) \\ + (V_{s1_x} - V_{s2_x}) \cdot (T_{ip29_{1,1}} \cdot M_{sd} + T_{ip29_{1,2}} \cdot M_{sq} + T_{ip31_{1,1}} \cdot U_{sd} \\ + T_{ip31_{1,2}} \cdot (K_{pdc} \cdot (V_{dcr} - V_{dc}) + K_{idc} \cdot M_{dc})) \\ + (V_{s1_y} - V_{s2_y}) \cdot (T_{ip29_{2,1}} \cdot M_{sd} + T_{ip29_{2,2}} \cdot M_{sq} + T_{ip31_{2,1}} \cdot U_{sd} \\ + T_{ip31_{2,2}} \cdot (K_{pdc} \cdot (V_{dcr} - V_{dc}) + K_{idc} \cdot M_{dc}) \Big)$$

$$G_{ip_{1,2}} = \frac{S_b}{C_{dc} \cdot V_{dc}} \cdot \Big( T_{ip18_{2,1}} \cdot M_{sd} + T_{ip18_{2,2}} \cdot M_{sq} + T_{ip19_{2,1}} \cdot U_{sd} \\ + T_{ip19_{2,2}} \cdot (K_{pdc} \cdot (V_{dcr} - V_{dc}) + K_{idc} \cdot M_{dc}) + 2T_{ip20_{1,1}} \cdot (V_{s1_y} - V_{s2_y}) \\ + (V_{s1_x} - V_{s2_x}) \cdot (T_{ip30_{1,1}} \cdot M_{sd} + T_{ip30_{1,2}} \cdot M_{sq} + T_{ip32_{1,1}} \cdot U_{sd} \\ + T_{ip32_{1,2}} \cdot (K_{pdc} \cdot (V_{dcr} - V_{dc}) + K_{idc} \cdot M_{dc})) \\ + (V_{s1_y} - V_{s2_y}) \cdot (T_{ip30_{2,1}} \cdot M_{sd} + T_{ip30_{2,2}} \cdot M_{sq} + T_{ip32_{2,1}} \cdot U_{sd} \\ + T_{ip32_{2,2}} \cdot (K_{pdc} \cdot (V_{dcr} - V_{dc}) + K_{idc} \cdot M_{dc}) \Big)$$

$$H_{ip_{1,1}} = \frac{-S_b}{C_{dc} \cdot V_{dc}} \cdot (T_{ip18_{1,1}} \cdot M_{sd} + T_{ip18_{1,2}} \cdot M_{sq} + T_{ip19_{1,1}} \cdot U_{sd} \\ + T_{ip19_{1,2}} \cdot (K_{pdc} \cdot (V_{dcr} - V_{dc}) + K_{idc} \cdot M_{dc}) + 2T_{ip20_{1,1}} \cdot (V_{s1_x} - V_{s2_x}))$$

$$H_{ip_{1,2}} = \frac{-S_b}{C_{dc} \cdot V_{dc}} \cdot (T_{ip18_{2,1}} \cdot M_{sd} + T_{ip18_{2,2}} \cdot M_{sq} + T_{ip19_{2,1}} \cdot U_{sd}$$
$$+ T_{ip19_{2,2}} \cdot (K_{pdc} \cdot (V_{dcr} - V_{dc}) + K_{idc} \cdot M_{dc}) + 2T_{ip20_{1,1}} \cdot (V_{s1_y} - V_{s2_y}))$$

It should be noted that matrixes T15-T19 contain variable $\theta_m$. $\theta_m$ is the function of $V_{m1x}$, and $V_{m1y}$. Then each entry in T15-T19 is function of $V_{m1x}$, and $V_{m1y}$. Here we define:

$$\Delta T_{ip1} = \begin{pmatrix} -sin\theta_m & -cos\theta_m \\ cos\theta_m & -sin\theta_m \end{pmatrix} \cdot \Delta\theta_m = T_{ip23} \cdot (T_{ip21_1} \cdot \Delta V_{m1_x} + T_{ip21_2} \cdot \Delta V_{m1_y})$$

$$\Delta T_{ip2} = \begin{pmatrix} -sin\theta_s & -cos\theta_s \\ cos\theta_s & -sin\theta_s \end{pmatrix} \cdot \Delta\theta_s = T_{ip24} \cdot (T_{ip22_1} \cdot \Delta V_{s1_x} + T_{ip22_2} \cdot \Delta V_{s1_y})$$

Where:

$$T_{ip23} = \begin{pmatrix} -sin\theta_m & -cos\theta_m \\ cos\theta_m & -sin\theta_m \end{pmatrix} \qquad T_{ip24} = \begin{pmatrix} -sin\theta_s & -cos\theta_s \\ cos\theta_s & -sin\theta_s \end{pmatrix}$$

Then $\Delta T_{ip15}$ can be expressed as:

$$\Delta T_{ip15} = T_{ip23} \cdot \begin{pmatrix} T_{ip3_1} & T_{ip3_2} \\ -T_{ip3_2} & T_{ip3_1} \end{pmatrix} = T_{ip25} \cdot \Delta V_{m1_x} + T_{ip26} \cdot \Delta V_{m1_y}$$

Where:

$$T_{ip25} = \begin{pmatrix} -sin\theta_m \cdot T_{ip3_1} + cos\theta_m \cdot T_{ip3_2} & -sin\theta_m \cdot T_{ip3_2} - cos\theta_m \cdot T_{ip3_1} \\ sin\theta_m \cdot T_{ip3_2} + cos\theta_m \cdot T_{ip3_1} & -sin\theta_m \cdot T_{ip3_1} + cos\theta_m \cdot T_{ip3_2} \end{pmatrix} \cdot T_{ip21_1}$$

$$T_{ip26} = \begin{pmatrix} -sin\theta_m \cdot T_{ip3_1} + cos\theta_m \cdot T_{ip3_2} & -sin\theta_m \cdot T_{ip3_2} - cos\theta_m \cdot T_{ip3_1} \\ sin\theta_m \cdot T_{ip3_2} + cos\theta_m \cdot T_{ip3_1} & -sin\theta_m \cdot T_{ip3_1} + cos\theta_m \cdot T_{ip3_2} \end{pmatrix} \cdot T_{ip21_2}$$

Similarly we have:

$$\Delta T_{ip16} = T_{ip27} \cdot \Delta V_{m1_x} + T_{ip28} \cdot \Delta V_{m1_y}$$

$$\Delta T_{ip18} = T_{ip29} \cdot \Delta V_{s1_x} + T_{ip30} \cdot \Delta V_{s1_y}$$

$$\Delta T_{ip19} = T_{ip31} \cdot \Delta V_{s1_x} + T_{ip32} \cdot \Delta V_{s1_y}$$

Where:

$$T_{ip27} = \begin{pmatrix} -sin\theta_m \cdot T_{ip4_1} + cos\theta_m \cdot T_{ip4_2} & -sin\theta_m \cdot T_{ip4_2} - cos\theta_m \cdot T_{ip4_1} \\ sin\theta_m \cdot T_{ip4_2} + cos\theta_m \cdot T_{ip4_1} & -sin\theta_m \cdot T_{ip4_1} + cos\theta_m \cdot T_{ip4_2} \end{pmatrix} \cdot T_{ip21_1}$$

$$T_{ip28} = \begin{pmatrix} -sin\theta_m \cdot T_{ip4_1} + cos\theta_m \cdot T_{ip4_2} & -sin\theta_m \cdot T_{ip4_2} - cos\theta_m \cdot T_{ip4_1} \\ sin\theta_m \cdot T_{ip4_2} + cos\theta_m \cdot T_{ip4_1} & -sin\theta_m \cdot T_{ip4_1} + cos\theta_m \cdot T_{ip4_2} \end{pmatrix} \cdot T_{ip21_2}$$

$$T_{ip29} = \begin{pmatrix} -sin\theta_s \cdot T_{ip9_1} + cos\theta_s \cdot T_{ip9_2} & -sin\theta_s \cdot T_{ip9_2} - cos\theta_s \cdot T_{ip9_1} \\ sin\theta_s \cdot T_{ip9_2} + cos\theta_s \cdot T_{ip9_1} & -sin\theta_s \cdot T_{ip9_1} + cos\theta_s \cdot T_{ip9_2} \end{pmatrix} \cdot T_{ip22_1}$$

$$T_{ip30} = \begin{pmatrix} -sin\theta_s \cdot T_{ip9_1} + cos\theta_s \cdot T_{ip9_2} & -sin\theta_s \cdot T_{ip9_2} - cos\theta_s \cdot T_{ip9_1} \\ sin\theta_s \cdot T_{ip9_2} + cos\theta_s \cdot T_{ip9_1} & -sin\theta_s \cdot T_{ip9_1} + cos\theta_s \cdot T_{ip9_2} \end{pmatrix} \cdot T_{ip22_2}$$

$$T_{ip31} = \begin{pmatrix} -sin\theta_s \cdot T_{ip10_1} + cos\theta_s \cdot T_{ip10_2} & -sin\theta_s \cdot T_{ip10_2} - cos\theta_s \cdot T_{ip10_1} \\ sin\theta_s \cdot T_{ip10_2} + cos\theta_s \cdot T_{ip10_1} & -sin\theta_s \cdot T_{ip10_1} + cos\theta_s \cdot T_{ip10_2} \end{pmatrix} \cdot T_{ip22_1}$$

$$T_{ip32} = \begin{pmatrix} -sin\theta_s \cdot T_{ip10_1} + cos\theta_s \cdot T_{ip10_2} & -sin\theta_s \cdot T_{ip10_2} - cos\theta_s \cdot T_{ip10_1} \\ sin\theta_s \cdot T_{ip10_2} + cos\theta_s \cdot T_{ip10_1} & -sin\theta_s \cdot T_{ip10_1} + cos\theta_s \cdot T_{ip10_2} \end{pmatrix} \cdot T_{ip22_2}$$

Linearizing equation (C-26) gives:

$$\frac{d}{dt}\Delta M_{dc} = -\Delta V_{dc} \tag{C-35}$$

Because $V_{m1dq}$, $V_{m2dq}$, $V_{s1dq}$ and $V_{s2dq}$ are functions of $\theta_m$, $\theta_s$ and their x-y counterparts. Before linearizing equations (C-27)-(C-30), we define:

$$\Delta T_{ip1} = \begin{pmatrix} -sin\theta_m & -cos\theta_m \\ cos\theta_m & -sin\theta_m \end{pmatrix} \cdot \Delta\theta_m = T_{ip23} \cdot (T_{ip21_1} \cdot \Delta V_{m1_x} + T_{ip21_2} \cdot \Delta V_{m1_y})$$

$$\Delta T_{ip2} = \begin{pmatrix} -sin\theta_s & -cos\theta_s \\ cos\theta_s & -sin\theta_s \end{pmatrix} \cdot \Delta\theta_s = T_{ip24} \cdot (T_{ip22_1} \cdot \Delta V_{s1_x} + T_{ip22_2} \cdot \Delta V_{s1_y})$$

Where:

$$T_{ip33} = \begin{pmatrix} -sin\theta_m & cos\theta_m \\ -cos\theta_m & -sin\theta_m \end{pmatrix} \qquad T_{ip34} = \begin{pmatrix} -sin\theta_s & cos\theta_s \\ -cos\theta_s & -sin\theta_s \end{pmatrix}$$

Linearizing equation (C-27)-(C-30) gives equations (C-36)-(C-39) respectively:

$$\begin{aligned} \frac{d}{dt}\Delta M_{md} = & -T_{ip3_1} \cdot \Delta M_{md} - T_{ip3_2} \cdot \Delta M_{mq} + (1 - T_{ip4_1}) \cdot \Delta U_{md} - T_{ip4_2} \cdot \Delta U_{mq} \\ & -(const\_M_{md} \cdot T_{ip21_1} + T_{ip35_1}) \cdot \Delta V_{m1_x} + T_{ip35_1} \cdot \Delta V_{m2_x} \\ & -(const\_M_{md} \cdot T_{ip21_2} + T_{ip35_2}) \cdot \Delta V_{m1_y} + T_{ip35_2} \cdot \Delta V_{m2_y} \end{aligned} \tag{C-36}$$

$$\begin{aligned}\frac{d}{dt}\Delta M_{mq} = &-T_{ip6_1}\cdot\Delta M_{md} - T_{ip6_2}\cdot\Delta M_{bq} - T_{ip7_1}\cdot\Delta U_{bd} + (1-T_{ip7_2})\cdot\Delta U_{mq}\\ &-(const\_M_{md}\cdot T_{ip21_1}+T_{ip36_1})\cdot\Delta V_{m1_x}+T_{ip36_1}\cdot\Delta V_{m2_x}\\ &-(const\_M_{md}\cdot T_{ip21_2}+T_{ip36_2})\cdot\Delta V_{m1_y}+T_{ip36_2}\cdot\Delta V_{m2_y}\end{aligned} \tag{C-37}$$

$$\begin{aligned}\frac{d}{dt}\Delta M_{sd} = &-T_{ip9_1}\cdot\Delta M_{sd} - T_{ip9_2}\cdot\Delta M_{sq} + (1-T_{ip10_1})\cdot\Delta U_{sd}\\ &-T_{ip10_2}\cdot(-K_{pdc}\cdot\Delta V_{dc}+K_{idc}\cdot\Delta M_{dc})\\ &-(const\_M_{sd}\cdot T_{ip22_1}+T_{ip37_1})\cdot\Delta V_{s1_x}+T_{ip37_1}\cdot\Delta V_{s2_x}\\ &-(const\_M_{sd}\cdot T_{ip22_2}+T_{ip37_2})\cdot\Delta V_{s1_y}+T_{ip37_2}\cdot\Delta V_{s2_y}\end{aligned} \tag{C-38}$$

$$\begin{aligned}\frac{d}{dt}\Delta M_{sq} = &-T_{ip12_1}\cdot\Delta M_{sd} - T_{ip12_2}\cdot\Delta M_{sq} - T_{ip13_1}\cdot\Delta U_{sd}\\ &+(1-T_{ip13_2})\cdot(-K_{pdc}\cdot\Delta V_{dc}+K_{idc}\cdot\Delta M_{dc})\\ &-(const\_M_{sq}\cdot T_{ip22_1}+T_{ip38_1})\cdot\Delta V_{s1_x}+T_{ip38_1}\cdot\Delta V_{s2_x}\\ &-(const\_M_{sq}\cdot T_{ip22_2}+T_{ip38_2})\cdot\Delta V_{s1_y}+T_{ip38_2}\cdot\Delta V_{s2_y}\end{aligned} \tag{C-39}$$

Where:

$$const\_M_{md} = T_{ip5}\cdot T_{ip33}\cdot\begin{pmatrix}V_{m1_x}-V_{m2_x}\\ V_{m1_y}-V_{m2_y}\end{pmatrix} \qquad T_{ip36}\text{ }T_{ip35}=\begin{pmatrix}T_{ip35_1} & T_{ip35_2}\end{pmatrix}=T_{ip5}\cdot T_{ip1}^{-1}$$

$$const\_M_{mq} = T_{ip8}\cdot T_{ip33}\cdot\begin{pmatrix}V_{m1_x}-V_{m2_x}\\ V_{m1_y}-V_{m2_y}\end{pmatrix} \qquad T_{ip36}=\begin{pmatrix}T_{ip36_1} & T_{ip36_2}\end{pmatrix}=T_{ip8}\cdot T_{ip1}^{-1}$$

$$const\_M_{sd} = T_{ip11}\cdot T_{ip34}\cdot\begin{pmatrix}V_{s1_x}-V_{s2_x}\\ V_{s1_y}-V_{s2_y}\end{pmatrix} \qquad T_{ip37}=\begin{pmatrix}T_{ip37_1} & T_{ip37_2}\end{pmatrix}=T_{ip11}\cdot T_{ip2}^{-1}$$

$$const\_M_{sq} = T_{ip14}\cdot T_{ip34}\cdot\begin{pmatrix}V_{s1_x}-V_{s2_x}\\ V_{s1_y}-V_{s2_y}\end{pmatrix} \qquad T_{ip38}=\begin{pmatrix}T_{ip38_1} & T_{ip38_2}\end{pmatrix}=T_{ip14}\cdot T_{ip2}^{-1}$$

Linearizing algebraic equations (C-23)-(C-24) gives equations (C-40)-(C-43) respectively:

$$\begin{aligned}\Delta I_{m_x} = &\,T_{ip15_{1,1}}\cdot\Delta M_{md}+T_{ip15_{1,2}}\cdot\Delta M_{mq}+T_{ip16_{1,1}}\cdot\Delta U_{md}+T_{ip16_{1,2}}\cdot\Delta U_{mq}\\ &+(T_{ip25_{1,1}}\cdot M_{md}+T_{ip25_{1,2}}\cdot M_{mq}+T_{ip27_{1,1}}\cdot U_{md}+T_{ip27_{1,2}}\cdot U_{mq}+T_{ip17_{1,1}})\Delta V_{m1_x}\\ &+(T_{ip26_{1,1}}\cdot M_{md}+T_{ip26_{1,2}}\cdot M_{mq}+T_{ip28_{1,1}}\cdot U_{md}+T_{ip28_{1,2}}\cdot U_{mq}+T_{ip17_{1,2}})\Delta V_{m1_y}\\ &-T_{ip17_{1,1}}\cdot\Delta V_{m2_x}-T_{ip17_{1,2}}\cdot\Delta V_{m2_y}\end{aligned} \tag{C-40}$$

$$\begin{aligned}\Delta I_{m_y} &= T_{ip15_{2,1}} \cdot \Delta M_{md} + T_{ip15_{2,2}} \cdot \Delta M_{mq} + T_{ip16_{2,1}} \cdot \Delta U_{md} + T_{ip16_{2,2}} \cdot \Delta U_{mq} \\ &\quad + (T_{ip25_{2,1}} \cdot M_{md} T_{ip25_{2,2}} \cdot M_{mq} + T_{ip27_{2,1}} \cdot U_{md} + T_{ip27_{2,2}} \cdot U_{mq} + T_{ip17_{2,1}}) \Delta V_{m1_x} \\ &\quad + (T_{ip26_{2,1}} \cdot M_{md} + T_{ip26_{2,2}} \cdot M_{mq} + T_{ip28_{2,1}} \cdot U_{md} + T_{ip28_{2,2}} \cdot U_{mq} + T_{ip17_{2,2}}) \Delta V_{m1_y} \\ &\quad - T_{ip17_{2,1}} \cdot \Delta V_{m2_x} - T_{ip17_{2,2}} \cdot \Delta V_{m2_y}\end{aligned} \tag{C-41}$$

$$\begin{aligned}\Delta I_{s_x} &= -T_{ip19_{1,2}} \cdot K_{pdc} \cdot \Delta V_{dc} + T_{ip19_{1,2}} \cdot K_{idc} \cdot \Delta M_{dc} \\ &\quad + T_{ip18_{1,1}} \cdot \Delta M_{sd} + T_{ip18_{1,2}} \cdot \Delta M_{sq} + T_{ip19_{1,1}} \cdot \Delta U_{sd} \\ &\quad + (T_{ip29_{1,1}} \cdot M_{sd} + T_{ip29_{1,2}} \cdot M_{sq} + T_{ip31_{1,1}} \cdot U_{sd} + T_{ip31_{1,2}} \cdot U_{sq} + T_{ip20_{1,1}}) \Delta V_{s1_x} \\ &\quad + (T_{ip30_{1,1}} \cdot M_{sd} + T_{ip30_{1,2}} \cdot M_{sq} + T_{ip32_{1,1}} \cdot U_{sd} + T_{ip32_{1,2}} \cdot U_{sq} + T_{ip20_{1,2}}) \Delta V_{s1_y} \\ &\quad - T_{ip20_{1,1}} \cdot \Delta V_{s2_x} - T_{ip20_{1,2}} \cdot \Delta V_{s2_y}\end{aligned} \tag{C-42}$$

$$\begin{aligned}\Delta I_{s_y} &= -T_{ip19_{2,2}} \cdot K_{pdc} \cdot \Delta V_{dc} + T_{ip19_{2,2}} \cdot K_{idc} \cdot \Delta M_{dc} \\ &\quad + T_{ip18_{2,1}} \cdot \Delta M_{sd} + T_{ip18_{2,2}} \cdot \Delta M_{sq} + T_{ip19_{2,1}} \cdot \Delta U_{sd} \\ &\quad + (T_{ip29_{2,1}} \cdot M_{sd} + T_{ip29_{2,2}} \cdot M_{sq} + T_{ip31_{2,1}} \cdot U_{sd} + T_{ip31_{2,2}} \cdot U_{sq} + T_{ip20_{2,1}}) \Delta V_{s1_x} \\ &\quad + (T_{ip30_{2,1}} \cdot M_{sd} + T_{ip30_{2,2}} \cdot M_{sq} + T_{ip32_{2,1}} \cdot U_{sd} + T_{ip32_{2,2}} \cdot U_{sq} + T_{ip20_{2,2}}) \Delta V_{s1_y} \\ &\quad - T_{ip20_{2,1}} \cdot \Delta V_{s2_x} - T_{ip20_{2,2}} \cdot \Delta V_{s2_y}\end{aligned} \tag{C-43}$$

The above linearized state equations (C-34)-(C-39) and algebraic equations (C-40)-(C-43) can be rewritten in standard compact forms as follows:

$$\Delta \dot{X}_{ip} = A_{ip} \cdot \Delta X_{ip} + B_{ip} \cdot \Delta U_{ip} + E_{ip} \cdot \Delta V_{m1} + F_{ip} \cdot \Delta V_{m2} + G_{ip} \cdot \Delta V_{s1} + H_{ip} \cdot \Delta V_{s2} \tag{C-44}$$

$$\Delta I_m = T_{ip39} \cdot \Delta X_{ip} + T_{ip40} \cdot \Delta U_{ip} + T_{ip41} \cdot \Delta V_{m1} + T_{ip42} \cdot \Delta V_{m2} \tag{C-45}$$

$$\Delta I_s = T_{ip43} \cdot \Delta X_{ip} + T_{ip44} \cdot \Delta U_{ip} + T_{ip45} \cdot \Delta V_{s1} + T_{ip46} \cdot \Delta V_{s2} \tag{C-46}$$

Where:

$$\Delta X_{ip} = \begin{pmatrix} \Delta V_{dc} \\ \Delta M_{dc} \\ \Delta M_{md} \\ \Delta M_{mq} \\ \Delta M_{sd} \\ \Delta M_{sq} \end{pmatrix} \qquad \Delta U_{ip} = \begin{pmatrix} \Delta U_{md} \\ \Delta U_{mq} \\ \Delta U_{sd} \end{pmatrix}$$

$$A_{ip} = \begin{pmatrix} Aip_{1,1} & Aip_{1,2} & Aip_{1,3} & Aip_{1,4} & Aip_{1,5} & Aip_{1,6} \\ -1 & 0 & 0 & 0 & 0 & 0 \\ 0 & 0 & -Tip3_1 & -Tip3_2 & 0 & 0 \\ 0 & 0 & -Tip6_1 & -Tip6_2 & 0 & 0 \\ Tip10_2 \cdot Kpdc & -Tip10_2 \cdot Kidc & 0 & 0 & -Tip9_1 & -Tip9_2 \\ -(1-Tip13_2)\cdot Kpdc & -(1-Tip13_2)\cdot Kidc & 0 & 0 & -Tip12_1 & -Tip12_2 \end{pmatrix}$$

$$B_{ip} = \begin{pmatrix} Bip_{1,1} & Bip_{1,2} & Bip_{1,3} \\ 0 & 0 & 0 \\ 1-Tip4_1 & -Tip4_2 & 0 \\ -Tip7_1 & 1-Tip7_2 & 0 \\ 0 & 0 & -Tip10_1 \\ 0 & 0 & 1-Tip13_1 \end{pmatrix}$$

$$E_{ip} = \begin{pmatrix} Eip_{1,1} & Eip_{1,2} \\ 0 & 0 \\ -(const\_Mmd \cdot Tip21_1 + Tip35_1) & -(const\_Mmd \cdot Tip21_2 + Tip35_2) \\ -(const\_Mmq \cdot Tip21_1 + Tip36_1) & -(const\_Mmq \cdot Tip21_2 + Tip36_2) \\ 0 & 0 \\ 0 & 0 \end{pmatrix}$$

$$F_{ip} = \begin{pmatrix} Fip_{1,1} & Fip_{1,2} \\ 0 & 0 \\ Tip35_1 & Tip35_2 \\ Tip36_1 & Tip36_2 \\ 0 & 0 \\ 0 & 0 \end{pmatrix}$$

$$G_{ip} = \begin{pmatrix} Gip_{1,1} & Gip_{1,2} \\ 0 & 0 \\ 0 & 0 \\ 0 & 0 \\ -(const\_Msd \cdot Tip22_1 + Tip37_1) & -(const\_Msd \cdot Tip22_2 + Tip37_2) \\ -(const\_Msq \cdot Tip22_1 + Tip38_1) & -(const\_Msq \cdot Tip22_2 + Tip38_2) \end{pmatrix}$$

$$Hip = \begin{pmatrix} Hip_{1,1} & Hip_{1,2} \\ 0 & 0 \\ 0 & 0 \\ 0 & 0 \\ Tip37_1 & Tip37_2 \\ Tip38_1 & Tip38_2 \end{pmatrix}$$

$$Tip39 = \begin{pmatrix} 0 & 0 & Tip15_{1,1} & Tip15_{1,2} & 0 & 0 \\ 0 & 0 & Tip15_{2,1} & Tip15_{2,2} & 0 & 0 \end{pmatrix} \qquad Tip40 = \begin{pmatrix} Tip16_{1,1} & Tip16_{1,2} & 0 \\ Tip16_{2,1} & Tip16_{2,2} & 0 \end{pmatrix}$$

$$Tip41 = \begin{pmatrix} Tip41_{1,1} & Tip41_{1,2} \\ Tip41_{2,1} & Tip41_{2,2} \end{pmatrix}$$

$$Tip41_{1,1} = Tip25_{1,1} \cdot Mmd + Tip25_{1,2} \cdot Mmq + Tip27_{1,1} \cdot Umd + Tip27_{1,2} \cdot Umq + Tip17_{1,1}$$

$$Tip41_{1,2} = Tip26_{1,1} \cdot Mmd + Tip26_{1,2} \cdot Mmq + Tip28_{1,1} \cdot Umd + Tip28_{1,2} \cdot Umq + Tip17_{1,2}$$

$$Tip41_{2,1} = Tip25_{2,1} \cdot Mmd + Tip25_{2,2} \cdot Mmq + Tip27_{2,1} \cdot Umd + Tip27_{2,2} \cdot Umq + Tip17_{2,1}$$

$$Tip41_{2,2} = Tip26_{2,1} \cdot Mmd + Tip26_{2,2} \cdot Mmq + Tip28_{2,1} \cdot Umd + Tip28_{2,2} \cdot Umq + Tip17_{2,2}$$

$$Tip42 = \begin{pmatrix} Tip42_{1,1} & Tip42_{1,2} \\ Tip42_{2,1} & Tip42_{2,2} \end{pmatrix} = -Tip17$$

$$Tip43 = \begin{pmatrix} -Tip19_{1,2} \cdot Kpdc & Tip19_{1,2} \cdot Kidc & 0 & 0 & Tip18_{1,1} & Tip18_{1,2} \\ -Tip19_{2,2} \cdot Kpdc & Tip19_{2,2} \cdot Kidc & 0 & 0 & Tip18_{2,1} & Tip18_{2,2} \end{pmatrix}$$

$$Tip44 = \begin{pmatrix} 0 & 0 & Tip19_{1,1} \\ 0 & 0 & Tip19_{2,1} \end{pmatrix}$$

$$Tip45 = \begin{pmatrix} Tip45_{1,1} & Tip45_{1,2} \\ Tip45_{2,1} & Tip45_{2,2} \end{pmatrix}$$

$$Tip45_{1,1} = Tip29_{1,1} \cdot Msd + Tip29_{1,2} \cdot Msq + Tip31_{1,1} \cdot Usd + Tip31_{1,2} \cdot Usq + Tip20_{1,1}$$

$$Tip45_{1,2} = Tip30_{1,1} \cdot Msd + Tip30_{1,2} \cdot Msq + Tip32_{1,1} \cdot Usd + Tip32_{1,2} \cdot Usq + Tip20_{1,2}$$

$$Tip45_{2,1} = Tip29_{2,1} \cdot Msd + Tip29_{2,2} \cdot Msq + Tip31_{2,1} \cdot Usd + Tip31_{2,2} \cdot Usq + Tip20_{2,1}$$

$$Tip45_{2,2} = Tip30_{2,1} \cdot Msd + Tip30_{2,2} \cdot Msq + Tip32_{2,1} \cdot Usd + Tip32_{2,2} \cdot Usq + Tip20_{2,2}$$

$$Tip46 = -Tip20$$

## C.2 Small Signal Models of Generators and Exciters

The small signal models of generators and exciters were given in Appendix B and are repeated here for reference.

$$\Delta \dot{X}_{g_k} = A_{g_k} \cdot \Delta X_{g_k} + B_{g_k} \cdot \Delta U_{g_k} + E_{g_k} \cdot \Delta V_{g_k} \tag{A-11}$$

$$\Delta I_{g_k} = S_{g_k} \cdot \Delta X_{g_k} - Y_{g_k} \cdot \Delta V_{g_k} \tag{A-12}$$

## C.3 Small Signal Model of Test System with Embedded IPFC

### C.3.1 Linearization of the Network State Equations

The IPFC has two series branches with each introducing one extra bus. Hence the network with the IPFC has 14 buses (the infinite bus is not included). Assuming there are p generators, then the buses of the system are sequenced as follows:

1~p: generator 1 to generator p,

p+1: the sending end bus of the IPFC master branch,

p+2: the receiving end bus of the IPFC master branch,

p+3: the sending end bus of the IPFC slave branch,

p+4: the receiving end bus of the IPFC slave branch,

p+5~n: remainder network buses (not including the infinite bus).

The corresponding network node equation can be represented by equation (C-47):

$$\begin{pmatrix} YN_{g1,1} & \cdots & YN_{g1,p} & YN_{g1,m1} & YN_{g1,m2} & YN_{g1,s1} & YN_{g1,s1} & YN_{g1,s2} & \cdots & YN_{g1,n} \\ \cdots & \cdots & \cdots & \cdots & \cdots & \cdots & \cdots & \cdots & \cdots & \cdots \\ YN_{gp,1} & \cdots & YN_{gp,p} & YN_{gp,m1} & YN_{gp,m2} & YN_{gp,s1} & YN_{gp,s1} & YN_{gp,s2} & \cdots & YN_{gp,n} \\ YN_{m1,1} & \cdots & YN_{m1,p} & YN_{m1,m1} & YN_{m1,m2} & YN_{m1,s1} & YN_{m1,s1} & YN_{m1,s2} & \cdots & YN_{m1,n} \\ YN_{m2,1} & \cdots & YN_{m2,p} & YN_{m2,m1} & YN_{m2,m2} & YN_{m2,s1} & YN_{m2,s1} & YN_{m2,s2} & \cdots & YN_{m2,n} \\ YN_{s1,1} & \cdots & YN_{s1,p} & YN_{s1,m1} & YN_{s1,m2} & YN_{s1,s1} & YN_{s1,s1} & YN_{s1,s2} & \cdots & YN_{s1,n} \\ YN_{s2,1} & \cdots & YN_{s2,p} & YN_{s2,m1} & YN_{s2,m2} & YN_{s2,s1} & YN_{s2,s1} & YN_{s2,s2} & \cdots & YN_{s2,n} \\ YN_{i,1} & \cdots & YN_{i,p} & YN_{i,m1} & YN_{i,m2} & YN_{i,s1} & YN_{i,s1} & YN_{i,s2} & \cdots & YN_{i,n} \\ \cdots & \cdots & \cdots & \cdots & \cdots & \cdots & \cdots & \cdots & \cdots & \cdots \\ YN_{n,1} & \cdots & YN_{n,p} & YN_{n,m1} & YN_{n,m2} & YN_{n,s1} & YN_{n,s1} & YN_{n,s2} & \cdots & YN_{n,n} \end{pmatrix} \cdot \begin{pmatrix} \Delta V_{g_1} \\ \cdots \\ \Delta V_{g_p} \\ \Delta V_{m1} \\ \Delta V_{m2} \\ \Delta V_{s1} \\ \Delta V_{s2} \\ \Delta V_i \\ \cdots \\ \Delta V_n \end{pmatrix}$$

$$= \begin{pmatrix} \Delta IN_{g_1} \\ \cdots \\ \Delta IN_{g_p} \\ \Delta IN_{m1} \\ \Delta IN_{m2} \\ \Delta IN_{s1} \\ \Delta IN_{s2} \\ \Delta IN_i \\ \cdots \\ \Delta IN_n \end{pmatrix} = \begin{pmatrix} \Delta I_{g_1} \\ \cdots \\ \Delta I_{g_p} \\ -\Delta I_m \\ \Delta I_m \\ -\Delta I_s \\ \Delta I_s \\ \Delta IN_i \\ \cdots \\ \Delta IN_n \end{pmatrix}$$

………………………………………..(C-47)

Substituting $\Delta I_{gk}$ of (A-12) into (C-47), the k[th] generator bus node equation is expressed as:

$$S_{g_k} \cdot \Delta X_{g_k} = \sum_{j=1, j\neq k}^{n} YN_{gk,j} \cdot \Delta Vj + (YN_{gk,k} + Y_{g_k}) \cdot \Delta V_{g_k} \tag{C-48}$$

Substituting $\Delta I_m$ , $\Delta I_s$ of (C-45), (C-46) into (C-47), the node equations of the IPFC sending and receiving end bus are expressed as:

$$\begin{aligned} & -T_{ip39} \cdot \Delta X_{ip} - T_{ip40} \cdot \Delta U_{ip} \\ & = \sum_{j=1, j\neq m1,m2}^{n} YN_{m1,j} \cdot \Delta Vj + (YN_{m1,m1} + T_{ip41}) \cdot \Delta V_{m1} + (YN_{m1,m2} + T_{ip42}) \cdot \Delta V_{m2} \end{aligned} \tag{C-49}$$

$$T_{ip39} \cdot \Delta X_{ip} + T_{ip40} \cdot \Delta U_{ip} = \sum_{j=1, j \neq m1, m2}^{n} YN_{m2,j} \cdot \Delta Vj + (YN_{m2,m1} - T_{ip41}) \cdot \Delta V_{m1} + (YN_{m2,m2} - T_{ip42}) \cdot \Delta V_{m2} \tag{C-50}$$

$$-T_{ip43} \cdot \Delta X_{ip} - T_{ip44} \cdot \Delta U_{ip} = \sum_{j=1, j \neq s1, s2}^{n} YN_{s1,j} \cdot \Delta V_j + (YN_{s1,s1} + T_{ip45}) \cdot \Delta V_{s1} + (YN_{s1,s2} + T_{ip46}) \cdot \Delta V_{s2} \tag{C-51}$$

$$T_{ip43} \cdot \Delta X_{ip} + T_{ip44} \cdot \Delta U_{ip} = \sum_{j=1, j \neq s1, s2}^{n} YN_{s2,j} \cdot \Delta V_j + (YN_{s2,s1} - T_{ip45}) \cdot \Delta V_{s1} + (YN_{s2,s2} - T_{ip46}) \cdot \Delta V_{s2} \tag{C-52}$$

For other buses which are not connected to dynamic devices:

$$0 = \sum_{j=1}^{n} YN_{i,j} \cdot \Delta V_j \tag{C-53}$$

The above equations (C-48)-(C-53) form a new network equation in which the current components of dynamic devices are eliminated by replacing them with linear combinations of states and reference inputs:

$$\begin{pmatrix} YM_{g,g} & YM_{g,m1} & YM_{g,m2} & YM_{g,s1} & YM_{g,s2} & YM_{g,j} \\ YM_{m1,g} & YM_{m1,m1} & YM_{m1,m2} & YM_{m1,s1} & YM_{m1,s2} & YM_{m1,j} \\ YM_{m2,g} & YM_{m2,m1} & YM_{m2,m2} & YM_{m2,s1} & YM_{m2,s2} & YM_{m2,j} \\ YM_{s1,g} & YM_{s1,m1} & YM_{s1,m2} & YM_{s1,s1} & YM_{s1,s2} & YM_{s1,j} \\ YM_{s2,g} & YM_{s2,m1} & YM_{s2,m2} & YM_{s2,s1} & YM_{s2,s2} & YM_{s2,j} \\ YM_{i,g} & YM_{i,m1} & YM_{i,m2} & YM_{i,s1} & YM_{i,s2} & YM_{i,j} \end{pmatrix} \cdot \begin{pmatrix} \Delta V_g \\ \Delta V_{m1} \\ \Delta V_{m2} \\ \Delta V_{s1} \\ \Delta V_{s2} \\ \Delta V_j \end{pmatrix} = \begin{pmatrix} S_g \cdot \Delta X_g \\ -T_{ip39} \cdot \Delta X_{ip} - T_{ip40} \cdot \Delta U_{ip} \\ T_{ip39} \cdot \Delta X_{ip} + T_{ip40} \cdot \Delta U_{ip} \\ -T_{ip43} \cdot \Delta X_{ip} - T_{ip44} \cdot \Delta U_{ip} \\ T_{ip43} \cdot \Delta X_{ip} + T_{ip44} \cdot \Delta U_{ip} \\ 0 \end{pmatrix} \tag{C-54}$$

Where:

$$Sg = \begin{pmatrix} Sg_1 & \cdots & 0 \\ \vdots & Sg_k & \vdots \\ 0 & \cdots & Sg_p \end{pmatrix} \qquad \Delta Xg = \begin{pmatrix} \Delta Xg_1 \\ \ldots \\ \Delta Xg_p \end{pmatrix}$$

$$YM_{g,g} = \begin{pmatrix} YN_{gk,1} + Yg_1 & \ldots & YN_{g1,p} \\ \ldots & \ldots & \ldots \\ YN_{gp,1} & \ldots & YN_{gp,p} + Yg_{p,p} \end{pmatrix} \qquad YM_{g,m1} = \begin{pmatrix} YN_{g1,m1} \\ \ldots \\ YN_{gp,m1} \end{pmatrix}$$

$$YM_{g,m2} = \begin{pmatrix} YN_{g1,m2} \\ \ldots \\ YN_{gp,m2} \end{pmatrix} \qquad YM_{g,s1} = \begin{pmatrix} YN_{g1,s1} \\ \ldots \\ YN_{gp,s1} \end{pmatrix} \qquad YM_{g,s2} = \begin{pmatrix} YN_{g1,s2} \\ \ldots \\ YN_{gp,s2} \end{pmatrix}$$

$$YM_{g,j} = \begin{pmatrix} YN_{g1,j} & \ldots & YN_{g1,n} \\ \ldots & \ldots & \ldots \\ YN_{gp,j} & \ldots & YN_{gp,n} \end{pmatrix}$$

$$YM_{i,g} = \begin{pmatrix} YN_{i,j} & \ldots & YN_{i,p} \\ \ldots & \ldots & \ldots \\ YN_{n,1} & \ldots & YN_{n,p} \end{pmatrix} \qquad YM_{i,m1} = \begin{pmatrix} YN_{i,m1} \\ \ldots \\ YN_{n,m1} \end{pmatrix} \qquad YM_{i,m2} = \begin{pmatrix} YN_{i,m2} \\ \ldots \\ YN_{n,m2} \end{pmatrix}$$

$$YM_{i,s1} = \begin{pmatrix} YN_{i,s1} \\ \ldots \\ YN_{n,s1} \end{pmatrix} \qquad YM_{i,s2} = \begin{pmatrix} YN_{i,s2} \\ \ldots \\ YN_{n,s2} \end{pmatrix} \qquad YM_{i,j} = \begin{pmatrix} YN_{i,j} & \ldots & YN_{i,i} \\ \ldots & \ldots & \ldots \\ YN_{n,j} & \ldots & YN_{n,n} \end{pmatrix}$$

$$YM_{m1,g} = \begin{pmatrix} YN_{m1,1} & \ldots & YN_{m1,p} \end{pmatrix} \qquad YM_{m1,m1} = YN_{m1,m1} + Tip41 \qquad YM_{m1,m2} = YN_{m1,m2} + Tip42$$

$$YM_{m1,s1} = YN_{m1,s1} \qquad YM_{m1,s2} = YN_{m1,s2} \qquad YM_{m1,j} = \begin{pmatrix} YN_{m1,j} & \ldots & YN_{m1,n} \end{pmatrix}$$

$$YM_{m2,g} = \begin{pmatrix} YN_{m2,1} & \ldots & YN_{m2,p} \end{pmatrix} \qquad YM_{m2,m1} = YN_{m2,m1} - Tip41 \qquad YM_{m2,m2} = YN_{m2,m2} - Tip42$$

$$YM_{m2,s1} = YN_{m2,s1} \qquad YM_{m2,s2} = YN_{m2,s2} \qquad YM_{m2,j} = \begin{pmatrix} YN_{m2,j} & \ldots & YN_{m2,n} \end{pmatrix}$$

$$YM_{s1,g} = \begin{pmatrix} YN_{s1,1} & \ldots & YN_{s1,p} \end{pmatrix} \qquad YM_{s1,m1} = YN_{s1,m1} \qquad YM_{s1,m2} = YN_{s1,m2}$$

$$YM_{s1,s1} = YN_{s1,s1} + T_{ip45} \qquad YM_{s1,s2} = YN_{s1,s2} + T_{ip46} \qquad YM_{s1,j} = \begin{pmatrix} YN_{s1,j} & \ldots & YN_{s1,n} \end{pmatrix}$$

$$YM_{s2,g} = \begin{pmatrix} YN_{s2,1} & \ldots & YN_{s2,p} \end{pmatrix} \qquad YM_{s2,m1} = YN_{s2,m1} \qquad YM_{s2,m2} = YN_{s2,m2}$$

$$YM_{s2,s1} = YN_{s2,s1} - T_{ip45} \qquad YM_{s2,s2} = YN_{s2,s2} - T_{ip46} \qquad YM_{s2,j} = \begin{pmatrix} YN_{s2,j} & \ldots & YN_{s2,n} \end{pmatrix}$$

Equation (C-54) can be rewritten as:

$$\begin{pmatrix} \Delta V_g \\ \Delta V_{m1} \\ \Delta V_{m2} \\ \Delta V_{s1} \\ \Delta V_{s2} \\ \Delta V_j \end{pmatrix} = ZM \cdot \begin{pmatrix} S_g \cdot \Delta X_g \\ -T_{ip39} \cdot \Delta X_{ip} - T_{ip40} \cdot \Delta U_{ip} \\ T_{ip39} \cdot \Delta X_{ip} + T_{ip40} \cdot \Delta U_{ip} \\ -T_{ip43} \cdot \Delta X_{ip} - T_{ip44} \cdot \Delta U_{ip} \\ T_{ip43} \cdot \Delta X_{ip} + T_{ip44} \cdot \Delta U_{ip} \\ 0 \end{pmatrix} \tag{C-55}$$

Where:

$$ZM = YM^{-1} = \begin{pmatrix} ZM_{g,g} & ZM_{g,m1} & ZM_{g,m2} & ZM_{g,s1} & ZM_{g,s2} & ZM_{g,j} \\ ZM_{m1,g} & ZM_{m1,m1} & ZM_{m1,m2} & ZM_{m1,s1} & ZM_{m1,s2} & ZM_{m1,j} \\ ZM_{m2,g} & ZM_{m2,m1} & ZM_{m2,m2} & ZM_{m2,s1} & ZM_{m2,s2} & ZM_{m2,j} \\ ZM_{s1,g} & ZM_{s1,m1} & ZM_{s1,m2} & ZM_{s1,s1} & ZM_{s1,s2} & ZM_{s1,j} \\ ZM_{s2,g} & ZM_{s2,m1} & ZM_{s2,m2} & ZM_{s2,s1} & ZM_{s2,s2} & ZM_{s2,j} \\ ZM_{i,g} & ZM_{i,m1} & ZM_{i,m2} & ZM_{i,s1} & ZM_{i,s2} & ZM_{i,j} \end{pmatrix}$$

Equation (C-55) can be split into following five equations:

$$\begin{aligned} \Delta V_{g_k} = & \sum_{j=1}^{p} ZM_{gk,gj} \cdot S_{g_j} \cdot \Delta X_{g_j} \\ & -((ZM_{gk,m1} - ZM_{gk,m2}) \cdot T_{ip39} + (ZM_{gk,m1} - ZM_{gk,m2}) \cdot T_{ip43}) \cdot \Delta X_{ip} \\ & -((ZM_{gk,m1} - ZM_{gk,m2}) \cdot T_{ip40} + (ZM_{gk,s1} - ZM_{gk,s2}) \cdot T_{ip44}) \cdot \Delta U_{ip} \end{aligned} \tag{C-56}$$

$$\begin{aligned} \Delta V_{m1} = & \sum_{j=1}^{p} ZM_{m1,gj} \cdot S_{g_j} \cdot \Delta X_{g_j} \\ & -((ZM_{m1,m1} - ZM_{m1,m2}) \cdot T_{ip39} + (ZM_{m1,s1} - ZM_{m1,s2}) \cdot T_{ip43}) \cdot \Delta X_{ip} \\ & -((ZM_{m1,m1} - ZM_{m1,m2}) \cdot T_{ip40} + (ZM_{m1,s1} - ZM_{m1,s2}) \cdot T_{ip44}) \cdot \Delta U_{ip} \end{aligned} \tag{C-57}$$

$$\Delta V_{m2} = \sum_{j=1}^{p} ZM_{m2,gj} \cdot Sg_j \cdot \Delta Xg_j$$
$$- ((ZM_{m2,m1} - ZM_{m2,m2}) \cdot T_{ip39} + (ZM_{m2,s1} - ZM_{m2,s2}) \cdot T_{ip43}) \cdot \Delta X_{ip} \quad \text{(C-58)}$$
$$- ((ZM_{m2,m1} - ZM_{m2,m2}) \cdot T_{ip40} + (ZM_{m2,s1} - ZM_{m2,s2}) \cdot T_{ip44}) \cdot \Delta U_{ip}$$

$$\Delta V_{s1} = \sum_{j=1}^{p} ZM_{s1,gj} \cdot Sg_j \cdot \Delta Xg_j$$
$$- ((ZM_{s1,m1} - ZM_{s1,m2}) \cdot T_{ip39} + (ZM_{s1,s1} - ZM_{s1,s2}) \cdot T_{ip43}) \cdot \Delta X_{ip} \quad \text{(C-59)}$$
$$- ((ZM_{s1,m1} - ZM_{s1,m2}) \cdot T_{ip40} + (ZM_{s1,s1} - ZM_{s1,s2}) \cdot T_{ip44}) \cdot \Delta U_{ip}$$

$$\Delta V_{s2} = \sum_{j=1}^{p} ZM_{s2,gj} \cdot Sg_j \cdot \Delta Xg_j$$
$$- ((ZM_{s2,m1} - ZM_{s2,m2}) \cdot T_{ip39} + (ZM_{s2,s1} - ZM_{s2,s2}) \cdot T_{ip43}) \cdot \Delta X_{ip} \quad \text{(C-60)}$$
$$- ((ZM_{s2,m1} - ZM_{s2,m2}) \cdot T_{ip40} + (ZM_{s2,s1} - ZM_{s2,s2}) \cdot T_{ip44}) \cdot \Delta U_{ip}$$

Substituting equation (C-56) into (A-11); and (C-57)-(C-60) into (C-44) results in the linearized state equations of the system:

$$\Delta \dot{X}g_k = \sum_{j=1}^{p} AGG_{k,j} \cdot \Delta Xg_j + AGI_k \cdot \Delta X_{ip} + \sum_{j=1}^{p} BGG_{k,j} \cdot \Delta Ug_j + BGI_k \cdot \Delta U_{ip} \quad \text{(C-61)}$$

$$\Delta \dot{X}_{ip} = \sum_{j=1}^{p} AIG_j \cdot \Delta Xg_j + A_{II} \cdot \Delta X_{ip} + B_{II} \cdot \Delta U_{ip} \quad \text{(C-62)}$$

Where:

$$AGG_{k,j} = Eg_k \cdot ZM_{gk,gj} \cdot Sg_j \qquad (j \neq k)$$

$$AGG_{k,k} = -Eg_k \cdot ZM_{gk,gk} \cdot Sg_k + Ag_k$$

$$AGI_k = -Eg_k \cdot ((ZM_{gk,m1} - ZM_{gk,m2}) \cdot T_{ip39} + (ZM_{gk,s1} - ZM_{gk,s2}) \cdot T_{ip43})$$

$$BGG_k = Bg_k$$

$$BGG_j = 0 \qquad (j \neq k)$$

$$BGI_k = -Eg_k \cdot ((ZM_{gk,m1} - ZM_{gk,m2}) \cdot T_{ip40} + (ZM_{gk,s1} - ZM_{gk,s2}) \cdot T_{ip44})$$

$$AIG_j = (E_{ip} \cdot ZM_{m1,gj} + F_{ip} \cdot ZM_{m2,gj} + G_{ip} \cdot ZM_{s1,gj} + H_{ip} \cdot ZM_{s2,gj}) \cdot Sg_j \qquad (j=1,...,p)$$

$$A_{II} = A_{ip} - E_{ip} \cdot ((ZM_{m1,m1} - ZM_{m1,m2}) \cdot T_{ip39} + (ZM_{m1,s1} - ZM_{m1,s2}) \cdot T_{ip43})$$
$$- F_{ip} \cdot ((ZM_{m2,m1} - ZM_{m2,m2}) \cdot T_{ip39} + (ZM_{m2,s1} - ZM_{m2,s2}) \cdot T_{ip43})$$
$$- G_{ip} \cdot ((ZM_{s1,m1} - ZM_{s1,m2}) \cdot T_{ip39} + (ZM_{s1,s1} - ZM_{s1,s2}) \cdot T_{ip43})$$
$$- H_{ip} \cdot ((ZM_{s2,m1} - ZM_{s2,m2}) \cdot T_{ip39} + (ZM_{s2,s1} - ZM_{s2,s2}) \cdot T_{ip43})$$

$$B_{II} = B_{ip} - E_{ip} \cdot ((ZM_{m1,m1} - ZM_{m1,m2}) \cdot T_{ip40} + (ZM_{m1,s1} - ZM_{m1,s2}) \cdot T_{ip44})$$
$$- F_{ip} \cdot ((ZM_{m2,m1} - ZM_{m2,m2}) \cdot T_{ip40} + (ZM_{m2,s1} - ZM_{m2,s2}) \cdot T_{ip44})$$
$$- G_{ip} \cdot ((ZM_{s1,m1} - ZM_{s1,m2}) \cdot T_{ip40} + (ZM_{s1,s1} - ZM_{s1,s2}) \cdot T_{ip44})$$
$$- H_{ip} \cdot ((ZM_{s2,m1} - ZM_{s2,m2}) \cdot T_{ip40} + (ZM_{s2,s1} - ZM_{s2,s2}) \cdot T_{ip44})$$

Equations (C-61) and (C-62) can be written in matrix form to give the standard linearized state equation:

$$\begin{pmatrix} \Delta \dot{X}_g \\ \Delta \dot{X}_{ip} \end{pmatrix} = \begin{pmatrix} A_{GG} & A_{GI} \\ A_{IG} & A_{II} \end{pmatrix} \cdot \begin{pmatrix} \Delta X_g \\ \Delta X_{ip} \end{pmatrix} + \begin{pmatrix} B_{GG} & B_{GI} \\ B_{IG} & B_{II} \end{pmatrix} \begin{pmatrix} \Delta U_G \\ \Delta U_{ip} \end{pmatrix} \tag{C-63}$$

Or: $\Delta \dot{X} = A \cdot \Delta X + B \cdot \Delta U$

Where:

$$A_{GG} = \begin{pmatrix} A_{GG_{1,1}} & \dots & A_{GG_{1,p}} \\ \dots & \dots & \dots \\ A_{GG_{p,1}} & \dots & A_{GG_{p,p}} \end{pmatrix} \qquad A_{GI} = \begin{pmatrix} A_{IG_1} \\ \dots \\ A_{IG_p} \end{pmatrix} \qquad A_{IG} = \begin{pmatrix} A_{IG_1} & \dots & A_{IG_p} \end{pmatrix}$$

$$B_{GG} = \begin{pmatrix} B_{GG_{1,1}} & \dots & 0 \\ \dots & \dots & \dots \\ 0 & \dots & B_{GG_{p,p}} \end{pmatrix} \qquad B_{GI} = \begin{pmatrix} B_{GI_1} \\ \dots \\ B_{GI_p} \end{pmatrix} \qquad B_{IG} = \begin{pmatrix} B_{IG_1} & \dots & B_{IG_p} \end{pmatrix}$$

$$\Delta \dot{X} = \begin{pmatrix} \Delta \dot{X}_{g1} \\ \dots \\ \Delta \dot{X}_{gp} \\ \Delta \dot{X}_{ip} \end{pmatrix}$$ : 1x18 matrix (3 generator and exciters, 4 states from each generator and exciter unit; 6 states from the IPFC);

$$\Delta U = \begin{pmatrix} \Delta U_{g1} \\ \ldots \\ \Delta U_{gp} \\ \Delta U_{ip} \end{pmatrix}$$: 1x9 matrix (2 inputs from each generator and exciter, 3 inputs from the IPFC).

When the generator governor and exciter input vector $\Delta U_g$ is set to zero, equation (C-63) can be written as:

$$\begin{pmatrix} \Delta \dot{X}_g \\ \Delta \dot{X}_{ip} \end{pmatrix} = \begin{pmatrix} A_{GG} & A_{GI} \\ A_{IG} & A_{II} \end{pmatrix} \cdot \begin{pmatrix} \Delta X_g \\ \Delta X_{ip} \end{pmatrix} + \begin{pmatrix} B_{GI} \\ B_{II} \end{pmatrix} \Delta U_{ip}$$

## C.3.2 Output Equations

Using equations (A-12) and (C-56) the real power deviation of the kth generator can be expressed as:

$$\Delta P_{g_k} = V_{g_k}^T \cdot \Delta I_{g_k} + I_{g_k}^T \cdot \Delta V_{g_k} = CPG_{g_k} \cdot \Delta X_g + CPG_{ip_k} \cdot \Delta X_{ip} + DPG_k \cdot \Delta U_{ip} \tag{C-64}$$

Where:

$$\begin{aligned} CPG_{g_k} = ((I_{g_k}^T - V_{g_k}^T \cdot Y_{g_k}) \cdot ZM_{g_{k,}g_1} \cdot S_{g_1} \ \ \ldots \ \ V_{g_k}^T \cdot S_{g_k} + (I_{g_k}^T - V_{g_k}^T \cdot Y_{g_k}) \cdot ZM_{g_{k,}g_k} \cdot S_{g_k} \ \ \ldots \\ (I_{g_k}^T - V_{g_k}^T \cdot Y_{g_k}) \cdot ZM_{g_{k,}g_p} \cdot S_{g_p}) \end{aligned}$$

$$CPG_{ip_k} = -(I_{g_k}^T - V_{g_k}^T \cdot Y_{g_k}) \cdot ((ZM_{gk,m1} - ZM_{gk,m2}) \cdot T_{ip39} + (ZM_{gk,s1} - ZM_{gk,s2}) \cdot T_{ip43})$$

$$DPG_k = -(I_{g_k}^T - V_{g_k}^T \cdot Y_{g_k}) \cdot ((ZM_{gk,m1} - ZM_{gk,m2}) \cdot T_{ip40} + (ZM_{gk,s1} - ZM_{gk,s2}) \cdot T_{ip44})$$

The reactive power derivation of the kth generator can be expressed as:

$$\begin{aligned} \Delta Q_{g_k} &= (V_{g_{ky}} \quad -V_{g_{kx}}) \cdot \Delta I_{g_k} + (-I_{g_{ky}} \quad I_{g_{kx}}) \cdot \Delta V_{g_k} \\ &= CQG_{g_k} \cdot \Delta X_g + CQG_{ip_k} \cdot \Delta X_{ip} + DQG_k \cdot \Delta U_{ip} \end{aligned} \tag{C-65}$$

Where:

$$CQMg = (((-Im_y \quad Im_x) + (Vm1_y \quad -Vm1_x) \cdot Tip41) \cdot ZM_{m1,g1} \cdot Sg_1 + (Vm1_y \quad -Vm1_x) \cdot Tip42 \cdot ZM_{m2,g1} \cdot Sg_1 \ \ldots$$
$$((-Im_y \quad Im_x) + (Vm1_y \quad -Vm1_x) \cdot Tip41) \cdot ZM_{m1,gp} \cdot Sg_p + (Vm1_y \quad -Vm1_x) \cdot Tip42 \cdot ZM_{m2,gp} \cdot Sg_p)$$

$$CQMip = (Vm1_y \quad -Vm1_x) \cdot Tip39$$
$$-((-Im_y \quad Im_x) + (Vm1_y \quad -Vm1_x) \cdot Tip41) \cdot ((ZM_{m1,m1} - ZM_{m1,m2}) \cdot Tip39 + (ZM_{m1,s1} - ZM_{m1,s2}) \cdot Tip43)$$
$$-(Vm1_y \quad -Vm1_x) \cdot Tip42 \cdot ((ZM_{m2,m1} - ZM_{m2,m2}) \cdot Tip39 + (ZM_{m2,s1} - ZM_{m2,s2}) \cdot Tip43)$$

$$DQM = (Vm1_y \quad -Vm1_x) \cdot Tip40$$
$$-((-Im_y \quad Im_x) + (Vm1_y \quad -Vm1_x) \cdot Tip41) \cdot ((ZM_{m1,m1} - ZM_{m1,m2}) \cdot Tip40 + (ZM_{m1,s1} - ZM_{m1,s2}) \cdot Tip44)$$
$$-(Vm1_y \quad -Vm1_x) \cdot Tip42 \cdot ((ZM_{m2,m1} - ZM_{m2,m2}) \cdot Tip40 + (ZM_{m2,s1} - ZM_{m2,s2}) \cdot Tip44)$$

The real power derivation of the master line of the IPFC can be derived by equations (C-45) and (C-57) as:

$$\Delta Pm = Vm1^T \cdot \Delta Im + Im^T \cdot \Delta Vm1 = CPMg \cdot \Delta Xg + CPMip \cdot \Delta Xip + DPM \cdot \Delta Uip \tag{C-66}$$

Where:

$$CPMg = ((Vm1^T \cdot Tip41 + Im^T) \cdot ZM_{m1,g1} \cdot Sg_1 + Vm1^T \cdot Tip42 \cdot ZM_{m2,g1} \cdot Sg_1 \ \ldots$$
$$(Vm1^T \cdot Tip41 + Im^T) \cdot ZM_{m1,gp} \cdot Sg_p + Vm1^T \cdot Tip42 \cdot ZM_{m2,gp} \cdot Sg_p)$$

$$CPMip = Vm1^T \cdot Tip39$$
$$-(Vm1^T \cdot Tip41 + Im^T) \cdot ((ZM_{m1,m1} - ZM_{m1,m2}) \cdot Tip39 + (ZM_{m1,s1} - ZM_{m1,s2}) \cdot Tip43)$$
$$-Vm1^T \cdot Tip42 \cdot ((ZM_{m2,m1} - ZM_{m2,m2}) \cdot Tip39 + (ZM_{m2,s1} - ZM_{m2,s2}) \cdot Tip43)$$

$$DPM = Vm1^T \cdot Tip40$$
$$-(Vm1^T \cdot Tip41 + Im^T) \cdot ((ZM_{m1,m1} - ZM_{m1,m2}) \cdot Tip40 + (ZM_{m1,s1} - ZM_{m1,s2}) \cdot Tip44)$$
$$-Vm1^T \cdot Tip42 \cdot ((ZM_{m2,m1} - ZM_{m2,m2}) \cdot Tip40 + (ZM_{m2,s1} - ZM_{m2,s2}) \cdot Tip44)$$

The reactive power derivation of master line of the IPFC can be expressed as:

$$\begin{aligned} \Delta Qm &= (Vm1_y \quad -Vm1_x) \cdot \Delta Im + (-Im_y \quad Im_x) \cdot \Delta Vm1 \\ &= CQMg \cdot \Delta Xg + CQMip \cdot \Delta Xip + DQM \cdot \Delta Uip \end{aligned} \tag{C-67}$$

Where:

$$CQMg = (((-Im_y \quad Im_x) + (Vm1_y \quad -Vm1_x) \cdot Tip41) \cdot ZM_{m1,g1} \cdot Sg_1 + (Vm1_y \quad -Vm1_x) \cdot Tip42 \cdot ZM_{m2,g1} \cdot Sg_1 \ \ldots$$
$$((-Im_y \quad Im_x) + (Vm1_y \quad -Vm1_x) \cdot Tip41) \cdot ZM_{m1,gp} \cdot Sg_p + (Vm1_y \quad -Vm1_x) \cdot Tip42 \cdot ZM_{m2,gp} \cdot Sg_p)$$

$$CQM_{ip} = (Vm1_y \quad -Vm1_x) \cdot T_{ip}39$$
$$-((-Im_y \quad Im_x) + (Vm1_y \quad -Vm1_x) \cdot T_{ip}41) \cdot ((ZM_{m1,m1} - ZM_{m1,m2}) \cdot T_{ip}39 + (ZM_{m1,s1} - ZM_{m1,s2}) \cdot T_{ip}43)$$
$$-(Vm1_y \quad -Vm1_x) \cdot T_{ip}42 \cdot ((ZM_{m2,m1} - ZM_{m2,m2}) \cdot T_{ip}39 + (ZM_{m2,s1} - ZM_{m2,s2}) \cdot T_{ip}43)$$

$$DQM = (Vm1_y \quad -Vm1_x) \cdot T_{ip}40$$
$$-((-Im_y \quad Im_x) + (Vm1_y \quad -Vm1_x) \cdot T_{ip}41) \cdot ((ZM_{m1,m1} - ZM_{m1,m2}) \cdot T_{ip}40 + (ZM_{m1,s1} - ZM_{m1,s2}) \cdot T_{ip}44)$$
$$-(Vm1_y \quad -Vm1_x) \cdot T_{ip}42 \cdot ((ZM_{m2,m1} - ZM_{m2,m2}) \cdot T_{ip}40 + (ZM_{m2,s1} - ZM_{m2,s2}) \cdot T_{ip}44)$$

Similarly the power derivations of the slave line of the IPFC can be derived by equations (C-46) and (C-59) as:

$$\Delta P_s = CPS_g \cdot \Delta X_g + CPS_{ip} \cdot \Delta X_{ip} + DPS \cdot \Delta U_{ip} \tag{C-68}$$

Where:

$$CPS_g = ((V_{s1}{}^T \cdot T_{ip}45 + I_s{}^T) \cdot ZM_{s1,g1} \cdot S_{g_1} + V_{s1}{}^T \cdot T_{ip}46 \cdot ZM_{s2,g1} \cdot S_{g_1} \ \ldots$$
$$(V_{s1}{}^T \cdot T_{ip}45 + I_s{}^T) \cdot ZM_{s1,gp} \cdot S_{g_p} + V_{s1}{}^T \cdot T_{ip}46 \cdot ZM_{s2,gp} \cdot S_{g_p})$$

$$CPS_{ip} = V_{s1}{}^T \cdot T_{ip}43$$
$$-(V_{s1}{}^T \cdot T_{ip}45 + I_s{}^T) \cdot ((ZM_{s1,m1} - ZM_{s1,m2}) \cdot T_{ip}39 + (ZM_{s1,s1} - ZM_{s1,s2}) \cdot T_{ip}43)$$
$$-V_{s1}{}^T \cdot T_{ip}46 \cdot ((ZM_{s2,m1} - ZM_{s2,m2}) \cdot T_{ip}39 + (ZM_{s2,s1} - ZM_{s2,s2}) \cdot T_{ip}43)$$

$$DPS = V_{s1}{}^T \cdot T_{ip}44$$
$$-(V_{s1}{}^T \cdot T_{ip}45 + I_s{}^T) \cdot ((ZM_{s1,m1} - ZM_{s1,m2}) \cdot T_{ip}40 + (ZM_{s1,s1} - ZM_{s1,s2}) \cdot T_{ip}44)$$
$$-V_{s1}{}^T \cdot T_{ip}46 \cdot ((ZM_{s2,m1} - ZM_{s2,m2}) \cdot T_{ip}40 + (ZM_{s2,s1} - ZM_{s2,s2}) \cdot T_{ip}44)$$

and $\Delta Q_s = CQS_g \cdot \Delta X_g + CQS_{ip} \cdot \Delta X_{ip} + DQS \cdot \Delta U_{ip}$ (C-69)

Where:

$$CQS_g = (((-Is_y \quad Is_x) + (Vs1_y \quad -Vs1_x) \cdot T_{ip}45) \cdot ZM_{s1,g1} \cdot S_{g_1} + (Vs1_y \quad -Vs1_x) \cdot T_{ip}46 \cdot ZM_{s2,g1} \cdot S_{g_1} \ \ldots$$
$$((-Is_y \quad Is_x) + (Vs1_y \quad -Vs1_x) \cdot T_{ip}45) \cdot ZM_{s1,gp} \cdot S_{g_p} + (Vs1_y \quad -Vs1_x) \cdot T_{ip}46 \cdot ZM_{s2,gp} \cdot S_{g_p})$$

$$CQS_{ip} = (Vs1_y \quad -Vs1_x) \cdot T_{ip}43$$
$$-((-Is_y \quad Is_x) + (Vs1_y \quad -Vs1_x) \cdot T_{ip}45) \cdot ((ZM_{s1,m1} - ZM_{s1,m2}) \cdot T_{ip}40 + (ZM_{s1,s1} - ZM_{s1,s2}) \cdot T_{ip}43)$$
$$-(Vs1_y \quad -Vs1_x) \cdot T_{ip}46 \cdot ((ZM_{s2,m1} - ZM_{s2,m2}) \cdot T_{ip}39 + (ZM_{s2,s1} - ZM_{s2,s2}) \cdot T_{ip}43)$$

$$DQS = (Vs1_y \quad -Vs1_x) \cdot T_{ip}44$$
$$-((-Is_y \quad Is_x) + (Vs1_y \quad -Vs1_x) \cdot T_{ip}45) \cdot ((ZM_{s1,m1} - ZM_{s1,m2}) \cdot T_{ip}40 + (ZM_{s1,s1} - ZM_{s1,s2}) \cdot T_{ip}44)$$
$$-(Vs1_y \quad -Vs1_x) \cdot T_{ip}46 \cdot ((ZM_{s2,m1} - ZM_{s2,m2}) \cdot T_{ip}40 + (ZM_{s2,s1} - ZM_{s2,s2}) \cdot T_{ip}44)$$

# Appendix D Derivation of the Small Signal Model of the 12 Bus Test System with Embedded UPFC

The derivation procedure is similar to that in Appendix C. The only difference lies in the differences between the UPFC's and the IPFC's equations.

## D.1 Small Signal Model of the UPFC

### D.1.1 State Equations and Algebraic Equations of the UPFC

The series part possessing two degrees is called the booster, and the shunt part is called the exciter. All of the variables and ratios of the booster and exciter sides are denoted with the subscripts 'b' and 'e' respectively. Two coordinate systems are adopted in this model. The sending end voltage vectors ($V_s$) are selected as the d-axis of the UPFC's coordinate system, so the real and reactive power ($P_b$, $Q_b$ and $P_e$, $Q_e$) can be represented by their corresponding d, q current components ($I_{bd}$, $I_{bq}$ and $I_{ed}$, $I_{eq}$). The other coordinate system is the network's coordinate system (x-y system) which takes the infinite bus voltage as its x-axis. All vectors of the network are finally expressed as x-y components.

The DC capacitor dynamics are modeled by:

$$C_{dc} \cdot V_{dc} \cdot \frac{d}{dt} V_{dc} = S_b \cdot (P_e - P_b) \tag{D-1}$$

Where:

$C_{dc}$: the capacitance of the dc bus capacitor.

$V_{dc}$: the voltage of the dc bus.

$P_e$: the real power drawn into the dc link from the exciter branch of UPFC

$P_b$: the real power flowing out of the dc link into the transmission line through the booster side of UPFC.

The PI Controller that maintains $V_{dc}$ at the reference setting of $V_{dcr}$ is modeled as:

$$U_{ed} = K_{pdc} \cdot (V_{dcr} - V_{dc}) + K_{idc} \cdot \int (V_{dcr} - V_{dc}) \cdot dt \tag{D-2}$$

Where, $U_{ed}$ is the reference of the d-axis of the exciter current that is in phase with the voltage $V_s$, and $K_{pdc}$, $K_{idc}$ are PI controller gains.

Equation (D-2) can be rewritten as following two equations:

$$\frac{d}{dt} M_{dc} = V_{dcr} - V_{dc} \tag{D-3}$$

$$U_{ed} = K_{pdc} \cdot (V_{dcr} - V_{dc}) + K_{idc} \cdot M_{dc} \tag{D-4}$$

The decoupled controllers of the UPFC are modeled as:

$$V_{b_d} = K_{bp} \cdot (U_{bd} - I_{b_d}) + \frac{1}{T_b} \cdot M_{bd} - K_{bp} \cdot \omega_0 \cdot M_{bq} \tag{D-5}$$

$$V_{b_q} = K_{bp} \cdot (U_{bq} - I_{b_q}) + \frac{1}{T_b} \cdot M_{bq} + K_{bp} \cdot \omega_0 \cdot M_{bq} \tag{D-6}$$

$$V_{e_d} = V_{s_d} - \left( K_{ep} \cdot (U_{ed} - I_{e_d}) + \frac{1}{T_e} \cdot M_{ed} - K_{ep} \cdot \omega_0 \cdot M_{eq} \right) \tag{D-7}$$

$$V_{e_q} = V_{s_q} - \left( K_{ep} \cdot (U_{eq} - I_{e_q}) + \frac{1}{T_e} \cdot M_{eq} + K_{ep} \cdot \omega_0 \cdot M_{ed} \right) \tag{D-8}$$

Where $M_{bd}$, $M_{bq}$, $M_{ed}$ and $M_{eq}$ are the integrals of the errors of UPFC's current components ($I_{bd}$, $I_{bq}$, $I_{ed}$ and $I_{eq}$) and their references ($U_{bd}$, $U_{bq}$, $U_{ed}$ and $U_{eq}$).

$$\frac{d}{dt} M_{bd} = U_{bd} - I_{b_d} \tag{D-9}$$

$$\frac{d}{dt} M_{bq} = U_{bd} - I_{b_q} \tag{D-10}$$

$$\frac{d}{dt} M_{ed} = U_{ed} - I_{e_d} \tag{D-11}$$

$$\frac{d}{dt}M_{eq} = U_{eq} - I_{e_q} \tag{D-12}$$

Where, $I_{bd}$ and $I_{bq}$ are the in-phase and quadrature component of the booster current; $I_{ed}$ and $I_{eq}$ are the in-phase and quadrature component of the exciter current.

The V-I relation of the UPFC can be represented with x-y coordinate vectors by the following equations:

$$V_b = -(V_s - V_r) + Z_b \cdot I_b = -\begin{pmatrix} V_{s_x} - V_{r_x} \\ V_{s_y} - V_{r_y} \end{pmatrix} + \begin{pmatrix} 0 & -X_b \\ X_b & 0 \end{pmatrix} \cdot \begin{pmatrix} I_{b_x} \\ I_{b_y} \end{pmatrix} \text{ or}$$

$$V_{bdq} = Z_b \cdot I_{bdq} - V_{sdq} + V_{rdq} \tag{D-13}$$

$$V_e = V_s - Z_e \cdot I_e = -\begin{pmatrix} V_{s_x} \\ V_{s_y} \end{pmatrix} - \begin{pmatrix} 0 & -X_e \\ X_e & 0 \end{pmatrix} \cdot \begin{pmatrix} I_{e_x} \\ I_{e_y} \end{pmatrix} \text{ or}$$

$$V_{edq} = V_{sdq} - Z_e \cdot I_{edq} \tag{D-14}$$

$$P_b = (V_{b_x} \quad V_{b_y}) \cdot I_b = -(V_{s_x} - V_{r_x}) \cdot I_{b_x} - (V_{s_y} - V_{r_y}) \cdot I_{b_y} \tag{D-15}$$

$$P_e = V_{e_x} \cdot I_{e_x} + V_{e_y} \cdot I_{e_y} = V_{s_x} \cdot I_{e_x} + V_{s_y} \cdot I_{e_y} \tag{D-16}$$

Where:

$V_s = \begin{pmatrix} V_{s_x} \\ V_{s_y} \end{pmatrix}$: the sending end voltage vector.

$V_r = \begin{pmatrix} V_{r_x} \\ V_{r_y} \end{pmatrix}$: the receiving end voltage vector.

$V_b = \begin{pmatrix} V_{b_x} \\ V_{b_y} \end{pmatrix} = T_{up1} \cdot V_{bdq} = T_{up1} \cdot \begin{pmatrix} V_{b_d} \\ V_{b_q} \end{pmatrix}$: the booster voltage vector of the UPFC.

$V_e = \begin{pmatrix} V_{e_x} \\ V_{e_y} \end{pmatrix} = T_{up1} \cdot V_{edq} = T_{up1} \cdot \begin{pmatrix} V_{e_d} \\ V_{e_q} \end{pmatrix}$: the exciter voltage vector of the UPFC.

$Vb_{dq} = \begin{pmatrix} Vb_d \\ Vb_q \end{pmatrix}$: in phase-quadrature (d-q) vector of the booster voltage of the UPFC.

$Ve_{dq} = \begin{pmatrix} Ve_d \\ Ve_q \end{pmatrix}$: in phase-quadrature (d-q) vector of the exciter voltage of the UPFC.

$Ib = \begin{pmatrix} Ib_x \\ Ib_y \end{pmatrix}$: the line current vector flowing through booster.

$Ie = \begin{pmatrix} Ie_x \\ Ie_y \end{pmatrix}$: the line current vector flowing through exciter.

$Ib_{dq} = \begin{pmatrix} Ib_d \\ Ib_q \end{pmatrix}$: in phase-quadrature (d-q) vector of the booster current of the UPFC.

$Ie_{dq} = \begin{pmatrix} Ie_d \\ Ie_q \end{pmatrix}$: in phase-quadrature (d-q) vector of the exciter current of the UPFC.

$Zb = \begin{pmatrix} Rb & -Xb \\ Xb & Rb \end{pmatrix}$: the booster impedance matrix of theUPFC.

$Ze = \begin{pmatrix} Re & -Xe \\ Xe & Re \end{pmatrix}$: the exciter impedance matrix of theUPFC.

$T_{up1} = \begin{pmatrix} cos\theta & -sin\theta \\ sin\theta & cos\theta \end{pmatrix}$: the dq to xy transformation matrix.

Substituting equations (D-5), (D-6) into (D-13) gives:

$$-Xb \cdot Ib_q = Kbp \cdot (Ubd - Ib_d) + \frac{1}{Tb} \cdot Mbd - Kbp \cdot \omega 0 \cdot Mbq + Vs_d - Vr_d \tag{D-17}$$

$$Xb \cdot Ib_d = Kbp \cdot (Ubq - Ib_q) + \frac{1}{Tb} \cdot Mbq + Kbp \cdot \omega 0 \cdot Mbd + Vs_q - Vr_q \tag{D-18}$$

Eliminating the d or q current component in equations (D-17) and (D-18) gives:

$$Ib_d = T_{up2} \cdot \begin{pmatrix} Mbd \\ Mbq \end{pmatrix} + T_{up3} \cdot \begin{pmatrix} Ubd \\ Ubq \end{pmatrix} + T_{up4} \cdot \begin{pmatrix} Vs_d - Vr_d \\ Vs_q - Vr_q \end{pmatrix} \tag{D-19}$$

$$I_{b_q} = T_{up5} \cdot \begin{pmatrix} M_{bd} \\ M_{bq} \end{pmatrix} + T_{up6} \cdot \begin{pmatrix} U_{bd} \\ U_{bq} \end{pmatrix} + T_{up7} \cdot \begin{pmatrix} V_{s_d} - V_{r_d} \\ V_{s_q} - V_{r_q} \end{pmatrix} \tag{D-20}$$

Where:

$$T_{up2} = \begin{pmatrix} \dfrac{\dfrac{K_{bp}}{T_b} + K_{bp} \cdot X_b \cdot \omega_0}{X_b^2 + K_{bp}^2} & \dfrac{\dfrac{X_b}{T_b} - K_{bp}^2 \cdot \omega_0}{X_b^2 + K_{bp}^2} \end{pmatrix}$$

$$T_{up3} = \begin{pmatrix} \dfrac{K_{bp}^2}{X_b^2 + K_{bp}^2} & \dfrac{K_{bp} \cdot X_b}{X_b^2 + K_{bp}^2} \end{pmatrix}$$

$$T_{up4} = \begin{pmatrix} \dfrac{K_{bp}}{X_b^2 + K_{bp}^2} & \dfrac{X_b}{X_b^2 + K_{bp}^2} \end{pmatrix}$$

$$T_{up5} = \begin{pmatrix} T_{up5_1} & T_{up5_2} \end{pmatrix} = \begin{pmatrix} -T_{up2_2} & T_{up2_1} \end{pmatrix} \qquad T_{up6} = \begin{pmatrix} T_{up6_1} & T_{up6_2} \end{pmatrix} = \begin{pmatrix} -T_{up3_2} & T_{up3_1} \end{pmatrix}$$

$$T_{up7} = \begin{pmatrix} T_{up7_1} & T_{up7_2} \end{pmatrix} = \begin{pmatrix} -T_{up4_2} & T_{up4_1} \end{pmatrix}$$

Similarly equations (D-21) and (D-22) can be obtained from equations (D-7), (D-8) and (D-14):

$$I_{e_d} = T_{up8} \cdot \begin{pmatrix} M_{ed} \\ M_{eq} \end{pmatrix} + T_{up9} \cdot \begin{pmatrix} U_{ed} \\ U_{eq} \end{pmatrix} \tag{D-21}$$

$$I_{e_q} = T_{up10} \cdot \begin{pmatrix} M_{ed} \\ M_{eq} \end{pmatrix} + T_{up11} \cdot \begin{pmatrix} U_{ed} \\ U_{eq} \end{pmatrix} \tag{D-22}$$

Where:

$$T_{up8} = \begin{pmatrix} \dfrac{\dfrac{K_{ep}}{T_e} + K_{ep} \cdot X_e \cdot \omega_0}{X_e^2 + K_{ep}^2} & \dfrac{\dfrac{X_e}{T_e} - K_{ep}^2 \cdot \omega_0}{X_e^2 + K_{ep}^2} \end{pmatrix} \qquad T_{up9} = \begin{pmatrix} \dfrac{K_{ep}^2}{X_e^2 + K_{ep}^2} & \dfrac{K_{ep} \cdot X_e}{X_e^2 + K_{ep}^2} \end{pmatrix}$$

$$T_{up10} = \begin{pmatrix} -T_{up8_2} & T_{up8_1} \end{pmatrix} \qquad T_{up11} = \begin{pmatrix} -T_{up9_2} & T_{up9_1} \end{pmatrix}$$

The algebraic equations can be obtained by expressing equations (D-19)-(D-22) with x-y coordinate vectors:

$$I_b = \begin{pmatrix} I_{b_x} \\ I_{b_y} \end{pmatrix} = T_{up1} \cdot \begin{pmatrix} I_{b_d} \\ I_{b_q} \end{pmatrix} = T_{up12} \cdot \begin{pmatrix} M_{bd} \\ M_{bq} \end{pmatrix} + T_{up13} \cdot \begin{pmatrix} U_{bd} \\ U_{bq} \end{pmatrix} + T_{up14} \cdot \begin{pmatrix} V_{s_x} - V_{r_x} \\ V_{s_y} - V_{r_y} \end{pmatrix} \tag{D-23}$$

$$Ie = \begin{pmatrix} Ie_x \\ Ie_y \end{pmatrix} = Tup1 \cdot \begin{pmatrix} Ie_d \\ Ie_q \end{pmatrix} = Tup15 \cdot \begin{pmatrix} Med \\ Meq \end{pmatrix} + Tup16 \cdot \begin{pmatrix} Ued \\ Ueq \end{pmatrix} \tag{D-24}$$

Where:

$$Tup12 = \begin{pmatrix} Tup12_{1,1} & Tup12_{1,2} \\ Tup12_{2,1} & Tup12_{2,2} \end{pmatrix} = \begin{pmatrix} cos\theta \cdot Tup2_1 + sin\theta \cdot Tup2_2 & -sin\theta \cdot Tup2_1 + cos\theta \cdot Tup2_2 \\ sin\theta \cdot Tup2_1 - cos\theta \cdot Tup2_2 & cos\theta \cdot Tup2_1 + sin\theta \cdot Tup2_2 \end{pmatrix}$$

$$Tup13 = \begin{pmatrix} Tup13_{1,1} & Tup13_{1,2} \\ Tup13_{2,1} & Tup13_{2,2} \end{pmatrix} = \begin{pmatrix} cos\theta \cdot Tup3_1 + sin\theta \cdot Tup3_2 & -sin\theta \cdot Tup3_1 + cos\theta \cdot Tup3_2 \\ sin\theta \cdot Tup3_1 - cos\theta \cdot Tup3_2 & cos\theta \cdot Tup3_1 + sin\theta \cdot Tup3_2 \end{pmatrix}$$

$$Tup14 = \begin{pmatrix} Tup4_1 & Tup4_2 \\ Tup7_1 & Tup7_2 \end{pmatrix} \qquad Tup15 = Tup1 \cdot \begin{pmatrix} Tup8_1 & Tup8_2 \\ Tup10_1 & Tup10_2 \end{pmatrix}$$

$$Tup16 = Tup1 \cdot \begin{pmatrix} Tup9_1 & Tup9_2 \\ Tup11_1 & Tup11_2 \end{pmatrix}$$

By substituting equations (D-4), (D-19)-(D-24) into (D-1), (D-3) and (D-9)-(D-12) to eliminate current components and $Ued$, these states equations are obtained:

$$\begin{aligned} \frac{d}{dt}Vdc = \frac{Sb}{Cdc \cdot Vdc} \cdot \Big( & (Vs_x - Vr_x) \cdot \big( Tup12_{1,1} \cdot Mbd + Tup12_{1,2} \cdot Mbq + Tup13_{1,1} \cdot Ubd \\ & \quad + Tup13_{1,2} \cdot Ubq + Tup14_{1,1} \cdot (Vs_x - Vr_x) \big) \\ & + (Vs_y - Vr_y) \cdot \big( -Tup12_{1,2} \cdot Mbd + Tup12_{1,1} \cdot Mbq - Tup13_{1,2} \cdot Ubd \\ & \quad + Tup13_{1,1} \cdot Ubq + Tup14_{1.1} \cdot (Vs_y - Vr_y) \big) \\ & + Vs_x \cdot \big( Tup15_{1,1} \cdot Med + Tup15_{1,2} \cdot Meq + Tup16_{1,2} \cdot Ueq \\ & \quad + Tup16_{1,1} \cdot (Kpdc \cdot (Vdcr - Vdc) + Kidc \cdot Mdc) \big) \\ & + Vs_y \cdot \big( -Tup15_{1,2} \cdot Med + Tup15_{1,1} \cdot Meq + Tup16_{1,1} \cdot Ueq \\ & \quad - Tup16_{1,2} \cdot (Kpdc \cdot (Vdcr - Vdc) + Kidc \cdot Mdc) \big) \Big) \end{aligned} \tag{D-25}$$

$$\frac{d}{dt}Mdc = Vdcr - Vdc \tag{D-26}$$

$$\begin{aligned} \frac{d}{dt}Mbd = & -Tup2_1 \cdot Mbd - Tup2_2 \cdot Mbq + (1 - Tup3_1) \cdot Ubd - Tup3_2 \cdot Ubq \\ & - Tup4_1 \cdot (\cos\theta \cdot (Vs_x - Vr_x) + \sin\theta \cdot (Vs_y - Vr_y)) \\ & - Tup4_2 \cdot (-\sin\theta \cdot (Vs_x - Vr_x) + \cos\theta \cdot (Vs_y - Vr_y)) \end{aligned} \tag{D-27}$$

$$\frac{d}{dt}Mbq = -Tup5_1 \cdot Mbd - Tup5_2 \cdot Mbq - Tup6_1 \cdot Ubd + (1 - Tup6_2) \cdot Ubq$$
$$- Tup7_1 \cdot (\cos\theta \cdot (Vs_x - Vr_x) + \sin\theta \cdot (Vs_y - Vr_y)) \tag{D-28}$$
$$- Tup7_2 \cdot (-\sin\theta \cdot (Vs_x - Vr_x) + \cos\theta \cdot (Vs_y - Vr_y))$$

$$\frac{d}{dt}Med = -Tup8_1 \cdot Med - Tup8_2 \cdot Meq$$
$$+ (1 - Tup9_1) \cdot (Kpdc \cdot (Vdcr - Vdc) + Kidc \cdot Mdc) - Tup9_2 \cdot Ueq \tag{D-29}$$

$$\frac{d}{dt}Meq = -Tup10_1 \cdot Med - Tup10_2 \cdot Meq$$
$$- Tup11_1 \cdot (Kpdc \cdot (Vdcr - Vdc) + Kidc \cdot Mdc) + (1 - Tup11_2) \cdot Ueq \tag{D-30}$$

## D.1.2 Linearization of State Equations and Algebraic Equations of the UPFC

The x-y components of the magnitude of voltage vectors can be represented by:

$$\begin{pmatrix} Vs_x \\ Vs_y \end{pmatrix} = |Vs| \cdot \begin{pmatrix} cos\theta \\ sin\theta \end{pmatrix} \tag{D-31}$$

Linearizing equation (D-31) yields:

$$\begin{pmatrix} \Delta Vs_x \\ \Delta Vs_y \end{pmatrix} = \begin{pmatrix} cos\theta & -|Vs| \cdot sin\theta \\ sin\theta & |Vs| \cdot cos\theta \end{pmatrix} \cdot \begin{pmatrix} |\Delta Vs| \\ \Delta\theta \end{pmatrix} \tag{D-32}$$

$$\Delta\theta = Tup17 \cdot \begin{pmatrix} \Delta Vs_x \\ \Delta Vs_y \end{pmatrix} = Tup17_1 \cdot \Delta Vs_x + Tup17_2 \cdot \Delta Vs_y \tag{D-33}$$

Where:

$$Tup17_1 = -\frac{1}{|Vs|} \cdot \sin\theta \qquad Tup17_2 = \frac{1}{|Vs|} \cdot \cos\theta$$

Linearizing equation (D-25) gives:

$$
\begin{aligned}
\frac{d}{dt}\Delta V_{dc} = {} & A_{up_{1,1}} \cdot \Delta V_{dc} + A_{up_{1,2}} \cdot \Delta M_{dc} + A_{up_{1,3}} \cdot \Delta M_{bd} + A_{up_{1,4}} \cdot \Delta M_{bq} \\
& + A_{up_{1,5}} \cdot \Delta M_{ed} + A_{up_{1,6}} \cdot \Delta M_{eq} \\
& + B_{up_{1,1}} \cdot \Delta U_{bd} + B_{up_{1,2}} \cdot \Delta U_{bq} + B_{up_{1,3}} \cdot \Delta U_{eq} \\
& + E_{up_{1,1}} \cdot \Delta V_{s_x} + E_{up_{1,2}} \cdot \Delta V_{s_y} + F_{up_{1,1}} \cdot \Delta V_{r_x} + F_{up_{1,2}} \cdot \Delta V_{r_y}
\end{aligned} \tag{D-34}
$$

Where:

$$
\begin{aligned}
A_{up_{1,1}} = \frac{-S_b}{C_{dc} \cdot V_{dc}^{\,2}} \cdot \Big( & (V_{s_x} - V_{r_x}) \cdot \big( T_{up12_{1,1}} \cdot M_{bd} + T_{up12_{1,2}} \cdot M_{bq} + T_{up13_{1,1}} \cdot U_{bd} \\
& \quad + T_{up13_{1,2}} \cdot U_{bq} + T_{up14_{1,1}} \cdot (V_{s_x} - V_{r_x}) \big) \\
& + (V_{s_y} - V_{r_y}) \cdot \big( T_{up12_{2,2}} \cdot M_{bd} + T_{up12_{2,2}} \cdot M_{bq} + T_{up13_{2,1}} \cdot U_{bd} \\
& \quad + T_{up13_{2,2}} \cdot U_{bq} + T_{up14_{1,1}} \cdot (V_{s_y} - V_{r_y}) \big) \\
& + V_{s_x} \cdot \big( T_{up15_{1,1}} \cdot M_{ed} + T_{up15_{1,2}} \cdot M_{eq} + T_{up16_{1,2}} \cdot U_{eq} \\
& \quad + T_{up16_{1,1}} \cdot (K_{pdc} \cdot V_{dcr} + K_{idc} \cdot M_{dc}) \big) \\
& + V_{s_y} \cdot \big( T_{up15_{2,1}} \cdot M_{ed} + T_{up15_{2,2}} \cdot M_{eq} + T_{up16_{2,2}} \cdot U_{eq} \\
& \quad + T_{up16_{2,1}} \cdot (K_{pdc} \cdot V_{dcr} + K_{idc} \cdot M_{dc}) \big) \Big)
\end{aligned}
$$

$$
A_{up_{1,2}} = \frac{S_b}{C_{dc} \cdot V_{dc}} \cdot (V_{s_x} \cdot T_{up16_{1,1}} \cdot K_{idc} + V_{s_y} \cdot T_{up16_{2,1}} \cdot K_{idc})
$$

$$
Aup_{1,3} = \frac{S_b}{C_{dc} \cdot V_{dc}} \cdot ((V_{s_x} - V_{r_x}) \cdot T_{up12_{1,1}} + (V_{s_y} - V_{r_y}) \cdot T_{up12_{2,1}})
$$

$$
A_{up_{1,4}} = \frac{S_b}{C_{dc} \cdot V_{dc}} \cdot ((V_{s_x} - V_{r_x}) \cdot T_{up12_{1,2}} + (V_{s_y} - V_{r_y}) \cdot T_{up12_{2,2}})
$$

$$
A_{up_{1,5}} = \frac{S_b}{C_{dc} \cdot V_{dc}} \cdot (V_{s_x} \cdot T_{up15_{1,1}} + V_{s_y} \cdot T_{up15_{2,1}})
$$

$$
A_{up_{1,6}} = \frac{S_b}{C_{dc} \cdot V_{dc}} \cdot (V_{s_x} \cdot T_{up15_{1,2}} + V_{s_y} \cdot T_{up15_{2,2}})
$$

$$
B_{up_{1,1}} = \frac{S_b}{C_{dc} \cdot V_{dc}} \cdot ((V_{s_x} - V_{r_x}) \cdot T_{up13_{1,1}} + (V_{s_y} - V_{r_y}) T_{up13_{2,1}})
$$

$$
B_{up_{1,2}} = \frac{S_b}{C_{dc} \cdot V_{dc}} \cdot ((V_{s_x} - V_{r_x}) \cdot T_{up13_{1,2}} + (V_{s_y} - V_{r_y}) \cdot T_{up13_{2,2}})
$$

$$
B_{up_{1,3}} = \frac{S_b}{C_{dc} \cdot V_{dc}} \cdot (V_{s_x} \cdot T_{up16_{1,2}} + V_{s_y} \cdot T_{up16_{2,2}})
$$

$$E_{up_{1,1}} = \frac{S_b}{C_{dc} \cdot V_{dc}} \cdot \Big( T_{up12_{1,1}} \cdot M_{bd} + T_{up12_{1,2}} \cdot M_{bq} + T_{up13_{1,1}} \cdot U_{bd} + T_{up13_{1,2}} \cdot U_{bq}$$
$$+ 2T_{up14_{1,1}} \cdot (V_{s_x} - V_{r_x}) + T_{up15_{1,1}} \cdot M_{ed} + T_{up15_{1,2}} \cdot M_{eq}$$
$$+ T_{up16_{1,2}} \cdot U_{eq} + T_{up16_{1,1}} \cdot (K_{pdc} \cdot (V_{dcr} - V_{dc}) + K_{idc} \cdot M_{dc})$$
$$+ (V_{s_x} - V_{r_x}) \cdot (T_{up19_{1,1}} \cdot M_{bd} + T_{up19_{1,2}} \cdot M_{bq} + T_{up21_{1,1}} \cdot U_{bd} + T_{up21_{1,2}} \cdot U_{bq})$$
$$+ (V_{s_y} - V_{r_y}) \cdot (T_{up19_{2,1}} \cdot M_{bd} + T_{up19_{2,2}} \cdot M_{bq} + T_{up21_{2,1}} \cdot U_{bd} + T_{up21_{2,2}} \cdot U_{bq})$$
$$+ V_{s_x} \cdot \Big( T_{up23_{1,1}} \cdot M_{ed} + T_{up23_{1,2}} \cdot M_{eq} + T_{up25_{1,2}} \cdot U_{eq}$$
$$+ T_{up25_{1,1}} \cdot (K_{pdc} \cdot (V_{dcr} - V_{dc}) + K_{idc} \cdot M_{dc}) \Big)$$
$$+ V_{s_y} \cdot \Big( T_{up23_{2,1}} \cdot M_{ed} + T_{up23_{2,2}} \cdot M_{eq} + T_{up25_{2,2}} \cdot U_{eq}$$
$$+ T_{up25_{2,1}} \cdot (K_{pdc} \cdot (V_{dcr} - V_{dc}) + K_{idc} \cdot M_{dc}) \Big) \Big)$$

$$E_{up_{1,2}} = \frac{S_b}{C_{dc} \cdot V_{dc}} \cdot \Big( T_{up12_{2,1}} \cdot M_{bd} + T_{up12_{2,2}} \cdot M_{bq} + T_{up13_{2,1}} \cdot U_{bd} + T_{up13_{2,2}} \cdot U_{bq}$$
$$+ 2T_{up14_{1,1}} \cdot (V_{s_y} - V_{r_y}) + T_{up15_{2,1}} \cdot M_{ed} + T_{up15_{2,2}} \cdot M_{eq}$$
$$+ T_{up16_{2,2}} \cdot U_{eq} + T_{up16_{2,1}} \cdot (K_{pdc} \cdot (V_{dcr} - V_{dc}) + K_{idc} \cdot M_{dc})$$
$$+ (V_{s_x} - V_{r_x}) \cdot (T_{up20_{1,1}} \cdot M_{bd} + T_{up20_{1,2}} \cdot M_{bq} + T_{up22_{1,1}} \cdot U_{bd} + T_{up22_{1,2}} \cdot U_{bq})$$
$$+ (V_{s_y} - V_{r_y}) \cdot (T_{up20_{2,1}} \cdot M_{bd} + T_{up20_{2,2}} \cdot M_{bq} + T_{up22_{2,1}} \cdot U_{bd} + T_{up22_{2,2}} \cdot U_{bq})$$
$$+ V_{s_x} \cdot \Big( T_{up24_{1,1}} \cdot M_{ed} + T_{up24_{1,2}} \cdot M_{eq} + T_{up26_{1,2}} \cdot U_{eq}$$
$$+ T_{up26_{1,1}} \cdot (K_{pdc} \cdot (V_{dcr} - V_{dc}) + K_{idc} \cdot M_{dc}) \Big)$$
$$+ V_{s_y} \cdot \Big( T_{up24_{2,1}} \cdot M_{ed} + T_{up24_{2,2}} \cdot M_{eq} + T_{up26_{2,2}} \cdot U_{eq}$$
$$+ T_{up26_{2,1}} \cdot (K_{pdc} \cdot (V_{dcr} - V_{dc}) + K_{idc} \cdot M_{dc}) \Big) \Big)$$

$$F_{up_{1,1}} = \frac{-S_b}{C_{dc} \cdot V_{dc}} \cdot (T_{up12_{1,1}} \cdot M_{bd} + T_{up12_{1,2}} \cdot M_{bq} + T_{up13_{1,1}} \cdot U_{bd} + T_{up13_{1,2}} \cdot U_{bq} + 2T_{up14_{1,1}} \cdot (V_{s_x} - V_{r_x}))$$

$$F_{up_{1,2}} = \frac{-S_b}{C_{dc} \cdot V_{dc}} \cdot (T_{up12_{2,1}} \cdot M_{bd} + T_{up12_{2,2}} \cdot M_{bq} + T_{up13_{2,1}} \cdot U_{bd} + T_{up13_{2,2}} \cdot U_{bq} + 2T_{up14_{1,1}} \cdot (V_{s_y} - V_{r_y}))$$

It should be noted that matrixes T12-T16 contain the variable $\theta$. $\theta$ is the function of $V_{sx}$, and $V_{sy}$. Then each entry in T12-T16 is function of $V_{sx}$, and $V_{sy}$. Here we define:

$$\Delta T_{up1} = \begin{pmatrix} -sin\theta & -cos\theta \\ cos\theta & -sin\theta \end{pmatrix} \cdot \Delta\theta = T_{up18} \cdot (T_{up17_1} \cdot \Delta V_{s_x} + T_{up17_2} \cdot \Delta V_{s_y})$$

Where:

$$T_{up18} = \begin{pmatrix} -sin\theta & -cos\theta \\ cos\theta & -sin\theta \end{pmatrix}$$

Then $\Delta T_{ip12}$ can be expressed as:

$$\Delta T_{up12} = T_{up18} \cdot \begin{pmatrix} T_{up2_1} & T_{up2_2} \\ -T_{up_2} & T_{up2_1} \end{pmatrix} = T_{up19} \cdot \Delta V_{s_x} + T_{up20} \cdot \Delta V_{s_y}$$

Where:

$$T_{up19} = \begin{pmatrix} -sin\theta \cdot T_{up2_1} + cos\theta \cdot T_{up2_2} & -sin\theta \cdot T_{up2_2} - cos\theta \cdot T_{up2_1} \\ sin\theta \cdot T_{up2_2} + cos\theta \cdot T_{up2_1} & -sin\theta \cdot T_{up2_1} + cos\theta \cdot T_{up2_2} \end{pmatrix} \cdot T_{up17_1}$$

$$T_{up20} = \begin{pmatrix} -sin\theta \cdot T_{up2_1} + cos\theta \cdot T_{up2_2} & -sin\theta \cdot T_{up2_2} - cos\theta \cdot T_{up2_1} \\ sin\theta \cdot T_{up2_2} + cos\theta \cdot T_{up2_1} & -sin\theta \cdot T_{up2_1} + cos\theta \cdot T_{up2_2} \end{pmatrix} \cdot T_{up17_2}$$

Similarly we have:

$$\Delta T_{up13} = T_{up21} \cdot \Delta V_{s_x} + T_{up22} \cdot \Delta V_{s_y}$$

$$\Delta T_{up15} = T_{up23} \cdot \Delta V_{s_x} + T_{up24} \cdot \Delta V_{s_y}$$

$$\Delta T_{up16} = T_{up25} \cdot \Delta V_{s_x} + T_{up26} \cdot \Delta V_{s_y}$$

Where:

$$T_{up21} = \begin{pmatrix} -sin\theta \cdot T_{up3_1} + cos\theta \cdot T_{up3_2} & -sin\theta \cdot T_{up3_2} - cos\theta \cdot T_{up3_1} \\ cos\theta \cdot T_{up3_1} + sin\theta \cdot T_{up3_2} & cos\theta \cdot T_{up3_2} - sin\theta \cdot T_{up3_1} \end{pmatrix} \cdot T_{up17_1}$$

$$T_{up22} = \begin{pmatrix} -sin\theta \cdot T_{up3_1} + cos\theta \cdot T_{up3_2} & -sin\theta \cdot T_{up3_2} - cos\theta \cdot T_{up3_1} \\ cos\theta \cdot T_{up3_1} + sin\theta \cdot T_{up3_2} & cos\theta \cdot T_{up3_2} - sin\theta \cdot T_{up3_1} \end{pmatrix} \cdot T_{up17_2}$$

$$T_{up23} = \begin{pmatrix} -sin\theta \cdot T_{up8_1} + cos\theta \cdot T_{up8_2} & -sin\theta \cdot T_{up8_2} - cos\theta \cdot T_{up8_1} \\ cos\theta \cdot T_{up8_1} + sin\theta \cdot T_{up8_2} & \cos\theta \cdot T8_2 - sin\theta \cdot T_{up8_1} \end{pmatrix} \cdot T_{up17_1}$$

$$T_{up24} = \begin{pmatrix} -sin\theta \cdot T_{up8_1} + cos\theta \cdot T_{up8_2} & -sin\theta \cdot T_{up8_2} - cos\theta \cdot T_{up8_1} \\ cos\theta \cdot T_{up8_1} + sin\theta \cdot T_{up8_2} & \cos\theta \cdot T8_2 - sin\theta \cdot T_{up8_1} \end{pmatrix} \cdot T_{up17_2}$$

$$T_{up25} = \begin{pmatrix} -sin\theta \cdot T_{up9_1} + cos\theta \cdot T_{up9_2} & -sin\theta \cdot T_{up9_2} - cos\theta \cdot T_{up9_1} \\ cos\theta \cdot T_{up9_1} + sin\theta \cdot T_{up9_2} & cos\theta \cdot T_{up9_2} - sin\theta \cdot T_{up9_1} \end{pmatrix} \cdot T_{up17_1}$$

$$T_{up26} = \begin{pmatrix} -sin\theta \cdot T_{up9_1} + cos\theta \cdot T_{up9_2} & -sin\theta \cdot T_{up9_2} - cos\theta \cdot T_{up9_1} \\ cos\theta \cdot T_{up9_1} + sin\theta \cdot T_{up9_2} & cos\theta \cdot T_{up9_2} - sin\theta \cdot T_{up9_1} \end{pmatrix} \cdot T_{up17_2}$$

Linearizing equation (D-26) gives:

$$\frac{d}{dt}\Delta M_{dc} = -\Delta V_{dc} \tag{D-35}$$

Because $V_{sdq}$, and $V_{rdq}$ are functions of $\theta$ and their x-y counterparts, before linearizing equations (D-27)-(D-30), we define:

$$\Delta T_{up1}{}^{-1} = \begin{pmatrix} -sin\theta & cos\theta \\ -cos\theta & -sin\theta \end{pmatrix} \cdot \Delta\theta = T_{up27} \cdot (T_{up17_1} \cdot \Delta V_{s_x} + T_{up17_2} \cdot \Delta V_{s_y})$$

Where:

$$T_{up27} = \begin{pmatrix} -sin\theta & cos\theta \\ -cos\theta & -sin\theta \end{pmatrix}$$

Linearizing equation (D-27)-(D-30) gives equations (D-36)-(D-39) respectively:

$$\begin{aligned} \frac{d}{dt}\Delta M_{bd} = & -T_{up2_1} \cdot \Delta M_{bd} - T_{up2_2} \cdot \Delta M_{bq} + (1 - T_{up3_1}) \cdot \Delta U_{bd} - T_{up3_2} \cdot \Delta U_{bq} \\ & -(const\_M_{bd} \cdot T_{up17_1} + T_{up28_1}) \cdot \Delta V_{s_x} + T_{up28_1} \cdot \Delta V_{r_x} \\ & -(const\_M_{bd} \cdot T_{up17_2} + T_{up28_2}) \cdot \Delta V_{s_y} + T_{up28_2} \cdot \Delta V_{r_y} \end{aligned} \tag{D-36}$$

$$\begin{aligned} \frac{d}{dt}\Delta M_{bq} = & -T_{up5_1} \cdot \Delta M_{bd} - T_{up5_2} \cdot \Delta M_{bq} - T_{up6_1} \cdot \Delta U_{bd} + (1 - T_{up6_2}) \cdot \Delta U_{bq} \\ & -(const\_M_{bd} \cdot T_{up17_1} + T_{up29_1}) \cdot \Delta V_{s_x} + T_{up29_1} \cdot \Delta V_{r_x} \\ & -(const\_M_{bd} \cdot T_{up17_2} + T_{up29_2}) \cdot \Delta V_{s_y} + T_{up29_2} \cdot \Delta V_{r_y} \end{aligned} \tag{D-37}$$

$$\begin{aligned} \frac{d}{dt}\Delta M_{ed} = & -T_{up8_1} \cdot \Delta M_{ed} - T_{up8_2} \cdot \Delta M_{eq} \\ & + (1 - T_{up9_1}) \cdot (-K_{pdc} \cdot \Delta V_{dc} + K_{idc} \cdot \Delta M_{dc}) - T_{up9_2} \cdot \Delta U_{eq} \end{aligned} \tag{D-38}$$

$$\begin{aligned} \frac{d}{dt}\Delta M_{sq} = & -T_{up10_1} \cdot \Delta M_{ed} - T_{up10_2} \cdot \Delta M_{eq} \\ & - T_{up11_1} \cdot (-K_{pdc} \cdot \Delta V_{dc} + K_{idc} \cdot \Delta M_{dc}) + (1 - T_{up11_2}) \cdot \Delta U_{eq} \end{aligned} \tag{D-39}$$

Where:

$$const\_M_{bd} = T_{up4} \cdot T_{up27} \cdot \begin{pmatrix} V_{s_x} - V_{r_x} \\ V_{s_y} - V_{r_y} \end{pmatrix} \qquad T_{up28} = \begin{pmatrix} T_{up28_1} & T_{up28_2} \end{pmatrix} = T_{up4} \cdot T_{up1}{}^{-1}$$

$$const\_M_{bq} = T_{up7} \cdot T_{up27} \cdot \begin{pmatrix} V_{s_x} - V_{r_x} \\ V_{s_y} - V_{r_y} \end{pmatrix} \qquad T_{up29} = \begin{pmatrix} T_{up29_1} & T_{up29_2} \end{pmatrix} = T_{up7} \cdot T_{up1}{}^{-1}$$

Linearizing algebraic equations (D-23)-(D-24) gives equations (D-40)-(D-43) respectively:

$$
\begin{aligned}
\Delta Ib_x = {} & Tup12_{1,1} \cdot \Delta Mbd + Tup12_{1,2} \cdot \Delta Mbq + Tup13_{1,1} \cdot \Delta Ubd + Tup13_{1,2} \cdot \Delta Ubq \\
& + (Tup19_{1,1} \cdot Mbd + Tup19_{1,2} \cdot Mbq + Tup21_{1,1} \cdot Ubd + Tup21_{1,2} \cdot Ubq + Tup14_{1,1})\Delta Vs_x \\
& + (Tup20_{1,1} \cdot Mbd + Tup20_{1,2} \cdot Mbq + Tup22_{1,1} \cdot Ubd + Tup22_{1,2} \cdot Ubq + Tup14_{1,2})\Delta Vs_y \\
& - Tup14_{1,1} \cdot \Delta Vr_x - Tup14_{1,2} \cdot \Delta Vr_y
\end{aligned} \tag{D-40}
$$

$$
\begin{aligned}
\Delta Ib_y = {} & Tup12_{2,1} \cdot \Delta Mbd + Tup12_{2,2} \cdot \Delta Mbq + Tup13_{2,1} \cdot \Delta Ubd + Tup13_{2,2} \cdot \Delta Ubq \\
& + (Tup19_{2,1} \cdot Mbd + Tup19_{2,2} \cdot Mbq + Tup21_{2,1} \cdot Ubd + Tup21_{2,2} \cdot Ubq + Tup14_{2,1})\Delta Vs_x \\
& + (Tup20_{2,1} \cdot Mbd + Tup20_{2,2} \cdot Mbq + Tup22_{2,1} \cdot Ubd + Tup22_{2,2} \cdot Ubq + Tup14_{2,2})\Delta Vs_y \\
& - Tup14_{2,1} \cdot \Delta Vr_x - Tup14_{2,2} \cdot \Delta Vr_y
\end{aligned} \tag{D-41}
$$

$$
\begin{aligned}
\Delta Ie_x = {} & -Tup16_{1,1} \cdot Kpdc \cdot \Delta Vdc + Tup16_{1,1} \cdot Kidc \cdot \Delta Mdc \\
& + Tup15_{1,1} \cdot \Delta Med + Tup15_{1,2} \cdot \Delta Meq + Tup16_{1,2} \cdot \Delta Ueq \\
& + (Tup23_{1,1} \cdot Med + Tup23_{1,2} \cdot Meq + Tup25_{1,1} \cdot Ued + Tup25_{1,2} \cdot Ueq)\Delta Vs_x \\
& + (Tup24_{1,1} \cdot Med + Tup24_{1,2} \cdot Meq + Tup26_{1,1} \cdot Ued + Tup26_{1,2} \cdot Ueq)\Delta Vs_y
\end{aligned} \tag{D-42}
$$

$$
\begin{aligned}
\Delta Ie_y = {} & -Tup16_{2,1} \cdot Kpdc \cdot \Delta Vdc + Tup16_{2,1} \cdot Kidc \cdot \Delta Mdc \\
& + Tup15_{2,1} \cdot \Delta Med + Tup15_{2,2} \cdot \Delta Meq + Tup16_{2,2} \cdot \Delta Ueq \\
& + (Tup23_{2,1} \cdot Med + Tup23_{2,2} \cdot Meq + Tup25_{2,1} \cdot Ued + Tup25_{2,2} \cdot Ueq)\Delta Vs_x \\
& + (Tup24_{2,1} \cdot Med + Tup24_{2,2} \cdot Meq + Tup26_{2,1} \cdot Ued + Tup26_{2,2} \cdot Ueq)\Delta Vs_y
\end{aligned} \tag{D-43}
$$

The above linearized state equations (D-34)-(D-39) and algebraic equations (D-40)-(D-43) can be rewritten in standard compact forms as following:

$$\Delta \dot{X}up = Aup \cdot \Delta Xup + Bup \cdot \Delta Uup + Eup \cdot \Delta Vs + Fup \cdot \Delta Vr \tag{D-44}$$

$$\Delta Ib = Tup30 \cdot \Delta Xup + Tup31 \cdot \Delta Uup + Tup32 \cdot \Delta Vs + Tup33 \cdot \Delta Vr \tag{D-45}$$

$$\Delta Ie = Tup34 \cdot \Delta Xup + Tup35 \cdot \Delta Uup + Tup36 \cdot \Delta Vs \tag{D-46}$$

Where:

$$\Delta Xup = \begin{pmatrix} \Delta Vdc \\ \Delta Mdc \\ \Delta Mbd \\ \Delta Mbq \\ \Delta Med \\ \Delta Meq \end{pmatrix} \qquad \Delta Uup = \begin{pmatrix} \Delta Ubd \\ \Delta Ubq \\ \Delta Ueq \end{pmatrix}$$

$$Aup = \begin{pmatrix} Aup_{1,1} & Aup_{1,2} & Aup_{1,3} & Aup_{1,4} & Aup_{1,5} & Aup_{1,6} \\ -1 & 0 & 0 & 0 & 0 & 0 \\ 0 & 0 & -Tup2_1 & -Tup2_2 & 0 & 0 \\ 0 & 0 & -Tup5_1 & -Tup5_2 & 0 & 0 \\ -(1-Tup9_1)\cdot Kpdc & (1-Tup9_1)\cdot Kidc & 0 & 0 & -Tup8_1 & -Tup8_2 \\ Tup11_1\cdot Kpdc & -Tup11_1\cdot Kidc & 0 & 0 & -Tup10_1 & -Tup10_2 \end{pmatrix}$$

$$Bup = \begin{pmatrix} Bup_{1,1} & Bup_{1,2} & Bup_{1,3} \\ 0 & 0 & 0 \\ 1-Tup3_1 & -Tup3_2 & 0 \\ -Tup6_1 & 1-Tup_2 & 0 \\ 0 & 0 & -Tup9_2 \\ 0 & 0 & 1-Tup11_2 \end{pmatrix}$$

$$Eup = \begin{pmatrix} Eup_{1,1} & Eup_{1,2} \\ 0 & 0 \\ -(const\_Mbd\cdot Tup17_1 + Tup28_1) & -(const\_Mbd\cdot Tup17_2 + Tup28_2) \\ -(const\_Mbq\cdot Tup17_1 + Tup29_1) & -(const\_Mbq\cdot Tup17_2 + Tup29_2) \\ 0 & 0 \\ 0 & 0 \end{pmatrix}$$

$$Fup = \begin{pmatrix} Fup_{1,1} & Fup_{1,2} \\ 0 & 0 \\ Tup28_1 & Tup28_2 \\ Tup29_1 & Tup29_2 \\ 0 & 0 \\ 0 & 0 \end{pmatrix}$$

$$Tup30 = \begin{pmatrix} 0 & 0 & Tup12_{1,1} & Tup12_{1,2} & 0 & 0 \\ 0 & 0 & Tup12_{2,1} & Tup12_{2,2} & 0 & 0 \end{pmatrix}$$

$$Tup31 = \begin{pmatrix} Tup13_{1,1} & Tup13_{1,2} & 0 \\ Tup13_{2,1} & Tup13_{2,2} & 0 \end{pmatrix}$$

$$Tup32 = \begin{pmatrix} Tup32_{1,1} & Tup32_{1,2} \\ Tup32_{2,1} & Tup32_{2,2} \end{pmatrix}$$

$$Tup32_{1,1} = Tup19_{1,1}\cdot Mbd + Tup19_{1,2}\cdot Mbq + Tup21_{1,1}\cdot Ubd + Tup21_{1,2}\cdot Ubq + Tup14_{1,1}$$

$$Tup32_{1,2} = Tup20_{1,1}\cdot Mbd + Tup20_{1,2}\cdot Mbq + Tup22_{1,1}\cdot Ubd + Tup22_{1,2}\cdot Ubq + Tup14_{1,2}$$

$$Tup32_{2,1} = Tup19_{2,1} \cdot Mbd + Tup19_{2,2} \cdot Mbq + Tup21_{2,1} \cdot Ubd + Tup21_{2,2} \cdot Ubq + Tup14_{2,1}$$

$$Tup_{2,2} = Tup20_{2,1} \cdot Mbd + Tup20_{2,2} \cdot Mbq + Tup20_{2,1} \cdot Ubd + Tup20_{2,2} \cdot Ubq + Tup14_{2,2}$$

$$Tup33 = \begin{pmatrix} Tup33_{1,1} & Tup33_{1,2} \\ Tup33_{2,1} & Tup33_{2,2} \end{pmatrix} = -Tup14$$

$$Tup34 = \begin{pmatrix} -Tup16_{1,1} \cdot Kpdc & Tup16_{1,1} \cdot Kidc & 0 & 0 & Tup15_{1,1} & Tup15_{1,2} \\ -Tup16_{2,1} \cdot Kpdc & Tup16_{2,1} \cdot Kidc & 0 & 0 & Tup15_{2,1} & Tup15_{2,2} \end{pmatrix}$$

$$Tup35 = \begin{pmatrix} 0 & 0 & Tup16_{1,2} \\ 0 & 0 & Tup16_{2,2} \end{pmatrix}$$

$$Tup36 = \begin{pmatrix} Tup36_{1,1} & Tup36_{1,2} \\ Tup36_{2,1} & Tup36_{2,2} \end{pmatrix}$$

$$Tup36_{1,1} = Tup23_{1,1} \cdot Med + Tup23_{1,2} \cdot Meq + Tup25_{1,1} \cdot Ued + Tup25_{1,2} \cdot Ueq$$

$$Tup36_{1,2} = Tup24_{1,1} \cdot Med + Tup24_{1,2} \cdot Meq + Tup26_{1,1} \cdot Ued + Tup26_{1,2} \cdot Ueq$$

$$Tup36_{2,1} = Tup23_{2,1} \cdot Med + Tup23_{2,2} \cdot Meq + Tup25_{2,1} \cdot Ued + Tup25_{2,2} \cdot Ueq$$

$$Tup36_{2,2} = Tup24_{2,1} \cdot Med + Tup24_{2,2} \cdot Meq + Tup26_{2,1} \cdot Ued + Tup26_{2,2} \cdot Ueq$$

## D.2 Small Signal Models of Generators and Exciters

The small signal models of generators and exciters were given in Appendix B and are repeated here for reference.

$$\Delta \dot{X}g_k = Ag_k \cdot \Delta Xg_k + Bg_k \cdot \Delta Ug_k + Eg_k \cdot \Delta Vg_k \tag{A-11}$$

$$\Delta Ig_k = Sg_k \cdot \Delta Xg_k - Yg_k \cdot \Delta Vg_k \tag{A-12}$$

## D.3 Small Signal Model of Test System with Embedded UPFC

### D.3.1 Linearization of the Network State Equations

The UPFC has one series branch which introduces one extra bus. Hence the network with the UPFC has 13 buses (the infinite bus is not included). The buses of the system are sequenced as follows:

1~p: generator 1 to generator p,

p+1: the sending end bus of the UPFC,

p+2: the receiving end bus of the UPFC,

p+3~n: remainder network buses (not including the infinite bus).

The corresponding network node equation can be represented by equation (D-47):

$$\begin{pmatrix} YN_{g1,1} & \dots & YN_{g1,p} & YN_{g1,s} & YN_{g1,r} & YN_{g1,i} & \dots & YN_{g1,n} \\ \dots & \dots & \dots & \dots & \dots & \dots & \dots & \dots \\ YN_{gp,1} & \dots & YN_{gp,p} & YN_{gp,s} & YN_{gp,r} & YN_{gp,i} & \dots & YN_{gp,n} \\ YN_{s,1} & \dots & YN_{s,p} & YN_{s,s} & YN_{s,r} & YN_{s,i} & \dots & YN_{s,n} \\ YN_{r,1} & \dots & YN_{r,p} & YN_{r,s} & YN_{r,r} & YN_{r,i} & \dots & YN_{r,n} \\ YN_{i,1} & \dots & YN_{i,p} & YN_{i,s} & YN_{i,r} & YN_{i,i} & \dots & YN_{i,n} \\ \dots & \dots & \dots & \dots & \dots & \dots & \dots & \dots \\ YN_{n,1} & \dots & YN_{n,p} & YN_{n,s} & YN_{n,r} & YN_{n,i} & \dots & YN_{n,n} \end{pmatrix} \cdot \begin{pmatrix} \Delta V_{g_1} \\ \dots \\ \Delta V_{g_p} \\ \Delta V_s \\ \Delta V_r \\ \Delta V_i \\ \dots \\ \Delta V_n \end{pmatrix} = \begin{pmatrix} \Delta I_{g_1} \\ \dots \\ \Delta I_{g_p} \\ -\Delta I_b - \Delta I_e \\ \Delta I_b \\ \Delta IN_i \\ \dots \\ \Delta IN_n \end{pmatrix}$$

………………………………………..(D-47)

Substituting $\Delta I_{gk}$ of (A-12) into (D-47), the k$^{th}$ generator bus node equation is expressed as:

$$S_{g_k} \cdot \Delta X_{g_k} = \sum_{j=1, j\neq k}^{n} YN_{gk,j} \cdot \Delta Vj + (YN_{gk,k} + Y_{g_k}) \cdot \Delta V_{g_k} \tag{D-48}$$

Substituting $\Delta I_b$ and $\Delta I_e$ of (D-45), (D-46) into (D-47), the node equations of the UPFC sending and receiving end bus are expressed as:

$$\begin{aligned} &-(T_{up30} + T_{up34}) \cdot \Delta X_{up} - (T_{up31} + T_{up35}) \cdot \Delta U_{up} \\ &= \sum_{j=1, j\neq s,r}^{n} YN_{s,j} \cdot \Delta Vj + (YN_{s,s} + T_{up32} + T_{up36}) \cdot \Delta V_{g_s} + (YN_{s,r} + T_{up33}) \cdot \Delta V_r \end{aligned} \tag{D-49}$$

$$T_{up30} \cdot \Delta X_{up} + T_{up31} \cdot \Delta U_{up}$$
$$= \sum_{j=1, j \neq s,r}^{n} YN_{r,j} \cdot \Delta V_j + (YN_{r,s} - T_{up32}) \cdot \Delta V_s + (YN_{r,r} - T_{up33}) \cdot \Delta V_r \tag{D-50}$$

For other buses which are not connected to dynamic devices:

$$0 = \sum_{j=1}^{n} YN_{i,j} \cdot \Delta V_j \tag{D-51}$$

The above equations (D-48)-(D-51) form a new network equation in which the current components of dynamic devices are eliminated by replacing them with linear combinations of states and reference inputs:

$$\begin{pmatrix} YM_{g,g} & YM_{g,s} & YM_{g,r} & YM_{g,j} \\ YM_{s,g} & YM_{s,s} & YM_{s,r} & YM_{s,j} \\ YM_{r,g} & YM_{r,s} & YM_{r,r} & YM_{r,j} \\ YM_{i,g} & YM_{i,s} & YM_{i,r} & YM_{i,j} \end{pmatrix} \cdot \begin{pmatrix} \Delta V_g \\ \Delta V_s \\ \Delta V_r \\ \Delta V_j \end{pmatrix} = \begin{pmatrix} S_g \cdot \Delta X_g \\ -(T_{up30} + T_{up34}) \cdot \Delta X_{up} - (T_{up31} + T_{up35}) \cdot \Delta U_{up} \\ T_{up30} \cdot \Delta X_{up} + T_{up31} \cdot \Delta U_{up} \\ 0 \end{pmatrix}$$

………………………..(D-52)

Where:

$$S_g = \begin{pmatrix} S_{g_1} & \cdots & 0 \\ \vdots & S_{g_k} & \vdots \\ 0 & \cdots & S_{g_p} \end{pmatrix} \qquad \Delta X_g = \begin{pmatrix} \Delta X_{g_1} \\ \ldots \\ \Delta X_{g_p} \end{pmatrix}$$

$$YM_{g,g} = \begin{pmatrix} YN_{gk,1} + Y_{g_1} & \ldots & YN_{g1,p} \\ \ldots & \ldots & \ldots \\ YN_{gp,1} & \ldots & YN_{gp,p} + Y_{g_{p,p}} \end{pmatrix} \qquad YM_{g,s} = \begin{pmatrix} YN_{g1,s} \\ \ldots \\ YN_{gp,s} \end{pmatrix} \qquad YM_{g,r} = \begin{pmatrix} YN_{g1,r} \\ \ldots \\ YN_{gp,r} \end{pmatrix}$$

$$YM_{g,j} = \begin{pmatrix} YN_{g1,j} & \ldots & YN_{g1,n} \\ \ldots & \ldots & \ldots \\ YN_{gp,j} & \ldots & YN_{gp,n} \end{pmatrix}$$

$$YM_{i,g} = \begin{pmatrix} YN_{i,j} & \ldots & YN_{i,p} \\ \ldots & \ldots & \ldots \\ YN_{n,1} & \ldots & YN_{n,p} \end{pmatrix} \qquad YM_{i,s} = \begin{pmatrix} YN_{i,s} \\ \ldots \\ YN_{n,s} \end{pmatrix} \qquad YM_{i,r} = \begin{pmatrix} YN_{i,r} \\ \ldots \\ YN_{n,r} \end{pmatrix}$$

$$YM_{i,j} = \begin{pmatrix} YN_{i,j} & \ldots & YN_{i,i} \\ \ldots & \ldots & \ldots \\ YN_{n,j} & \ldots & YN_{n,n} \end{pmatrix}$$

$$YM_{s,g} = \begin{pmatrix} YN_{s,1} & \ldots & YN_{s,p} \end{pmatrix} \qquad YM_{s,s} = YN_{s,s} + T_{up32} + T_{up36} \qquad YM_{s,r} = YN_{s,r} + T_{up33}$$

$$YM_{s,j} = \begin{pmatrix} YN_{s,j} & \ldots & YN_{s,n} \end{pmatrix}$$

$$YM_{r,g} = \begin{pmatrix} YN_{r,1} & \ldots & YN_{r,p} \end{pmatrix} \qquad YM_{r,s} = YN_{r,s} - T_{up32} \qquad YM_{r,r} = YN_{r,r} - T_{up33}$$

$$YM_{r,j} = \begin{pmatrix} YN_{r,j} & \ldots & YN_{r,n} \end{pmatrix}$$

Equation (D-52) can be rewritten as:

$$\begin{pmatrix} \Delta V_g \\ \Delta V_s \\ \Delta V_r \\ \Delta V_j \end{pmatrix} = ZM \cdot \begin{pmatrix} S_g \cdot \Delta X_g \\ -(T_{up30} + T_{up34}) \cdot \Delta X_{up} - (T_{up31} + T_{up35}) \cdot \Delta U_{up} \\ T_{up30} \cdot \Delta X_{up} + T_{up31} \cdot \Delta U_{up} \\ 0 \end{pmatrix} \tag{D-53}$$

Where:

$$ZM = YM^{-1} = \begin{pmatrix} ZM_{g,g} & ZM_{g,s} & ZM_{g,r} & ZM_{g,j} \\ ZM_{s,g} & ZM_{s,s} & ZM_{s,r} & ZM_{s,j} \\ ZM_{r,g} & ZM_{r,s} & ZM_{r,r} & ZM_{r,j} \\ ZM_{i,g} & ZM_{i,s} & ZM_{i,r} & ZM_{i,j} \end{pmatrix}$$

Equation (D-53) can be split into following five equations:

$$\begin{aligned} \Delta Vg_k = & \sum_{j=1}^{p} ZM_{gk,gj} \cdot Sg_j \cdot \Delta Xg_j - ((ZM_{gk,s} - ZM_{gk,r}) \cdot T_{up30} + ZM_{gk,s} \cdot T_{up34}) \cdot \Delta X_{up} \\ & - ((ZM_{gk,s} - ZM_{gk,r}) \cdot T_{up31} + ZM_{gk,s} \cdot T_{up35}) \cdot \Delta U_{up} \end{aligned} \tag{D-54}$$

$$\begin{aligned} \Delta V_s = & \sum_{j=1}^{p} ZM_{s,gj} \cdot Sg_j \cdot \Delta Xg_j - ((ZM_{s,s} - ZM_{s,r}) \cdot T_{up30} + ZM_{s,s} \cdot T_{up34}) \cdot \Delta X_{up} \\ & - ((ZM_{s,s} - ZM_{s,r}) \cdot T_{up31} + ZM_{s,s} \cdot T_{up35}) \cdot \Delta U_{up} \end{aligned} \tag{D-55}$$

$$\Delta V_r = \sum_{j=1}^{p} ZM_{r,gj} \cdot Sg_j \cdot \Delta Xg_j - ((ZM_{r,s} - ZM_{r,r}) \cdot T_{up30} + ZM_{r,s} \cdot T_{up34}) \cdot \Delta X_{up}$$
$$- ((ZM_{r,s} - ZM_{r,r}) \cdot T_{up31} + ZM_{r,s} \cdot T_{up35}) \cdot \Delta U_{up} \quad \text{(D-56)}$$

Substituting equation (D-54) into (A-11); and (D-55)-(D-56) into (D-44) gives the linearized state equations of the system:

$$\Delta \dot{X}g_k = \sum_{j=1}^{p} AGG_{k,j} \cdot \Delta Xg_j + AGU_k \cdot \Delta X_{up} + \sum_{j=1}^{p} BGG_{k,j} \cdot \Delta Ug_j + BGU_k \cdot \Delta U_{up} \quad \text{(D-57)}$$

$$\Delta \dot{X}_{up} = \sum_{j=1}^{p} AUG_j \cdot \Delta Xg_j + AUU \cdot \Delta X_{up} + BUU \cdot \Delta U_{up} \quad \text{(D-58)}$$

Where:

$$AGG_{k,j} = Eg_k \cdot ZM_{gk,gj} \cdot Sg_j \qquad (j \neq k)$$

$$AGG_{k,k} = -Eg_k \cdot ZM_{gk,gk} \cdot Sg_k + Ag_k$$

$$AGU_k = -Eg_k \cdot ((ZM_{gk,s} - ZM_{gk,r}) \cdot T_{up30} + ZM_{gk,s} \cdot T_{up34})$$

$$BGG_k = Bg_k$$

$$BGG_j = 0 \qquad (j \neq k)$$

$$BGU_k = -Eg_k \cdot ((ZM_{gk,s} - ZM_{gk,r}) \cdot T_{up31} + ZM_{gk,s} \cdot T_{up35})$$

$$AUG_j = (E_{up} \cdot ZM_{s,gj} + F_{up} \cdot ZM_{r,gj}) \cdot Sg_j \qquad (j=1,...,p)$$

$$AUU = A_{up} - E_{up} \cdot ((ZM_{s,s} - ZM_{s,r}) \cdot T_{up30} + ZM_{s,s} \cdot T_{up34})$$
$$- F_{up} \cdot ((ZM_{r,s} - ZM_{r,r}) \cdot T_{up30} + ZM_{r,s} \cdot T_{up34})$$

$$BUU = B_{up} - E_{up} \cdot ((ZM_{s,s} - ZM_{s,r}) \cdot T_{up31} + ZM_{s,s} \cdot T_{up35})$$
$$- F_{up} \cdot ((ZM_{r,s} - ZM_{r,r}) \cdot T_{up31} + ZM_{r,s} \cdot T_{up35})$$

Equations (D-57) and (D-58) can be written in matrix form to give the standard linearized state equation:

$$\begin{pmatrix} \Delta \dot{X}_g \\ \Delta \dot{X}_{up} \end{pmatrix} = \begin{pmatrix} AGG & AGU \\ AUG & AUU \end{pmatrix} \cdot \begin{pmatrix} \Delta X_g \\ \Delta X_{up} \end{pmatrix} + \begin{pmatrix} BGU \\ BUU \end{pmatrix} \cdot \Delta U_{up} \quad \text{(D-59)}$$

Or: $\Delta \dot{X} = A \cdot \Delta X + B \cdot \Delta U_{up}$

Where:

$$\Delta \dot{X} = \begin{pmatrix} \Delta \dot{X}_{g1} \\ \ldots \\ \Delta \dot{X}_{gp} \\ \Delta \dot{X}_{up} \end{pmatrix} \qquad \Delta U = \begin{pmatrix} \Delta U_{g1} \\ \ldots \\ \Delta U_{gp} \\ \Delta U_{ip} \end{pmatrix}$$

$$A_{GG} = \begin{pmatrix} A_{GG_{1,1}} & \ldots & A_{GG_{1,p}} \\ \ldots & \ldots & \ldots \\ A_{GG_{p,1}} & \ldots & A_{GG_{p,p}} \end{pmatrix} \qquad A_{GU} = \begin{pmatrix} A_{UG_1} \\ \ldots \\ A_{UG_p} \end{pmatrix} \qquad A_{UG} = \begin{pmatrix} A_{UG_1} & \ldots & A_{UG_p} \end{pmatrix}$$

$$B_{GU} = \begin{pmatrix} B_{GU_1} \\ \ldots \\ B_{GU_p} \end{pmatrix} \qquad B = \begin{pmatrix} B_{GU} \\ B_{UU} \end{pmatrix}$$

## D.3.2 Output Equations

Using equations (A-12) and (D-54) the real power deviation of the kth generator can be expressed as：

$$\Delta P_{g_k} = V_{g_k}^T \cdot \Delta I_{g_k} + I_{g_k}^T \cdot \Delta V_{g_k} = CPG_{g_k} \cdot \Delta X_g + CPG_{up_k} \cdot \Delta X_{up} + DPG_k \cdot \Delta U_{up} \tag{D-60}$$

Where:

$$CPG_{g_k} = ((I_{g_k}^T - V_{g_k}^T \cdot Y_{g_k}) \cdot ZM_{g_k,g_1} \cdot S_{g_1} \ \ldots \ V_{g_k}^T \cdot S_{g_k} + (I_{g_k}^T - V_{g_k}^T \cdot Y_{g_k}) \cdot ZM_{g_k,g_k} \cdot S_{g_k} \ \ldots$$
$$(I_{g_k}^T - V_{g_k}^T \cdot Y_{g_k}) \cdot ZM_{g_k,g_p} \cdot S_{g_p})$$

$$CPG_{up_k} = -(I_{g_k}^T - V_{g_k}^T \cdot Y_{g_k}) \cdot ((ZM_{gk,s} - ZM_{gk,r}) \cdot T_{up30} + ZM_{gk,s} \cdot T_{up34})$$

$$DPG_k = -(I_{g_k}^T - V_{g_k}^T \cdot Y_{g_k}) \cdot ((ZM_{gk,s} - ZM_{gk,r}) \cdot T_{up31} + ZM_{gk,s} \cdot T_{up35})$$

The reactive power derivation of the kth generator can be expressed as:

$$\begin{aligned}\Delta Qg_k &= (Vg_{ky} \quad -Vg_{kx}) \cdot \Delta Ig_k + (-Ig_{ky} \quad Ig_{kx}) \cdot \Delta Vg_k \\ &= CQGg_k \cdot \Delta Xg + CQGup_k \cdot \Delta Xup + DQG_k \cdot \Delta Uup\end{aligned} \tag{D-61}$$

Where:

$$\begin{aligned}CQGg_k = (((&-Ig_{ky} \quad Ig_{kx}) - (Vg_{ky} \quad -Vg_{kx}) \cdot Yg_1) \cdot ZMg_{k,g_1} \cdot Sg_1 \;\ldots \\ &(Vg_{ky} \quad -Vg_{kx}) \cdot Sg_k + ((-Ig_{ky} \quad Ig_{kx}) - (Vg_{ky} \quad -Vg_{kx}) \cdot Yg_k) \cdot ZMg_{k,g_k} \cdot Sg_k \ldots \\ &((-Ig_{ky} \quad Ig_{kx}) - (Vg_{ky} \quad -Vg_{kx}) \cdot Yg_k) \cdot ZMg_{k,g_p} \cdot Sg_p)\end{aligned}$$

$$CQGup_k = -((-Ig_{ky} \quad Ig_{kx}) - (Vg_{ky} \quad -Vg_{kx}) \cdot Yg_k) \cdot ((ZM_{gk,s} - ZM_{gk,r}) \cdot Tip30 + ZM_{gk,s} \cdot Tip34)$$

$$DQGup_k = -((-Ig_{ky} \quad Ig_{kx}) - (Vg_{ky} \quad -Vg_{kx}) \cdot Yg_k) \cdot ((ZM_{gk,s} - ZM_{gk,r}) \cdot Tip31 + ZM_{gk,s} \cdot Tip35)$$

The sending ending real power derivation of the UPFC can be derived by equations (D-45) and (D-55) as:

$$\Delta Ps = Vs^T \cdot (\Delta Ib + \Delta Ie) + (Ib + Ie)^T \cdot \Delta Vs = CPSg \cdot \Delta Xg + CPSup \cdot \Delta Xup + DPS \cdot \Delta Uup \tag{D-62}$$

Where:

$$\begin{aligned}CPSg = ((&Vs^T \cdot (Tup32 + Tup36) + (Ib + Ie)^T) \cdot ZM_{s,g1} \cdot Sg_1 + Vs^T \cdot Tup33 \cdot ZM_{r,g1} \cdot Sg_1 \;\ldots \\ &(Vs^T \cdot (Tup32 + Tup36) + (Ib + Ie)^T) \cdot ZM_{s,gp} \cdot Sg_p + Vs^T \cdot Tup33 \cdot ZM_{r,gp} \cdot Sg_p)\end{aligned}$$

$$\begin{aligned}CPSup = &Vs^T \cdot (Tup30 + Tup34) \\ &-(Vs^T \cdot (Tup32 + Tup36) + (Ib + Ie)^T) \cdot (ZM_{s,s} - ZM_{s,r}) \cdot Tup30 + ZM_{s,s} \cdot Tup34) \\ &-Vs^T \cdot Tup33 \cdot ((ZM_{r,s} - ZM_{r,r}) \cdot Tup30 + ZM_{r,s} \cdot Tup34)\end{aligned}$$

$$\begin{aligned}DPS = &Vs^T \cdot (Tup31 + Tup35) \\ &-(Vs^T \cdot (Tup32 + Tup36) + (Ib + Ie)^T) \cdot (ZM_{r,s} - ZM_{r,r}) \cdot Tup31 + ZM_{r,s} \cdot Tup35) \\ &-Vs^T \cdot Tup33 \cdot ((ZM_{r,s} - ZM_{r,r}) \cdot Tup31 + ZM_{r,s} \cdot Tup35)\end{aligned}$$

The reactive power derivation of the master line of the UPFC can be expressed as:

$$\begin{aligned}\Delta Qs &= (Vs_y \quad -Vs_x) \cdot (\Delta Ib + \Delta Ie) + ((-Ib_y \quad Ib_x) + (-Ie_y \quad Ie_x)) \cdot \Delta Vs \\ &= CQSg \cdot \Delta Xg + CQSup \cdot \Delta Xup + DQS \cdot \Delta Uup\end{aligned} \tag{D-63}$$

Where:

$$CQSg = (((-Ib_y \quad Ib_x) + (-Ie_y \quad Ie_x) + (Vs_y \quad -Vs_x) \cdot (Tup32 + Tup36)) \cdot ZM_{s,g1} \cdot Sg_1$$
$$+ (Vs_y \quad -Vs_x) \cdot Tup33 \cdot ZM_{s,g1} \cdot Sg_1 \;\; \ldots$$
$$((-Ib_y \quad Ib_x) + (-Ie_y \quad Ie_x) + (Vs_y \quad -Vs_x) \cdot (Tup32 + Tup36)) \cdot ZM_{s,gp} \cdot Sg_p$$
$$+ (Vs_y \quad -Vs_x) \cdot Tup33 \cdot ZM_{s,gp} \cdot Sg_p)$$

$$CQSup = (Vs_y \quad -Vs_x) \cdot (Tup30 + Tup34)$$
$$-((-Ib_y \quad Ib_x) + (-Ie_y \quad Ie_x) + (Vs_y \quad -Vs_x) \cdot (Tup32 + Tup36)) \cdot ((ZM_{s,s} - ZM_{s,r}) \cdot Tup30 + ZM_{s,s} \cdot Tup34)$$
$$-(Vs_y \quad -Vs_x) \cdot Tup33 \cdot ((ZM_{r,s} - ZM_{r,r}) \cdot Tup30 + ZM_{r,s} \cdot Tup34)$$

$$DQS = (Vs_y \quad -Vs_x) \cdot (Tup31 + Tup35)$$
$$-((-Ib_y \quad Ib_x) + (-Ie_y \quad Ie_x) + (Vs_y \quad -Vs_x) \cdot (Tup32 + Tup36)) \cdot ((ZM_{s,s} - ZM_{s,r}) \cdot Tup31 + ZM_{s,s} \cdot Tup35)$$
$$-(Vs_y \quad -Vs_x) \cdot Tup33 \cdot ((ZM_{r,s} - ZM_{r,r}) \cdot Tup31 + ZM_{r,s} \cdot Tup35)$$